2022 Annual Cancer Research Symposium

NCI Cancer Center

Friday | March 4, 2022

Hosted by

OU Health | Stephenson Cancer Center

OU Health Stephenson Cancer Center wishes to recognize and thank the Oklahoma Tobacco Settlement Endowment Trust (TSET) for co-sponsoring the 2022 Stephenson Cancer Research Symposium.

In 2012 TSET awarded a five-year, $30.25 million grant to Stephenson Cancer Center to establish the Oklahoma TSET Cancer Research Program. In 2017 TSET renewed this award for an additional five year period.

The mission of the Oklahoma TSET Cancer Research Program is to decrease the burden of cancer in Oklahoma and nationally through promoting, coordinating and supporting innovative cancer research. It seeks to accomplish this mission through:

- Attracting cancer researchers with grant funding from the National Cancer Institute and other national sponsors to Oklahoma
- Developing trans-disciplinary, collaborative cancer research programs
- Promoting inter-institutional partnerships to leverage unique strengths at research institutions in Oklahoma
- Enhancing research infrastructure and shared resources to enable and support innovative and nationally-competitive cancer research
- Serving as a statewide resource for researchers and institutions that conduct cancer research

The Oklahoma TSET Cancer Research Program supports a wide range of programs, shared resources and initiatives designed to accomplish these goals.

Five Year Highlights

With support from the Oklahoma TSET Cancer Research Program Stephenson Cancer Center accomplished the following:

- Increased cancer center membership from 75 to 273 members at nine academic institutions across Oklahoma
- Recruited thirty eight new cancer researchers to Oklahoma
- Funded over fifty seed and directed-research grants to cancer investigators in Oklahoma
- Enhanced five Shared Resource facilities
- Hosted over 330 research seminar speakers
- Hosted annual statewide Cancer Research Symposium that bring together over 250 researchers from around the state
- Hosted over 75 undergraduate students from 26 different universities for a summer cancer research experience
- Since the inception of the TSET grant, the SCC has enrolled more than 7,000 patients to interventional clinical trials.

Health Promotion Research Center

OU Health Stephenson Cancer Center wishes to recognize and thank the TSET Health Promotion Research Center (HPRC) for co-sponsoring the 2022 Annual Cancer Research Symposium

---

The TSET Health Promotion Research Center (HPRC; formerly the Oklahoma Tobacco Research Center [OTRC]) is a leading research program with a focus on the entire translational continuum – from the discovery of basic mechanisms of health behavior and behavior change, to the development and evaluation of novel interventions, to the dissemination and implementation of interventions, policies, and education throughout Oklahoma.

The **mission** of the HPRC is to reduce the burden of disease in Oklahoma by addressing modifiable health risk factors such as tobacco use, sedentary lifestyle, poor diet, and risky alcohol and other substance use through research, novel intervention development, and dissemination of research findings.

The HPRC contains four major resources that facilitate research: Mobile Health Shared Resource, Tobacco Treatment Research Program, Postdoctoral Fellowship Training Program, and Tobacco Regulatory Science Clinical Laboratory.

The center was established in 2007 with funding from the Oklahoma Tobacco Settlement Endowment Trust (TSET). Recognizing the investments that TSET has made in statewide and community-based cessation and intervention projects, a key feature of the HPRC is establishing partnerships with existing and future TSET-funded projects and the Oklahoma State Department of Health (OSDH) tobacco-related programs. Those partnerships directly link HPRC researchers with health-related issues and initiatives in Oklahoma.

HPRC Directors, Faculty, and Fellows

Michael S. Businelle, PhD (Director, Faculty)
Darla E. Kendzor, PhD (Director, Faculty)
Adam C. Alexander, PhD (Faculty)
Than C. Bui, MD, DrPh (Faculty)
Amy Cohn, PhD (Faculty)
Sarah Ehlke, PhD (Fellow)
Summer Frank-Pearce, PhD (Faculty)
Julia McQuoid, PhD (Faculty)
Chaelin Karen Ra, PhD. (Fellow)

TSET

OU Health | Stephenson Cancer Center

2022 Annual Cancer Research Symposium

9:30 – 9:45	Welcome & State of the Cancer Center
9:45 – 9:50	Keynote Introduction
9:50 – 10:35	Keynote Address
10:35 – 11:05	Grab Lunch and Move to Breakouts Rooms
11:05 – 12:20	Poster Sessions / Lunch
12:25 – 1:30	Session I
1:35 – 2:40	Session II
2:45 – 3:50	Session III
3:50 – 4:00	Awards & Closing Remarks

2022 Annual Cancer Research Symposium
Detailed Agenda

9:30 – 9:45	Welcome & State of the Cancer Center Dr. Robert S. Mannel, MD
9:45 – 9:50	Keynote Introduction Dr. Rajagopal Ramesh
9:50 – 10:35	Keynote Address: **Promoting and Retaining Women in Senior Faculty Positions in Academic Research: Challenges and Opportunities.** Dr. Elizabeth Travis – MD Anderson
10:35 – 11:05	Break; Grab lunch and move to Poster Breakout Rooms
11:05 – 12:20	Poster Session/Lunch
12:25 – 1:30	**Session I** **Mechanisms of Cancer Progression & Therapy** Moderators: Resham Bhattacharya, Desiree Azizoddin **Genomic Instability Genes in Cancers** Hiroshi Yamada **Role of DNPH1 in Cancer** Ralf Janknecht **Cancer-Related Outcomes Among Children with Acute Lymphoblastic Leukemia** Amanda Janitz

OU Health | Stephenson Cancer Center

2022 Annual Cancer Research Symposium

Laser Immunotherapy Induced *de novo* T Cell Responses Against Poorly Immunogenic Tumors
Wei Chen

1:35 – 2:40

Session II
Cancer Prevention Strategies in Oklahoma
Moderators: Min Li, Priyabrata Mukherjee

FGF-Mediated ER Activation in Obesity-Associated Breast Cancer: Upstream Influences and Downstream Consequences
Elizabeth Wellberg

Tribally Engaged Approaches to Lung Screening (TEALS) Study - Year 2 Pilot
Zsolt Nagykaldi

Barriers to Care Faced by Head and Neck Cancer Patients in Oklahoma
Christina Henson

Age-Dependent Endothelial Regulation of Ovarian Cancer Stem Cell Fate
Stefano Tarantini

2:45 – 3:50

Session III
Bench to Bedside
Moderators: Lurdes Queimado, Lacey McNally

FLT Pet Imaging as an Imaging Biomarker for Transplantation Events
Jennifer Holter-Chakrabarty

OU Health | Stephenson Cancer Center

2022 Annual Cancer Research Symposium

Mechanisms of Resistance to RET-Targeted Cancer Therapy
Jie Wu

Development of an MHealth App to Improve Pain Coping Skills for Patients with Advanced Cancer
Desiree Azizoddin

Drug and Target Discovery at the Oklahoma Center for Therapeutic Sciences
Matthew Hart

3:50 – 4:00 Awards & Closing Remarks

KEYNOTE SPEAKER

Elizabeth LaTorre Travis, Ph.D., FASTRO

Dr. Travis is the Associate Vice President for Faculty Diversity, Equity and Inclusion, and Mattie Allen Fair Professor in Cancer Research in the Department of Experimental Radiation Oncology and Pulmonary Medicine at The University of Texas MD Anderson Cancer Center., Dr Travis is a consummate advocate for women and minority faculty and committed to furthering their academic careers by ensuring that they are appointed to high profile committees and leadership positions and are nominated for awards, by leading institutional policy change to address obstacles that interfere with their success, and by providing career guidance to countless women and minority faculty. She publishes and speaks extensively on sponsorship as a path to leadership for women and minority faculty. Dr Travis's scientific research interest is in the complications of cancer treatments, primarily in the lung, which has made significant contributions to our understanding of the effects of radiation on normal tissues.

She is a fellow of the American Society of Radiation Oncology, recipient of the Association of American Medical Colleges' Group on Women in Medicine and Science Leadership Development Award for an individual (2009) and for an institution (2012), and recipient of the 2014 Marie Sklodowska-Curie Award by The American Association for Women Radiologists. In 2012 she was inducted into the Greater Houston Women's Chamber of Commerce Hall of Fame.

Dr. Travis served as a member of the Board of Directors of the Association of American Medical Colleges (AAMC) from 2018-2022 and is past Chair of the Steering Committee of the Group on Women in Medicine and Science of the AAMC. Dr Travis serves as a member of the Board of Directors of the Association for Women in Science from 2014-2021. Dr. Travis is a member of the Board of Directors of the Greater Houston Women's Chamber of Commerce and served as Chair

of the Board in 2017.She also serves on the Board of Directors of the Girl Scouts of San Jacinto Council.

Dr. Travis is a principal investigator on an NIH U54 grant with Puerto Rico, “Partnership for Excellence in Cancer Research,” and co-leader of the training program, the goal of which is to increase the number of Hispanic physicians and scientists in cancer research and medicine. She founded and leads the Partnership for Careers in Cancer Science and Medicine, a comprehensive program to diversify the cancer research and clinical trainee pipeline at all levels. In 2021 she was awarded the NIH prize for Enhancing Faculty Gender Diversity in Biomedical and Behavioral Science.

PROMOTING AND RETAINING WOMEN IN SENIOR FACULTY POSITIONS IN ACADEMIC RESEARCH: CHALLENGES AND OPPORTUNITIES.

Elizabeth LaTorre Travis, Ph. D. FASTRO

Despite decades of programs designed to advance women in academic medicine and science to senior ranks and leadership positions, the numbers remain dismally low. Less than 20% of cancer center directors and deans of medical schools are women, and 28% of professors are women, up from 19% a decade ago. So, the question remains “Why so Slow? This presentation will briefly dissect the problem and explore evidenced based solutions including what the elusive concept of inclusion looks like.

Mechanisms of Cancer Progression & Therapy

GENOMIC INSTABILITY GENES IN CANCERS

Chinthalapally V. Rao, Chao, Xu, Yuting Zhang, Adam S. Asch, Hiroshi Y. Yamada

Background Colorectal cancers (CRCs) is the third most commonly diagnosed cancer and the second most lethal cancer worldwide. CRCs carry high degrees of genomic instability (GI), which enables cancer evolution and makes prognosis poorer. Thus, GI is an exploitable target for therapy purposes. GI can be caused by gene mutation, alteration in gene expression, epigenetic modification, and other infectious or environmental factors. Several mutated genes involved in Chromosome instability and/or microsatellite instability have been identified. Yet it has not been technically feasible to modify functions of mutated genes (e.g., APC, TP53). From the drug development' standpoint, inhibition of over-expressed target gene is preferred. However, specific genes involved in GI via expression alterations in CRCs have not been comprehensively identified. The gap in knowledge hinders development of CRC therapies targeting GI in CRC.

In a previous study, we developed a data mining strategy (Gene Expression to Copy Number Alterations; "GE-CNA") and comprehensively identified 1,578 genes that associate with CNA in lung adenocarcinoma, among which 39 were survival-critical (i.e., expression levels correlate with significant differences in patients' survival).

Rationale Causal genes for GI via expressions have not been comprehensively identified in CRCs. Thus, the mechanistic understanding of GI generation in CRC remains incomplete. Few attempts have been made to understand the organ-specificity of genomic instability in cancer.

Main Results We applied the GE-CNA approach to 592 TCGA CRC datasets, and identified 500 genes whose expression levels associate with CNA. Among these, 27 were survival-critical, and 18 remained significant after adjustment with covariates. Comparison with previous results and new pathway analysis results from CRCs will be presented.

Implications The 18 survival-critical genomic instability genes are potential targets to suppress CRC genomic instability and therefore are targets for CRC drug development. Causal genes for genomic instability via expressions differ among organs. Hence, the "targeting genomic instability and/or aneuploidy" approach will need to be tailored for the specific target organ.

ROLE OF DNPH1 IN CANCER

Ralf Janknecht

DNPH1 is a 2'-deoxynucleoside 5'-monophosphate *N*-hydrolase, whose enzymatic activity might affect nucleotide metabolism and increase levels of 2-deoxyribose that may act as an angiogenic factor. However, the precise physiological functions of DNPH1 and its mechanisms of action have remained unresolved. Here, we provide *in vivo* evidence that DNPH1 is a promoter of tumor development: its ablation in mice impairs mammary tumor formation, angiogenesis and metastasis induced by the HER2 oncogene. Moreover, DNPH1 may sanitize nucleoside-based drugs and thereby contribute to chemotherapy resistance. Overall, our research is expected to highlight DNPH1 as a promising new drug target for breast and other cancers. Of note, because DNPH1 is an enzyme, small molecule drugs can be designed to inhibit its catalytic activity. Lastly, since our DNPH1 knockout mice are viable and present no obvious pathological phenotype, DNPH1 inhibitors are predicted to selectively affect cancer cells and thus display minimal side effects, a highly desirable scenario for any therapeutic drug.

CANCER-RELATED OUTCOMES AMONG CHILDREN WITH ACUTE LYMPHOBLASTIC LEUKEMIA

Amanda E. Janitz[1], Rylee Barber[1], Janis E. Campbell[1], Jessica Blanchard[2], Chao Xu[1], Hanumantha R. Pokala[1], René McNall-Knapp[1] 1.University of Oklahoma Health Sciences Center, Oklahoma City, OK 2. University of Oklahoma – Norman Campus, Norman, OK

Background: Childhood cancer is the leading cause of disease-related death among children aged 5-19 years in the US. While there have been great successes in the treatment of cancer, little information is available on disparities in access to treatment and survival among underrepresented populations.

Methods: We partnered with a children's hospital at an academic medical center to abstract data from electronic medical records and the institution's cancer registry on cancer diagnosis, treatment, and outcomes for children with acute lymphoblastic leukemia (ALL) (n=287) diagnosed from 2005-2019 prior to age 20. We evaluated the relation between 1) race/ethnicity and 2) distance to care (<25, 25-74, and ≥75 miles) from residence at diagnosis to the children's hospital and event-free survival. We evaluated the difference in survival times from diagnosis to date of first recurrence, death, or end of the study period by race using Kaplan-Meier analysis with the log-rank test. We used the Cox Proportional Hazards Model for multivariable survival analyses of race/ethnicity and distance to care.

Results: The median age of ALL diagnosis was 5 years, with 41% being female, the most common insurance types were Medicaid (56%) and private insurance (39%), and the majority of children had Pre-B ALL (85%). Non-Hispanic (NH) Black children had poorer event-free survival compared to NH White children (Adjusted HR: 2.12, 95% CI: 0.89, 5.05), though the estimate was imprecise. We observed no differences for AI, NH Asian, or Hispanic children and observed similar results when restricting to children with Pre-B ALL. We observed no association between distance to the children's hospital and cancer recurrence.

Conclusion: As a next step, we will link our dataset with the state cancer registry to allow for a more comprehensive, population-based evaluation of cancer disparities in Oklahoma and explore disparities in outcomes for other common childhood cancers.

LASER IMMUNOTHERAPY INDUCED *DE NOVO* T CELL RESPONSES AGAINST POORLY IMMUNOGENIC TUMORS

Wei R. Chen[1], Ashley R. Hoover[1,2], Saghar Kaabinejadian[3], and William H. Hildebrand[3]
[1] Biophotonics & ImmunoEngineering Laboratory, Stephenson School of Biomedical Engineering, Gallogly College of Engineering, University of Oklahoma, Norman, OK 73019, Oklahoma, 73034, USA
[2]Arthritis and Clinical Immunology Research Program, Oklahoma Medical Research Foundation, Oklahoma City, OK 73015, USA
[3]Department of Microbiology and Immunology, University of Oklahoma Health Sciences Center, Oklahoma City, OK 73015, USA

The tumor microenvironment (TME) remains a major challenge to current cancer treatments. We have developed an immune-ablative approach, laser immunotherapy (LIT), that combines localized photothermal therapy (PTT) and intratumoral administration of a potent immune stimulant, N-dihydrogalactochitosan (GC), to overcome the immunosuppressive, treatment resistant TME. We hypothesize three phases to this therapy. 1) PTT ablation disrupts tumor homeostasis and releases danger associated molecular patterns (DAMPs) resulting in the recruitment of immune cells into the TME. 2) The cellular necrosis caused by PTT also releases tumor associated antigens (TAAs) and tumor specific antigens (TSAs), capable of enhancing the existing antitumor T cell responses and generating *de novo* antitumor T cell responses. 3) Intratumoral injection of GC, which induces a potent type I IFN response, enhances the activation of antigen-presenting cells and the uptake/presentation of TAAs and TSAs, leading to a tumor-specific immune response. To understand the immune modulating mechanism of LIT, we examined the importance of establishing a strong type I IFN signature in B16-F10 melanoma tumors in mice and its effects on antitumor T cell activation/differentiation. We discovered that type I IFN was critical for the therapeutic effect of LIT, and that STING mediated type I IFN production was essential for enhancing T cell mediated antitumor immune memory after LIT treatment. Furthermore, we discovered that LIT generates *de novo* $CD8^+$ T cell responses that strongly correlate with animal survival and long-term tumor resistance. Our results suggest that LIT is a viable option to overcome the immunosuppressive TME to enhance responses to cancer therapies and mediate immune mediated tumor killing.

Keywords: Laser Immunotherapy, Tumor Specific Antigens, *de novo* T cell response, poorly immunogenic

Cancer Prevention Strategies in Oklahoma

FGF-MEDIATED ER ACTIVATION IN OBESITY-ASSOCIATED BREAST CANCER: UPSTREAM INFLUENCES AND DOWNSTREAM CONSEQUENCES

Marisol Castillo-Castrejon, Stevi Johnson Murguia, Abasi-ama Udeme, Nisha S. Thomas, Emma Turner, Barbara Sankofi Mensah, and Elizabeth A. Wellberg

Breast cancer is one of thirteen obesity-associated cancer types. Beyond body mass index (BMI), adult weight gain is independently linked to breast cancer risk and progression, particularly for the prevalent estrogen receptor (ER) positive subtype. Anti-estrogen therapies for ER-positive breast cancer are very effective, but these tumors can recur after a long latency (>10 years) and up to 40% of patients display *de novo* or acquired resistance. Rodents do not typically develop ER-positive tumors, which was a gap in our ability to study mechanisms of obesity-associated breast cancer. We developed a mouse model of diet-induced obesity that can grow human ER-positive tumors and paired this with a rat model of chemical carcinogen-induced ER-positive mammary tumors. In general, after anti-estrogen therapy, more tumors continued to grow in obese compared to lean rodents. Mammary adipose tissue developed adipocyte hypertrophy and produced FGF1, which activated cancer cell FGFR1. Tumor growth and FGF1 signaling occurred during the window of weight gain that followed anti-estrogen therapy, providing a possible mechanism that supported cancer progression. Consistent with this, preventing weight gain during estrogen deprivation inhibited tumor growth in rats and mice. In cultured breast cancer cells, FGF1 treatment increased phosphorylation of ER only in therapy-resistant cells. Downstream effects of FGF1-mediated ER activation included a shift towards a glycolytic phenotype, potentially mediated through ETV4 and altered ER transcriptional activity. Studies are ongoing to identify differences in ER transcriptional activity in the presence and absence of ETV4 and the role of metabolic reprogramming in obesity-associated breast cancer therapy resistance.

TRIBALLY ENGAGED APPROACHES TO LUNG SCREENING (TEALS) STUDY – YEAR 2 PILOT

Zsolt Nagykaldi, PhD; Mark Doescher, MD; Dorothy Rhoades, MD, MPH; Kathleen Dwyer, PhD, RN; Ann Chou, PhD, MPH; Brook McCann, RN

University of Oklahoma Health Sciences Center, Department of Family Medicine
University of Oklahoma Health Sciences Center, Department of Internal Medicine
University of Oklahoma Health Sciences Center, College of Nursing
University of Oklahoma Health Sciences Center, Department of Biostatistics and Epidemiology
Choctaw Nation Health Services Authority

Corresponding Author: Zsolt Nagykaldi, PhD (znagykal@ouhsc.edu)

Context: Lung cancer is the leading cause of cancer mortality among American Indians and Alaska Natives (AI/AN), and AI/AN have worse lung cancer incidence rates, survival, and death compared to the general population. Although lung cancer screening (LCS) with low-dose computed tomography is a grade-B USPSTF recommendation, uptake of LCS has been slow in most healthcare systems. LCS implementation among AI/AN has not been studied before in detail.
Objective: To address this knowledge and implementation gap, we initiated a multi-phase, 5-year “Tribally Engaged Approaches to Lung Screening" (TEALS) study in 2019 to co-design and test a tribal community-engaged LCS implementation program.
Setting: TEALS will be conducted in 8 primary care centers of the Choctaw Nation Health Services Authority (CNHSA) in Southeast Oklahoma using a Community-Engaged Research (CEnR) approach.
Study Design: In Year 2 of TEALS, we initiated a pre-post pilot implementation study in 2 CNHSA health centers to prepare for a subsequent RCT.
Population Studied: AI patients (N=100), who meet LCS criteria and clinicians/staff/leadership (N~20) from all CNHSA primary care centers.
Intervention: Two CNHSA practices received EHR reminders for LCS and access to smoking cessation services, in addition to care system improvements, including an LCS Care Coordinator, quality benchmarking and feedback, academic detailing, practice facilitation, and technical support.
Outcomes: Changes in LCS care pathways and care delivery (primary), patient morbidity profile and care experiences (secondary/patient-level), and practice LCS care system improvements (secondary/practice-level).
Results: By the end of Year 2, our team will have implemented and evaluated a pilot LCS program in 2 CNHSA health centers. Many lessons will have been learned regarding major barriers and some solutions arising from the implementation and from the COVID-19 pandemic.
Future Steps: Initiation of a CHNSA-wide RCT in Years 3 & 4.
Poster’s Learning Objectives:
First Objective: Translate emerging evidence into practice by designing and pilot testing a low-dose CT lung cancer screening (LCS) program in tribal communities.

Second Objective: Demonstrate planning and implementation of an LCS program in rurally located tribal communities and identify barriers and facilitators of implementing an LCS program.
Third Objective: Discuss how a community-wide LCS program can be implemented despite major challenges due to the COVID-19 pandemic.

BARRIERS TO CARE FACED BY HEAD AND NECK CANCER PATIENTS IN OKLAHOMA

Christina E. Henson

Head and neck squamous cell carcinoma (HNSCC) is the most common cancer involving the mucosal surfaces of the head and neck and is associated with a number of etiological factors, including cigarette smoking, alcohol consumption, and exposure to high-risk human papillomavirus. The risk of HNSCC increases with age, peaking in the seventh and eighth decade. Despite several advancements in the treatment of head and neck cancer (HNC) in recent decades, undertaking curative treatment still subjects patients to substantial toxicity, leaving this population at risk of psychosocial distress and unmet needs. Stephenson Cancer Center researchers are currently evaluating the use of virtual reality and mHealth to help meet these needs.

AGE-DEPENDENT ENDOTHELIAL REGULATION OF OVARIAN CANCER STEM CELL FATE

Stefano Tarantini

High grade serous ovarian cancer (HGSOC) is the most common and lethal form of ovarian cancer, due to lack of early detection methods and development of chemotherapy resistance. Ovarian cancer is mostly diagnosed in women ≥ 63 years of age. Ovarian cancer stem cells (OCSC) account not only for the primary tumor growth, the peritoneal spread and the relapse, but also for the development of chemoresistance, thus having profound implication for the treatment of this deadly disease. OCSC's fate is primarily dependent on the surrounding microenvironment, which is defined by blood vessels and that provide niches for stem cells. Previous work showed that age-related decrease in brain vascular functionality is driven by cellular senescence. In this pilot study we set out to investigate the age-related changes in ovarian vasculature and look at endothelial senescence burden as a critical contributing factor to the commitment and development of OCSC.

Bench to Bedside

FLT PET IMAGING AS AN IMAGING BIOMARKER FOR TRANSPLANTATION EVENTS

Jennifer Holter-Chakrabarty

Background: Noninvasive methods to diagnose and follow response in acute graft versus host disease (aGVHD) would be valuable. We performed this secondary analysis on our prospective pilot study (NCT01338987) to evaluate whether Fluorothymidine PET (FLT-PET) imaging could identify acute GVHD of liver and gastrointestinal tract (GI-GVHD) 28 days after first allogeneic myeloablative hematopoietic cell transplantation for hematologic malignancies (HCT, n=23).
Methods: Regions of interest (ROI) of were drawn in Liver (2cm3), Spleen (3cm3), and colon (1cm3), jejunum (1cm3), ileum (1cm3) on scans from evaluable patients (with FLT and without relapse by day 28, n=20). Standardized uptake values (SUV) were captured within the ROI and compared between those with and without GI-GVHD of the GI tract (ileum, jejunum, colon, liver) using Mann-Whitney U test.
Results: The median age of the HCT recipients was 33.5 years, included 11 females and 9 males, and 8/8 matched related marrow (n=6), 8/8 matched related PBSC (n=10), matched unrelated donor 8/8 marrow (n=3), and 7/8 matched related donor (n=1). 7/20 had developed GI-GVHD by 28 days after HCT. Of these, 7/7 were diagnosed with GI-GVHD, mean stage 1.7 (range 1-3) and 1/7 were liver (stage 1), with 2/7 and 1 additional individual with skin GVHD in the non-GI GVHD group (stage 1-3). The SUV of the jejunum were significantly different between those with (n=7) and without GI-GVHD (n=13): MAX SUV (p=0.01), Mean SUV (p=0.03) and Total SUV(p=0.05) Figure 1 A-C. Data on the liver, colon, and ileum were not significant between those with and without GI-GVHD.
Conclusions: This data suggests that FLT-PET may identify acute GI-GVHD at Day 28 and may yield information about location and inflammation. Further studies to identify FLT-PET to identify and follow acute GI-GVHD are warranted.

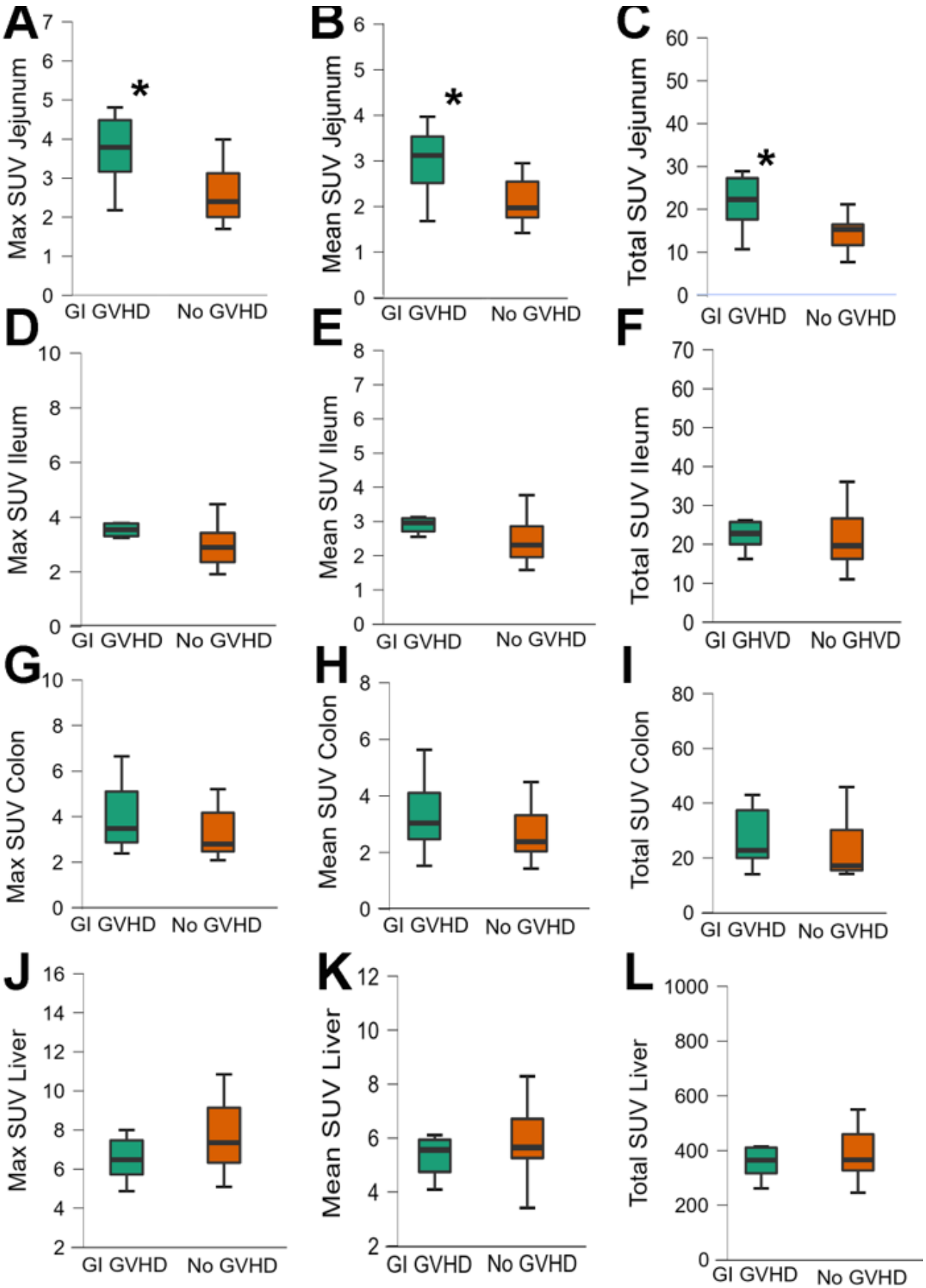
A
Max SUV Jejunum
*
GI GVHD
No GVHD
B
Mean SUV Jejunum
*
GI GVHD
No GVHD
C
Total SUV Jejunum
*
GI GVHD
No GVHD
D
Max SUV Ileum
GI GVHD
No GVHD
E
Mean SUV Ileum
GI GVHD
No GVHD
F
Total SUV Ileum
GI GHVD
No GHVD
G
Max SUV Colon
GI GVHD
No GVHD
H
Mean SUV Colon
GI GVHD
No GVHD
I
Total SUV Colon
GI GVHD
No GVHD
J
Max SUV Liver
GI GVHD
No GVHD
K
Mean SUV Liver
GI GVHD
No GVHD
L
Total SUV Liver
GI GVHD
No GVHD

MECHANISMS OF RESISTANCE TO RET-TARGETED CANCER THERAPY

Tao Shen[1,2], Xuan Liu[1,2], Xueqing Hu[1,2], Ujjwol Khatri[1,2], Simon S. Terzyan[1,3], Blaine H.M. Mooers[1,3], Vivek Subbiah[4], and Jie Wu[1,2*]

[1]Stephenson Cancer Center, [2]Department of Pathology, and [3]Department of Biochemistry and Molecular Biology, University of Oklahoma Health Sciences Center, Oklahoma City, OK; [4]Department of Investigational Cancer Therapeutics, The University of Texas MD Anderson Cancer Center, Houston, TX; *presenter

Cancers with oncogenic RET protein tyrosine kinase (PTK) are excellent responders to RET protein tyrosine kinase inhibitors (TKIs). However, like other PTK-targeted therapies, residual tumors persist in most patients, which eventually evolve to RET TKI resistance. A mechanism of acquired resistance is the secondary mutations in the targeted kinase that disrupt the TKI binding. Using a proactive approach, we screened random mutation pools for resistance to RET TKIs selpercatinib (LOXO-292) or pralsetinib (BLU-667). Eleven RET mutations in the kinase domain were identified from 98 LOXO-292- or BLU-667-resistant cell lines. Cross-profiling of these mutations revealed that the G810C/R/S mutations at the solvent-front site caused the strongest resistance to both of these TKIs. Consistently, G810 mutations were the predominant RET mutations found in the cfDNA of LOXO-292-resistant patients. Interestingly, the L730V/I mutations located at the roof position of the RET kinase domain were selectively resistant to BLU-667 in cell and tumor models. These findings point to the need of developing G810 mutants effective next-gen RET TKIs to overcome LOXO-292 and BLU-667 resistance and suggest LOXO-292 as an option for treating the BLU-667-resistant L730V/I tumors. Another possible mechanism of TKI resistance is activation of an alternative oncogene. In a collaborative study, a KHDRBS1-NTRK3 fusion gene was identified from a tumor biopsy of a NSCLC patient whose tumors developed LOXO-292 resistance after the initial response. Laboratory experiments confirmed that the NTRK3 fusion kinase caused LOXO-292 resistance. Significantly, our new evidence suggests the existence of a RET TKI-induced transition state of resistance during the evolution of cancer cells to the RET TKI-resistant cancer. Grant support: NIH R01CA17456, NIH P30CA225520, PHF Team and SEED grants, OCAST HR19-026, and TSET.

DEVELOPMENT OF AN MHEALTH APP TO IMPROVE PAIN COPING SKILLS FOR PATIENTS WITH ADVANCED CANCER

Authors: Desiree Azizoddin[1,2], Kris-Ann Anderson[1], Ashton Baltazar[1]

Email: Desiree-Azizoddin@ouhsc.edu

Health Promotion Research Center, Stephenson Cancer Center[1] & The Department of Psychosocial Oncology and Palliative Care, Dana-Farber Cancer[2]

Background: Pain affects 40-90% of patients with advanced cancer. Evidence suggests that supplementing pharmacologic therapy with behavioral skills may be helpful for pain outcomes. We sought to evaluate patients' perspectives of cognitive behavioral therapy for pain delivered through mobile health.

Methods: We recruited patients from Dana-Faber Cancer Institute: outpatient palliative care. Patients engaged in individual, qualitative interviews to review pain-focused cognitive behavioral therapy content modified for advanced cancer and mHealth delivery, provided feedback on the relevance of the content, and discussed their current approaches to cancer pain self-management. Patients who were ≥21 years old, had an incurable solid malignancy, chronic pain related to their cancer, and were using opioids for cancer were invited to participate. We excluded those who were currently hospitalized, had pain from a recent surgery, dementia/delirium, or history of opioid use disorder.

Results: 14 patients were interviewed; they were mostly female (57%), 54 years old on average, white (100%), with variable cancer types, and mostly taking short-acting opioids (93%). Six subthemes were identified through patients' descriptions of their approaches to managing cancer pain. Individuals endorsed using *physical coping* skills including using devices, engaging in physical activity, and at times struggling to recognize physical limits. Most endorsed utilizing *psychological coping* such as accepting their pain, reframing thoughts about pain, and using distraction or relaxation to cope. *Social support* was also identified as relevant to coping for almost all patients, and many described COVID-19 distancing guidelines as disruptive. Patients' endorsed a complex *relationship to opioids* for coping - half described being hesitant to use opioids due to shame and stigma, and many acknowledged that pain management requires "more than just taking your medications." Lastly, most patients emphasized the *relationship between sleep, stress, and pain* as central to their management. Regarding mobile health delivery of the content, most patients rated the content as highly usable, informative, aesthetically pleasing, relevant to their experiences, and they noted appreciating its convenience in access. In several instances, they requested revising technical content (e.g. "catastrophizing") to improve literacy, shortening length of text,

adding an option for daily opioid tracking, and increasing the presence of visuals throughout the app.

Conclusion: MHealth interventions seeking to alleviate cancer pain should consider addressing factors from patient perspectives of current cancer pain management and supplementing medications with behavioral skills. A future pilot study will evaluate the apps feasibility and acceptability.

Funded by: The National Palliative Care Research Center (Azizoddin)

DRUG AND TARGET DISCOVERY AT THE OKLAHOMA CENTER FOR THERAPEUTIC SCIENCES

Matthew J. Hart

The Center for Therapeutic Sciences (CTS) at University of Oklahoma is a trans-institutional hub for drug discovery and development. The CTS comprises the Laboratory for Drug and Target Discovery (DTD), the Med Chem Laboratory (MCL) and the Pharmacology Laboratory (PHL), that coordinately support a multi-entry pipeline of both target and drug discovery and drug development. The DTD is a state-of-the-art technological hub that provides lab space, cell culture facilities and a full suite of integrated detection, robotic and imaging equipment designed to enable HTS in 96, 384-or 1536 well microplate formats. The goal of the DTD is to enable the translation of basic discoveries into therapeutics by working along with investigators during each stage of the drug discovery process, including screen design, high throughput screening, candidate identification and lead validation. DTD has also added structure-guided drug identification and development to its portfolio of services available to investigators. Drug candidates are then optimized through medicinal chemistry at the MCL and ADME and PD/PK among other parameters are defined at the PHL to generate intellectual property as novel therapeutics. Dr. Matthew Hart, Director of the CTS and the DTD has over 25 years of experience in drug and target discovery using high throughput screening technologies. Dr. Hart will discuss activities at the CTS and how CTS can add to the translational directions available to OUHSC investigators.

Poster Presentations

Cancer Biology

CANCER BIOLOGY POSTERS

POSTER PRESENTATION LIST
(Listed A-Z by Presenter Last Name)

ELUCIDATING THE ROLE OF XRN2 IN GLIOBLASTOMA MULTIFORME METASTASIS
Tuyen T. Dang

CHARACTERIZATION OF A NOVEL BIPHENOTYPIC CELLULAR SUBTYPE RESEMBLING EARLY LYMPHOID PROGENITORS
Clay A. Foster

REGULATION OF HISTONE DEMETHYLASE JMJD2A BY SET7/9-MEDIATED METHYLATION
Ruicai Gu

THE ROLE OF NECROPTOSIS-MEDIATED INFLAMMATION IN NASH-INDUCED HEPATOCELLULAR CARCINOMA
Sabira Mohammed Jazir

QUANTITATIVE ANALYSIS OF SINGLE CELL NITRIC OXIDE DETECTION
Yunpeng Lan

INVESTIGATING THE ROLE OF KRCC1 IN THE DNA DAMAGE RESPONSE
Fiifi Neizer-Ashun

SINGLE CELL MASS SPECTROMETRY METABOLOMIC STUDIES OF PRIMARY AND METASTATIC CANCERS
Tra D. Nguyen

A NOVEL SCALE BIOPSY TECHNIQUE IDENTIFIES ZEBRAFISH EPITHELIAL LYMPHOCYTES AND ALLOWS BIOMARKER DISCOVERY TO PREDICT GLUCOCORTICOID RESPONSE IN ACUTE LYMPHOBLASTIC LEUKEMIA
Gilseung Park

WHEN A DICER1 MUTATION OF UNCERTAIN SIGNIFICANCE IS ACTUALLY SIGNIFICANT
Loretta Parker

OPPOSITE ROLES OF THE JMJD1A INTERACTION PARTNERS MDFI AND MDFIC IN COLORECTAL CANCER
Yuan Sui

POLARIZED MACROPHAGES ALTER DNA METHYLATION AND GENE EXPRESSION IN COLON EPITHELIAL CELLS THROUGH A MICROBIOTA-INDUCED BYSTANDER EFFECT
Ram Babu Undi

A NOVEL ACYL-COA SYNTHETASE PROMOTES PANCREATIC DUCTAL ADENOCARCINOMA PROGRESSION
Zhijun Zhou

ELUCIDATING THE ROLE OF XRN2 IN GLIOBLASTOMA MULTIFORME METASTASIS

Tuyen T. Dang, PhD. and Julio C. Morales, PhD.
University of Oklahoma Health Science Center, Neurosurgery Department, Stephenson Cancer Center
tuyen-dang@ouhsc.edu

Glioblastoma multiforme (GBM) is a highly aggressive brain cancer. The standard course of treatment is a combination of radiation and chemotherapy. Even with the dual treatment, the 5-year survival rate of patients with GBM is between 4-10%. Therefore, there is an urgent need to develop novel therapies to increase the survivorship. A possible cause of the low survival rate for GBM patients is the presence of therapeutic resistant motile neoplastic cells. These motile cells have been shown to be resilient against chemotherapy and radiation. Even though GBMs rarely metastasize outside of the brain, these cancer cells often undergo intracranial metastasis. They often continue to grow unchecked leading to lethal secondary tumor disease.

XRN2 is upregulated in GBMs as compared to normal brain tissues. XRN2 is a 5'-3' exonuclease that resolve DNA:RNA hybrids (R loops) that arise during transcription. R loops can affect gene expression by modulating the access of genes to transcription factors, miRNA transcription, and methylation status of genes. Our group have shown that loss of XRN2 sensitizes to a variety of DNA damaging agents but in particular ionizing radiation and Parp-1 treatment. Previously we have shown that XRN2 is required for DNA repair, specifically DNA double stranded break repair.

To understand how XRN2 modulates cell motility, we conducted RNA-Seq analyses of two GBM cell lines with and without XRN2 expression and found that XRN2 can regulate genes involved in cell movement, cell development and cellular organization programs. It has been shown that cancer cells have utilized these programs to metastasize. To determine if XRN2 is required for the initial steps of metastasis of cell motility and invasion, we conducted spontaneous cell motility and invasion through a matrix assays. Through live-cell imaging of two-dimensional movement and invasion through an extracellular matrix, we found that XRN2 was required for motility and invasion. In addition, using a GBM xenograft model, we found that XRN2 was required for tumor growth.

Lastly based on our RNA-Seq data, we have conducted a mini-cherry picked screen of the XRN2 targets and found at least 16 genes to be required for cell motility. Additionally, we also found a number of XRN2 targets required for DNA double stranded break repair. A number of these XRN2-regulated genes have inhibitors. The next phase of the project is to determine if the XRN2-target inhibitors can synergize with DNA damaging agents such as ionizing radiation to increase the death of neoplastic cells.

Our goal is to develop a patient signature that can better predict patient outcome and if possible a new synergetic treatment plan to increase the efficacy of radio-therapies.

Elucidating the role of XRN2 in Glioblastoma Multiforme Metastasis

Tuyen T. Dang, PhD., Julio C. Morales, PhD.
The University of Oklahoma Health Science Center
Stephenson Cancer Center
Department of Neurosurgery, Oklahoma City, OK, USA
tuyen-dang@ouhsc.edu, julio-morales@ouhsc.edu

Introduction: Glioblastoma multiforme (GBM) is a highly aggressive brain cancer. The standard course of treatment is a combination of radiation and chemotherapy. Even with the dual treatment, the 5-year survival rate of patients with GBM is between 4-10%. Therefore, there is an urgent need to develop novel therapies to increase the survivorship. A possible cause of the low survival rate for GBM patients is the presence of motile neoplastic cells with efficient DNA repair abilities. These motile cells have been shown to be resilient against chemotherapy and radiation. They often continue to grow unchecked leading to lethal secondary tumors.

XRN2 is upregulated in GBMs as compared to normal and other brain cancer types. XRN2 is a 5'-3' exonuclease that resolve DNA:RNA hybrids (R loops) that arise during transcription, especially at the 3' end of genes. R-loop biology can affect gene expression by modulating the access of genes to transcription factors, miRNA transcription, and methylation status of genes. Our previous data have shown that loss of XRN2 sensitizes to a variety of DNA damaging agents but in particular ionizing radiation (IR).

Additionally, we found that XRN2 is required cell motility and invasion through a matrix. Cell motility and invasion through a matrix are the initial steps in the metastatic cascade. Upon orthotopic injection of GBM cells with and without XRN2, we found that XRN2 is required for tumor establishment. These data suggest that XRN2 plays a vital role in GBM.

To understand how XRN2 modulates metastasis, we conducted RNA-Seq analyses of two GBM cell lines with and without XRN2 expression and found that XRN2 can regulate genes involved in DNA repair pathway and cell motility. We have conducted a mini-cherry picked screen of the XRN2 targets and found at least 16 genes to be required for cell motility. A number of these XRN2-regulated genes have inhibitors. The next phase of the project is to determine if the XRN2-target inhibitors can synergize with DNA damaging agents such as ionizing radiation to increase the death of neoplastic cells.

Hypothesis: Based on these observations, we hypothesized that XRN2 contributes to glioma disease progression by acting as a therapy protectant and driver of neoplastic cell motility and/or invasion.

Impact: Findings from these studies would impact on radio/chemo- treatment of cancer patients by identifying who would best benefit from conventional therapy(s). Additionally, this project may find new drug targets to work in concert with standard of care therapeutics to increase therapy efficacy.

XRN2 expression correlates with disease and poor patient outcome

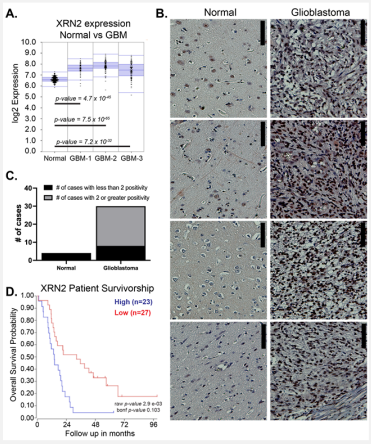

A. Log2 XRN2 mRNA expression levels in normal (Berchtold, 172 samples), GBM-1 (Pfister, 46 samples), GBM-2 (Loeffler, 70 samples), and GBM-3 (Hegi, 84 samples) databases. Graph generated from R2: Genomics Analysis and Visualization Platform. **B.** IHC of XRN2 (brown) in patient tumor tissues. Counterstained with hematoxylin (nuclei, blue). Scale bar is 200 micron. Samples from US Biomax TMA. **C.** Quantification of XRN2 expression from US Biomax TMA. Samples with 2+% pixels positive for XRN2 were considered positive for XRN2 expression. **D.** Kaplan-Meier graph of XRN2 expression shows a poorer outcome in XRN2 high (blue) compared to XRN2 low (red) patients. Graph from R2: Genomics Analysis .

XRN2 is required for GBM cell motility

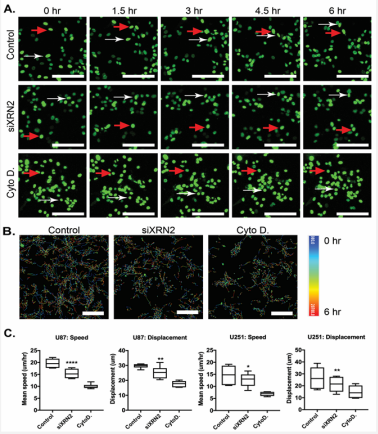

A. Subconfluent imaging of U87 H2B-GFP transfected for 72 hrs or treated with 0.2 uM of cytochlasin D (non-motile control). Images were taken with LSM710 confocal microscope with an environmental chamber. Images were taken every 30 minutes. Tracking duration 6 hours. Arrows are representative tracking over time. Scale bars are 100 um. **B.** Tracks of cell movement over time. Scale bars are 100 micron. **C.** Quantification of live cell imaging of U87 and U251 GBM cells using TrackMate. *= p-value 0.05, **= p-value 0.01

XRN2 is required for GBM invasion through a matrix

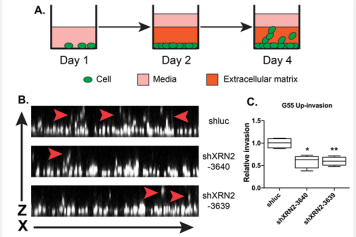

A. Schematic of vertical invasion assay. Briefly cells are plated on day 1. Day 2, matrix is added on top of confluent cultures. Day 4, cultures are fixed and imaged on an LSM710. Z-stacks span 140 um with images taken at every 5 um. **B.** Representative images of vertical invasion using G55 shluc (control) and G55 expressing two different shRNAs targeting XRN2 expression. Arrows point to invading cells. Invading cells are cells that transverse 50+ um from monolayer. **C.** Quantification of vertical invasion. *= p-value 0.05, **= p-value 0.01

XRN2 is required for GBM tumor establishment

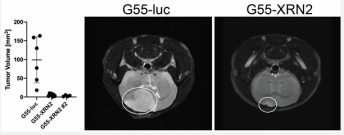

Tumor volume and representative MRI images of mouse brain xenografts using G55 GBM patient cell line. Cells expressed a shRNA targeting either luciferase (luc) or XRN2 and were orthotopically injected into the brain. Shluc is our control.

XRN2 regulates genes involved in cell motility and invasion

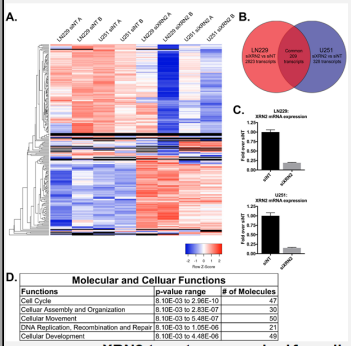

MiSeq on GBM cell lines transfected with corresponding siRNAs. **A.** Expression heatmap of the 209 transcripts in B. **B.** Venn-diagram of transcription landscape in LN229 and U251 from A. **C.** qPCR of XRN2 mRNA expression in samples transfected with the corresponding siRNAs. **D.** Cellular programs for which XRN2 targets are involved in.

XRN2-targets are required for cell motility

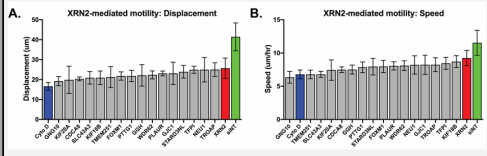

Quantification of live-cell imaging of U251 cells transfected with siRNAs targeting listed genes. Subconfluent tracking of 72 hrs siRNA transfection or treated with 0.2 uM of cytochlasin D (non-motile control). Images were taken with LSM710 confocal microscope with an environmental chamber. Images were taken every 30 minutes. Tracking duration 6 hours. **A.** Displacement quantification **B.** Speed quantification. TrackMate (Fiji) was used to track and measure the movement of the cells.

Loss of XRN2 increases E-cadherin expression independent of Slug

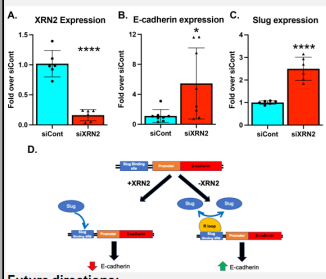

RT-qPCR of LN229 transfected with siCont or siXRN2. **A.** XRN2 expression. **B.** E-cadherin expression. **C.** Slug expression. *= p-value 0.05, ****= p-value 0.0001. **D.** Proposed hypothesis of R-loop mediated E-cadherin expression. In the presence of XRN2, there is no R loop present in the Slug binding site allowing Slug to repress E-cadherin expression. In XRN2 deficient conditions, R loops are formed at the Slug binding site, blocking Slug from repressing E-cadherin expression.

Future directions:

1. Determine if XRN2-targets are required for GBM motility/invasion.
2. Determine if XRN2-targets are required for GBM tumor establishment.
3. Determine the mechanism of XRN2- mediated epithelial-to-mesenchymal transition.

Acknowledgments:
I would like to thank the OMRF imaging core facility for the usage of their LSM710 microscope and OUHSC Laboratory for Molecular Biology and Cytometer Research for their assistance with the MiSeq. I would like to express my appreciation to Dr. Rheal Towner's group for their collaboration on the mouse xenograft experiments. Funding source: P20GM103639 (to JCM).

CHARACTERIZATION OF A NOVEL BIPHENOTYPIC CELLULAR SUBTYPE RESEMBLING EARLY LYMPHOID PROGENITORS

Clay A. Foster[1], José J. Macias[1], Katie M. Foster[1], Megan Malone-Perez[1], Arpan A. Sinha[1], J. Kimble Frazer[1]

[1]Jimmy Everest Section of Pediatric Hematology/Oncology, Department of Pediatrics, University of Oklahoma Health Sciences Center, Oklahoma City, OK, USA
Email: Clay-Foster@ouhsc.edu
Acknowledgment of funding: This work is supported by awards from the Oklahoma Center for the Advancement of Science and Technology (OCAST) and the Oklahoma Center for Adult Stem Cell Research (OCASCR).

Acute lymphoblastic leukemia (ALL) is the most common and 2nd most lethal form of pediatric cancer. Prognoses in adults are even worse, and nearly 80% of relapsed ALL patients will die. Driving ALL relapse is a rare cellular subtype known as a leukemia stem cell (LSC). Our understanding of LSC (and normal lymphoid progenitor) biology is woefully incomplete. To assess relapse risk and target tumor-initiating LSCs during therapy, better techniques are needed to enrich for and characterize these early lymphoid progenitors (ELPs).

We previously demonstrated a transgenic ALL zebrafish model that develops both B- and T-ALL in the same background. Most cells exhibited either B or T cell signatures, but we discovered a rare subpopulation that simultaneously co-expressed genes of both lineages (dubbed 'biphenotypic' or BiP cells). *We hypothesize that (1) in healthy fish, BiP cells include ELPs not yet committed to the B or T lineage, and (2) in ALL, BiP cells LSCs*. To test this, we generated a novel dual-transgenic line incorporating both B- (*cd79:GFP*; green) and T-specific (*lck:mCherry*; red) markers. LSCs (and other stem-like cells, including ELPs) typically express high levels of multi-functional efflux transporters, leading to chemoresistance and post-treatment relapse. We also developed an optimized flow cytometric side population (SP) assay to exploit this phenomenon as an adjunct method for detecting BiP cells.

We found that the labeled subtypes (*cd79+* and *lck+*) effectively represent B- and T-lineage cells, respectively. Flow cytometric analyses revealed multiple BiP subpopulations in both healthy and malignant tissues, likely representing distinct subtypes or developmental stages. The SP assay and dual-transgenic lines will reveal if BiP cells are indeed enriched for in the SP+ phenotype. Purification and further analysis of BiP cells by RNA-seq will reveal the exact nature of the various subpopulations. Functional transplantation assays will also be used to test the capacity of the BiP cells to

rescue lymphopoiesis in deficient individuals (healthy BiP cells) or to engraft into sub-lethally irradiated hosts (malignant BiP cells). Future studies will focus on identifying specific and novel LSC biomarkers for use in evaluating ALL treatment efficacy/patient relapse risk and to further our understanding of general lymphoid development.

Clay Foster[1], Jesús Macias[1], Katie Foster[1], Megan Malone-Perez[1], Ameera Hasan[1], Jessica Garcia-Burroughs[1], Arpan Sinha[1], J. Kimble Frazer[1]
[1]Section of Pediatric Hematology/Oncology, Department of Pediatrics, University of Oklahoma Health Sciences Center, Oklahoma City, OK, USA

CANCER RESEARCH SYMPOSIUM

UNIVERSITY OF OKLAHOMA - ANNUAL CANCER RESEARCH SYMPOSIUM 2022

CHARACTERIZATION OF A NOVEL BIPHENOTYPIC CELLULAR SUBTYPE RESEMBLING EARLY LYMPHOID PROGENITORS

CONTACT
PRESENTED BY: Clay A. Foster, Ph.D.
EMAIL: clay-foster@ouhsc.edu
FOR: ACRS 2022
DATE :03/04/2022

01 BACKGROUND

Acute lymphoblastic leukemia (ALL) is the most common form of pediatric cancer. 1 in 5 children with ALL will relapse, and ~80% of relapsed patients die. Driving relapse is a rare cellular subtype known as **leukemia stem cells (LSCs)**. Our understanding of LSCs and closely related **early lymphoid progenitor cells (ELPs)** is incomplete. We recently described a MYC-transgenic ALL model that develops B- and/or T-ALL.[1,2] Most cells exhibit either B or T signatures, but some rare cells co-express genes of both lineages (dubbed '**biphenotypic**' or **BiP cells**).

HYPOTHESIS: BiP cells represent a form of early lymphoid progenitors not yet committed to the B or T lineage, resembling LSCs in ALL (BiP-ALL).

The rarity of BiP/LSCs/ELPs makes study challenging. We built dual-transgenic models featuring B/T cell-specific reporters to further characterize the relationship between these rare cellular subtypes.

02 RESULTS

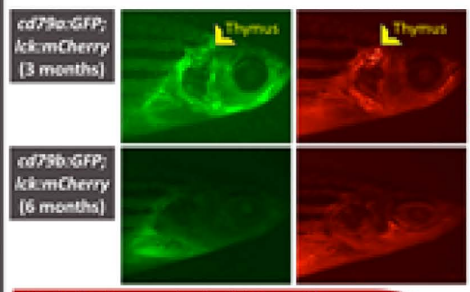

Fig. 1. Dual-transgenic zebrafish lines with fluorescently labeled B/T cells.

Top (2): Dual-transgenic zebrafish (3m) with markers *cd79a:GFP* and *lck:mCherry* allow us to **visualize B (green) and T (red) cells. Bottom (2):** Dual-transgenic zebrafish (6m) featuring markers *cd79b:GFP* and *lck:mCherry*. Thymus is no longer visible due to involution.

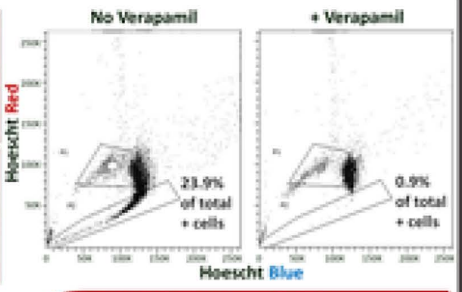

Fig. 2. Optimized side population (SP) assay allows for isolation of stem cell-like subtype in ALL (LSCs).[4]

Populations enriched for LSCs visualized using SP assay. **Left:** Hoescht dye is extruded by a stem cell-like SP from zebrafish ALL. **Right:** Ability to extrude Hoescht dye is ablated by ABC-transport inhibitor verapamil (VP). **We predict a BiP+SP subgroup will be enriched for LSCs.**

03 RESULTS

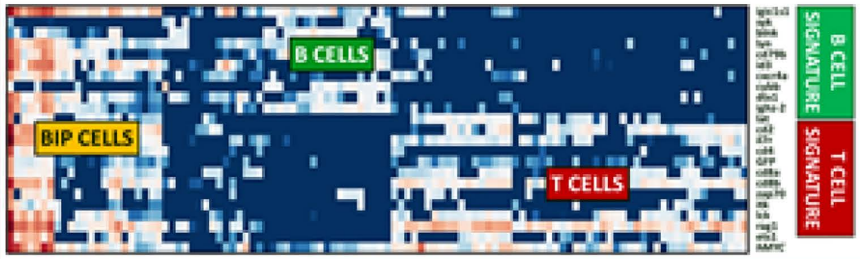

Fig. 4. Single-cell qPCR shows BiP-ALL population resembles both B and T cells.

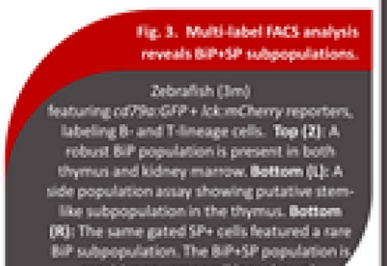

Fig. 3. Multi-label FACS analysis reveals BiP+SP subpopulations.

Zebrafish (3m) featuring *cd79a:GFP* + *lck:mCherry* reporters, labeling B- and T-lineage cells. **Top (2):** A robust BiP population is present in both thymus and kidney marrow. **Bottom (L):** A side population assay showing putative stem-like subpopulation in the thymus. **Bottom (R):** The same gated SP+ cells featured a rare BiP subpopulation. The BiP+SP population is sensitive to verapamil (not shown).

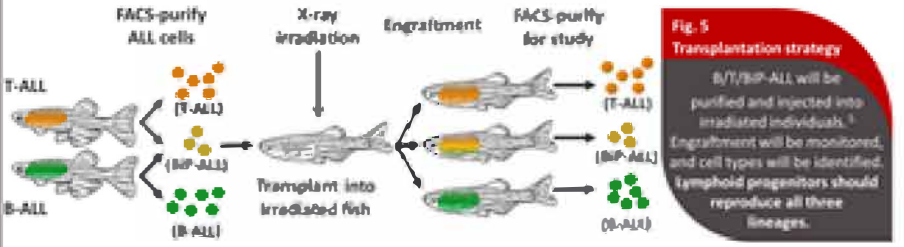

Fig. 5 Transplantation strategy

B/T/BiP-ALL will be purified and injected into irradiated individuals.[3] Engraftment will be monitored, and cell types will be identified. **Lymphoid progenitors should reproduce all three lineages.**

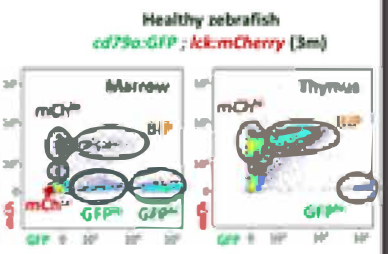

Fig. 6 Representative engraftment time course.

ALL cells can be allo-transplanted, indicating LSCs are present. ALL cells were injected into irradiated subject. Engraftment was monitored over 4 weeks.

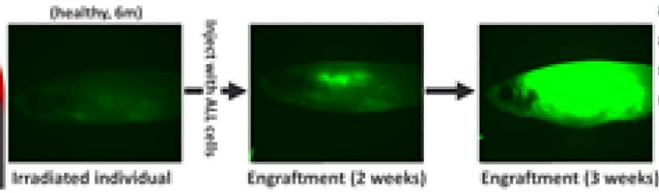

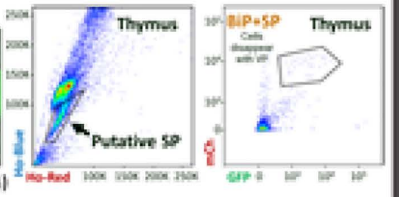

04 DISCUSSION

We identified a novel population of cells that **exhibit B- and T-lineage gene signatures simultaneously** in healthy (**BiP**) and ALL (**BiP-ALL**) samples. We hypothesized that a subpopulation of BiP cells represents an uncommitted form of **early lymphoid progenitor (ELP)**, and the same group in BiP-ALL represents a subset of **leukemia stem cells (LSCs)**. To facilitate purification of the rare BiP cell type for further study, we built multiple dual-transgenic fish lines, incorporating separate B and T cell-specific fluorescent reporters (green and red, respectively). We predicted that BiP cells would exhibit a distinct green + red profile in these lines. We also speculated that the BiP population itself may be enriched for stem cell-like subtypes (either normal ELPs or malignant LSCs in BiP-ALL).

The new transgenic lines allow us to determine if BiP cells in fact resemble LSCs/ELPs. FACS-based purification of the corresponding populations is now possible, allowing for further characterization through sequencing. Using allo-transplantation experiments, we can test the functional properties of the BiP/BiP-ALL/SP cells. By transplanting healthy BiP cells into mutant fish (lacking B/T cells), we will assess the differentiative capacity of the BiP subpopulations. A similar experiment will demonstrate whether malignant BiP-ALL are capable of engrafting ALL more efficiently than bulk tumor cells, suggesting that they feature true LSC. Finally, our newly optimized SP assay will demonstrate if BiP cells are enriched for in stem cell-like side populations and also provide a means of further purification for single-cell sequencing experiments (i.e. by isolating a smaller BiP+SP subset).

The ultimate goals of these efforts are two-fold: first, we seek to increase our understanding of and/or our ability to monitor/target leukemia stem cells; second, we seek insight into normal lymphopoiesis and the role of a population of cells that we believe have not yet committed to a B-/T-lineage.

References

1. Borga, C. et al. Molecularly distinct models of zebrafish Myc-induced B cell leukemia. Leukemia **33**, 559-562 (2019).
2. Borga, C. et al. Simultaneous B and T cell acute lymphoblastic leukemias in zebrafish driven by transgenic MYC: implications for oncogenesis and lymphopoiesis. Leukemia **33**, 133-147 (2019).
3. Park, G. et al. Zebrafish B cell acute lymphoblastic leukemia: new findings in an old model. Oncotarget **11**, 1292-1305 (2020).
4. Boehm, J.T. et al. The side population enriches for leukemia propagating cell activity and Wnt pathway expression in zebrafish acute lymphoblastic leukemia. Haematologica **104**, 1388-1395 (2019).
5. Rudner, L.A. et al. Shared acquired genomic changes in zebrafish and human T-ALL. Oncogene **30**, 4289-96 (2011).

REGULATION OF HISTONE DEMETHYLASE JMJD2A BY SET7/9-MEDIATED METHYLATION

Ruicai Gu[1], Ralf Janknecht[1,2,3]
Presenting Author's Email Address：Ruicai-Gu@ouhsc.edu
[1]Department of Cell Biology, University of Oklahoma Health Sciences Center, Oklahoma City;
[2]Stephenson Cancer Center, Oklahoma City; [3]Department of Pathology, University of Oklahoma Health Sciences Center, Oklahoma City

Abstract: Jumonji C domain-containing 2A (JMJD2A) is a histone H3 demethylase and its overexpression aids prostate tumorigenesis. However, how JMJD2A is regulated in its activity is unknown. We found that JMJD2A is directly methylated by SET7/9 in LNCaP prostate cancer cells. SET7/9 methylates JMJD2A on up to six lysine residues (K505, K506, K507, K563, K564, K594). In LNCaP cells, JMJD2A cooperated with its interaction partner, the ETS transcription factor ETV1, in enhancing the activity of the MMP1 promoter. However, mutation of K505/506/507 (3xR mutant) or of all six methylation sites (6xR mutant) decreased the transcriptional synergy between JMJD2A and ETV1 at the MMP1 promoter. Further, mutation of JMJD2A methylation sites reduced the physical interaction of JMJD2A and ETV1. The JMJD2A 6xR or 3xR mutants also caused reduced invasion in LNCaP cells and diminished proliferation and invasion in DU145 prostate cancer cells. Meanwhile, normal RWPE-1 prostate cells were not affected upon mutation of JMJD2A methylation sites, suggesting that JMJD2A methylation is specifically modulating cancer cells. Altogether, our data indicate that JMJD2A methylation by SET7/9 affects JMJD2A function in prostate cancer cells and thereby promotes tumorigenesis. This implies that blocking JMJD2A methylation may have therapeutic value.

Acknowledgement of funding: This work was in part funded by grant R03 CA223615 from the National Institutes of Health/National Cancer Institute.

Regulation of Histone Demethylase JMJD2A by SET7/9-Mediated Methylation

Ruicai Gu[1](Ruicai-Gu@ouhsc.edu), Tae-Dong Kim[1], Hoogeun Song[1], Sangphil Oh[1,2], Sook Shin[1,2] and Ralf Janknecht[1,2,3]

[1]Department of Cell Biology, OUHSC, Oklahoma City; [2]Stephenson Cancer Center, Oklahoma City; [3]Department of Pathology, OUHSC, Oklahoma City

ABSTRACT Jumonji C domain-containing 2A (JMJD2A) is a histone H3 demethylase and its overexpression aids prostate tumorigenesis. However, how JMJD2A is regulated in its activity is unknown. We found that JMJD2A is directly methylated by SET7/9 in vitro and in vivo on up to six lysine residues. In LNCaP prostate cancer cells, JMJD2A cooperated with its interaction partner, the ETS transcription factor ETV1, in enhancing the activity of the MMP1 promoter, which was decreased upon mutation of JMJD2A lysines K505/506/507 (3xR mutant) or of all six methylation sites (6xR mutant). Further, mutation of JMJD2A methylation sites impaired the physical interaction of JMJD2A with ETV1. The JMJD2A methylation site mutants also caused reduced invasion (LNCaP) and diminished proliferation, invasion and metastasis in DU145 prostate cancer cells. Altogether, our data indicate that methylation by SET7/9 affects JMJD2A function in prostate cancer cells and thereby promotes tumorigenesis.

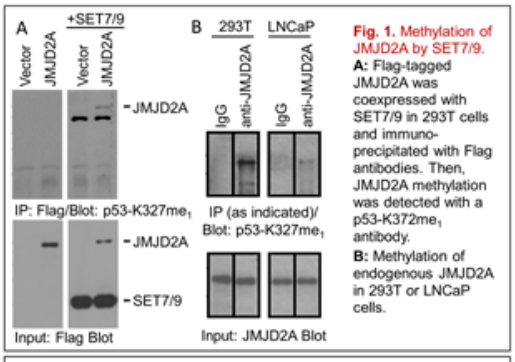

Fig. 1. Methylation of JMJD2A by SET7/9. **A:** Flag-tagged JMJD2A was coexpressed with SET7/9 in 293T cells and immuno-precipitated with Flag antibodies. Then, JMJD2A methylation was detected with a p53-K372me$_1$ antibody. **B:** Methylation of endogenous JMJD2A in 293T or LNCaP cells.

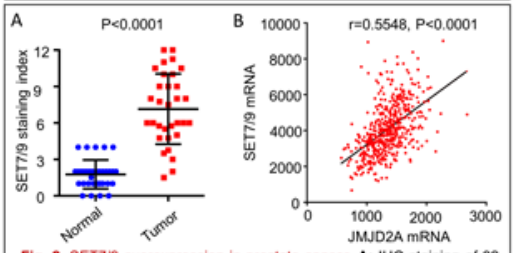

Fig. 2. SET7/9 overexpression in prostate cancer. **A:** IHC staining of 32 matching normal and tumor prostate specimens. **B:** Correlation of SET7/9 and JMJD2A mRNA levels in 493 prostate adenocarcinomas.

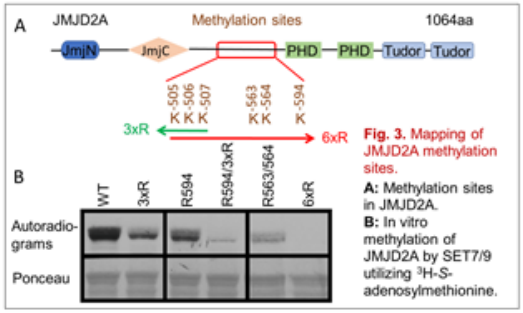

Fig. 3. Mapping of JMJD2A methylation sites. **A:** Methylation sites in JMJD2A. **B:** In vitro methylation of JMJD2A by SET7/9 utilizing ^{3}H-*S*-adenosylmethionine.

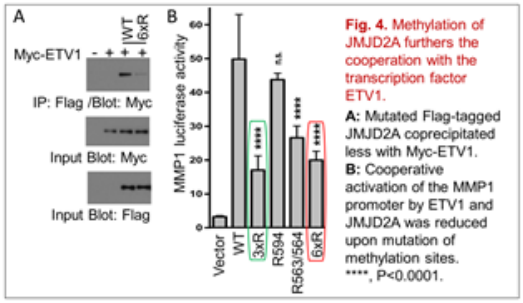

Fig. 4. Methylation of JMJD2A furthers the cooperation with the transcription factor ETV1. **A:** Mutated Flag-tagged JMJD2A coprecipitated less with Myc-ETV1. **B:** Cooperative activation of the MMP1 promoter by ETV1 and JMJD2A was reduced upon mutation of methylation sites. ****, P<0.0001.

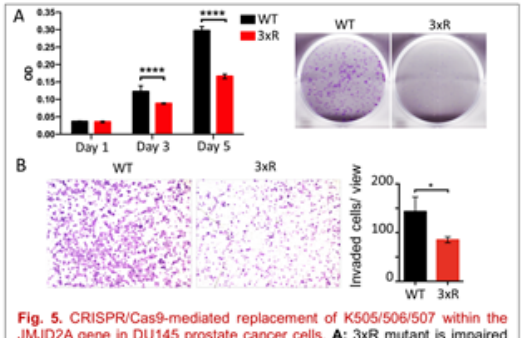

Fig. 5. CRISPR/Cas9-mediated replacement of K505/506/507 within the JMJD2A gene in DU145 prostate cancer cells. **A:** 3xR mutant is impaired in cell growth (MTT and clonogenic assays). ****, P<0.0001. **B,** 3xR mutant invades less. Representative trans-well assays. * , P<0.05.

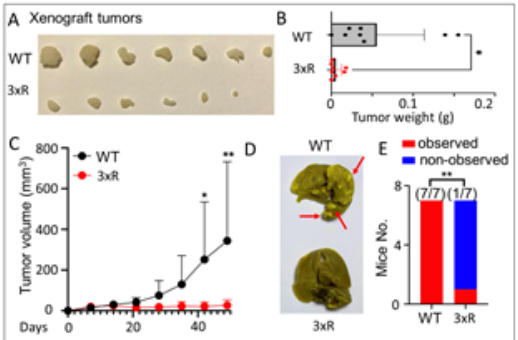

Fig. 6. Mutation of JMJD2A reduces DU145 prostate cancer tumor growth and metastatic potential. **A-C:** DU145 cells stably expressing JMJD2A WT or 3xR mutant were *s.c.* injected into nude mice (n=8). Photographs of harvested tumors (**A**), tumor weights (**B**), and tumor growth curves (**C**). **D:** DU145 cells (JMJD2A WT or 3xR mutant) were injected into nude mice through the tail vein (n=7). Representative images of lungs with metastases (red arrows). **E:** Quantification of mice with and without metastases. * , P<0.05, **, P<0.01.

Fig. 7. Model how JMJD2A methylation by SET7/9 stimulates prostate cancer.

CONCLUSIONS

- JMJD2A is directly methylated by SET7/9, which itself is overexpressed in prostate tumors similar to JMJD2A.
- SET7/9 methylates JMJD2A on up to six lysine residues (K505, K506, K507, K563, K564, K594).
- Mutation of three (3xR) or six (6xR) methylation sites decreased interaction and transcriptional synergy between JMJD2A and ETV1.
- Blocking JMJD2A methylation can cause reduced cell proliferation, invasion, tumor growth and metastasis.
- Suppression of SET7/9-mediated JMJD2A methylation may have therapeutic benefit in prostate and other cancers.

Acknowledgements: This work was in part funded by grant R03 CA223615 from the NIH/NCI and the Stephenson Cancer Center.

THE ROLE OF NECROPTOSIS-MEDIATED INFLAMMATION IN NASH-INDUCED HEPATOCELLULAR CARCINOMA

Sabira Mohammed Jazir[1], Evan Nicklas[2], Constantin Georgescu[4], Jonathan Wren[4], Wenyi Luo[3] , Arlan Richardson[1,2,5] and Deepa Sathyaseelan[1, 2]
[1]Stephenson Cancer Center, [2]Department of Biochemistry & Molecular Biology, [3]Department of Pathology, The University of Oklahoma Health Sciences Center, [4] Genes and Human Disease Research Program, Oklahoma Medical Research Foundation, and [5]Oklahoma City VA medical Center.
Sabira-Jazir@ouhsc.edu

Non-alcoholic hepatosteatosis (NASH) due to metabolic syndrome or diabetes mellitus has been identified as the fastest growing cause of hepatocellular carcinoma (HCC), the fourth leading cause of cancer related deaths in the world. Therapeutic options for HCC are limited, and survival after diagnosis is poor (>10%). Thus, a better understanding of the mechanisms that drive the progression of NASH to HCC is critical in developing new strategies to prevent/treat HCC. Chronic inflammation is a key player in the pathogenesis of HCC, however, pathways that drive chronic hepatic inflammation in NASH-driven HCC is not known. Necroptosis is a regulated mode of cell death that causes inflammation and is activated in the livers of patients with NASH. Therefore, we tested whether necroptosis-mediated inflammation plays a role in the progression of NASH to HCC in a mouse model of NASH-induced HCC. Three groups of male and female mice were used for the study: wild type (WT), mouse models where necroptosis is blocked, *Ripk3*$^{-/-}$ or *Mlkl*$^{-/-}$ mice. Mice were fed a choline deficient high fat diet (CD-HFD, 60% fat) starting at 2 months for 6 months (NASH-induced HCC model) . Mice fed normal chow or CD-low fat diet (CD-LFD, 10% fat) were used as controls.

After 6-months of CD-HFD feeding, 100% of WT mice developed liver tumors and tumor incidence was 2-3 folds higher in male mice relative to female mice, which agrees with the clinical scenario where men are more susceptible to liver cancer. Blocking necroptosis using *Ripk3*$^{-/-}$ and *Mlkl*$^{-/-}$ mice showed a significant reduction in tumor incidence in male and female mice. Analysis of innate immune cells (in particular, macrophages) that are activated by necroptosis showed a significant increase in total macrophages (F4/80+ cells) and inflammatory monocytic (Ly6C^{hi} CCR2^{+} cells) populations in the livers of WT mice fed CD-HFD, which was significantly reduced in the livers of *Ripk3*$^{-/-}$ *and Mlkl*$^{-/-}$ mice fed CD-HFD. Consistent with this, levels of proinflammatory cytokine IL-6, chemokine CCL2 and activation of oncogenic transcription factor STAT3, which is triggered by IL6, were increased in the livers of WT mice and blocking necroptosis reduced their expression. RNA sequencing analysis showed that several cancer related genes are altered in WT mice fed CD-HFD and blocking necroptosis reversed their expression. Thus, our findings show for the first time

that blocking necroptosis could reduce inflammation and tumor incidence in a mouse model of NASH-induced HCC, suggesting that necroptosis-mediated inflammation plays an important role in the progression of NASH to HCC.

Funding: NIH/NIA R01 grant, Geroncology pilot grant.

THE ROLE OF NECROPTOSIS-MEDIATED INFLAMMATION IN NASH-INDUCED HEPATOCELLULAR CARCINOMA

Sabira Mohammed Jazir[1], Evan Nicklas[2], Albert Tran[2], Wenyi Luo[3], Constantin Georgescu[4], Jonathan Wren[4], Arlan Richardson[1,2,5] and Deepa Sathyaseelan[1,2]

[1]Stephenson Cancer Center, [2]Department of Biochemistry & Molecular Biology, [3]Department of Pathology, The University of Oklahoma Health Sciences Center, [4] Genes and Human Disease Research Program, Oklahoma Medical Research Foundation, and [5]Oklahoma City VA medical Center.

First report that shows blocking necroptosis reduces inflammation and tumor incidence in a mouse model of NASH-induced HCC

Background of the study

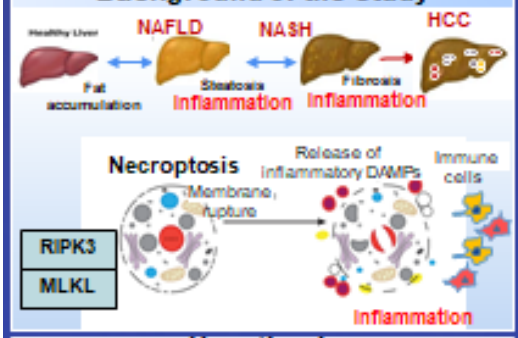

Hypothesis

Inflammation arising from hepatic necroptosis plays a major role in the progression of NASH (Non alcoholic steatohepatitis) to HCC and preventing necroptosis will reduce inflammation and the progression of NASH to HCC.

Results

1. Blocking necroptosis reduces inflammation in response to CD-HFD feeding

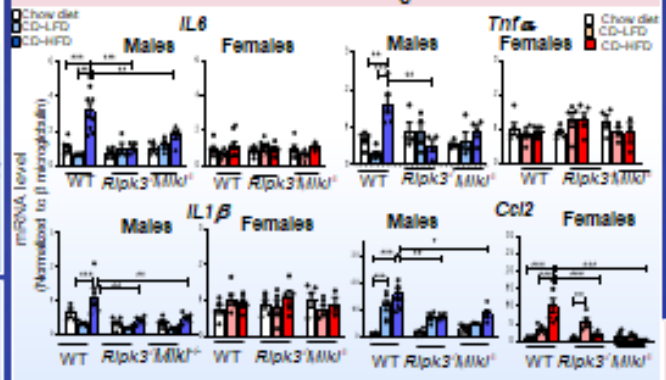

Fig.1:Transcript levels of inflammatory makes in WT, *Rlpk3*$^{-/-}$ and *Mlkl*$^{-/-}$ lives fed with normal chow , CD-LFD or CD-HFD for 6 months. ***p<0.0005, **p<0.005, *p<0.05

3. Tumor incidence is reduced in *Rlpk3*$^{-/-}$ and *Mlkl*$^{-/-}$ mice in response to CD-HFD feeding

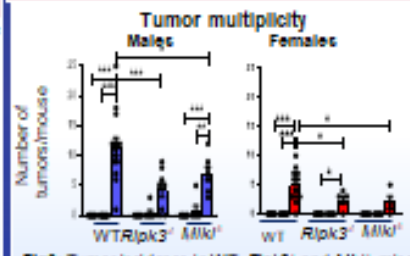

Fig3: Tumor incidence in WT, *Rlpk3*$^{-/-}$ and *Mlkl*$^{-/-}$ mice fed with normal chow , CD-LFD or CD-HFD for 6 months.. ***p<0.0005, **p<0.005, *p<0.05

4. Absence of necroptosis markers reverses expression of genes involved in inflammation and HCC development in response to CD-HFD feeding

Experimental Design

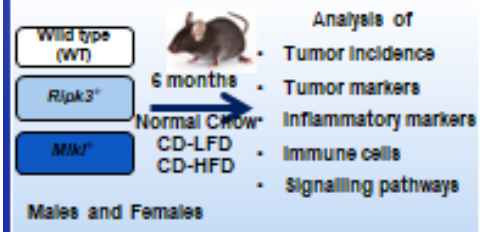

CD-LFD/HFD: Choline deficient amino acid defined – Low (10%)/High Fat diet (60%))

2. Flow cytometric analysis of immune cell infiltration in response to CD-HFD feeding

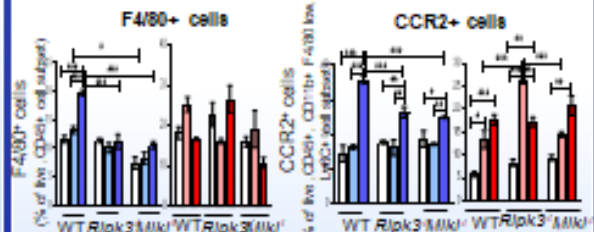

Fig.2: Flow cytometric analysis of immune cells in the lives of WT, *Rlpk3*$^{-/-}$ and *Mlkl*$^{-/-}$ fed with normal chow , CD-LFD or CD-HFD for 6 months. ***p<0.0005, **p<0.005, *p<0.05

Fig4: (a)RNA sequanding analysis, (b) top5 up and down regulated genes in WT-CD HFD reversed by the absence of necroptotic proteins, (c) validation of selected genes in lives of WT, *Rlpk3*$^{-/-}$ and *Mlkl*$^{-/-}$ fed with normal chow , CD-LFD or CD-HFD for 6 months.

Take home message

NASH induced HCC exhibits sex difference which reflects in inflammation, immune cell filtration and tumor incidence, and blocking necroptosis reduces these features.

QUANTITATIVE ANALYSIS OF SINGLE CELL NITRIC OXIDE DETECTION

Yunpeng Lan, Xingxiu Chen. Advisor: Dr. Zhibo Yang
University of Oklhoma, Department of Chemistry and Biochemistry

Nitric oxide or nitrogen monoxide (NO) is a colorless gas in nature, which is a very volatile molecule. As an important intermediate in industrial chemistry, nitric oxide is involved in a lot of industrial products, such as nitric acid. In nature, nitric oxide also forms under lightning in thunderstorms. However, as a precursor of nitric acid which is the main reason for acid rain, nitric oxide has a negative impact on the environment especially as increasing industrial utilization. However, after the impacts of biology were discovered and rewarded by the 1998 Nobel Prize, more and more efforts were applied to understand nitric oxide and human health. As a biological signaling molecule, almost every organism, including bacteria, plants, fungi, and animal cells, have nitric oxide synthase, the enzyme for bile synthesized endogenously from L-arginine, oxygen and NADPH. Nitric oxide is involved in multiple biological processes including the ion transformation and blood vessels adjustment. New drugs were developed and many lives were saved. However, as the further understanding of nitric oxide, the relationship between nitric oxide and tumor was discovered.

Tumor is a comprehensive disease that is related with different functions of humans, such as the immune system and remodeling and maturation of blood vessels. Nitric oxide was found to be a significant factor. In the immune system, low concentrations of nitric oxide produce anti-inflammatory effects by inhibiting the proliferation of T helper cells. Oppositely, high concentration of nitric oxide leads to a strong proinflammatory response under abnormal conditions. The concentration of nitric oxide directly influences the growth of the tumor. Low concentration of nitric oxide induces the growth and nutrition of tumors which are related with the formation of blood vessels. Therefore, quantitative monitoring of nitric oxide in cancers or health cells is important. However, one of the difficulties for tumor therapy showed up for monitoring nitric oxide, cell heterogeneity. Cell heterogeneity represents the difference between cells altering due to the microenvironmental change such as nutrition and oxygen. The cell responses differently with nitric oxide also increase the difficulty to further understand the function of nitric oxide by bulk analysis. In this case, we would like to develop a quantitative nitric oxide detection method for single cell analysis.

The UNIVERSITY of OKLAHOMA

Department of Chemistry and Biochemistry

Quantification of Nitric Oxide (NO) in Single Cells using Mass Spectrometry

Yunpeng Lan, Xingxiu Chen, Dr. Zhibo Yang*

Department of Chemistry and Biochemistry

Introduction

- Nitric oxide (NO) is an important biological molecule.
- NO plays critical roles in tumor processes such as remodeling and maturation of blood vessels.
- NO functions are highly dependent on its concentration.
- NO is a highly reactive molecule with very short lifetime (several seconds) and relatively low concentrations (pM - nM) in cells.
- Tumor heterogeneity requires the quantification of NO at single cell level, while traditional bulk analysis only gives average results.
- Mass spectrometry (MS) is a powerful tool for molecular detection and quantification, and single cell MS is capable of molecular analysis of single cells.
- Amlodipine (AML, m/z 409.1524) specifically reacts with NO (**~100% conversion efficiency**), producing **dehydro Amlodipine (DAM, m/z 407.1368)** for MS quantification.
- However, a common background ion (m/z 407.2118) interferes with direct quantification of DAM.
- **Oxaisoluron (OXF, m/z 407.1020)** was used as the internal standard, which can be co-isolated with DAM for MS2 quantification.

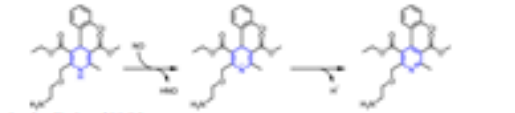

Zhibo Yang, et al. Anal. Chem. 2021, 93, 9950-9955

Results

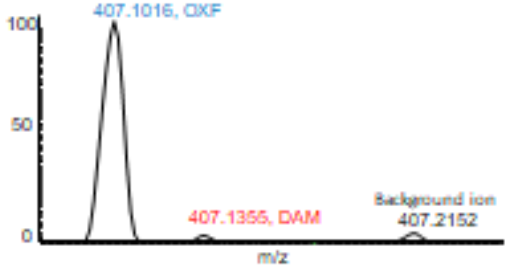

Figure 3. co-isolation of internal standard and DAM

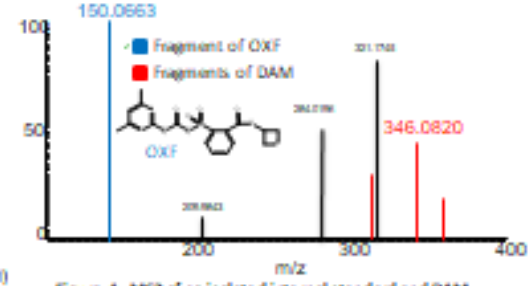

Figure 4. MS2 of co-isolated internal standard and DAM

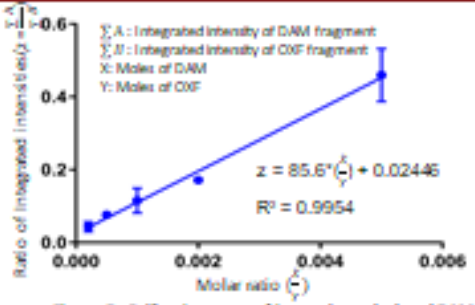

Figure 5. Calibration curve of internal standard and DAM

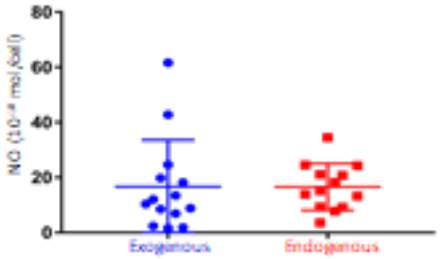

Figure 6. Concentrations of NO in single cells

Method

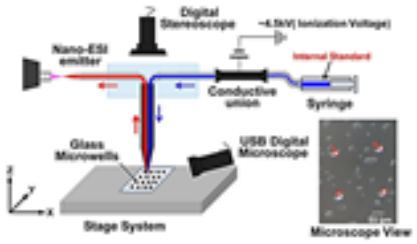

Figure 1. Technique details

Li Yun, et al. Anal. Chem. 2019, 91, 14, 9016-9024

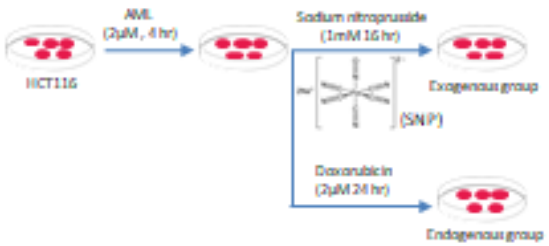

Figure 2. Cell culture and treatment

Conclusion

- Chemical reaction was successfully used to convert NO into DAM to facilitate its detection in live single cells.
- Calibration curve was established using the major MS2 fragments and corresponding molar ratios of DAM and OXF.
- The amounts of DAM in single cells were measured based on the calibration curve.
- Our results are within the range of published values ($2 * 10^{-17}$ mole/cell).

Zhibo Yang, et al. Anal. Chem. 2021, 93, 9950-9955

Acknowledgement

This research was supported by a grant from the Research Council of the University of Oklahoma Norman Campus, National Institutes of Health (R01GM116116) and National Science Foundation (OCE-1654690).

INVESTIGATING THE ROLE OF KRCC1 IN THE DNA DAMAGE RESPONSE

Fiifi Neizer-Ashun[1, 3], Shailendra Dwivedi[2, 3], Anindya Dey[2, 3] Resham Bhattacharya[1, 2, 3] [1]Department of Cell Biology, University of Oklahoma Health Sciences Center. [2]Department of Obstetrics and Gynecology, University of Oklahoma Health Sciences Center.
[3]Peggy and Charles Stephenson Cancer Center, University of Oklahoma Health Sciences Center.

The ATR-CHK1 axis regulates the intra-S checkpoint which responds to DNA damage from extrinsic sources as well as to replication associated stress and endogenous damage. Typically, activation of checkpoint delays origin firing and ultimately blocks mitotic entry allowing time for efficient DNA repair. Although this checkpoint has been much studied, the mechanisms underlying activation and its contribution towards cell cycle remain unclear.

We previously demonstrated that the lysine-rich coiled coil 1 (KRCC1), a protein with unknown biology is overexpressed in cancer. Silencing KRCC1 causes DNA damage, decreases clonal growth, and potentiates apoptosis resulting in reduced tumor growth. At the molecular level, silencing KRCC1 increased CHK1 phosphorylation at S345 and H2AX at S139 (γH2AX) which suggests enhanced DNA damage. Additionally, histone 3 phosphorylation at S10 (pH3S10), a mitotic marker, was also increased in KRCC1 silenced cells. We reasoned that the intriguing dichotomy of enhanced DNA damage and augmented mitotic progression could be attributed to checkpoint inadequacy.

Interestingly, we find that silencing KRCC1 decreased CHK1 phosphorylation at S296 and stabilized CDC25A, suggesting impaired CHK1 activity. Cell cycle evaluation by EdU/ PI, revealed that depleting KRCC1 impaired cell cycle progression, which coupled with a defective checkpoint resulted in premature mitotic entry. Concurrently, DNA repair via homologous recombination was significantly decreased corroborating decreased RAD51 foci formation in KRCC1 silenced cells.

Altogether, these results suggest that KRCC1 may play a critical role in the CHK1-mediated DNA damage response, associated DNA repair, and in overall cell cycle progression.

Investigating the role of KRCC1 in the DNA damage response.

Fiifi Neizer-Ashun[1,3], Shailendra Dwivedi[2,3], Anindya Dey[2,3], Resham Bhattacharya[1,2,3]

[1]Department of Cell Biology, [2]Department of Obstetrics and Gynecology, [3]Peggy and Charles Stephenson Cancer Center, University of Oklahoma Health Sciences Center.

ABSTRACT

The ATR-CHK1 axis regulates the intra-S checkpoint which responds to DNA damage from extrinsic sources as well as to replication associated stress and endogenous damage. Typically, activation of checkpoint delays origin firing and ultimately blocks mitotic entry allowing time for efficient DNA repair. Although this checkpoint has been much studied, the mechanisms underlying activation and its contribution towards cell cycle remain unclear. We previously demonstrated that the lysine-rich coiled coil 1 (KRCC1), a protein with unknown biology is overexpressed in cancer. Silencing KRCC1 causes DNA damage, decreases clonal growth, and potentiates apoptosis resulting in reduced tumor growth. At the molecular level, silencing KRCC1 increased CHK1 phosphorylation at S345 and H2AX at S139 (γH2AX) which suggests enhanced DNA damage. Additionally, histone 3 phosphorylation at S10 (pH3S10), a mitotic marker, was also increased in KRCC1 silenced cells. We reasoned that the intriguing dichotomy of enhanced DNA damage and augmented mitotic progression could be attributed to checkpoint inadequacy. Interestingly, we find that silencing KRCC1 decreased CHK1 phosphorylation at S296 and stabilized CDC25A, suggesting impaired CHK1 activity. Cell cycle evaluation by EdU/PI, revealed that depleting KRCC1 impaired cell cycle progression, which coupled with a defective checkpoint resulted in premature mitotic entry. Concurrently, DNA repair via homologous recombination was significantly decreased corroborating decreased RAD51 foci formation in KRCC1 silenced cells. Altogether, these results suggest that KRCC1 may play a critical role in the CHK1-mediated DNA damage response, associated DNA repair, and in cell cycle progression.

RESULTS

Localization and interactions of KRCC1.

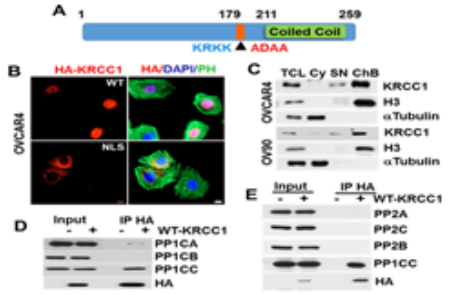

Fig.1- A. Schematic representation of KRCC1 with nuclear localization signal sequence (NLS, blue mutated to red). **B.** OVCAR4 cells were transfected with HA-tagged WT or NLS mutant KRCC1 and KRCC1 localization determined by immunofluorescence with phalloidin (PH) and DAPI. (Bar=20 μm) **C.** Subcellular fractionation was performed in OVCAR4 and OV90 cells to detect endogenous KRCC1, total cell lysate (TCL), cytoplasm (Cy), soluble nuclear (SN), chromatin bound fraction (ChB). Fraction purity determined by respective markers. **D, E.** OV90 cells were transfected with HA-tagged WT-KRCC1 for 30h. Association of KRCC1 with various catalytic subunits of protein phosphoatase 1 and 2 (PP1 and PP2) were determined by immunoprecipitation.

Expression of KRCC1 correlates with poor prognosis in cancer.

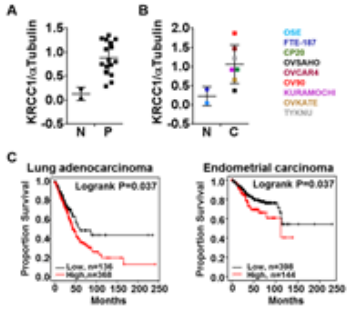

Fig.2- A. Relative quantitation of KRCC1 expression in normal fallopian tissue (N) and ovarian tumors (P) **B.** Relative quantitation of KRCC1 expression in respective normal (N) and ovarian cancer (C) cell lines. **C.** Kaplan-Meier curves evaluated by log-rank test to determine association between expression of KRCC1 with overall survival in lung adenocarcinoma and endometrial carcinoma.

Effect of KRCC1 silencing on clonal growth and apoptosis.

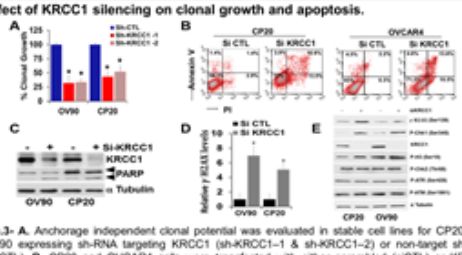

Fig.3- A. Anchorage independent clonal potential was evaluated in stable cell lines for CP20 and OV90 expressing sh-RNA targeting KRCC1 (sh-KRCC1–1 & sh-KRCC1–2) or non-target shRNA (shCTL). **B.** CP20 and OVCAR4 cells were transfected with either scrambled (siCTL) or KRCC1 siRNA (siKRCC1) for 72h, stained with AnnexinV/PI and analyzed by flow cytometry. **C.** OV90 and CP20 cells were transfected with either scrambled (siCTL) or KRCC1 siRNA (siKRCC1) for 72h and immunoblotted for cleaved PARP. **D.** Relative quantitation of phosphorylated histone H2AX (γH2AX) in OV90 and CP20 cells after KRCC1 silencing evaluated by immunofluorescence. **E.** CP20 and OV90 cells were transfected with either scrambled (siCTL) or KRCC1 siRNA (siKRCC1) for 72h. Expression of checkpoint and DNA damage response markers was determined by immunoblotting.

Effect of KRCC1 silencing on CHK1-mediated DDR.

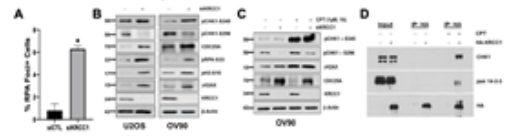

Fig.4- A. OV90 cells were transfected with either scrambled (siCTL) or KRCC1 siRNA (siKRCC1) for 72h and evaluated for replication protein A 32 (RPA32) foci positivity by immunofluorescence, an indication of replication stress. **B.** U2OS and OV90 cells were transfected with either scrambled (siCTL) or KRCC1 siRNA (siKRCC1) for 72h. Markers of CHK1 activation and expression of CHK1-dependent DDR markers were determined by immunoblotting. **C.** To evaluate checkpoint activation in the presence of extrinsic damage, OV90 and U2OS cells were transfected with either scrambled (siCTL) or KRCC1 siRNA (siKRCC1) and treated with camptothecin (CPT,1μM for 1h). Cells were collected immediately following treatment and immunoblotted for CHK1-mediated DDR markers. **D.** KRCC1 interaction with CHK1 and 14-3-3 was evaluated using co-immunoprecipitation in empty vector (EV) or HA-tagged KRCC1 (HA-KRCC1) overexpressed OV90 cells.

Effect of KRCC1 silencing on homologous recombination.

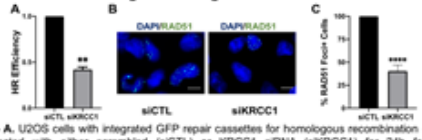

Fig.5- A. U2OS cells with integrated GFP repair cassettes for homologous recombination (HR) were transfected with either scrambled (siCTL) or KROC1 siRNA (siKRCC1) for 24h followed by transfection with the rare cutting I-SceI endonuclease for 48h. Quantitation of GFP expression, indicative of efficient repair is plotted. **B,C.** To elucidate the mechanism for KRCC1-mediated HR, OV90 cells were transfected with either scrambled (siCTL) or KRCC1 siRNA (siKRCC1) and treated with camptothecin (CPT,1μM for 1h). Cells were washed and allowed to recover in fresh warm media for 2h and evaluated for RAD51 foci positivity by immunofluorescence (2h recovery time point is where RAD51 foci is most prominent in control cells).

Effect of KRCC1 silencing on cell cycle progression.

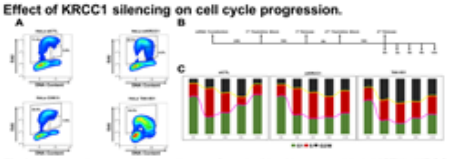

Fig.6- A. Asynchronous HeLa cells transfected with either scrambled (siCTL), KRCC1 siRNA (siKRCC1) or treated with CHK1 inhibitor, AZD7762 (CHK1i) or CDC7 inhibitor, TAK-931 (CDC7i) were pulse labeled with 5-ethynyl-2'-deoxyuridine (EdU) for 15 minutes followed by propidium iodide (PI) staining and cell cycle analysis by flow cytometry. **B.** Experimental scheme of **C.** HeLa cells transfected with either scrambled (siCTL), KRCC1 siRNA (siKRCC1) or treated with CDC7i were synchronized in G1/S by double thymidine block. After synchronization, cells were released in fresh warm FBS containing media for 12h, collected at 3h intervals, and processed for PI cell cycle.

Effect of KRCC1 silencing KRCC1 on mitotic entry.

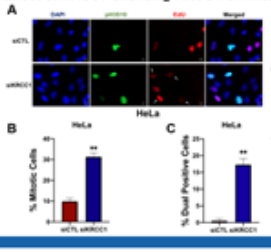

Fig.7- A. HeLa cells transfected with either scrambled (siCTL) or KRCC1 siRNA (siKRCC1) were pulse labeled with EdU for 15 minutes, fixed and processed for immunofluorescence for EdU, to denote S-phase cells and pH3S10, a mitotic marker. **B.** Quantitation of mitotic (pH3S10+) cells. **C.** Relative quantitation of dual positive (EdU+ and pH3S10+) cells.

PROPOSED MODEL & CONCLUSION

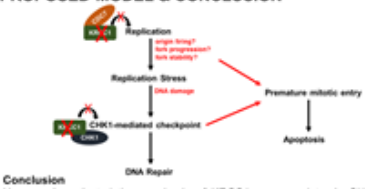

Conclusion

Here we investigated the novel role of KRCC1 as a regulator in CHK1-mediated DNA damage response. We report that KRCC1 is overexpressed in cancer and overexpression correlates with poor overall survival. Silencing KRCC1 induces DNA damage, impairs CHK1 activation resulting in a defective checkpoint. Additionally, silencing KRCC1 decreases RAD51 foci formation leading to suppressed HR repair. Interestingly, depleting KRCC1 results in slower S phase progression and stalling at late S/G2.

Presence of damage, a defective checkpoint, and stalling at the late S-G2 boundary in KRCC1 silenced cells resulted in premature mitotic entry, i.e, cells that have not fully replicated their genome (EdU+) also being positive for a mitotic marker (pH3S10).

Altogether, our findings introduce a new protein in the DNA damage response that bridges the gap between cell cycle integrity, associated replication stress response, and DNA repair.

ACKNOWLEDGEMENT

This study was supported by the Oklahoma Center for Adult Stem Cell Research - a program of TSET award, Department of Defense grants W81XWH1810073 and W81XWH1810073 awarded to Dr. Resham Bhattacharya, and Stephenson Cancer Center Trainee Conference and Workshop Award to Fiifi Neizer-Ashun.

SINGLE CELL MASS SPECTROMETRY METABOLOMIC STUDIES OF PRIMARY AND METASTATIC CANCERS

Tra D. Nguyen, Zhibo Yang*
Department of Chemistry and Biochemistry, Norman, OK 73019
Corresponding author: Zhibo.Yang@ou.edu
Presenting author: TraNguyen@ou.edu

Metastatic cancers are often more dangerous than the primary cancers, although genomic alterations between these two types of cancer are generally not significantly different. As the end products of cell metabolism, metabolites directly reflect metabolic programs and define sites of metastasis. Studying the difference of molecular characteristics and metabolomics of drug treatment is of great interest of cancer studies. Due to cell heterogeneity and rapid turnover rate of metabolites, metabolomics studies of live single cells can provide critical information for fundamental research and potentially clinical diagnosis. In this study, we used primary/metastatic melanoma cell lines as models, and conducted single cell mass spectrometry studies to investigate their metabolite biomarkers and their metabolomic profiles affected by drug treatment.

The Single-probe was designed to couple to a Thermo LTQ Orbitrap XL mass spectrometer to perform tandem MS and MS experiment. The Single-probe is constructed with three major components which include a laser-pulled dual-bore quartz needle and two capillaries (i.e., a nano-ESI emitter and a solvent-providing capillary). The two pairs of primary/metastatic melanoma cell lines (IGR 39/IGR 37 and WM 115/WM 266-4) were cultured and treated with Vemurafenib (an FDA-approved drug for melanoma treatment) at 0.5 μM for 48 hours. Both control and drug treated cells in each group were analyzed using Single-probe single cell MS technique.

In total, two pairs of primary/metastatic melanoma cells, with or without Vemurafenib treatment (n = 100 in each group for control and treated cells and 400 in total), were analyzed using the Single-probe single cell mass spectrometry. MS raw data were subjected to pretreatment (e.g., noise removal, peak alignment, and intensity normalization) and statistical analysis such as Principal Component Analysis (PCA), Volcano plot, and T-tests using MetaboAnalyst 5.0. T-test results provided targeted metabolites prior to perform MS/MS analysis. Tandem MS data's results were analyzed based upon the online database METLIN and HMDB.

Based on the experimental results, the metabolomic profiles of primary cells have distinct difference from those of metastatic cells. The differences in the profiles of control and treated cells were also detected. A series of molecules, such as drug compound, drug metabolites, cells metabolites, and lipids, were observed with significantly different abundances in comparative studies, and these species can be regarded as potential metabolite biomarkers representing the type of cells, response to drug treatment, and distinct metabolomic pathways of primary vs metastatic cells. Additional molecular identification of relative abundant ions will be performed at the single cell level, whereas complementary information for species with low abundances will be provided using LC/MS analysis of cell lysate. Analyzing the treated primary cells and treated metastatic cells provides more insights into the difference in metabolite biomarkers, cell metabolism, cell microenvironment, difference in drug resistance mechanisms, etc.

The first study to explore metabolomic profiles of primary and metastatic cancers with Vemurafenib treatment using single cell MS technique.

This work was supported in part by National Institutes of Health (R01GM116116).

Single Cell Mass Spectrometry Metabolomic Studies of Primary and Metastatic Cancers

Tra D. Nguyen, Zhibo Yang*
Department of Chemistry and Biochemistry, Norman, OK 73019
Corresponding author: Zhibo.Yang@ou.edu

Introduction

- Melanoma is the most aggressive type of skin cancer and metastasis mechanisms are underinvestigated. Primary melanoma is derived from melanocytes and later developed to metastatic melanoma. Metastatic cancers are often more dangerous than the primary cancers.
- As the end products of cell metabolism, metabolites directly reflect metabolic perturbations and define states of metastasis. Metabolites reflect the differences of molecular characteristics and metabolomics of drug treatment.
- Due to rapid turnover rate of metabolites, metabolomics studies of live single cells can analyze metabolites sensitive to living status of cells that are often masked during traditional bulk analysis.
- Single probe single cell mass spectrometry (SCMS) is employed to conduct the untargeted metabolomic profiling of melanoma cells.
- Two pairs of cell lines (primary melanoma WM 115 and metastatic melanoma WM 266-4, and primary melanoma 1120 SP and metastatic melanoma 1205 Lu) were examined to determine if cell biomarkers and treatment significance metabolites affected by drug treatment (Vemurafenib).
- Vemurafenib is a single agent inhibitor of the BRAF V600E kinase which has been approved to induce cell cycle arrest or G1/G0 phase that leads to the apoptosis of melanoma.

Methods

A. Sample Preparation

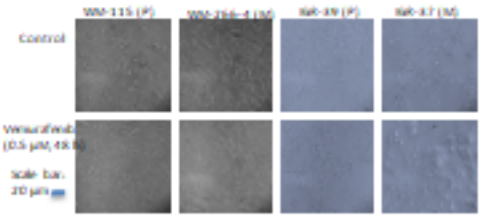

Figure 1. Microscopic images of two pairs of primary/metastatic melanoma cells before and after Vemurafenib treatment were captured prior to performing single cell analysis using Single probe SCMS technique.

B. Single-probe SCMS technique

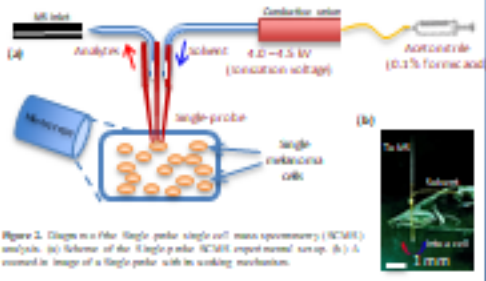

Figure 2. Diagram of the Single probe single cell mass spectrometry (SCMS) analysis. (a) Scheme of the Single probe SCMS experimental set-up. (b) A zoomed in image of a Single probe with its working mechanism.

Results

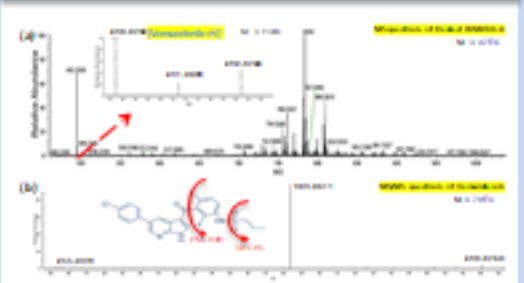

Figure 3. (a) Representative mass spectrum of an individual treated WM 266-4 cell treated by Vemurafenib (1 μM for 48 h) with drug molecules and cell metabolites are observed. The zoom in spectrum displays Vemurafenib, [C23H18F2N3O3S+H]+ (m/z 450.10760) and its isotopic peaks. (b) Confirmation of the detection of Vemurafenib using MS/MS of the single cell level.

Statistical analysis

Treatment influence, Control vs. Treated cells

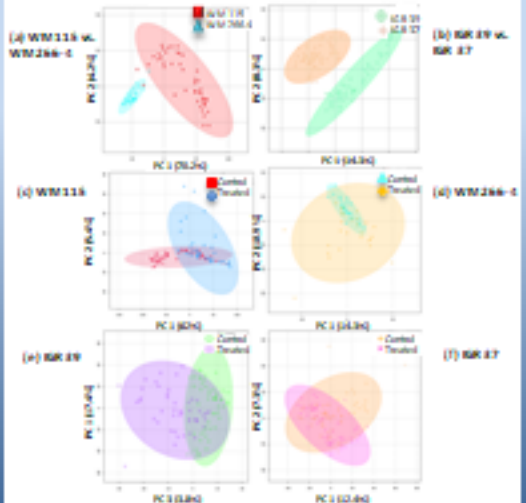

Figure 4. Principal Component Analysis (PCA) illustrating the metabolomic profiles of control cells (before treatment) with 3 pairs of primary vs. metastatic cells (a) WM 115 vs. WM 266-4, (b) SK-MEL-28 vs. SK-MEL-5 and the metabolomic profiles of control (untreated) cells and drug treated (0.5 μM, 48 h) cells in each cell line, (c) WM 115, (d) WM 266-4, (e) SK-MEL-28 and (f) SK-MEL-5.

Results

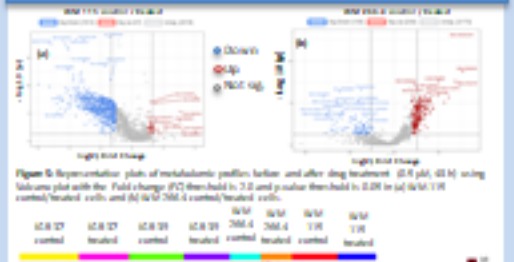

Figure 5. (a) Representative plots of metabolomic profiles before and after drug treatment (0.5 μM, 48 h) using Volcano plot with the Fold change (FC) threshold is 2.0 and p-value threshold is 0.05 in (a) WM 115 control/treated cells and (b) WM 266-4 control/treated cells.

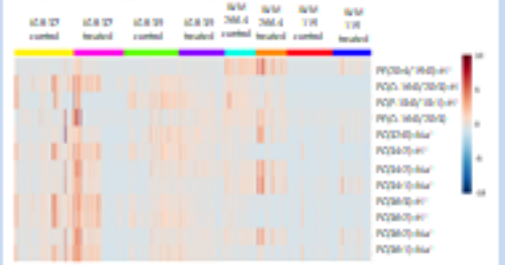

Figure 6. Hierarchical Clustering of metabolite features differing between control vs. treated cells in 2 pairs of primary/metastatic cells (WM 115/WM 266-4 and SK-MEL-28/SK-MEL-5).
*PC = Phosphatidylcholine; PE = Phosphatidylethanolamine

Conclusions

- Single probe SCMS technique was successfully utilized for performing metabolomic analysis of individual cells.
- The metabolomic profiles of primary cells have distinct metabolites difference from metastatic cells.
- Volcano plots provide metabolite biomarkers, which were significantly down regulated (blue) or upregulated (red) after treatment.
- Most metabolite biomarkers are identified as Phosphatidylcholine (PC), Phosphatidylethanolamine (PE) and Carnitine.
- The metastatic cells (WM 266-4 and SK-MEL-5) possess higher abundances of unsaturated lipids than their corresponding primary cells (WM 115 and SK-MEL-28). It is consistent with upregulation of lipids that were reported in melanoma cells.
- With Vemurafenib treatment, the treated melanoma cells display elevated level of PC and PE compared to their corresponding control cells.

Acknowledgement

- Professor Dr. Wenbing Wang from UC Riverside for providing cell lines.
- Professor Dr. Zhibo Yang and all group members, Dr. Yang Lab: Zhu Zhu, Mingxia Chen, Yunpeng Lan, Zonghui Peng, Tam Chen, Amit Singh.
- Funding: Funded by National Institutes of Health (R01GM116116).

A NOVEL SCALE BIOPSY TECHNIQUE IDENTIFIES ZEBRAFISH EPITHELIAL LYMPHOCYTES AND ALLOWS BIOMARKER DISCOVERY TO PREDICT GLUCOCORTICOID RESPONSE IN ACUTE LYMPHOBLASTIC LEUKEMIA

Gilseung Park[1], Clay A. Foster[2], Megan Malone-Perez[2], Ameera Hasan[3], Jose Juan Macias[3], and J. Kimble Frazer[1,2,3]

[1]Department of Cell Biology, University of Oklahoma Health Sciences Center, OK, USA, [2]Department of Pediatrics, University of Oklahoma Health Sciences Center, OK, USA, [3]Department of Microbiology & Immunology, University of Oklahoma Health Sciences Center, OK, USA

Zebrafish are a compelling model to study lymphocyte development and lymphocytic cancers because the zebrafish and human immune systems are similar, including their B and T cells. Several zebrafish T cell acute lymphoblastic leukemia (T-ALL) models are established, including human *MYC* (*hMYC*) transgenic fish. Recently, we reported that *rag2:hMYC* fish develop B-ALL also, making this line powerful to study both ALL types. However, non-lethal methods to serially obtain ALL samples from animals have not been described. In addition, the existence and identities of epidermal lymphocytes in zebrafish have not been studied. Here, we report a novel 'scale biopsy' method to collect lymphocytes from live zebrafish and identify epithelial lymphocytes in the scales of multiple fluorescently-labeled transgenic lines. Confocal imaging of normal scales reveals fluorescent lymphocytes in the attached epidermis, and scales of fish with ALL show dramatic infiltration of malignant lymphocytes. FACS analyses and gene expression studies of ALL cells from scales and other tissues of the same fish prove scale ALL cells are representative of those animals' cancers. Single-cell expression studies also reveal diverse lymphocyte populations in scales. Finally, scale ALL cells can respond to dexamethasone (DXM), a glucocorticoid used to treat ALL. As in patients, DXM responses varied across our fish cohort. We analyzed the least- and most-responsive ALL samples by RNA-seq, at multiple timepoints, seeking DXM response indicators. In summary, our new biopsy technique opens new avenues to study epithelial lymphocytes in zebrafish and describes a non-lethal method to study lymphocytes *ex vivo*, including malignant lymphocytes.

Presenter email: gpark1@ouhsc.edu

Acknowledgement of Funding: OCASCR & 2020 SCC Seed grant

A Novel Scale Biopsy Technique Identifies Zebrafish Epithelial Lymphocytes and Allows Biomarker Discovery to Predict Glucocorticoid Response in Acute Lymphoblastic Leukemia

Gilseung Park[1], Clay A. Foster[2], Megan Malone-Perez[2], Ameera Hasan[3], Jose Juan Macias[3], and J. Kimble Frazer[1,2,3]
[1]Department of Cell Biology, University of Oklahoma Health Sciences Center, OK, USA
[2]Department of Pediatrics, University of Oklahoma Health Sciences Center, OK, USA
[3]Department of Microbiology & Immunology, University of Oklahoma Health Sciences Center, OK, USA

INTRODUCTION

- Acute lymphoblastic leukemia (ALL) is the most common childhood cancer. Precursor-B and -T cell ALL (pre-B ALL, T-ALL) represent ~85% and ~15% of cases, respectively.
- We found transgenic *lck:GFP* zebrafish express GFP highly in T cells (or T-ALL with the additional transgene, human *MYC* regulated by a *D. rerio rag2* promoter), and B lymphocytes (or B-ALL*)* express *lck* at lower levels.
- Studies of *D. rerio* lymphocytes or acute lymphoblastic leukemia (ALL) typically require euthanizing animals to obtain lymphocytes.
- Here, we report **a new technique** using different zebrafish lines that mark either T or B cells to **biopsy living fish** and **obtain normal lymphocytes or ALL cells from fish scales.**
- Using this method, we can study **the resistance mechanism to dexamethasone (DXM)**, the key drug for human ALL treatment, at any time points during the treatment.

OBJECTIVES

- To identify epithelial lymphocyte populations in different transgenic zebrafish scales.
- To obtain ex vivo samples including both normal lymphocytes and ALL cells from live fish without euthanasia.
- To examine ALL gene expressions that can identify predictors of DXM response in different responsive groups: Responder, Respond-then-relapse, or Non-responder.

BACKGROUND & PREVIOUS DATA

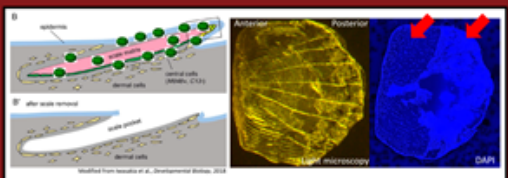

Zebrafish scale anatomy and an example of the scale biopsy sample. The scale of the zebrafish is a membranous bone (dermal bone) embedded in the skin (**left**). Single scale images show both scale matrix and epidermal layer cells on the posterior area (**right**). Zebrafish scales are **abundant** (600-800/fish) & can **regenerate in only a few days**, allowing multiple biopsies from each individual.

RESULTS: Confocal Images & FACS Analyses

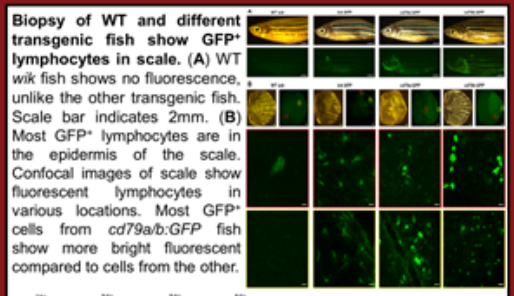

Biopsy of WT and different transgenic fish show GFP⁺ lymphocytes in scale. (**A**) WT *wik* fish shows no fluorescence, unlike the other transgenic fish. Scale bar indicates 2mm. (**B**) Most GFP⁺ lymphocytes are in the epidermis of the scale. Confocal images of scale show fluorescent lymphocytes in various locations. Most GFP⁺ cells from *cd79a/b:GFP* fish show more bright fluorescent compared to cells from the other.

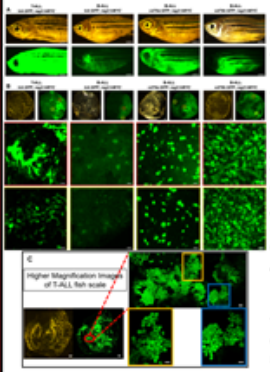

Scale biopsy samples of different transgenic zebrafish with T- or B-ALL show GFP⁺ lymphocytes. (**A**) Different transgenic fish exhibit highly infiltrated T- and B-ALL all over the body. (**B**) T-ALL cells from *lck:GFP* background are highly fluorescent compared to dimly fluorescent B-ALL cells. Most ALL cells from both *cd79a* and *cd79b* fish spread through the entire scale, on the other hand, ALL cells from *lck:GFP* fish are mostly in the epidermis. (**C**) Higher magnification images of the T-ALL fish scale reveal clustering of T-ALL cells on the surface.

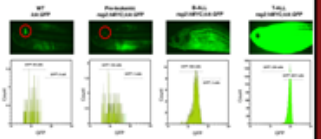

FACS of scale cells can quantify lymphocytes. One scale from a WT fish has **~100 B cells**, but **0-1 T cells**. ALL scale has **hundreds-to-thousands** of ALL cells.

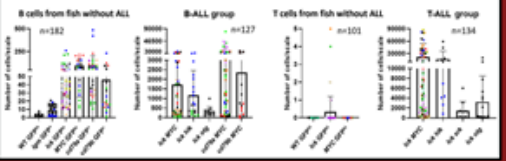

RESULTS: DXM Scheme & ALL Responsiveness

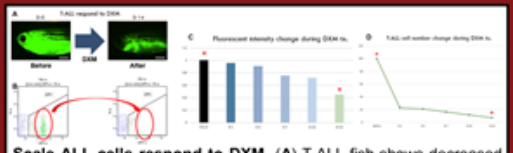

Scale ALL cells respond to DXM. (**A**) T-ALL fish shows decreased GFP fluorescence after DXM treatment. (**B**) FACS data reveal the actual decline of GFP⁺ cell numbers. (**C**) Fluorescent intensity of fish on each treatment day also shows reduction of entire fish fluorescent. (**D**) Total GFP⁺ cell numbers are reduced during DXM treatment.

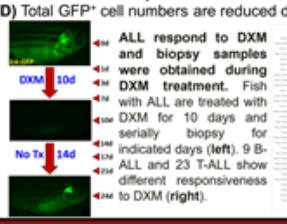

ALL respond to DXM and biopsy samples were obtained during DXM treatment. Fish with ALL are treated with DXM for 10 days and serially biopsy for indicated days (**left**). 9 B-ALL and 23 T-ALL show different responsiveness to DXM (**right**).

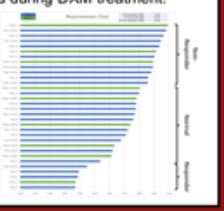

RESULTS: DXM & ALL Gene Expression Changes

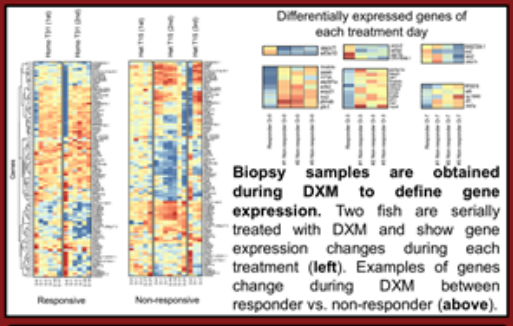

Biopsy samples are obtained during DXM to define gene expression. Two fish are serially treated with DXM and show gene expression changes during each treatment (**left**). Examples of genes change during DXM between responder vs. non-responder (**above**).

CONCLUSIONS

- We developed a novel technique to serially-biopsy live zebrafish.
- Our study reveals diverse lymphocyte populations in zebrafish scales from multiple transgenic lines.
- Serial biopsy can decipher DXM treatment effects in real-time, with our ultimate goal being to find genes that predict DXM-response in ALL.

WHEN A DICER1 MUTATION OF UNCERTAIN SIGNIFICANCE IS ACTUALLY SIGNIFICANT

Authors: Parker, Loretta[1]; Journeycake, Janna[1]; Pokala, Hanumantha[1]
Institutions: 1. Pediatric Hematology/Oncology, The University of Oklahoma Health Sciences Center, Oklahoma City, OK, United States
Email Address: loretta-parker@ouhsc.edu

Background

DICER1 is a cancer predisposition syndrome caused by mutations within the DICER1 gene on chromosome 14. DICER is an enzyme that cleaves RNA into microRNA and is integral in inhibiting unregulated cell growth and protein expression. We report a case of a young girl with two DICER1-associated tumors, who was found to have a variant of uncertain significance (VUS) in the DICER1 gene. Immediate family members also demonstrated the mutation, with two of three exhibiting DICER1-associated diagnoses. While DICER1 is typically inherited in an autosomal dominant fashion and manifests with low penetrance, this report illustrates high penetrance with this mutation, suggesting re-designation of the VUS to pathogenic.

Objective

1. Recognize potentially late presentation in DICER1 syndrome
2. Understand that a VUS can be pathogenic and may warrant re-designation
3. Understand the importance of testing patients presenting with DICER1-typical tumors

Design/Method

Case Report and Literature Review

Results

A 9-year-old female with past medical history significant for cerebral palsy and right ovarian torsion with oophorectomy at 6 years of age presented with a 2 week history of abdominal pain, distention, and decreased appetite. Imaging revealed a large 24 x 21 x 5.5 cm solid, cystic mass, with concern of origin from the left ovary. Alpha-fetoprotein and Inhibin A were within normal limits. CA-125 was elevated to 377 u/mL. Pathology showed poorly differentiated retiform Sertoli-Leydig Cell Tumor (SLCT) with rhabdomyosarcoma components after removal. Due to a strong family history of tumors associated with DICER1 syndrome, DICER1 testing was initiated. A heterozygous missense mutation in c.2408G>A (p.Gly803Glu) was detected and classified as a VUS. Subsequently, her mother and two sisters underwent testing and possess the same

germline mutation. Almost one year off-therapy from 4 cycles of Cisplatin, Ifosfamide, and Etoposide for her primary tumor, she developed a second abdominal malignancy, with pathology revealing Spindle Cell Sarcoma/Embryonal Rhabdomyosarcoma.

Conclusion

DICER1 syndrome is a rare genetic disorder, with development of DICER1- associated tumors occurring even less commonly. Our patient's VUS has not yet been designated a pathogenic variant for DICER1 syndrome. However, re-designation may be warranted due to the presence of multiple DICER1-associated tumors in the proband, as well as discovery of the same variant in her mother and sisters. This case exemplifies the importance of DICER1 testing in response to typical tumors associated with this mutation, as well as testing of family members. This will ideally lead to initiation of surveillance strategies with hopes of early diagnosis of potentially ominous malignancies.

References:

1. Schultz KAP, Williams GM, Kamihara J, et al. *DICER1* and Associated Conditions: Identification of At-risk Individuals and Recommended Surveillance Strategies. *Clin Cancer Res*. 2018;24(10):2251-2261. doi:10.1158/1078-0432.CCR-17-3089
2. McCluggage WG, Foulkes WD. DICER1-associated sarcomas: towards a unified nomenclature. *Mod Pathol*. 2021;34(6):1226-1228. doi:10.1038/s41379-020-0602-4
3. https://www.chop.edu/conditions-diseases/dicer1-syndrome
4. Caroleo AM, De Ioris MA, Boccuto L, et al. DICER1 Syndrome and Cancer Predisposition: From a Rare Pediatric Tumor to Lifetime Risk. *Front Oncol*. 2021;10:614541. Published 2021 Jan 21. doi:10.3389/fonc.2020.614541
5. Robertson JC, Jorcyk CL, Oxford JT. DICER1 Syndrome: DICER1 Mutations in Rare Cancers. *Cancers (Basel)*. 2018;10(5):143. Published 2018 May 15. doi:10.3390/cancers10050143
6. Bailey KM, Jacobs MF, Anderson B, et al. DICER1 Mutations in the Era of Expanding Integrative Clinical Sequencing in Pediatric Oncology. *JCO Precis Oncol*. 2019;3:PO.18.00172. doi:10.1200/po.18.00172

When a DICER1 Mutation of Uncertain Significance is Actually Significant

COLLEGE OF MEDICINE
The UNIVERSITY of OKLAHOMA

Parker L, Journeycake J, Pokala H
Pediatric Hematology/Oncology at The University of Oklahoma College of Medicine

Jimmy Everest Section of Pediatric Hematology/Oncology

Background

- DICER is an enzyme that cleaves RNA into microRNA
- DICER1 is a cancer predisposition syndrome caused by mutations within the DICER1 gene on Chromosome 14
- Mutations within the DICER1 gene lead to unregulated cell growth and protein expression
- We present a case of a girl with 2 DICER1-associated tumors but with a variant of uncertain significance (VUS)

Objectives

- Recognize potentially late presentation in DICER1 syndrome
- Understand that a VUS can be pathogenic and may warrant re-designation
- Understand the importance of testing patients presenting with DICER1-typical tumors

Case Presentation

- 9-year-old female with past medical history significant for cerebral palsy and right ovarian torsion with oophorectomy who presented with 2-week history of abdominal pain and distension
- Imaging showed 24 x 21 x 5.5 cm solid/cystic mass with concern of origin from left ovary
- CA-125 elevated to 377 u/mL, AFP and Inhibin A within normal limits
- Mass removed and pathology showed Sertoli-Leydig Cell Tumor (SLCT) with rhabdomyosarcoma components

Case Presentation

- DICER1 testing conducted due to strong family history of DICER1-associated tumors
  - Heterozygous missense mutation in c.2408G>A (p.Gly803Glu) was detected and classified as a VUS
  - Mother and two sisters found to possess the same germline mutation
- SLCT was treated with Cisplatin, Ifosfamide, and Etoposide
- Diagnosed with a second abdominal malignancy 1 year off therapy (Spindle Cell Sarcoma/Embryonal Rhabdomyosarcoma)

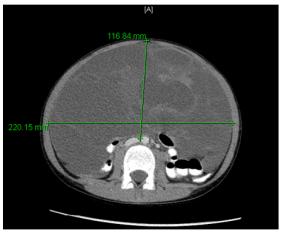

Figure 1: SLCT – Tumor#1 9/8/2019

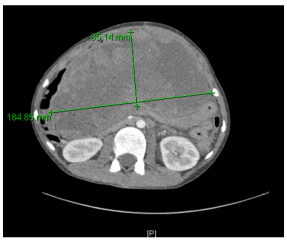

Figure 2: Spindle Cell Sarcoma – Tumor#2 12/6/2020

Discussion

- Prevalence of DICER1 syndrome pathogenic mutations is approximately 1:4,600-10,600 and affects about 30,000 people in the US
- DICER1 syndrome is inherited in an autosomal dominant fashion, typically presenting with decreased penetrance
- Our patient has a VUS, but has now had two malignancies associated with DICER1
- Additionally, two of three immediate family members have had DICER1-associated diagnoses
- Diagnoses associated with DICER1 syndrome include: Pleuropulmonary Blastoma, Sertoli-Leydig Cell tumor, Pineoblastoma, Wilms tumor, thyroid nodules, lung and renal cysts, among others
- Germline testing is imperative with DICER1-associated tumors

Conclusion

- DICER1 syndrome is a rare genetic disorder, with DICER1-associated tumors occurring even less commonly
- Our patient has a DICER mutation leading to multiple malignancies
- Re-designation should be considered for c.2408G>A (p.Gly803Glu) due to significant prevalence
- Testing in patients with DICER1-typical tumors is important to detect germline mutations in the patient and family
- Earlier detection can lead to improved surveillance and potentially decreased morbidity.

References

- Schultz KAP, Williams GM, Kamihara J, et al. DICER1 and Associated Conditions: Identification of At-risk Individuals and Recommended Surveillance Strategies. Clin Cancer Res. 2018;24(10):2251-2261. doi:10.1158/1078-0432.CCR-17-3089
- McCluggage WG, Foulkes WD. DICER1-associated sarcomas: towards a unified nomenclature. Mod Pathol. 2021;34(6):1226-1228. doi:10.1038/s41379-020-0602-4
- https://www.chop.edu/conditions-diseases/dicer1-syndrome
- Further references upon request

OPPOSITE ROLES OF THE JMJD1A INTERACTION PARTNERS MDFI AND MDFIC IN COLORECTAL CANCER

Yuan Sui[1], Xiaomeng Li[2,3], Sangphil Oh[3,4], Bin Zhang[2], Willard M. Freeman[4,5], Sook Shin[3,4] and Ralf Janknecht[1,3,4]
Presenting Author's Email Address：yuan-sui@ouhsc.edu

[1]Department of Pathology, University of Oklahoma Health Sciences Center, Oklahoma City, USA; [2]China-Japan Union Hospital of Jilin University, Changchun, China; [3]Department of Cell Biology, University of Oklahoma Health Sciences Center, Oklahoma City, USA; [4]Stephenson Cancer Center, Oklahoma City, USA; [5]Oklahoma Medical Research Foundation, Oklahoma City, USA

Abstract: MyoD family inhibitor (MDFI) and MyoD family inhibitor domain-containing (MDFIC) are homologous proteins known to regulate myogenic transcription factors. Hitherto, their role in cancer is unknown. We discovered that *MDFI* is up- and *MDFIC* downregulated in colorectal tumors. Mirroring these different expression patterns, MDFI stimulated while MDFIC inhibited the growth of HCT116 colorectal cancer cells. Further, MDFI and MDFIC interacted with JMJD (Jumonji C domain-containing) 1A, a histone demethylase and epigenetic regulator involved in colorectal cancer. JMJD1A influenced transcription of several genes that were also regulated by MDFI or MDFIC. Notably, the *HIC1* tumor suppressor gene was stimulated by JMJD1A and MDFIC, but not MDFI, and HIC1 overexpression phenocopied the growth suppressive effects of MDFIC in HCT116 cells. Similar to colorectal cancer, *MDFI* was up- and *MDFIC* downregulated in breast, ovarian and prostate cancer, but both *MDFI* and *MDFIC* were overexpressed in brain, gastric and pancreatic tumors. This implies cancer-critical roles for MDFI and MDFIC beyond colorectal tumors and also points out that MDFIC might be a tissue-specific suppressor or promoter of tumorigenesis. Altogether, our data suggest a tumor modulating function for MDFI and MDFIC in colorectal and other cancers that may involve their interaction with JMJD1A and a MDFIC-HIC1 axis.

Acknowledgement of funding: This work was in part funded by a seed grant from the Stephenson Cancer Center (W.M.F. and R.J.).

Opposite Roles of the JMJD1A Interaction Partners MDFI and MDFIC in Colorectal Cancer

Yuan Sui[1], Xiaomeng Li[2,3], Sangphil Oh[3,4], Bin Zhang[2], Willard M. Freeman[4,5], Sook Shin[3,4] and Ralf Janknecht[1,3,4]

[1]Pathology Department, OUHSC; [2]China-Japan Union Hospital of Jilin University, China; [3]Cell Biology Department, OUHSC; [4]Stephenson Cancer Center; [5]Oklahoma Medical Research Foundation

ABSTRACT

MyoD family inhibitor (MDFI) and MyoD family inhibitor domain-containing (MDFIC) are homologous proteins known to regulate myogenic transcription factors. Hitherto, their role in cancer is unknown. We discovered that *MDFI* is up- and *MDFIC* downregulated in colorectal tumors. Mirroring these different expression patterns, MDFI stimulated and MDFIC inhibited growth of HCT116 colorectal cancer cells. Further, MDFI and MDFIC interacted with JMJD (Jumonji C domain-containing) 1A, a histone demethylase and epigenetic regulator involved in colorectal cancer. JMJD1A influenced transcription of several genes that were also regulated by MDFI or MDFIC. Notably, the *HIC1* tumor suppressor gene was stimulated by JMJD1A and MDFIC, but not MDFI, and HIC1 overexpression phenocopied the growth suppressive effects of MDFIC in HCT116 cells. Altogether, our data suggest a tumor modulating function for MDFI and MDFIC in colorectal cancer that may involve their interaction with JMJD1A and a MDFIC-HIC1 axis.

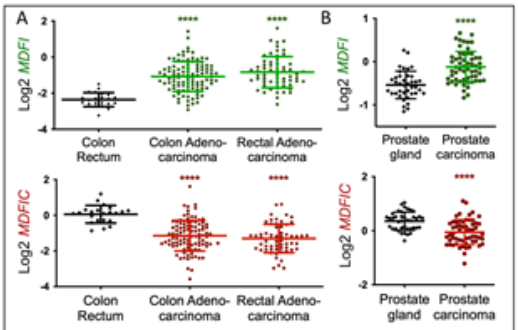

Fig. 1. Altered mRNA levels of *MDFI* and *MDFIC* in cancerous compared to healthy tissue. ****, P<0.0001. **A:** Colorectal tissues; **B:** Prostate tissues.

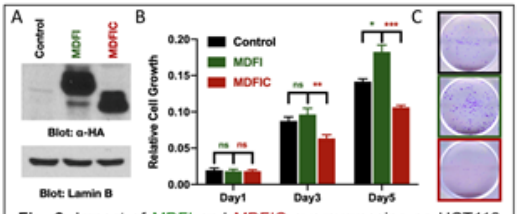

Fig. 2. Impact of MDFI and MDFIC overexpression on HCT116 cells. **A:** Western blot; **B:** Growth assay; **C:** Clonogenic assay.

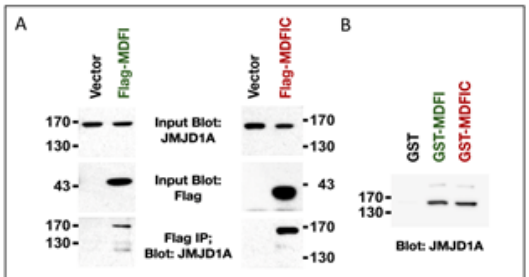

Fig. 3. Interaction of JMJD1A with MDFI and MDFIC. **A:** Co-immunoprecipitation of JMJD1A with MDFI and MDFIC; **B:** GST pull down assay with purified proteins.

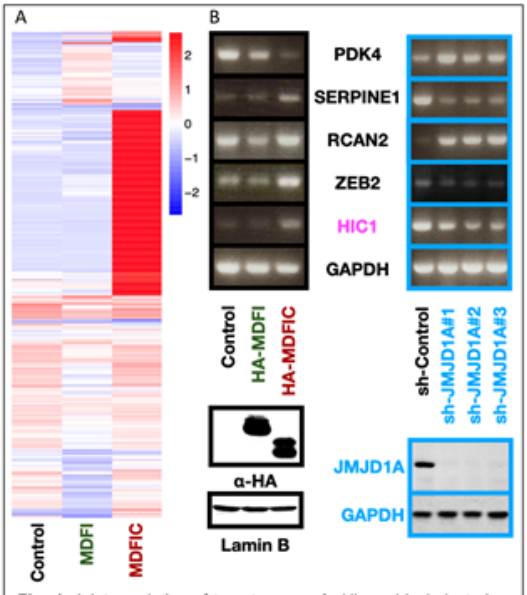

Fig. 4. Joint regulation of target genes. **A:** Hierarchical clustering of 525 target genes differentially regulated by MDFI and MDFIC. **B:** RT-PCR proving coregulation of several targets by JMJD1A.

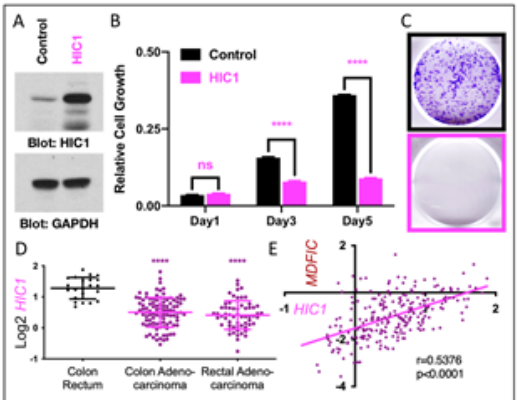

Fig. 5. Impact of HIC1 overexpression on HCT116 cancer cells. **A:** Western blot; **B:** Growth assay; **C:** Clonogenic assay; **D:** *HIC1* mRNA levels in normal and diseased colorectal tissues; **E:** Correlation between *HIC1* and *MDFIC* mRNA levels across all 234 samples shown in panel D. ****, P<0.0001.

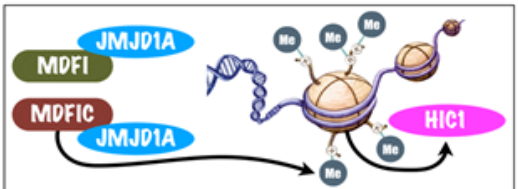

Fig. 6. Scheme of MDFI, MDFIC and JMJD1A interactions and resultant induction of HIC1 expression.

CONCLUSIONS

- First demonstration that MDFI and MDFIC are cancer-critical proteins;
- Perplexing potential opposite function of MDFI and MDFIC in colon, prostate and breast (not shown) cancer;
- MDFI and MDFIC can affect transcription through JMJD1A;
- Upregulation of *HIC1* by the MDFIC/JMJD1A complex may suppress colorectal tumorigenesis.

Acknowledgement: This work was in part funded by a seed grant from the Stephenson Cancer Center.

POLARIZED MACROPHAGES ALTER DNA METHYLATION AND GENE EXPRESSION IN COLON EPITHELIAL CELLS THROUGH A MICROBIOTA-INDUCED BYSTANDER EFFECT

Ram Babu Undi,[1,2] Hunter L. Porter [4], Adrian Filiberti,[1,2] Naushad Ali,[2,3] Jonathan D. Wren [4] and Mark M. Huycke [1,2]

[1]Department of Radiation Oncology, University of Oklahoma Health Sciences Center, Oklahoma City, OK 73104, USA.

[2]Stephenson Cancer Center, University of Oklahoma Health Sciences Center, Oklahoma City, OK 73104, USA.

[3]Department of Internal Medicine, Section of Digestive Diseases and Nutrition, University of Oklahoma Health Sciences Center, Oklahoma City, OK 73104, USA.

[4]Oklahoma Medical Research Foundation, Oklahoma City, OK 73104, USA.

Presenting author email: rambabu-undi@ouhsc.edu

Funding: R01-CA230641 (MMH)

Colitis-associated and sporadic colorectal cancer (CRC) arise from somatic mutations and epigenetic changes in tumor suppressors and oncogenes. The role of the intestinal microbiota in the initiation of CRC is poorly understood. One potential mechanism involves colon epithelial cell transformation due to chronically polarized macrophages. These cells produce endogenous mutagens and other diffusible factors that help drive cell transformation through the microbiota-induced bystander effect (MIBE).

To understand early responses of MIBE, young adult mouse colon epithelial (YAMC) cells were exposed to macrophages polarized to an M1 (lipopolysaccharide and interferon-γ) or M2 (IL-4) phenotype. DNA damage occurred in target cells as measured by γH2AX staining after exposure to either phenotype. RNAseq identified numerous pathways and protein interactions such as ubiquitination, hippo signaling, ER overload response, and lipid biosynthesis among others. Activation of signaling pathways was observed at the protein level by western blot (e.g., active β-Catenin and COX-2). In this same system, cells were repetitively exposed to M1-polarized macrophages or 4-hydroxy-2-nonenal (4-HNE) as a mutagen purified from M1 macrophages. Clones that were generated over 10 weeks were analyzed by whole genome sequencing, DNA methylation, and altered gene expression. Finally, to further assess MIBE *in vivo,* IL-10 knockout mice (*Il10*$^{-/-}$) were colonized with *Enterococcus faecalis* for 9 months and colon epithelial cells isolated.

These cells were grown as spheroids with or without niche (FGF, Noggin, Wnt3a, and R-Spondin).

In vitro study of YAMC cells and clones using RNAseq and high throughput bisulfite sequencing showed numerous changes in gene expression and DNA methylation. RNAseq showed upregulation of antigen processing pathways (ubiquitination) for cells exposed to M1 macrophages whereas countervailing downregulation was noted following exposure to M2 macrophages. Hypomethylation was identified near genes involved in cell adhesion and differentiation with additional changes noted in colon cancer driver genes. Colon epithelial cells isolated from *E. faecalis*-colonized IL-10 knockout mice that grew in the absence of growth factors formed poorly differentiated carcinomas in NOD-*scid* IL2Rg^{null} mice.

In conclusion, these results show that polarized macrophages alter gene expression and DNA methylation in target colon epithelial cells. Acute changes include DNA damage and dysregulation of antigen processing pathways. Finally, these data suggest polarized macrophages are capable of being cellular initiators of malignant transformation.

Polarized Macrophages alter DNA Methylation and Gene Expression in Colon Epithelial Cells Through a Microbiota-induced Bystander Effect

Ram Babu Undi,[1,2] Hunter L. Porter,[4] Adrian Filiberti,[1,2] Naushad Ali,[2,3] Jonathan D. Wren,[4] and Mark M. Huycke[1,2]

[1]Department of Radiation Oncology, [2]Stephenson Cancer Center, and [3]Section of Digestive Diseases and Nutrition in the Department of Internal Medicine, University of Oklahoma Health Sciences Center, and [4]Oklahoma Medical Research Foundation, Oklahoma City, OK 73104, USA.

ABSTRACT

Colitis-associated and sporadic colorectal cancer (CRC) arise from somatic mutations and epigenetic changes in tumor suppressors and oncogenes. The role of the intestinal microbiota in CRC initiation is poorly understood. One potential mechanism involves colon epithelial cell transformation due to chronic polarization of macrophages. These innate immune cells, when polarized, produce endogenous mutagens and other diffusible factors that can drive cell transformation through microbiota-induced bystander effects (MIBE).

To understand early responses of MIBE, young adult mouse colon (YAMC) cells were exposed to macrophages that were polarized to M1 or M2 phenotypes. Cells were also repetitively exposed to M1 macrophages or purified 4-hydroxy-2-nonenal (4-HNE) - a mutagen isolated from M1 macrophages. Clones were generated over 10 weeks. Acute DNA damage was measured in target cells by γH2AX staining. RNAseq of target cells identified numerous pathway and protein interactions (e.g., ubiquitination, hippo signaling, ER overload response, and lipid biosynthesis). Antigen processing was upregulated in cells exposed to M1 macrophages whereas downregulated in cells exposed to M2 macrophages. Western blotting showed activation of signaling and inflammatory pathways (e.g., β-catenin and COX-2). Acutely treated cells and clones derived after 10 weeks of treatment were also assessed using high throughput bisulfite sequencing and RNAseq. We have identified a number of significant changes in DNA methylation and gene expression DNA methylation was significantly enriched near genes involved in cell adhesion and differentiation. Collectively, these results show that classic and alternate polarized macrophages cause acute double-strand DNA damage in target cells. Changes in gene expression significantly enriched in dysregulation of antigen processing pathways after exposure to M1 macrophages. Exposure of clones to M1 macrophages (Fig.3B and C) showed a significant correlation between DNA methylation and gene expression of genes responsible for differentiation and at colon cancer driver genes.

BACKGROUND

The interaction of the colonic microbiota with immune cells to initiate colorectal cancer is poorly characterized. One potential mechanism involves mutation and transformation of colon epithelial cells by chronically polarized macrophages.

RESULTS

Acute changes due to the bystander effect

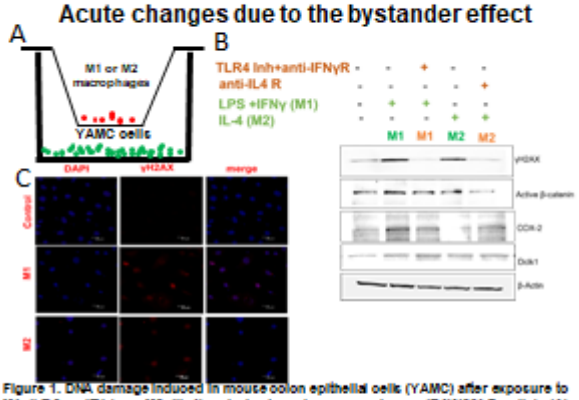

Figure 1. DNA damage induced in mouse colon epithelial cells (YAMC) after exposure to M1 (LPS + IFNγ) or M2 (IL-4) polarized murine macrophages (RAW264.7 cells). (A) Macrophages were cultured in upper compartment of a dual-chamber system with YAMC cells in lower compartment as target cells. (B) Protein expression of cellular proteins by western blot showed M1 and M2 macrophages (green) increased γh2ax, active β-catenin, COX2 and Ddk1 where as M1 and M2 macrophage blockers (red) inhibited(C) Immunofluorescence of γH2AX (red) is induced by both M1 and M2 macrophages.

Figure 2. (A) RNAseq-enriched terms for antigen processing and ubiquitination in YAMC cells that were acutely exposed to M1 (B) Protein interaction network of ubiquitination and antigen processing genes induced in YAMC cells exposed to M1 macrophages. (↓ is downregulated and ↑ is upregulated).

Methylation changes in 10-week treated clones

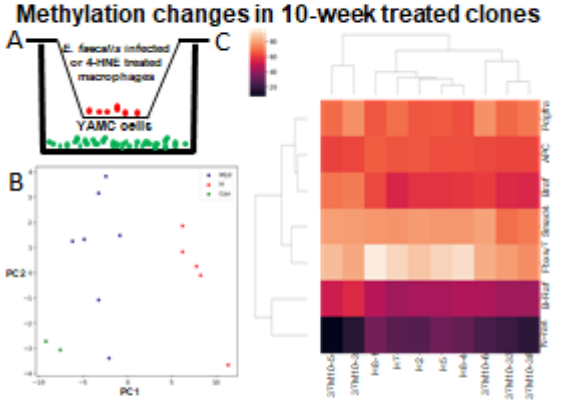

Figure 3. (A) YAMC clones generated by repeat exposure of *E. faecalis* or 4-HNE. (B) Molecular profiles identified in gene expression and (C) differential methylation in gene promoters of cancer driver genes after exposed to 4-HNE or M1-polarized macrophage.

Conclusions and future directions

Conclusions: Our results show that classic (M1) and alternate (M2) polarized macrophages alter gene expression and DNA methylation in target colon epithelial cells. Acute changes included DNA damage and dysregulation of antigen processing pathways. These data support polarized macrophages as drivers of cellular carcinogenesis.

Future directions: The role of antigen presentation and protein ubiquitination as an early event in MIBE is being investigated along with analyzing whole genome sequence data in conjunction with RNAseq and genome methylation to fully integrate the effects of MIBE in malignant transformation.

Acknowledgements: Nathan Shock Center on Aging **Funding:** R01-CA230641 (MMH)

Reference. Wang, X., et al. Commensal bacteria drive endogenous transformation and tumour stem cell marker expression through a bystander effect. Gut 64:459-468, 2015.

A NOVEL ACYL-COA SYNTHETASE PROMOTES PANCREATIC DUCTAL ADENOCARCINOMA PROGRESSION

Zhijun Zhou,[1,2] Jingxuan Yang,[1.2] Mingyang Liu,[1,2] Yuqing Zhang,[1,2]Xiuhui Shi,[1,2]Courtney Houchen,[1] Min Li,[1,2]
[1]Department of Medicine and [2]Department of Surgery, The University of Oklahoma Health Science Center, Oklahoma City, OK.

Background: Pancreatic ductal adenocarcinoma (PDAC) is characterized with dense stroma, which creates a nutrient deficient microenvironment. How PDAC cells survive in this nutrient deficient microenvironment remains elusive. Acyl-CoA Synthetase Short-Chain Family Member 2 (ACSS2) is an enzyme that converts acetate into acetyl-CoA. Emerging evidence has shown that ACSS2 grants tumor cells growth advantage under nutrient deficiency in several cancer types, such as breast cancer and glioblastoma. However, it remains uncharacterized whether and how ACSS2 promotes PDAC cell survival in a nutrient deficient microenvironment.

Methods: ACSS2 knockout and overexpressed stable cell lines were established by CRISPR/Cas9 system and lentivirus transfection. The function of ACSS2 was explored *in vitro*, *in vivo* and in patients' samples. The downstream pathway of ACSS2 was examined by in silico analysis, qPCR and western blotting.

Results: Nutrient deficient microenvironment can upregulate ACSS2 expression in AsPC-1 and CFPAC-1 cell lines. ACSS2 overexpression increased tumor growth while ACSS2 knockout decreased cell proliferation, especially under nutrient deficiency. *In vivo* study showed that ACSS2 knockout decreased tumor growth in an orthotopic PDAC mouse model. Mechanistic study identifies ZIP4, a zinc transporter, as a potential target of ACSS2. ACSS2 knockout can decrease ZIP4 transcription, and suppress the downstream AKT/GSK-3β pathway. ACSS2 overexpression upregulated ZIP4 expression. In silico analysis identified ETV4 as a potential transcript factor upstream of ZIP4. Overexpression of ETV4 can increase ZIP4 expression in PDAC cell lines. Human PDAC tissue showed higher expression of ACSS2 than that in adjacent benign pancreas tissue. High ACSS2 is associated with dismal prognosis in PDAC. ETV4/ZIP4 expression is positively correlated to ACSS2 expression in human PDAC tissue.

Conclusion: ACSS2 promotes tumor cell survival in nutrient deficient microenvironment by activating ETV4/ZIP4. Targeting this signaling pathway represents a novel therapeutic strategy in PDAC.

Presenting author: Zhijun Zhou, Zhijun-Zhou@ouhsc.edu

Acknowledgement of Funding: This work was supported in part by the William and Ella Owens Medical Research Foundation and the Department of Medicine at University of Oklahoma Health Sciences Center.

A Novel Acyl-CoA Synthetase Promotes Pancreatic Ductal Adenocarcinoma Survival in Nutrient Deficient Microenvironment

Z. Zhou, J. Yang, M. Liu, Y. Zhang, X. Shi, W. Luo, C. Houchen, M. Li.

Department of Medicine, Department of Surgery, The University of Oklahoma Health Sciences Center, Oklahoma City, OK

Abstract

Background: Pancreatic ductal adenocarcinoma (PDAC) is characterized with dense stroma, which creates a nutrient deficient microenvironment. How PDAC cells survive in this nutrient deficient microenvironment remains elusive. Acyl-CoA Synthetase Short-Chain Family Member 2 (ACSS2) is an enzyme that converts acetate into acetyl-CoA. Emerging evidence has shown that ACSS2 grants tumor cells growth advantage under nutrient deficiency in several cancer types, such as breast cancer and glioblastoma. However, it remains uncharacterized whether and how ACSS2 promotes PDAC cell survival in a nutrient deficient microenvironment.

Methods: ACSS2 knockout and overexpressed stable cell lines were established by CRISPR/Cas9 system and lentivirus transfection. The function of ACSS2 was explored in vitro, in vivo and in patients' samples. The downstream pathway of ACSS2 was examined by in silico analysis, qPCR and western blotting.

Results: Nutrient deficient microenvironment can upregulate ACSS2 expression in AsPC-1 and CFPAC-1 cell lines. ACSS2 overexpression increased tumor growth while ACSS2 knockout decreased cell proliferation, especially under nutrient deficiency. In vivo study showed that ACSS2 knockout decreased tumor growth in an orthotopic PDAC mouse model. Mechanistic study identifies a zinc transporter, ZIP4, as a potential target of ACSS2. ACSS2 knockout can decrease ZIP4 transcription, and suppress the downstream AKT/GSK-3β pathway. ACSS2 overexpression upregulated ZIP4 expression. In silico analysis identified ETV4 as a potential transcript factor upstream of ZIP4. Overexpression of ETV4 can increase ZIP4 expression in PDAC cell lines. Human PDAC tissue showed higher expression of ACSS2 than that in adjacent benign pancreas tissue. High ACSS2 is associated with dismal prognosis in PDAC. ETV4/ZIP4 expression is positively correlated to ACSS2 expression in human PDAC tissue.

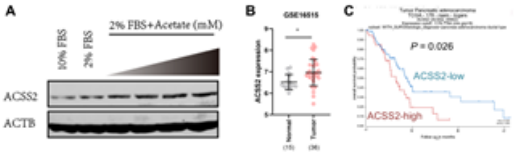

Fig.1 ACSS2 is upregulated in metabolic stress and in PDAC tissue.

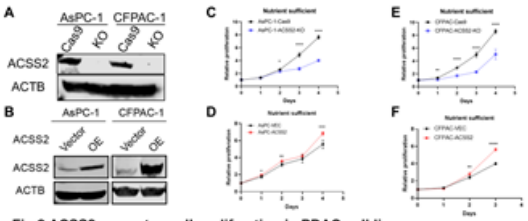

Fig.2 ACSS2 promotes cell proliferation in PDAC cell lines.

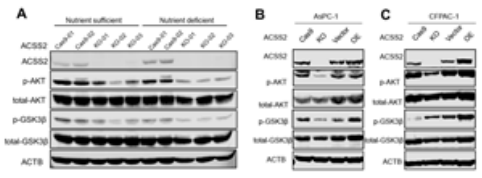

Fig.3 ACSS2 regulates AKT/GSK3B pathway.

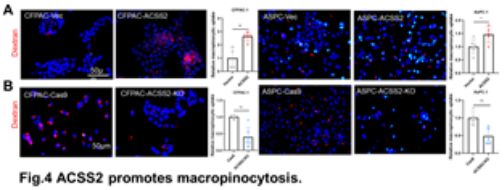

Fig.4 ACSS2 promotes macropinocytosis.

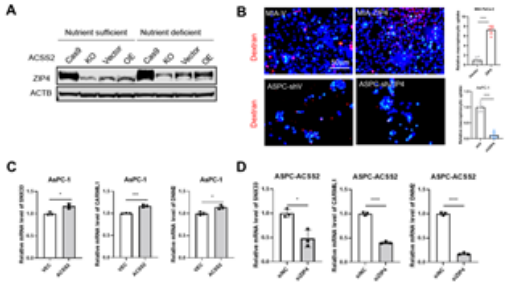

Fig.5 ACSS2 promoted macropinocytosis is dependent on ZIP4.

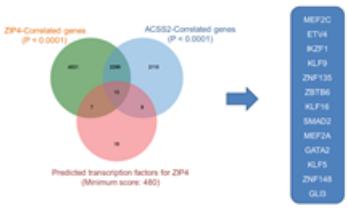

Fig.6 Predicted transcription factors for ZIP4.

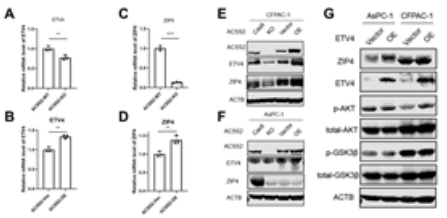

Fig.7 ACSS2 upregulates ZIP4 via ETV4

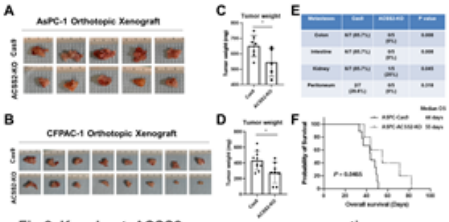

Fig.8 Knockout ACSS2 can suppress pancreatic cancer progression in orthotopic mouse model.

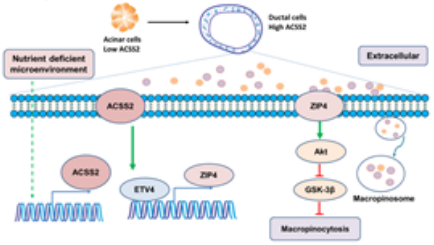

Fig.9 Schematic diagram showing ACSS2 promotes macropinocytosis via ZIP4/AKT/GSK3B pathway in PDAC .

Conclusion: ACSS2 promotes pancreatic cancer cell survival in nutrient deficient microenvironment by activating ETV4/ZIP4, thus representing a novel therapeutic target in PDAC.

Acknowledgements:
This work was supported by NIH grants R01CA138701, R01CA186338-01A1, R01CA203108-01, R01CA247234-01, P30CA225520.

Email: Min-Li@ouhsc.edu

Cancer Control & Prevention

CANCER CONTROL AND PREVENTION POSTERS

POSTER PRESENTATION LIST

Listed A-Z by Presenter Last Name

QUIT STAGE AND INTERVENTION TYPE DIFFERENCES IN THE MOMENTARY WITHIN-PERSON ASSOCIATION BETWEEN NEGATIVE AFFECT AND SMOKING URGES
Lizbeth Benson

PREVALENCE OF MARIJUANA USE AND CO-USE AMONG COMBUSTIBLE TOBACCO AND ELECTRONIC CIGARETTE USERS
Mayilvanan Chinnaiyan

PATTERNS OF ALCOHOL, TOBACCO, AND CANNABIS USE AMONG SEXUAL MINORITY AND HETEROSEXUAL FEMALES: IMPLICATIONS FOR CANCER RISK
Sarah J. Ehlke

SMOKING STATUS FOLLOWING LARYNGEAL CANCER DIAGNOSIS DETERMINES TREATMENT RESPONSE AND LARYNGECTOMY-FREE SURVIVAL
Jacey Elliott

DO CHANGES IN PATIENT-REPORTED COGNITION EXPLAIN CHANGE IN COGNITIVE PERFORMANCE DURING TAXANE CHEMOTHERAPY FOR WOMEN'S CANCERS?
Ashley Fox

PEPTIDE AGGREGATION INDUCED IMMUNOGENIC RUPTURE (PAIIR)
Gokhan Gunay

FUSION OF HANDCRAFTED AND DEEP TRANSFER LEARNING FEATURES TO IMPROVE PERFORMANCE OF BREAST LESION CLASSIFICATION
Meredith A. Jones

EFFECT OF TOBACCO CESSATION ON TREATMENT RESPONSE AND LONG-TERM SURVIVAL IN ORAL AND OROPHARYNGEAL CANCER
Matthew Krutz

PUFFING TOPOGRAPHY AMONG EXCLUSIVE COMBUSTIBLE CIGARETTE USERS AND DUAL USERS OF CIGARETTES AND POD-BASED OR MOD-BASED ELECTRONIC CIGARETTES
Austin Milton

NEGATIVE AFFECT AND STRESS ARE ASSOCIATED WITH MOMENT-TO-MOMENT CHANGE IN MOTIVATION DURING A SMOKING CESSATION ATTEMPT
Jiwon Min

EPIDEMIOLOGY OF LUNG CANCER IN OKLAHOMA, 2014-2018
Shayla R. Morin

CANCER CONTROL AND PREVENTION POSTERS

THE RELATION BETWEEN INSOMNIA SEVERITY AND SMOKING CESSATION OUTCOMES AMONG ADULTS PARTICIPATING IN TREATMENT: A LONGITUDINAL STUDY
Chaelin K. Ra

INTRA-SESSION RELIABILITY IN 1ST-RAY FORCE CONTRIBUTION TO PUSH-OFF DURING NEUROTOXIC CHEMOTHERAPY
Josiah Rippetoe

SECONDHAND SMOKE EXPOSURE ALTERS DRUG TRANSPORTERS AND INDUCES CISPLATIN-RESISTANT IN HEAD AND NECK CANCER CELLS
Balaji Sadhasivam

FACILITATORS AND BARRIERS TO LUNG CANCER SCREENING IMPLEMENTATION IN THE U.S: A SYSTEMATIC REVIEW
Ami E. Sedani

GAIT ANALYSIS USING DATA-DRIVEN LEARNING METHODS ON SPATIOTEMPORAL PLANTAR FORCE DATASET BY TEKSCAN STRIDEWAY SYSTEM
Kangjun Seo

QUIT STAGE AND INTERVENTION TYPE DIFFERENCES IN THE MOMENTARY WITHIN-PERSON ASSOCIATION BETWEEN NEGATIVE AFFECT AND SMOKING URGES

Lizbeth Benson,[1] Chaelin Karen K. Ra,[1] Emily T. Hébert,[2] Darla E. Kendzor,[1,3] Jason A. Oliver,[1,3] Summer G. Frank-Pearce,[1,4] Jordan M. Neil, [1,3] & Michael S. Businelle[1,3]

[1]TSET Health Promotion Research Center, Stephenson Cancer Center, University of Oklahoma Health Sciences Center, Oklahoma City, OK, United States

[2]Department of Health Promotion and Behavioral Sciences, UT Health School of Public Health, Austin, TX, United States

[3]Department of Family and Preventive Medicine, University of Oklahoma Health Sciences Center, Oklahoma City, OK, United States

[4]Department of Biostatistics and Epidemiology, Hudson College of Public Health, The University of Oklahoma Health Sciences Center, Oklahoma City, OK, United States

Presenting author's email address: lizbeth-benson@ouhsc.edu

Background: Smoking urges and negative affect play important roles in daily cigarette smoking and smoking lapse during a cessation attempt. Traditionally, laboratory research has considered negative affect as a potential cause of smoking urges. A deeper understanding of momentary associations between negative affect and smoking urges during a smoking cessation attempt can inform treatment development efforts. This study examined whether the within-person association between negative affect and smoking urges differed before and after a quit attempt, and by intervention type.

Methods: Data are from a pilot randomized controlled trial comparing 3 smoking cessation interventions. Participants were randomly assigned to: 1) a novel, smartphone-based just-in-time adaptive intervention that tailored treatment content in real-time (Smart-T2; *n*=24), 2) the National Cancer Institute QuitGuide app (*n*=25), or 3) a clinic-based tobacco cessation program (TTRP; *n*=23) that followed Clinical Practice Guidelines. All participants received up to 12 weeks of nicotine replacement therapy and completed up to 5 assessments per day ($M_{PreQuit}$=25.8 assessments, *SD*=6.0; $M_{PostQuit}$=107.7 assessments, *SD*=37.1) of their negative affect and smoking urges during the 7 days (*M*=6.6 days, *SD*=1.0) prior to their quit-date and the 29 days (*M*=25.8 days, *SD*=6.4) after their quit-date. Prior to analysis, repeated measures of smoking urges were decomposed into between-person and within-person components.

Results: After accounting for baseline nicotine dependence, Bayesian multilevel models indicated that the extent of within-person association between negative affect and smoking urges was stronger in the post-quit stage of the intervention than the pre-quit stage. Results also indicated that in the post-quit stage of the intervention, the within-person association between negative affect and smoking urges was weaker for those in the Smart-T2 and TTRP groups compared with those in the QuitGuide group. The extent of this within-person association did not differ between those in the Smart-T2 and TTRP groups.

Conclusions: These findings offer preliminary evidence that the momentary within-person association between negative affect and smoking urges increases following a quit attempt, and that the TTRP and Smart-T2 interventions may weaken this association. Research is needed to

replicate and expand upon current findings in a fully powered randomized controlled trial.

Trial Registration: ClinicalTrials.gov NCT02930200; https://clinicaltrials.gov/show/NCT02930200

Acknowledgement of Funding: This study was supported by the Oklahoma Tobacco Settlement Endowment Trust (grant number 092-016-0002) and used the mobile health shared resource of the Stephenson Cancer Center via an NCI Cancer Center Support Grant (grant number P30CA225520). Manuscript preparation was additionally supported by the National Institute on Drug Abuse of the National Institutes of Health under award number R00DA046564. The content is solely the responsibility of the authors and does not necessarily represent the official views of the National Institutes of Health.

TSET Health Promotion Research Center

OU Health | Stephenson Cancer Center

Quit Stage and Intervention Type Differences in the Momentary Within-Person Association between Negative Affect and Smoking Urges

Lizbeth Benson,[1] Chaelin K. Ra,[1] Emily T Hébert,[2] Darla E. Kendzor,[1,3] Jason A. Oliver,[1,3] Summer Frank-Pearce,[1,4] Jordan M. Neil,[1,3] & Michael S. Businelle[1,3]

[1]TSET Health Promotion Research Center, Stephenson Cancer Center, University of Oklahoma Health Sciences Center (OUHSC); [2]Department of Health Promotion and Behavioral Sciences, UT Health School of Public Health; [3]Department of Family and Preventive Medicine, OUHSC; [4]Department of Biostatistics and Epidemiology, Hudson College of Public Health, OUHSC

INTRODUCTION

Background:

- Cigarette smoking is the leading preventable cause of death
- Smoking cessation smartphone apps could:
  - Increase treatment accessibility
  - Capture people's experiences via ecological momentary assessment (EMA)
  - Inform development of Just-in-time adaptive interventions (JITAIs)
- Smoking urges and negative affect are risk factors for smoking cessation lapse

Present Study:

- Examined within-person associations between momentary negative affect and smoking urges (a) before and after a quit attempt, (b) by intervention type

METHOD

Participants (*N*=72):

- Recruited during a Tobacco Treatment Research Program (TTRP) clinic visit
  Participants were 50 years old (Range=23-73 years), 49% female, 64% White

Procedures (approved by the OUHSC IRB):

- Study provided study phones
- 5 EMAs/day via smartphone: 7 days pre-quit, 28 days post-quit

Intervention Types: all groups received nicotine replacement therapy

- SmartT2 (*n*=24): novel smartphone app, delivers tailored smoking risk messages
- QuitGuide (*n*=25): National Cancer Institute smartphone app with quit tips
- TTRP (*n*=23): clinic-based tobacco cessation treatment, once per week visit

Measures:

- Rating Scale: strongly disagree (=1) to strongly agree (=5)
- *Negative Affect:* irritable, frustrated, worried, restless, anxious, stress
- *Smoking Urges:* "I have an urge to smoke"

Analysis Plan:

- Inclusion criteria: 5 complete assessments during pre- and post-quit stages
  - $M_{Pre\text{-}Quit}$: 26 assessments; $M_{Post\text{-}Quit}$: 108 assessments
- Bayesian multilevel models: moments (*t*) nested within persons (*i*)

RESULTS: CHANGE ACROSS QUIT STAGE

- In moments when individuals' smoking urges were higher than usual, their negative affect also tended to be higher than usual (γ=0.11, 95% *CI*=[0.07, 0.16])
- The strength of the within-person association between negative affect and smoking urges differed across participants (faint background lines; σ=0.16, 95% *CI*=[0.12, 0.19])
- Stronger within-person association between negative affect and smoking urges during the post-quit phase (green, solid line) compared with the pre-quit phase (coral dashed line) (γ=0.06, 95% *CI*=[0.02, 0.10])

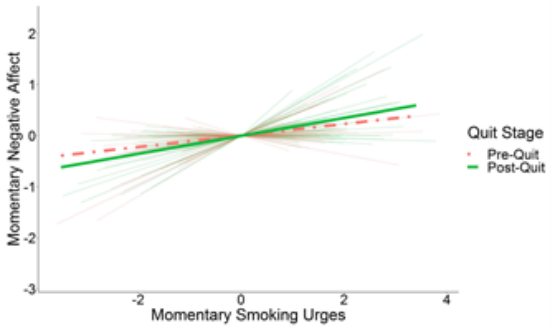

RESULTS: INTERVENTION TYPE DIFFERENCES

- Those who received Smart-T2 (solid green line) and TTRP (dotted blue line) showed a weaker within-person association between their momentary experiences of smoking urges and negative affect compared to those who received QuitGuide (coral dot-dash line) (γ=0.11, 95% *CI*=[0.01, 0.21]; γ=0.16, 95% *CI*=[0.04, 0.27])
- No differences between Smart-T2 and TTRP in the within-person association between smoking urges and negative affect (γ=-0.1, 95% *CI*=[-0.2, 0.0])

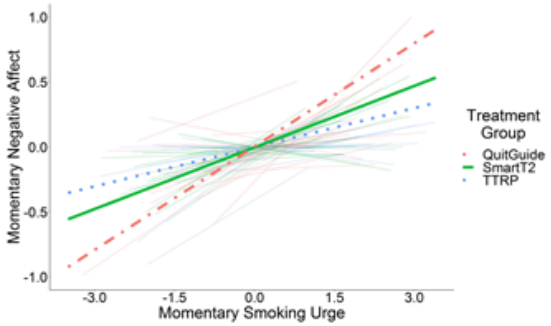

LIMITATIONS & FUTURE DIRECTIONS

Sample size: pilot study that may not be powered to adequately detect between-group differences

- Follow-up study underway with larger sample size

Modeling strategy: assumed stable post-quit association

- Future work: bidirectional and time varying-associations

CONCLUSIONS

Present Study Contributions:

- Momentary coupling between smoking urges and negative affect
- Extent of coupling between urges and negative affect increases post-quit
- Smartphone apps that deliver messages tailored to smoking risk factors may weaken the extent of coupling in service of smoking cessation

ACKNOWLEDGEMENTS

This study was supported by the Oklahoma Tobacco Settlement Endowment Trust (R21-02) and used the mobile health shared resource of the Stephenson Cancer Center via an NCI Cancer Center Support Grant (P30CA225520). Abstract preparation was additionally supported by the National Institute on Minority Health and Health Disparities (1K01MD015295-01A1).

PREVALENCE OF MARIJUANA USE AND CO-USE AMONG COMBUSTIBLE TOBACCO AND ELECTRONIC CIGARETTE USERS

Mayilvanan Chinnaiyan[1], Geraldine Chissoe[1], Pawan Acharya[4], Balaji Sadhasivam[1], Vengatesh Ganapathy[1], Daniel Brobast[1], Katie Johnson[1], Yan D. Zhao[4], Lurdes Queimado[1-3]

Departments of [1]Otorhinolaryngology, [2]Cell Biology, and [4]Biostatistics & Epidemiology. [3]TSET Health Promotion Research Center, Stephenson Cancer Center, The University of Oklahoma Health Sciences Center, Oklahoma.
Presenter email: Mayilvanan-Chinnaiyan@ouhsc.edu

Background: Tobacco use is the main cause of preventable death in the United States and an important health behavior to study among young adults. Cigarette smoking has been implicated as an initiation and gateway to marijuana and other illicit drugs use. In 2019, among young adults aged 18 to 25, the marijuana users increased from 29.8% (or 9.2 million people) to 35.4% (or 12.0 million people) in US. Tobacco and cannabis (marijuana) co-use are among the most common psychoactive substances used worldwide and are often used in combinations, either simultaneously or sequentially or by the same individual at different times in a day. Co-use of tobacco and cannabis smoke increases toxicant exposure, cancer risk, and other negative health effects. Although, e-cigarette use has increased alarmingly in recent years among teens and adults, there is limited knownledge about the frequency of co-use of cannabis and e-cig and the corresponding health effects.

Aim: 1. To estimate the prevalence of marijuana/cannabis use among young adults in Oklahoma metropolitan population. 2. To characterize the frequency of cannabis use among exclusive smokers (S), exclusive electronic cigarette (EC) users, dual users of combustible cigarette and e-cigarette (DU), and non-smokers/non-vapers (NS/NV).

Methods: Participants were recruited through mass e-mail, flyers, and facebook and twitter ads. Based on the online survey answers, participants were classified as exclusive smokers (S), dual users of combustible cigarette & e-cigarettes (DU), exclusive electronic cigarette users (EC) and non-smokers/non-vapers (NS/NV). Participants reported on whether they use marijuana and other drugs in the past 3 months. Survey was conducted between March 2021 to January 2022. Data were analyzed using independent t-test, ANOVA and Chi-square test. Logistic regression analysis was used to estimate the association between tobacco product user status and marijuana use.

Results: 784 participants were included in this study, of whom about half were women (N=390). There were 180 non-smokers, 143 exclusive smokers, 314 exclusive e-cigarette users, and 147 dual users of combustible cigarettes & e-cigarettes. Exclusive smokers (26±4 years) were significantly older than all other groups (23±4 years). Among all surveyed, prevalence of marijuana use was over 50%. The lowest prevalence was among non-tobacco product users (20%) and the highest was among exclusive EC users (68%). The odds of being using marijuana was 8 times higher among exclusive EC users [OR=8.27; 95%CI: 5.36-12.75] than among non-tobacco product users.

Conclusion: Our preliminary data shows that, among the surveyed population, over 20% of non-users of tobacco products reported using marijuana in the last 3 months. Among tobacco product users, exclusive EC users had the highest proportion of marijuana users followed by dual users and tobacco users. These type of studies are essential to develop and implement measures essential to reduce the risks associated long-term effects of substance abuse.

Grant support: This work was supported by NIH/NCI (R01CA242168, Queimado) and the Oklahoma Tobacco Settlement Endowment Trust. Dr. Queimado holds a Presbyterian Health Foundation Endowed Chair in Otorhinolaryngology.

TSET Health Promotion Research Center

OU Health | Stephenson Cancer Center

Prevalence of marijuana use and co-use among combustible tobacco and electronic cigarette users

Mayilvanan Chinnaiyan[1], Geraldine Chissoe[1], Pawan Acharya[4], Balaji Sadhasivam[1], Vengatesh Ganapathy[1], Daniel Brobast[1], Katie Johnson[1], Yan D. Zhao[4], Lurdes Queimado[1-3]

Departments of [1]Otorhinolaryngology, [2]Cell Biology, and [4]Biostatistics & Epidemiology. [3]TSET Health Promotion Research Center, Stephenson Cancer Center, The University of Oklahoma Health Sciences Center, Oklahoma.

Background

- Diversified tobacco products and cannabis legalization in many US states are associated with increased use.
- Oklahoma ranks 1 in the nation, with roughly 10% of the population having obtained a medical marijuana card in the past 2 years.
- Cannabis and tobacco smoke contain toxicants and carcinogens. Co-use may additively increase the risk.
- In 2020, 34.5% of young adults (18-25 y) were using marijuana, which was higher than other age groups.
- Smoking prevalence is decreasing nationally but, emerging nicotine products and electronic cigarettes (e-cig) use increased during the past years.
- E-cig and cannabis co-use trend is increasing among young adults in recent years. A national study reported that, among high school students, nearly four-in-ten current e-cig users also used marijuana or tetrahydrocannabinol (THC) related products.

Objectives

- To estimate the prevalence of marijuana/cannabis use among young adults in Oklahoma City metropolitan population.
- To characterize the frequency of cannabis use among exclusive smokers (S), exclusive electronic cigarette (EC) users, dual users of combustible cigarette and e-cigarette (DU), and non-smokers/non-vapers (NS/NV).

Study Methods

- Participants were recruited through mass e-mail, flyers and facebook ads.
- Participants tobacco products use habits, and past 3 months marijuana use details were collected by completing a survey.
- Based on survey answers, participants were classified as exclusive smokers (S), dual users of combustible cigarette & e-cigarettes (DU), exclusive electronic cigarette users (EC), and non-smokers/non-vapers (NS/NV).
- Data analysis was performed using independent t-test, ANOVA, Chi-square test and logistic regression analysis.

Results

Table 1. Participants demographics.

	Non-smokers/ Non-vapers (NS/NV)	Exclusive smokers (S)	Exclusive EC Users (EC)	Dual users (Tob Cig + E-cig)
Count (#)	180	143	314	147
Percentage (%)	23	18	40	19
Sex (M:F)	56:124	66:77	179:134	92:55
Age	26±4	29±4	26±4	26±4

Table 2. Marijuana use among different groups.

	Non-smokers/ Non-vapers (NS/NV)	Exclusive smokers (S)	Exclusive EC Users (EC)	Dual users (Tob Cig + E-cig)
Marijuana Use (%)	20.56	51.75	68.15	57.82

- There was significant difference across the groups. ($p<0.0001$).

Results

Figure 1. Logistic regression analysis of marijuana use between groups ($p<0.0001$).

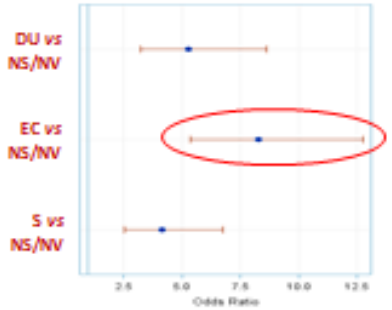

Table 3. Odds Ratio Estimates

Effect	Point Estimate	95% Wald Confidence Limits	
DU vs NS/NV	5.299	3.254	8.629
EC vs NS/NV	8.271	5.367	12.746
S vs NS/NV	4.145	2.544	6.753

Conclusions

- Exclusive EC users had the highest proportion of marijuana users (68%) followed by dual users (58%) and tobacco users (52%).
- Over 20% of non-users of tobacco products reported using marijuana in the last 3 months.
- These findings are essential to implement important measures to reduce long-term effects of substance abuse.

Grant support: NIH/NCI (R01CA242168) and Oklahoma Tobacco Settlement Endowment Trust (TSET). Dr. Queimado holds a PHF Endowed Chair in ORL.

PATTERNS OF ALCOHOL, TOBACCO, AND CANNABIS USE AMONG SEXUAL MINORITY AND HETEROSEXUAL FEMALES: IMPLICATIONS FOR CANCER RISK

Sarah J. Ehlke[a], Darla E. Kendzor[a,b], Michael A. Smith[a,c], Munjireen Sifat[a], Laili K. Boozary[a,d] & Amy M. Cohn[a,e]
[a]TSET Health Promotion Research Center, Stephenson Cancer Center, The University of Oklahoma Health Sciences Center
[b]Department of Family and Preventive Medicine, The University of Oklahoma Health Sciences Center
[c]Hudson College of Public Health, The University of Oklahoma Health Sciences Center
[d]Department of Psychology, Cellular and Behavioral Neurobiology, The University of Oklahoma
[e]Department of Pediatrics, The University of Oklahoma Health Sciences Center
Department: TSET Health Promotion Research Center, Stephenson Cancer Center, University of Oklahoma Health Sciences Center
Acknowledgements: This study was primarily supported by Oklahoma Tobacco Settlement Endowment Trust contract R21-02. Additional support was provided by National Cancer Institute Cancer Center Support Grant P30CA225520 awarded to the Stephenson Cancer Center.

Sexual minority females (SMF) have higher rates of alcohol, tobacco, and cannabis use compared to heterosexual women. The co-use of alcohol and tobacco are associated with increased risk of head and neck cancer, and the co-use of cannabis and tobacco is associated with higher prevalence of combustible tobacco product use, a primary cancer risk factor, compared to tobacco-only use. Few studies have examined sexual identity disparities of co-use and polysubstance use (use of ≥ three substances), which are each associated with greater health consequences. The current study examined differences between SMF and heterosexual women on patterns of past 30-day alcohol, tobacco, and cannabis use.

Participants were adult females (*N*=3020; 18.6% SMF) from Oklahoma who were recruited through an online panel for a cross-sectional three-wave study. Participants reported on their past 30-day alcohol, tobacco (cigarette, e-cigarette, cigar/little cigar or cigarillos [LCCs], and other tobacco products), and cannabis use. A single past 30-day substance use grouping variable was created to capture patterns of use: 1) no substance use, 2) alcohol use only, 3) tobacco use only, 4) cannabis use only, 5) alcohol and tobacco co-use, 6) alcohol and cannabis co-use, 7) tobacco and cannabis co-use, and 8) alcohol, tobacco, and cannabis (i.e., polysubstance) use. Chi-square analyses examined differences between heterosexual and SMF on substance use. A multinomial logistic regression model examined the association between sexual identity and substance use grouping, controlling for demographic factors.

Compared to heterosexual women, more SMF reported past 30-day use of e-cigarettes (14.9% vs. 27.9%), cigars/LCCs (10.9% vs. 19.4%), other tobacco products (4.7% vs. 8.6%), any tobacco product (40.3% vs. 51.3%), and cannabis (29.1% vs. 53.0%; *p*'s<.001). Sexual identity was not related to past 30-day cigarette (31.7% vs. 32.4%) or alcohol use (45.8% vs. 48.8%). Compared to heterosexual women, SMF were more likely to be cannabis only (AOR = 2.54, 95% CI: 1.56, 4.14), tobacco and cannabis (AOR = 1.73, 95% CI: 1.17, 2.55), alcohol and cannabis (AOR = 2.48, 95% CI: 1.57, 3.93), and polysubstance users (AOR =

2.58, 95% CI: 1.88, 3.53), relative to a non-user. There were no differences based on sexual identity between the likelihood of being a tobacco only, alcohol only, and alcohol and tobacco user, relative to non-user.

SMF have double the rates of cannabis use, relative to heterosexual women. Given their higher rates of polysubstance use, SMF may be at greater risk of health problems, including increased cancer risk due to the combined use of alcohol, tobacco, and cannabis together. SMF may benefit from interventions focused on polysubstance use, and particularly cannabis use, in order to reduce cancer-risk in this vulnerable group.

TSET Health Promotion Research Center

OU Health | Stephenson Cancer Center

Patterns of Alcohol, Tobacco, and Cannabis Use among Sexual Minority and Heterosexual Females: Implications for Cancer Risk

Sarah J. Ehlke[1], Darla E. Kendzor[1,2], Michael A. Smith[1,3], Munjireen Sifat[1], Laili K. Boozary[1,4], & Amy M. Cohn[1,5]

[1]TSET Health Promotion Research Center, Stephenson Cancer Center, OUHSC, [2]Department of Family and Preventative Medicine, OUHSC, [3]Hudson College of Public Health, [4]Department of Psychology, Cellular and Behavioral Neurobiology, OU, [5]Department of Pediatrics, OUHSC

Background

- Sexual minority females have higher rates of alcohol, tobacco, and cannabis use compared to heterosexual women.
- The co-use of alcohol and tobacco are associated with increased risk of head and neck cancer, and the co-use of cannabis and tobacco is associated with higher prevalence of combustible tobacco product use, a primary cancer risk factor, compared to tobacco-only use.
- Few studies have examined sexual identity disparities of co-use (2 substances) and polysubstance use (use of ≥ 3 substances), which are each associated with greater health consequences.

Objective

- To examine unique patterns of past 30-day tobacco, alcohol, and cannabis use and co-use (no use, single use, co-use, and polysubstance use).
- To examine differences between heterosexual and sexual minority females on patterns of past 30-day substance use.

Study Design

- N = 3,020 adult (≥ 18 years old) females who lived in Oklahoma and completed a brief online survey about cannabis use and related behaviors.

Measures

- **Demographic information**
- **Sexual Identity**
  - "Do you consider yourself to be:"
    - Heterosexual/Straight
    - Sexual minority female (lesbian/gay, bisexual, other, questioning, queer, or don't know/not sure)
- **Past 30-day Substance Use**
  - Tobacco
    - Cigarettes, e-cigarettes, large cigars/LCCs, other tobacco products (e.g., hookah, chew)
  - Alcohol
  - Cannabis
    - Combined medical and non-medical use

Data Analysis

- Single past 30-day patterns of substance use: 1) no substance use, 2) alcohol use only, 3) tobacco use only, 4) cannabis use only, 5) alcohol and tobacco co-use, 6) alcohol and cannabis co-use, 7) tobacco and cannabis co-use, and 8) alcohol, tobacco, and cannabis (i.e., polysubstance) use
- Chi-square tests examined differences between heterosexual and sexual minority females on substance use.
- A multinomial logistic regression model examined the association between sexual identity and substance use grouping, controlling for demographic factors.

Results

Table 1. Demographic Characteristics of Heterosexual and Sexual Minority Females

	Overall Sample N=3,020 n (%)	Heterosexual Females n=2,478, 81.2% n (%)	Sexual Minority Females n=573, 18.8% n (%)
Age			
18-24	673 (22.3%)	426 (17.3%)	247 (44.0%)
25-34	669 (22.2%)	509 (20.7%)	160 (28.5%)
35-44	525 (17.4%)	436 (17.7%)	89 (15.9%)
45-54	460 (15.2%)	422 (17.2%)	38 (6.8%)
55-64	401 (13.3%)	386 (15.7%)	15 (2.7%)
65 years old+	292 (9.7%)	280 (11.4%)	12 (2.1%)
Race/Ethnicity			
NH White	2153 (71.3%)	1813 (73.7%)	340 (60.6%)
NH Black	224 (7.4%)	172 (7.0%)	52 (9.3%)
NH Other	430 (14.2%)	320 (13.0%)	110 (19.6%)
Hispanic	213 (7.1%)	154 (6.3%)	59 (10.5%)
Relationship Status			
Single	767 (25.4%)	547 (22.2%)	220 (39.2%)
In a relationship	640 (21.2%)	455 (18.5%)	185 (33.0%)
Married	1083 (35.9%)	980 (39.9%)	103 (18.4%)
Other	530 (17.5%)	477 (19.4%)	53 (9.4%)
Employment			
Employed	1389 (46.0%)	1138 (46.3%)	251 (44.7%)
Unemployed	424 (14.0%)	309 (12.6%)	115 (20.5%)
Homemaker	363 (12.0%)	307 (12.5%)	56 (10.0%)
Student	154 (5.1%)	96 (3.9%)	58 (10.3%)
Retired	301 (10.0%)	290 (11.8%)	11 (2.0%)
Disabled	297 (9.8%)	251 (10.2%)	46 (8.2%)
Other	92 (3.0%)	68 (2.8%)	24 (4.3%)
Income			
≤ $19,999	875 (30.7%)	672 (28.8%)	203 (39.3%)
$20,000 - $39,999	798 (28.0%)	648 (27.8%)	150 (29.0%)
$40,000 - $59,999	486 (17.0%)	410 (17.6%)	76 (14.7%)
$60,000 - $79,999	290 (10.2%)	245 (10.5%)	45 (8.7%)
$80,000 - $99,9999	168 (5.9%)	148 (6.3%)	20 (3.9%)
≥ $100,000	235 (8.2%)	212 (9.1%)	23 (4.4%)

Results (cont.)

Table 2. Differences in Heterosexual and Sexual Minority Females on Past 30-day Substance Use

	Total n (%)	Heterosexual Females n (%)	Sexual Minority Females n (%)	p
Past 30-day Use				
Cigarette Use	954 (31.8%)	774 (31.7%)	180 (32.4%)	.752
E-cigarette Use	518 (17.3%)	363 (14.9%)	155 (27.9%)	<.001
Cigar/LCC Use	373 (12.4%)	265 (10.9%)	108 (19.4%)	<.001
Other Tobacco Use	164 (5.5%)	116 (4.7%)	48 (8.6%)	<.001
Any Tobacco Use	1273 (42.3%)	987 (40.3%)	286 (51.3%)	<.001
Alcohol Use	1390 (46.3%)	1119 (45.8%)	271 (48.8%)	.194
Cannabis Use	985 (33.5%)	697 (29.1%)	288 (53.0%)	<.001
Substance Use Group				<.001
No Use	906 (30.9%)	767 (32.1%)	139 (25.6%)	
Tobacco Only	276 (9.4%)	239 (10.0%)	37 (6.8%)	
Alcohol Only	501 (17.1%)	456 (19.1%)	45 (8.3%)	
Cannabis Only	133 (4.5%)	94 (3.9%)	39 (7.2%)	
Alcohol and Tobacco	263 (9.0%)	229 (9.6%)	34 (6.3%)	
Tobacco and Cannabis	255 (8.7%)	193 (8.1%)	62 (11.4%)	
Alcohol and Cannabis	156 (5.3%)	116 (4.9%)	40 (7.4%)	
Polysubstance Use	440 (15.0%)	293 (12.3%)	147 (27.1%)	

Table 3. Multinomial Logistic Regression Models of Associations between Sexual Identity and Past 30-day Substance Use (vs No Use): Significant Effects Presented

	Cannabis Only (vs. No Use) AOR (95% CI)	Tobacco and Cannabis (vs. No Use) AOR (95% CI)	Alcohol and Cannabis (vs. No Use) AOR (95% CI)	Polysubstance Use (vs. No Use) AOR (95% CI)
Sexual Identity				
Heterosexual	REF	REF	REF	REF
Sexual Minority	2.54 (1.56, 4.14)	1.73 (1.17, 2.55)	2.49 (1.57, 3.93)	2.58 (1.88, 3.53)

- No significant differences on sexual identity for tobacco only, alcohol only, and alcohol and tobacco use, relative to being a non-user.

Conclusions

- Past 30-day tobacco and cannabis use were high, particularly among sexual minority females, highlighting the need for targeted substance use intervention and prevention messaging for this group.
- Patterns of use that involved cannabis, including single use, dual-use with alcohol and tobacco, and polysubstance use were predominant among sexual minority females compared to heterosexual females.
- Data was collected during the COVID-19 pandemic when substance use may have increased, and it will be important to monitor if substance use patterns dissipate as people return to pre-pandemic lifestyles.

This study was primarily supported by Oklahoma Tobacco Settlement Endowment Trust contract R21-02. Additional support was provided by National Cancer Institute Cancer Center Support Grant P30CA225520 awarded to the Stephenson Cancer Center.

Questions Contact: Sarah Ehlke at Sarah-Ehlke@ouhsc.edu

SMOKING STATUS FOLLOWING LARYNGEAL CANCER DIAGNOSIS DETERMINES TREATMENT RESPONSE AND LARYNGECTOMY-FREE SURVIVAL

Matthew Krutz[1], Jacey Elliott[1], Pawan Acharya[4], Daniel Zhao[4], Lurdes Queimado[1-3], Rachad Mhawej[1]
Departments of [1]Otolaryngology, [2]Cell Biology, and [4]Biostatistics & Epidemiology; [3]TSET Health Promotion Research Center, Stephenson Cancer Center, The University of Oklahoma Health Sciences Center, Oklahoma

Author's email: Jacey-Elliott@ouhsc.edu

Introduction: Current smokers at the time of laryngeal cancer diagnosis have inferior outcomes compared to non-smokers, but the effect of tobacco cessation between the time of diagnosis and the initiation of treatment remains understudied. This study aims to evaluate the role of tobacco cessation between the time of diagnosis and treatment initiation on response to first-line therapy and laryngectomy-free survival for patients diagnosed with laryngeal cancer and treated with definitive radiation or chemo-radiation.

Methods: Patients diagnosed with laryngeal squamous cell carcinoma and treated at the University of Oklahoma Medical Center between 2005 and 2019 were identified. Electronic medical records for 600 patients were reviewed, resulting in 119 patients included in the study. These patients were active smokers at the time of diagnosis with a primary laryngeal tumor and underwent subsequent definitive radiation or chemo-radiation with intent to cure. Clinical and demographic data were retrospectively collected. Patients were categorized based on whether they ceased tobacco use (quitters) or continued tobacco use (active smokers) before the time of treatment initiation. Primary outcomes include response to first-line therapy and laryngectomy-free survival time.

Results: Data analysis includes 119 total patients with laryngeal squamous cell carcinoma who were treated with the intent to cure. 67 patients (56.3%) continued smoking throughout treatment, while 52 patients (43.7%) stopped smoking before treatment initiation. No significant differences in age, sex, race, tobacco pack years, or alcohol use were found between the two groups. Only 58.2% of patients who continued smoking achieved a complete response to therapy, compared to 82.7% of patients who ceased tobacco use before treatment (p=0.004). The difference in laryngectomy-free survival time between the two groups was statistically significant (p=0.034).

Conclusions: Our results show that patients who continue smoking throughout treatment have poorer responses to therapy and shorter laryngectomy-free survival time compared to patients who quit smoking before beginning treatment. This data

provides critical support for physicians to encourage patients to cease tobacco use following diagnosis with laryngeal cancer.

Grant Support: Oklahoma Center for Advancement of Science and Technology, NIH/NCI (R01CA242168, R33CA202898, and P30CA225520) and the Oklahoma Tobacco Settlement Endowment Trust. Dr. Queimado holds a Presbyterian Health Foundation Endowed Chair in Otorhinolaryngology.

TSET Health Promotion Research Center

OU Health | Stephenson Cancer Center

Smoking Status Following Laryngeal Cancer Diagnosis Determines Treatment Response and Laryngectomy-Free Survival

Matthew Krutz[1], Jacey Elliott[1], Pawan Acharya[4], Daniel Zhao[4], Lurdes Queimado[1-3], Rachad Mhawej[1]

Departments of [1]Otolaryngology, [2]Cell Biology, and [4]Biostatistics & Epidemiology; [3]TSET Health Promotion Research Center, Stephenson Cancer Center, The University of Oklahoma Health Sciences Center, Oklahoma

Background

- Laryngeal squamous cell carcinoma (LSCC) is a common cancer of the head
- Tobacco use is the single most important factor in the development of LSCC; 95% of patients diagnosed with LSCC have a history of tobacco use
- LSCC therapy is often bimodal, utilizing a combination of chemoradiation therapy (CRT) and laryngectomy
- Organ preservation therapy is preferred; laryngectomy leads to voice loss, difficulty swallowing, etc.
- Current smokers at the time of laryngeal cancer diagnosis have inferior outcomes compared to non-smokers, but the effect of tobacco cessation between the time of diagnosis and the initiation of treatment remains understudied

Objective

- To evaluate the role of tobacco cessation between the time of diagnosis and treatment initiation on response to first-line therapy
- To compare laryngectomy-free survival between active smokers and quitters following laryngeal cancer diagnosis

Study Design

- Electronic medical records for patients diagnosed with LSCC between 2006 and 2019 were reviewed (n=600)
- Active smokers at the time of diagnosis who underwent subsequent definitive radiation or chemo-radiation with intent to cure were included in the study (n=119)
- Clinical and demographic data were retrospectively collected
- Patients were categorized based on whether they ceased tobacco use (quitters) or continued tobacco use (active smokers) before the time of treatment initiation
- Primary outcomes include response to first-line therapy and laryngectomy-free survival time
- Chi-square test for categorical variables; t-test for continuous variables
- Difference in survival between smoking status groups estimated by Kaplan-Meier methods, log-rank test, and Cox proportional-hazard models

Results

Table 1. Characteristics of the Study Population by Smoking Status at Time of Treatment

Variable	Level	Active Smokers (N=67)	Quitters (N=52)	Parametric P-value*
Sex	Female	20 (30%)	12 (23%)	0.408
	Male	47 (70%)	40 (77%)	
Age at Diagnosis	Mean	59.9	60.8	0.573
	Median	59	61	
Race	White	58 (87%)	49 (94%)	0.262
	Black	6 (9%)	1 (2%)	
	American Indian/Alaska Native	3 (4%)	2 (4%)	
Tobacco Pack Years	Mean	55.6	51.4	0.394
	Median	50	50	
Alcohol Use	No	28 (42%)	23 (44%)	0.790
	Yes	39 (58%)	29 (56%)	

*ANOVA for numerical covariates and chi-square test for categorical covariates

No significant differences in sex, age, race, tobacco pack years, or alcohol use were found between active smokers and quitters.

Table 2. Smoking status determines response to therapy.

Smoking Status at Treatment	Response to First-Line Therapy	
	No/Partial Response (n=37)	Complete Response (n=82)
Active Smokers (n=67)	28 (42%)	39 (58%)
Quitters (n=52)	9 (17%)	43 (83%)
p = 0.0042		

Only 58% of LSCC patients who continued smoking achieved a complete response to therapy compared to 83% of patients who ceased tobacco use before treatment (p=0.004).

Figure 1. Laryngectomy-free survival.

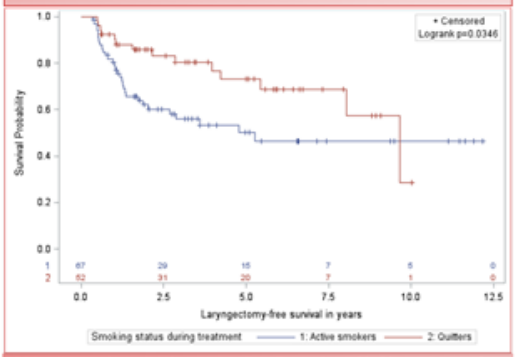

LSCC patients who quit tobacco use after diagnosis avoided laryngectomy for a significantly longer time than those who continued to smoke after diagnosis (p=0.035).

Conclusions

- LSCC patients who quit after cancer diagnosis have significantly better response to first-line therapy than active smokers
- LSCC patients who are active smokers have shorter laryngectomy-free survival time compared to those who quit after diagnosis
- Patients should cease tobacco use following laryngeal cancer diagnosis
- Smoking cessation programs should be an integral part of laryngeal cancer treatment.

Acknowledgements

- This work was supported by NIH/NCI (R01CA242168), the Oklahoma Center for the Advancement of Science and Technology, and the Oklahoma Tobacco Settlement Endowment Trust.
- Dr. Queimado holds a Presbyterian Health Foundation Endowed Chair in Otorhinolaryngology.

DO CHANGES IN PATIENT-REPORTED COGNITION EXPLAIN CHANGE IN COGNITIVE PERFORMANCE DURING TAXANE CHEMOTHERAPY FOR WOMEN'S CANCERS?

Ashley Fox, MS[1,3], Jo-Dane Bell[2], Chao Xu, PhD[4], Debra Richardson, MD[2], Kathleen Moore, MD, MS[2], Elizabeth Hile, PT, PhD[1,3]

[1]OU Health Stephenson Cancer Center, Cancer Rehabilitation, Oklahoma City, OK

[2]OU Health Stephenson Cancer Center, College of Medicine, Department of Obstetrics and Gynecology, Oklahoma City, OK

[3]The University of Oklahoma Health Science Center, College of Allied Health, Department of Rehabilitation Sciences, Oklahoma City

[4]The University of Oklahoma Health Sciences Center, College of Public Health, Department of Biostatistics and Epidemiology, Oklahoma City, OK

[5]University of New Mexico, Department of Health Exercise & Sports Sciences, Albuquerque, NM

Introduction: Neurotoxic chemotherapy (NtxChemo) can contribute to cancer-related cognitive impairment (CRCI), impacting the cognitive domains of memory, concentration, and processing speed for daily activities. In women receiving cumulative NtxChemo, we aim to explore associations between changes in patient-reported (PR) cognition and cognitive performance on the Digit Symbol Substitution Test (DSST), a test of working memory, processing speed, visuospatial attention, and motor planning.

Methods: For this exploratory secondary analysis, we identified 21 women with longitudinal data from one of two feasibility studies of cumulative taxane chemo: observation of mobility or exercise intervention. We performed univariate linear regression with change in DSST-90 (correct responses in 90 sec) as the dependent variable. The independent variable was cognitive PR as NCI-PRO Common Terminology Criteria for Adverse Events self-rating for "problems with" (1) concentration or (2) memory. For each, patients rated (1) severity & (2) interference with daily activities. To explore mechanisms, we repeated univariate models with DSST-90 score split as boxes completed in 1st ($DSST_{1st\text{-}45}$) or 2nd ($DSST_{1st\text{-}45}$) 45 sec intervals, and explored age and PR anxiety for associations with DSST performance.

Results: Participants were 68±10.5 yrs, 90% white non-Latinx with 48% ovarian/38% uterine/14% breast cancer, and 65% comorbid diabetes. Mean DSST-90 was 44.8 ±11.9 (range 26-72). Change in DSST-90 with cumulative NtxChemo was partly explained by change in PR concentration, both severity (p=0.020, y-intercept -4.31) and interference (p=0.019, intercept -6.0). $DSST_{1st\text{-}45}$ associated only with PR memory interference

(p=0.022, intercept -7.8). No PR change explained $DSST_{2nd-45}$. Results for age and anxiety were not significant (p=0.308-0.776).

Conclusion: In women's cancer survivors on taxane chemotherapy, self-perception of new or worse concentration problems partially explained declining performance during the entire 90 sec DSST, perhaps by impacting visuospatial attention and processing speed. New or worse memory interference explained performance more specifically, in the 1st 45-seconds, a critical interval for learning the symbol-digit pairings. Results should be validated in a larger sample, but may advance understanding of how PR-cognitive problems during NtxChemo relate to specific domains of cognitive performance on clinically-feasible tests, with a long-term goal of advancing CRCI screening and treatment in women's cancers.

Funding: Cancer Undergraduate Research Experience (CURE), NCI Cancer Center Support Grant P30CA225520 to OU Stephenson Cancer Center. Presbyterian Health Foundation, Oklahoma Tobacco Settlement Endowment Trust.

ASSOCIATIONS BETWEEN CHANGES IN PATIENT-REPORTED COGNITION AND COGNITIVE PERFORMANCE DURING TAXANE CHEMOTHERAPY FOR WOMEN'S CANCERS

Ashley Fox, M.S.[1,3], Jo-Dane Bell[5], Chao Xu, Ph.D.[4], Debra Richardson, M.D.[2], Kathleen Moore, M.D., M.S.[2] Elizabeth Hile, P.T., Ph.D.[1,3]

[1]OU Health Stephenson Cancer Center, Cancer Rehabilitation [2]OU Health Stephenson Cancer Center, Department of Obstetrics and Gynecology

[3]The University of Oklahoma Health Science Center, College of Allied Health, Department of Rehabilitation Sciences [4] The University of Oklahoma Health Sciences Center, Department of Biostatistics and Epidemiology

[5]University of New Mexico, Department of Health Exercise & Sports Sciences

INTRODUCTION

Cancer-Related Cognitive Impairment (CRCI) affects 50% of breast & gynecologic cancer survivors after chemotherapy, and threatens quality of life by limiting memory, concentration & processing speed for daily activities. Deficits may persist for years, and older age may be a risk factor for CRCI. [1-3]

- CRCI screening is not routine in clinics, but the use of patient-report is more common than performance tests. In 2011, the International Cancer & Cognition Task Force recommended tests of working memory.
- ***Digit Symbol Substitution Test (DSST)*** is a validated, sensitive test of working memory, processing speed, visuospatial attention, motor planning & coordination. Patients encode 9 digit-symbol pairs (implicit learning) to fill up to 90 boxes with the correct symbol (repeated retrieval) in 90 seconds. DSST scores depend on age and improve by 9% or more with practice. [4-7]

Fig 1: Digit Symbol Substitution Test

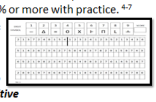

Purpose: ***We aimed to explore associations between changes in patient-reported cognition (memory & concentration) and change in cognitive performance (DSST) during neurotoxic chemo for women's cancers.***

Hypothesis: PRO Memory & Concentration problems will both decrease 90 sec DSST score, but *memory* problems will relate to score in the 1st 45 sec, interfering with the encoding of digit-symbol pairs. *Concentration* problems will impact sustained attention in the 2nd 45 sec.

METHODS

Design: Exploratory secondary analysis of longitudinal data from two longitudinal feasibility studies during taxane chemotherapy.

- Observational study of mobility for ≤6 chemo cycles (n=15)
- Exercise intervention for women with ovarian cancer >70 yrs old (n=6)

21 women had data for at least 2 timepoints. Baseline = before 1st chemo infusion. Repeated assessments = a few days before each subsequent dose.

Measures:

1) DSST – Administered at the start of each visit.

Instructions: *Complete as many boxes as you can in 90 seconds.*

- To minimize long-term encoding, participants cycled between 3 validated alternative versions of the DSST across study visits.

2) Self Reported Symptoms: NCI-PRO-CTCAE = NCI Patient-Reported Outcomes Common Criteria for Adverse Events

- At each visit, patients rated any problems over the past 7 days with (1) **Concentration** and (2) **Memory**, on a 5-point scale.
  - ***Severity*** of the problem at its worst: None to Very Severe
  - ***Interference*** with usual or daily activities: Not at all to Very Much
  - Patients also rated their **Anxiety** at each visit.[8]

Statistical Analysis: Univariate linear regression

- ***DSST Change***: Visit score= # of boxes correct in (1) 90, (2) 1st 45, (3) 2nd 45 s. *$DSST_{90}$ V2 change = V2 score – V1 score.*
- ***PRO Change***: **PRO V2 change = V2 score – V1 score** (Negative = improved)
  - Separate regression models for outcomes of $DSST_{90}$, $DSST_{1st-45}$, $DSST_{2nd-45}$, with PRO Items as predictor variables.

RESULTS

Table 1: Description of Sample at Baseline (n=21 women)

Age in Years	
Mean (SD)	68 (10.5)
Min-Max	46 – 85
Race n (%)	
White	19 (90%)
Black/African American	1 (5%)
Asian	1 (5%)
Ethnicity n (%)	
Non-Hispanic	21 (100%)
Cancer Type n (%)	
Ovarian	10 (48%)
Uterine	8 (38%)
Breast	3 (14%)
Chemo Regimen n (%)	
Paclitaxel + Carboplatin	17 (80%)
Docetaxel + Carboplatin	1 (5%)
Docetaxel Only	2 (10%)
Carboplatin Only	1 (5%)
DSST Boxes Correct in 90 sec (Best>90)	
Mean (SD)	44.8 (11.9)*
Min-Max	26 – 72
Diabetes n (%)	
Yes	13 (62%)
No	6 (29%)
Not Reported	2 (9%)

*By comparison, a sample of > 3,000 well-functioning community dwelling older adults 74.0 (4.6) yrs old completed **42.1 (12.3)** boxes in 90 sec. [9]

Figure 2: Sample Trajectory for Cognitive Performance and Patient-Report Over 1st Two Chemo Cycles

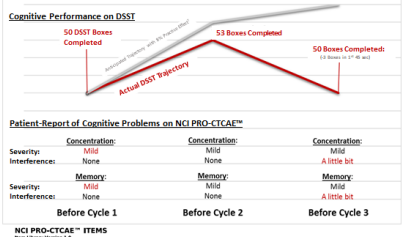

NCI PRO-CTCAE™ ITEMS

Item Library Version 1.0

In the last 7 days, what was the SEVERITY of your PROBLEMS WITH MEMORY at their WORST?

○ None ○ Mild ○ Moderate ○ Severe ○ Very severe

In the last 7 days, how much did PROBLEMS WITH MEMORY INTERFERE with your usual or daily activities?

○ Not at all ○ A little bit ○ Somewhat ○ Quite a bit ○ Very much

Table 2: Change in PRO Cognitive Domains That Explain Change in DSST Performance over Chemotherapy*

Results of Univariate Regression Analysis

Outcome: Change in DSST boxes completed in 1st 45 sec			
Predictor: Change in NCI-PRO-CTCAE	Coefficient	Std Error	Pr > |t|
Memory problems interfere with daily activities	-7.79	2.64	0.0215
Outcome: Change in DSST boxes completed in 90 sec			
Predictor: Change in NCI-PRO-CTCAE	Coefficient	Std Error	Pr > |t|
Severity of concentration problems at their worst	-4.31	1.58	0.0198
Concentration problems interfere with daily activities	-6.00	2.19	0.0192

*Note: Only significant relationships are shown. No PRO items predicted change in 2nd 45 sec.

Results for Age & Change in PRO Anxiety Associations with Change in DSST Performance During Neurotoxic Chemotherapy

Table 3: Age & Anxiety Do Not Associate with DSST Score Change (p-values)

	Age in Yrs	Anxiety PRO
$DSST_{90}$	0.549	0.643
1st 45 sec	0.308	0.776
2nd 45 sec	0.716	0.466

Figure 3: Comparing DSST Trajectories of the Oldest vs. Youngest Participant

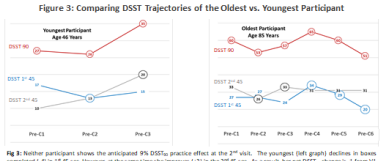

Fig 3: Neither participant shows the anticipated 9% $DSST_{90}$ practice effect at the 2nd visit. The youngest (left graph) declines in boxes completed (-4) in 1st 45 sec. However, at the same time she improves (+3) in the 2nd 45 sec. As a result, her net $DSST_{90}$ change is -1 from V1 to V2. In contrast, from V1 to V2 the oldest participant (right graph) declines only in the 2nd 45 sec, for a net $DSST_{90}$ decline (-7) when a 9% increase (+5 boxes) might be expected as a practice effect. From V1 to V3, the oldest participant's 90 sec DSST score is driven more by her performance in the 2nd 45-sec interval. However, from V3 to V6, her change in overall score appears to track her performance in 1st 45 sec.

CONCLUSIONS

Main Conclusions: In mid-life & older women with breast & gynecologic cancers, change in reported memory and concentration during taxane chemotherapy differentially associated with DSST change.

- ***Memory***: Change in memory PRO associated with **$DSST_{1st-45}$**, but the association was limited to memory **Interference** with activities.
  - For each Likert-scale unit increase in interference, DSST scores were nearly 8 boxes slower in only 45 sec.
  - *Interpretation: Patients who perceive memory interference may learn the DSST symbol-digit pairings more slowly.*
- ***Concentration***: Changes in concentration **Severity** & **Interference** PRO associated with DSST changes, but only in **$DSST_{90}$**, not $DSST_{2nd-45}$.
  - *Interpretation: The DSST 45-sec interval (1st vs 2nd) that is most impacted by self-reported concentration problems may vary across subgroups within this heterogeneous sample of women.*

Age & change in anxiety did not associate with DSST change in our sample.

Limitations: No control group/repeated baseline for DSST practice effects, or measure of writing time (greater in older adults & remains constant with practice[6]). Included participants from an exercise intervention study.

Post-hoc power analysis: n of 12 is 99% power to detect coefficient of 4.

Clinical Implications for CRCI Monitoring during Neurotoxic Chemo

- *To screen for performance changes on tasks requiring working memory & psychomotor processing, the NCI PRO-CTCAE™ concentration or memory interference rating may be more useful than the severity rating.*
- *Some clinical tests may be too brief to capture performance deficits associated with patient-reported concentration problems.*

Future Plans: Replicate in larger sample to identify CRCI subgroups, Quantify practice effect in cancer with/without chemo, Explore change in motor speed (gait speed) as a potential explanatory factor for DSST change.

Societal Impact: Understanding how patient-reported cognitive problems during neurotoxic chemo relate to specific domains of cognitive performance on clinically-feasible tests can advance CRCI screening and treatment in women's cancers. Helping women to maintain work and social roles during & after cancer treatment will improve their quality of life, reduce financial toxicity, and lessen the societal burden of cancer.

ACKNOWLEDGEMENTS

OUHSC Cancer Undergraduate Research Experience (CURE) and Stephenson Cancer Center

The research reported here was supported in part by the ***Presbyterian Health Foundation (PHF), Oklahoma Tobacco Settlement Endowment Trust (TSET)***, and the ***National Cancer Institute Cancer Center Support Grant P30CA225520*** awarded to the University of Oklahoma Stephenson Cancer Center. The content is solely the responsibility of the authors and does not necessarily represent the official views of the PHF, NIH/NCI, or Oklahoma TSET.

REFERENCES

(1) Lange, M., Joly, F., Vardy, J., et al. (2019). Cancer-related cognitive impairment: an update on state of the art, detection, and management strategies in cancer survivors. Annals of Oncol, 30(12), 1925-1940. (2) Wagner, L.I., Gray, R.J., Sparano, J.A. et al. (2020). Patient-reported cognitive-impairment among women with early breast cancer randomly assigned to endocrine therapy alone vs chemoendocrine therapy: Results from TAILORx. J Clin Oncol. (3) Hess, L.M. et al. (2015). Cognitive function during and six months following chemotherapy for front-line treatment of ovarian, primary peritoneal or fallopian tube cancer: An NRG oncology/ GOG study. Gyn Oncol. 139, 541-545 (4) Wechsler Adult Intelligence Scale-Revised. (1981). Psychological Corporation: San Antonio, TX. (5) Jaeger, J. (2018). Digit Symbol Substitution Test: The case for sensitivity over specificity in clinical neuropsychological testing. Journal of Clinical Psychopharmacology, 38(5), 513–519 (6) Cornelis, C., DePrickere, L.I., Huldtjin, W., et al. (2015) Preserved learning during the symbol-digit substitution test in patients with schizophrenia, age-matched controls, and elderly. Frontiers in Psychiatry, 5(189), 1-9. (7) Marsley, C.J., Sinnott, a., Hall, J.E., et al. (2017) Failure to account for practice effects leads to clinical misinterpretation of cognitive outcome following carotid endarterectomy. PhysioReports, 5(11), e13264. (8) Hormozi, M. et al. (2019). Investigating Relationship between Pre- and Post- Chemotherapy Cognitive Performance with Levels of Depression and Anxiety in Breast Cancer Patients: A Cross-Sectional Study. AJRCR 2019(2), 3831-3837. (9) Kosano, C., Newman, A., Katz, R. et al. (2008) Association between lower digit symbol substitution test score and slower gait and greater risk of mortality and of developing incident disability in well-functioning older adults. JAGS, 56(9), 1618.

PEPTIDE AGGREGATION INDUCED IMMUNOGENIC RUPTURE (PAIIR)

Gokhan Gunay[1], Seren Hamsici[1], Gillian A. Lang,[3] Mark L. Lang[3], Susan Kovats[3, 4], Handan Acar[1, 2*]

1- Stephenson School of Biomedical Engineering, University of Oklahoma, Norman, OK 73069, USA
2- Stephenson Cancer Center, University of Oklahoma Health Sciences Center, Oklahoma City, OK 73104, USA
3- Department of Microbiology and Immunology, University of Oklahoma Health Sciences Center, Oklahoma City, OK 73104, USA
4- Arthritis & Clinical Immunology Program, Oklahoma Medical Research Foundation, Oklahoma City, OK 73104, USA

Gokhan Gunay: Gokhan.Gunay-1@ou.edu

Immunogenic cell death (ICD) involves damage to the cell membrane and release of damage associated molecular patterns (DAMPs), molecules that can engage innate immune cells and are natural adjuvants for inducing immune response. In the presence of an antigen, released DAMPs can be a decisive factor regarding the type and magnitude of the immune response, and therefore the longevity and efficacy of an antigen-specific immunity. In the last decade, numerous studies highlighted the potential of ICD in immunotherapies and vaccine development, yet there is no tool that can induce controlled ICD with predictable results, regardless of the cell type. We used the co-assembling oppositely charged peptides (CoOP) strategy to design peptide-based mechanical tools for controlled damage to cell membrane. In this paper, we demonstrate the first peptide-aggregation induced immunogenic rupture (PAIIR) and DAMP release on various healthy and cancerous cells. We further demonstrate the efficacy of this aggregation for antibody production against influenza HA antigens. We show the induction of neutralizing antibodies as well as antibody isotype-switching with PAIIR technology. The system we developed represents an approach that can engage ICD and DAMP release for immunotherapy and vaccine applications.

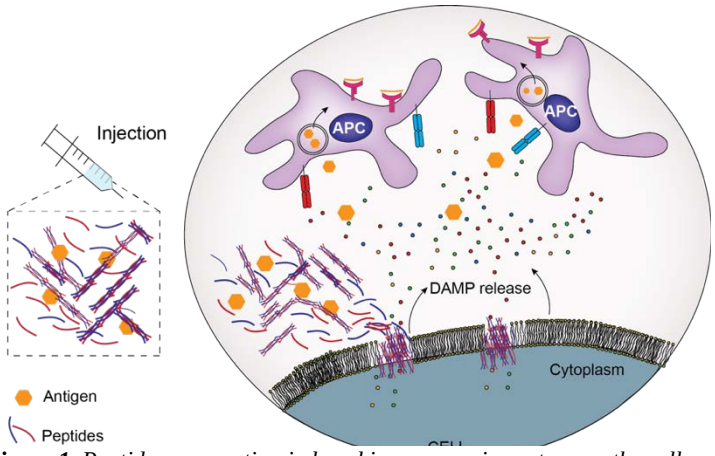

Figure 1. *Peptide-aggregation induced immunogenic rupture on the cell membrane induces the release of damage associated molecular patterns, which can activate the antigen presenting cells and adaptive immune response*

Peptide Aggregation Induced Immunogenic Rupture

Gokhan Gunay, Seren Hamsici, Gillian A. Lang, Mark L. Lang, Susan Kovats, Handan Acar*
University of Oklahoma
www.acar-lab.com

The UNIVERSITY of OKLAHOMA PEGGY AND CHARLES STEPHENSON SCHOOL OF BIOMEDICAL ENGINEERING

Background and significance

Immunogenic cell death (ICD) involves damage to the cell membrane and release of damage associated molecular patterns (DAMPs), natural adjuvants for inducing immune response. In the presence of an antigen, released DAMPs can be a decisive factor regarding the type and magnitude of the immune response, and therefore the longevity and efficacy of an antigen-specific immunity. In the last decade, numerous studies highlighted the potential of ICD in immunotherapies and vaccine development, yet there is no tool that can induce controlled ICD with predictable results, regardless of the cell type. We used the co-assembling oppositely charged peptides (CoOP) strategy to design peptide-based mechanical tools for controlled damage to cell membrane. In this paper, we demonstrate the first peptide-aggregation induced immunogenic rupture (PAIIR) on the membranes of various healthy and cancerous cells. We further demonstrate the efficacy of this aggregation for antibody production against influenza HA antigens.

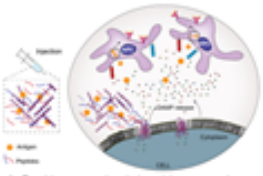

Figure 1. Peptide-aggregation induced immunogenic rupture on the cell membrane induces the release of damage associated molecular patterns, which can activate the antigen presenting cells and adaptive immune response

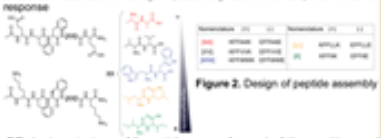

Figure 2. Design of peptide assembly

CoOP design strategy: All peptides were formed of the positive and negative counterparts of the same sequence. Only [XX], substitution domain were changed to study the effects on aggregation kinetics.

[II] peptide is cytotoxic to OVCAR-8 cells

Among all tested peptide groups, [II] peptide showed cytotoxicity to OVCAR-8 cells. While individual peptides were not toxic when they form [II] peptide they induced cytotoxicity. [WW] peptide cytotoxicity was correlated to tryptophan motif and excess positive charge, which upon charge neutralization completely abolished the cytotoxicity.

Preparation of the peptide was determined at this step.

We carried out the remainder of the experiment by mixing the [II] peptide for 30 min prior to administration to cells.

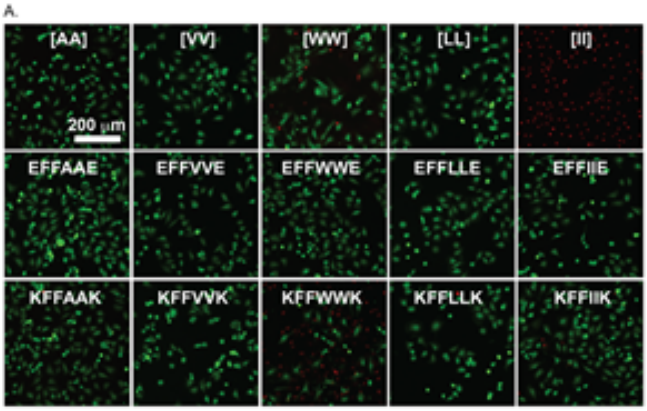

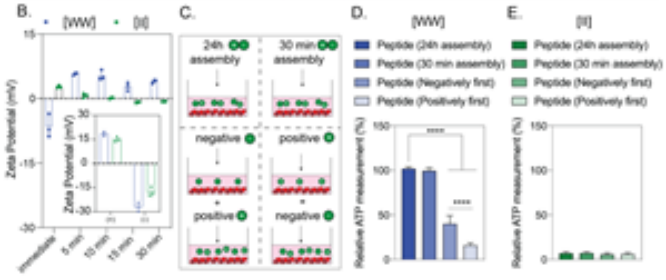

Figure 3. Cytotoxicity of peptides to OVCAR-8 cells. Negative peptides were added to the cells followed by the addition of corresponding positive peptides. (A) Live-dead images of OVCAR-8 cells treated with peptide combinations and corresponding individual counterparts at 6h (peptide concentration is 0.5mM. (B) Zeta potential of individual and combined peptides. (C) Illustration of peptide preparation for [WW] and [II]. The effect of peptide preparation on cell viability for [WW] (D) and [II] (E). Scale bar is 200 μm. Data are representative of at least three experiments. Statistical analysis via one-way ANOVA test, data are mean ±SD, ****p<0.0001.

[II] peptide aggregation induced cell death

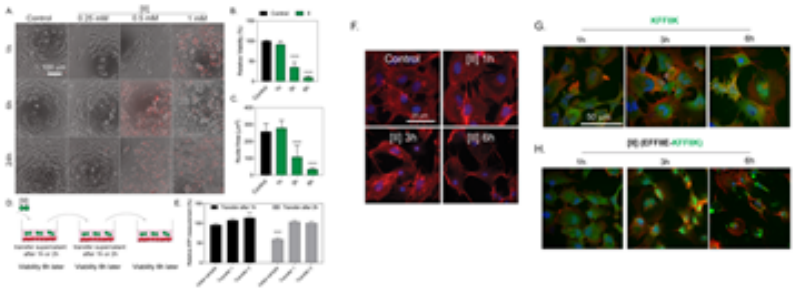

Figure 4. [II] aggregation induces membrane rupture. (A) Time and concentration dependent cytotoxicity of [II] analyzed through PI uptake, scale bar is 100 μm. Time dependent viability measurement (B), and time dependent nuclear size analysis (C). Experimental plan of [II] transfer and viability experiment (D). Effect of [II] transfer on cell viability at 6h (E). Actin cytoskeleton staining of [II] treated OVCAR-8 cells at 1,3 and 6h, scale bar is 20 μm(F). Internalization of FITC-KFFIIK (G) and FITC-[II] for 1,3 and 6h (H), scale bar is 100 μm. Data are representative of at least three experiments. Statistical analysis was done with one-way ANOVA test, data are mean ±SD, ****p<0.0001.

[II] peptide cytotoxicity is independent of pore-forming proteins

[II] peptide induced immunogenic cell death in all tested cell lines. Additionally, all tested cell lines secreted HMGB-1 and HSP90, important DAMPs for the activation of antigen presenting cells to stimulate adaptive immune responses. Fibroblasts are present in the subcutaneous layer, before the vaccination experiments, we showed ICD and DAMP release in these cell line as well.

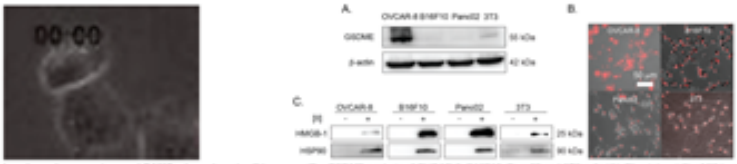

Figure 5. [II] induced membrane rupture and DAMP release is not cell type specific. GSDME analysis of OVCAR-8, B16F10, Panc02 and 3T3 cells (A). PI uptake at 6h of [II] treatment on cells (B). HMGB-1 and HSP90 release to the supernatant (SN) at 6h (C). Time dependent viability measurement (D). Time dependent LDH release (E). Phase contrast images of [II] treated fibroblasts at 1, 3 and 6h (F). Data are representative of at least three experiments. Statistical analysis was done by one-way ANOVA test, data shown are mean ± SD,****p<0.0001, ***p<0.001.

[II] peptide induces influenza-antigen specific antibody formation

[II] peptide is used as an adjuvant together with the mixture of HA antigens. [II] peptide induced the formation strong IgG1 and IgG2a antibody formation indicating Th2 and Th1 immunity, respectively.

No antibodies were formed against [II] peptide, showing that [II] is a **safe adjuvant.**

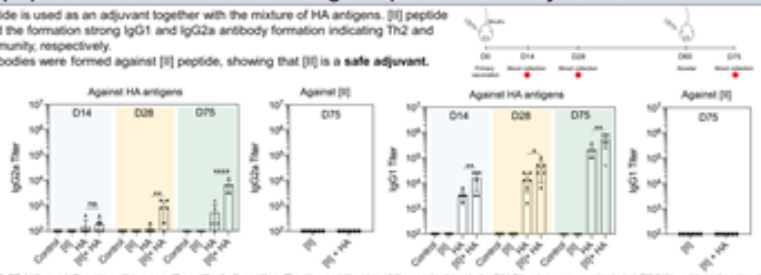

Figure 6. [II] induces influenza-antigen specific antibody formation. Timeline and the plan of the vaccination study: BALB/c mice were vaccinated at D0 followed by a booster at D60, serum was collected at D14, 28 and 75 (A). Serum IgG1 titers at D14, 28 and 75 (B). Serum IgG2a titers at D14, 28 and 75 (C). Statistical analysis was done by one-way ANOVA test, data shown are mean ± SD ****p<0.0001b, **p<0.01, *p<0.1 n=6 mice.

[II] peptide induced DAMP release can be controlled

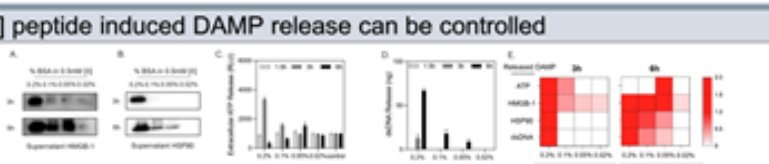

Figure 8. DAMP release can be controlled through controlling aggregation. Release of HMGB-1 (A), HSP90 (B), extracellular ATP (C) and dsDNA (D). Heat map of DAMP release at 3 and 6h (E)

Conclusions

Understanding and controlling ICD will play a paramount role in advancing cancer immunotherapy and vaccine development. Induction of ICD through membrane rupturing peptide aggregates can overcome limitations due to reduced levels of immune system activation in immunotherapies and vaccination strategies.

References

1- **Gokhan Gunay**, Seren Hamsici, Gillian A. Lang, Mark L. Lang, Susan Kovats, Handan Acar* "Peptide Aggregation Induced Immunogenic Rupture" (in revision Advanced Science)

2- Hamsici, S., White, A. D. and Acar, H., "Peptide framework for screening the effects of amino acids on assembly", *Science Advances*, 2021 *(in press)*

FUSION OF HANDCRAFTED AND DEEP TRANSFER LEARNING FEATURES TO IMPROVE PERFORMANCE OF BREAST LESION CLASSIFICATION

Meredith A. Jones*[a], Huong Pham[b], Tiancheng Gai[b], Bin Zheng[b]

[a] School of Biomedical Engineering, University of Oklahoma, Norman, OK 73019, USA
[b] School of Electrical and Computer Engineering, University of Oklahoma, Norman, OK 73019, USA

Purpose: Early detection of breast cancer through routine mammographic screening has significantly improved treatment efficacy and decreased patient mortality rate. While efficacious, only ~20% of women with breast lesions recommended for biopsy are confirmed as malignant. Computer aided detection and/or diagnosis (CAD) schemes are commonly employed to improve the sensitivity and specificity of mammography screening. CAD schemes traditionally follow one of two approaches. The first approach involves the extraction of a set of handcrafted image features, often referred to as radiomics features. The second approach uses deep learning to extract a set of features directly from the image. We hypothesize that the traditional handcrafted features and the deep learning model generated automated features contain complementary discriminatory information in representing clinically relevant phenotype of lesions. Thus, optimal fusion of these two types of features has the potential to improve the classification performance of breast lesions. We investigate this hypothesis by developing and evaluating a new CAD scheme that uses the fusion of traditional handcrafted features and automated features extracted from a deep transfer learning model to classify breast lesions.

Methods: We retrospectively assembled a dataset involving 1,535 lesions (740 malignant and 795 benign). Regions of interest surrounding suspicious lesions are extracted and two types of features are computed from each ROI. The first set includes 40 radiomic features and the second set includes automated features computed from a VGG16 network using a transfer learning method. A single channel ROI image is converted to three channel pseudo-ROI images by stacking the original image, a bilateral filtered image, and a histogram equalized image. Two VGG16 models using pseudo-ROIs and stacked original ROIs without pre-processing are used to extract automated features, resulting in a pseudo-ROI and stacked-ROI feature sets. Five linear SVMs are built using either the handcrafted features, the pseudo-ROI features, the stacked-ROI features, or the fusion of handcrafted features with pseudo-ROI and stacked-ROI features, independently.

Results: Using 10-fold cross-validation, the fusion SVM using pseudo-ROIs yields the highest lesion classification performance with area under ROC curve (AUC=0.756 ±0.042), which is significantly higher than those yielded by other SVMs trained using handcrafted or automated features only ($p<0.05$).

Conclusion: This study demonstrates that both handcrafted and automated futures contain useful information to classify breast lesions. Fusion of these two types of features can further increase CAD performance.

Acknowledgment of Funding: This work is supported in part by Grants of R01CA197150 from the National Cancer Institute, National Institutes of Health.

Fusion of Handcrafted and Deep Transfer Learning Features to Improve Performance of Breast Lesion Classification

Meredith Jones*[1], Huong Pham[2], Tiancheng Gai[2], Bin Zheng[2]

School of Biomedical Engineering, University of Oklahoma, Norman, OK 73019, USA, [1]

School of Electrical and Computer Engineering, University of Oklahoma, Norman, OK 73019, USA, [2]

Introduction

Early detection of breast cancer through routine mammographic screening has significantly improved treatment efficacy and decreased patient mortality rate. While efficacious, less than 30% of lesions are confirmed as malignant, highlighting the large false-positive recall rate associated with mammography[1]. Thus, there is an **unmet clinical need** to improve the accuracy of radiologists in classifying mammography-detected suspicious lesions.

Traditional CAD or deep learning CAD schemes have been used to improve the sensitivities and specificities of mammogram screening.

Fig. 1(A) Traditional CAD scheme

Fig. 1(B) Deep Learning CAD scheme

Traditional CAD Limitations	Deep Learning CAD Limitations
• Image feature extraction and optimal feature selection is time-intensive and varies drastically depending on study aims.	• Requires an extremely large training dataset which is often not possible in medical imaging. • Not easily interpretable by radiologists. • Transfer learning often requires transformation of input image.

Study Objective

The **objective of this study** is to develop and evaluate a new fusion CAD scheme to test the hypothesis that traditional handcrafted features and automated features generated from a deep transfer learning model contain complementary discriminatory information that when fused can increase CAD performance in classifying breast lesions.

Image Dataset

This study includes a dataset involving 1,535 craniocaudal full-field digital mammogram images with suspicious lesions. Among them

- 740 biopsy confirmed malignant lesions
- 795 biopsy confirmed benign lesions

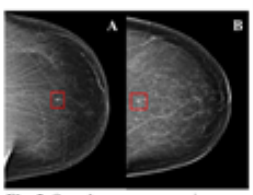

Fig. 2: Sample mammogram images. A is a malignant lesion and B is a benign lesion.

Methods

1) Preprocessing:

To generate images suitable for VGG16 network, we combine 2 prepeocessed images with the original image to create a 3-channel image.

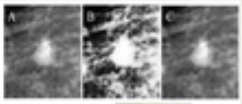

Fig. 3(A): Original greyscale ROI.

Fig. 3(B): Histogram Equalized Image to improve contrast.

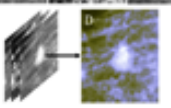

Fig. 3(C): Bilateral Filtered Image to reduce noise while preserving edges.

Fig. 3(D): Pseudo 3-channel color ROI.

Stacked ROIs were also created by stacking the original greyscale ROI in 3-channels

2) Handcrafted Feature Extraction

All handcrafted features were extracted from the original greyscale ROI.

- 6 First Order Statistical Features
- 12 gray level co-occurrence matrix features
- 22 gray level run length matrix features

Deep Transfer Learning Feature Extraction

The VGG16 Network pretrained on the ImageNet Dataset was used

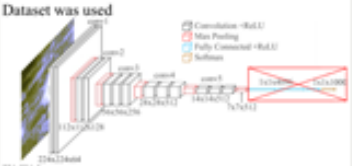

Figure 4: VGG16 architecture. The red box identifies the top fully-connected layers which are removed for this study. A 7x7x512 feature map was extracted after the last max pooling layer.

3) Handcrafted Feature Selection

Variance Thresholding at a threshold of 0.01.

Deep Transfer Learning Feature Selection

A 3-step feature selection pipeline is used, which includes

1. Variance Thresholding at a threshold of 0.01.
2. Relief-F.
3. Sequential Forward Floating Feature Selector.

4) Feature Level Fusion

Feature pools generated from the VGG16 network are fused with the handcrafted feature set to create two fused feature sets.

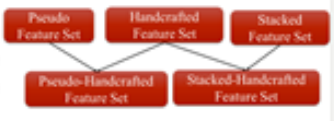

5) Classification

Five separate linear SVMs were trained using the five independent optimal feature vectors to test the hypothesis that the SVM trained using the optimal fusion feature set will perform better than the SVMs trained using either the handcrafted feature set or the automated feature set alone.

Results

	ROC AUC		Accuracy		Sensitivity		Specificity	
	mean	std	mean	std	mean	std	mean	std
SVM1	0.596	0.032	0.567	0.033	0.385	0.055	0.735	0.044
SVM2- Stacked	0.717	0.022	0.660	0.030	0.565	0.052	0.747	0.037
SVM3- Stacked	0.734	0.017	0.676	0.041	0.585	0.058	0.761	0.032
SVM2- Pseudo	0.750	0.043	0.699	0.036	0.665	0.064	0.731	0.028
SVM3- Pseudo	0.756	0.042	0.704	0.035	0.676	0.061	0.731	0.027

Table 1: Displays the mean value and standard deviation for each SVM after 10-fold cross validation.

Results

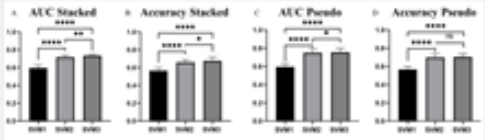

Fig 5: A paired t-test was used to determine if there was a statistically significant difference between the means of each group. A and B show that the SVM3-stacked model performed significantly better than both SVM1-stacked and SVM2-stacked models. C shows that the SVM3-pseudo model performed significantly better than both SVM1-pseudo and SVM2-pseudo models in terms of AUC, but D shows the accuracy of SVM3-pseudo model is not significantly different from SVM2-pseudo model ($p = 0.1363$).

Results

Fig 6: While there is only a statistically significant difference between the classification accuracies of SVM2, SVMs trained using pseudo-ROI features always perform with a higher AUC and classification accuracy than the classifiers trained using the stacked-ROIs.

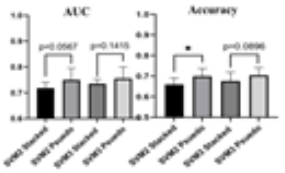

Conclusions

1. Deep transfer learning has significant advantages over the traditional or radiomics-based CAD schemes.
2. Fusion of traditional handcrafted features and deep transfer learning model generated features creates an optimal fusion feature pool that can improve classification performance of a machine learning classifier in classifying breast lesions as malignant or benign.
3. Features extracted using radiomics-based CAD schemes and deep learning-based CAD schemes contain complementary classification information.
4. Meaningful pre-processing of mammogram images has potential to play an important role to improve the overall performance of the classifier.

Funding Acknowledgements

This work is supported in part by Grants of R01CA197150 from the National Cancer Institute, National Institutes of Health, and Graduate Study Scholarship from the Stephenson School of Biomedical Engineering, University of Oklahoma.

References

Siegel, R.L., K.D. Miller, and A. Jemal, Cancer statistics, 2020. CA Cancer J Clin, 2020. **70**(1): p. 7-30.

EFFECT OF TOBACCO CESSATION ON TREATMENT RESPONSE AND LONG-TERM SURVIVAL IN ORAL AND OROPHARYNGEAL CANCER

Matthew Krutz[1], Pawan Acharya[4], Geraldine Chissoe[1], Vijay Raj[1], Lane Driskill[1], Daniel Zhao[3,4], Rachad Mhawej[1], Lurdes Queimado[1-3]

Departments of [1]Otorhinolaryngology, [2]Cell Biology, and [4]Biostatistics & Epidemiology;

[3]TSET Health Promotion Research Center, Stephenson Cancer Center, The University of Oklahoma Health Sciences Center, Oklahoma.

Author's email: matthew-krutz@ouhsc.edu

Background and Aims: Current smokers at diagnosis of head and neck cancer have inferior clinical outcomes compared to never smokers and previous smokers, but the impact of tobacco cessation even up to the point of treatment initiation remains understudied. Current smokers possess tumors with different mutational and epigenetic makeup than previous smokers and never smokers. Here, to precisely measure the impact of smoking cessation following head and neck cancer diagnosis on response to first-line therapy, disease-free survival and long-term overall survival, we included only current smokers at time of head and neck cancer diagnosis.

Methods: Patients diagnosed with oral or oropharyngeal squamous cell carcinoma (n=923) who were treated at the OU Medical Center between 2006 and 2018 were identified. The electronic medical records were reviewed and after exclusions, 134 patients who were current smokers at diagnosis and treated with intent to cure were included in this study. Clinical and demographic information was retrospectively collected. Patients were separated into two groups based on whether they quit smoking before treatment initiation (quitters) or not (active smokers). Primary outcomes included response to first line of therapy, disease-free survival, and overall survival.

Results: 55 patients (41%) of patients quit smoking before treatment initiation. There were no significant differences in sex, race, tumor stage, or treatment regimen between groups. Quitters were 3.7 times more likely to obtain a complete response to first-line therapy than active smokers (OR, 3.67; 95% CI, 1.142-11.79; p=0.03). Quitters had a statistically significant increase in overall survival compared to active smokers (p=0.016). In the oral cavity population, quitters had a statistically significant increase in disease-free survival compared to active smokers (p=0.04).

Conclusions: In our study population, current smokers at time of oral cavity or oropharyngeal cancer diagnosis who quit smoking before therapy have increased response to definitive radiation or chemoradiation regimens, longer disease-free survival, and longer overall survival. Our data suggests that patients who quit smoking

even up to the point of treatment initiation respond better to therapy and can obtain a survival benefit.

Grant support: Oklahoma Center for Advancement of Science and Technology, NIH/NCI (R01CA242168, R33CA202898, and P30CA225520), and the Oklahoma Tobacco Settlement Endowment Trust. Dr. Queimado holds a Presbyterian Health Foundation Endowed Chair in Otorhinolaryngology.

TSET Health Promotion Research Center

OU Health | Stephenson Cancer Center

Effect of Tobacco Cessation on Treatment Response and Long-Term Survival in Oral and Oropharyngeal Cancer

Matthew Krutz[1], Pawan Acharya[4], Geraldine Chissoe[1], Vijay Raj[1], Lane Driskill[1], Daniel Zhao[3, 4], PhD, Rachad Mhawej, MD[1], Lurdes Queimado, MD, PhD[1-3]

[1]Departments of [2]Otorhinolaryngology, [3]Cell Biology, and [4]Biostatistics & Epidemiology; [5]TSET Health Promotion Research Center, Stephenson Cancer Center, The University of Oklahoma Health Sciences Center, Oklahoma

Introduction

- Current smokers at diagnosis of head and neck cancer have inferior outcomes compared to previous smokers and never smokers.
- The impact of tobacco cessation following diagnosis, even up to the point of treatment initiation, remains understudied.
- Current smokers possess tumors with different mutational and epigenetic makeup than previous smokers and never smokers, and should be studied separately.
- We hypothesize that among current smokers at diagnosis, tobacco cessation prior to treatment initiation will improve response to therapy and survival outcomes.

Specific Aims

- To assess the impact of smoking cessation on response to first-line therapy among current smokers at diagnosis.
- To assess the impact of smoking cessation on disease-free survival and long-term survival among current smokers at diagnosis.

Study Design

- 134 patients with oral or oropharyngeal squamous cell carcinoma, who were current smokers at time of diagnosis, and were treated with chemoradiation with intent to cure, were included.
- Demographic and clinical data were retrospectively collected.
- Patients were separated into two groups based on whether they quit smoking before treatment initiation (quitters) or not (active smokers).
- Primary outcomes included response to first-line therapy, disease-free survival, and overall survival.

Results

Table 1. Characteristics of the Study Population by Smoking Status

Characteristics	Current Smokers at Diagnosis, No. (%)			
	Total (n=134)	Quitters before treatment (n=55)	Active smokers during treatment (n=79)	p-value[§]
Age, y	55.8 ± 9.9	56.1 ± 9.4	55.8 ± 9.9	0.099
Sex				
Male	108 (80.6%)	40 (72.7%)	68 (86.1%)	0.055
Female	26 (19.4%)	15 (27.3%)	11 (13.9%)	
Race				
White	117 (87.3%)	48 (87.3%)	69 (87.3%)	0.635
African American	9 (6.7%)	3 (5.5%)	6 (7.6%)	
American Indian/ Alaskan Native	6 (4.5%)	3 (5.5%)	3 (3.8%)	
Other	2 (1.5%)	1 (1.8%)	1 (1.3%)	
Alcohol use				
Yes	69 (51.5%)	22 (40.0%)	47 (59.5%)	0.026
No	65 (48.5%)	33 (60.0%)	32 (40.5%)	
Primary Site				
Oral Cavity	53 (39.6%)	30 (54.5%)	23 (29.1%)	0.003
Oropharynx	81 (60.4%)	25 (45.5%)	56 (70.9%)	
Treatment Group				
Surgery + Radiation	37 (27.6%)	20 (36.4%)	17 (21.5%)	0.088
Chemo + Radiation	60 (44.8%)	19 (34.5%)	41 (51.9%)	
Surgery + Chemo + Radiation	37 (27.6%)	16 (29.1%)	21 (26.6%)	

[§]p-value calculated using ANOVA (Age), Chi-square test (sex; alcohol, primary site, treatment group), or Fisher's exact test (race, tumor stage)

Abbreviation: y, Year; Other, Hispanic/Latino + Asian.

Table 2. Tobacco Status at Treatment and Response to First-Line Therapy

		Odds Ratio (95% CI); p-value	
		Crude	Adjusted
All Sites	Quitters	2.27 (0.93 – 5.56); 0.497	3.67 (1.14-11.79); 0.029
	Active Smokers	1 [Reference]	1 [Reference]
Oral Cavity	Quitters	1.44 (0.42 – 4.90); 0.560	1.90 (0.25 – 14.21); 0.53
	Active Smokers	1 [Reference]	1 [Reference]
Oropharynx	Quitters	8.78 (1.09 – 70.68); 0.041	7.42 (0.74 -74.7); 0.089
	Active Smokers	1 [Reference]	1 [Reference]

Crude and adjusted OR and 95% confidence intervals calculated by a Cox-proportional hazard model

Results (cont.)

Figure 1. Tobacco Cessation and Disease-Free Survival in Oral Cancer Patients

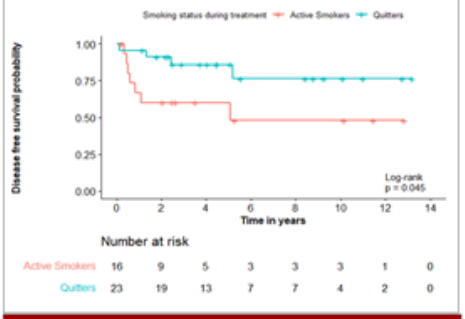

Figure 2. Tobacco Cessation and Overall Survival in the Total Population

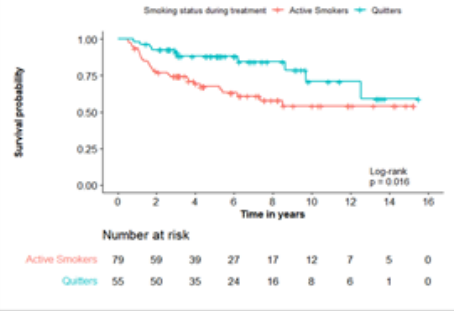

Conclusions

- Quitters respond better to treatment compared to active smokers, especially in those with oropharyngeal cancer.
- Quitters have increased disease-free survival and long-term survival than active smokers.
- Our data suggests that current smokers who quit smoking prior to treatment initiation respond better to first-line therapy and can survive longer than those who continue smoking.

PUFFING TOPOGRAPHY AMONG EXCLUSIVE COMBUSTIBLE CIGARETTE USERS AND DUAL USERS OF CIGARETTES AND POD-BASED OR MOD-BASED ELECTRONIC CIGARETTES

Austin Milton[1], Mayilvanan Chinnaiyan[1], Geraldine Chissoe[1], Daniel Brobst[1], Balaji Sadhasivam[1], Vengatesh Ganapathy[1], Lurdes Queimado[1-3]

Departments of [1]Otorhinolaryngologyand and [2]Cell Biology. [3]TSET Health Promotion Research Center, Stephenson Cancer Center, The University of Oklahoma Health Sciences Center, Oklahoma.
Presenter email: Austin-Milton@ouhsc.edu

Background: Puff topography affects the chemical composition of cigarette smoke and electronic cigarette (EC) aerosol and the total volume inhaled by the user. Consequently, topography is crucial in studying the health outcomes associated with the use of tobacco products. While the topography of exclusive combustible cigarette (CIG) users is well characterized, the impact of dual CIG and EC use on the topography of subsequent CIG or EC use is not.

Aims: 1. To characterize the puffing behavior of exclusive and dual CIG and EC users. 2. To determine whether the topography of dual users differs from that of exclusive users.

Methods: Participants answered an online survey and were assigned to 6 groups based on their reported tobacco habits: exclusive users of EC Mod devices; exclusive users of EC Pod devices; exclusive CIG users; dual users of CIGs and Mods; dual users of CIGs and Pods; and never-smokers/non-EC users. Eligible participants, 21-35 years old, were invited for 2 research visits. During each visit, tobacco product users were asked to smoke and/or vape as they normally would for 2 hours. The smoking and vaping patterns, including puff duration, flow rate, puff volume, and inter puff intervals, were recorded using a topography device. A two-tailed, unequal variance t-test was performed to compare each of the variables between the exclusive CIG user group and the dual user groups.

Results: This study included 11 sessions of smokers, 8 sessions of dual smokers and POD users, and 7 sessions of dual smokers and MOD users. Dual users of CIGs + Mod and CIGs + Pod had significantly shorter interpuff intervals than exclusive CIG smokers ($p=0.02$ & $p=0.04$, respectively). The maximum puff volumes of exclusive CIG users were higher than those of CIG + Mod dual users during the first interval of the session ($p=.049$) and overall ($p=0.01$). Preliminary data also suggest that EC puffing is significantly modified in the context of dual CIG + EC use.

Conclusion: Dual users have a smoking topography that is significantly different from the topography seen with exclusive CIG users. This includes shorter duration between puffs and smaller puff volumes among EC Pod and EC Mod dual users smoking CIGs compared with exclusive CIG smokers. Further evaluation of smoking and vaping puff characteristics is essential to further improve understanding of nicotine dependence and tobacco product toxicity.

Grant support: NIH/NCI (R01CA242168)

TSET Health Promotion Research Center

OU Health | Stephenson Cancer Center

Puffing Topography Among Exclusive Combustible Cigarette Users and Dual Users of Cigarettes and Pod-Based or Mod-Based Electronic Cigarettes

Austin Milton[1], Mayilvanan Chinnaiyan[1], Geraldine Chissoe[1], Daniel Brobst[1], Balaji Sadhasivam[1], Vengatesh Ganapathy[1], Lurdes Queimado[1-3]

Departments of [1]Otorhinolaryngologyand and [2]Cell Biology. [3]TSET Health Promotion Research Center, Stephenson Cancer Center, The University of Oklahoma Health Sciences Center, Oklahoma.

Background

- Electronic cigarettes (ECs) are the most used smoking method among youth, and are used by over 30% of adult tobacco smokers. Oklahoma has the highest EC use in the nation.
- Puff topography affects the chemical composition of cigarette smoke and EC aerosol and the total volume inhaled by the user.
- While the topography of exclusive combustible cigarette (CIG) users is well characterized, the impact of dual CIG and EC use on the topography of subsequent CIG or EC use is not.

Objectives

1. To characterize the puffing behavior of exclusive and dual CIG and EC users.
2. To determine whether the topography of dual users differs from that of exclusive users.

Study Design

- Participants were assigned to 6 groups:
  - MODs, exclusive users of EC Mod devices
  - PODs, exclusive users of EC Pod devices
  - S, smokers (exclusive users of combustible cigarettes)
  - S-MODs, dual users of Cigs and Mods
  - S-PODs, dual users of Cigs and Pods
  - NS/NEC, never-smokers/non-EC users
- Eligible participants, 21-35yo, attended 2 sessions, during which they smoked and/or vaped as they wished for 2 hours.
- A topography device from AUB Aerosol Research Lab recorded puff data.
- Groups were compared with a 2-tailed, unequal variance t-test.

Results

- This study includes 11 sessions of exclusive CIG smokers, 9 sessions of dual CIG + POD users, 8 sessions of dual CIG + MOD users, 6 sessions of exclusive MOD vapers, and 20 sessions of exclusive POD vapers.
- The max. puff volumes of exclusive CIG users were higher than the max. cigarette puff volumes of CIG + MOD dual users (for the overall session, p=0.01).
- CIG + MOD and CIG + POD dual users had significantly shorter interpuff intervals with cigarettes than exclusive CIG smokers.
- More MOD users need to be enrolled in order to analyze the differences between exclusive users and MOD + CIG dual users.

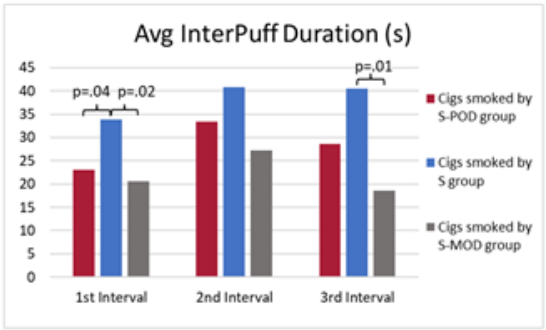

	Cig puffs by S-POD	Cig puffs by S	Cig puffs by S-MOD	Pod puffs by S-POD	Pod puffs by POD
Overall Session					
# of cigarettes	2.8	3.9	2.4		
Total # of Puffs	24.0	39.5	33.7	45.4	66.8
Puff Duration (avg, s)	1.58	1.59	1.63	2.1	3.1
Puff Volume (avg, ml)	45.1	45.2	38.1	53.5	88.1
Flow Rate (max, L/min)	3.4	3.4	2.9	3.3	3.5
Total Inhaled Volume (ml)	1124	1772	1330	2317	5220
1st Interval					
# of puffs in this interval	8.0	8.2	11.7	5.9	5.6
Puff Duration (avg, s)	1.51	1.68	1.65	2.2	3.0
Puff Volume (avg, ml)	45.8	50.5	40.2	58.7	71.0
Flow Rate (max, L/min)	3.3	3.3	2.8	2.5	2.5
2nd Interval					
# of puffs in this interval	6.9	8.2	12.5	7.2	5.5
Puff Duration (avg, s)	1.81	1.58	1.98	1.8	3.1
Puff Volume (avg, ml)	43.5	43.6	39.3	50.2	88.8
Flow Rate (max, L/min)	2.8	3.2	2.4	2.8	2.8

Boxed data pairs above have a statistically significant difference (p<.05).

Results (cont.)

- POD + CIG dual users with PODs had shorter average puff durations and shorter average interpuff durations than exclusive POD users.
- No statistically significant differences in flow rate were found between exclusive cigarette smokers and dual users smoking cigarettes or exclusive POD smokers and dual users smoking PODs.

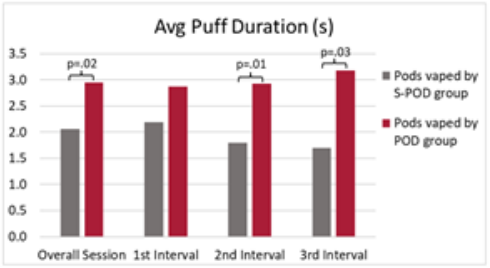

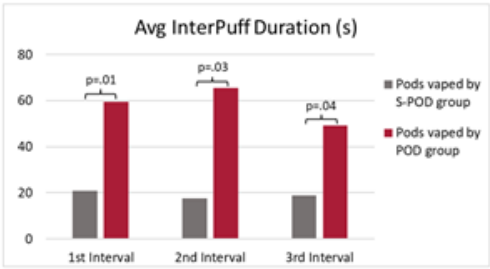

Conclusions

- The cigarette smoking topography seen among dual users is different from the topography seen among exclusive CIG users.
- The POD vaping topography seen among dual users is different from the topography seen among exclusive POD users.
- Longer puffs and/or shorter interpuff durations have been proposed to change the smoke/aerosol chemistry leading to higher concentration of toxins.
- Further evaluation of smoking and vaping puff characteristics is critical to improve understanding of dependence and toxicity.

This work was supported by NIH/NCI (R01CA242168, Queimado) and the Oklahoma Tobacco Settlement Endowment Trust.

NEGATIVE AFFECT AND STRESS ARE ASSOCIATED WITH MOMENT-TO-MOMENT CHANGE IN MOTIVATION DURING A SMOKING CESSATION ATTEMPT

Jiwon Min,[1,2] Lizbeth Benson,[2] Chaelin K. Ra,[2] Emily T. Hébert,[3] Darla E. Kendzor,[2,4] Summer Frank-Pearce,[2,5] & Michael S. Businelle[2,4]

[1]Department of Psychology, Oklahoma State University, Stillwater, OK, United States

[2]TSET Health Promotion Research Center, Stephenson Cancer Center, University of Oklahoma Health Sciences Center, Oklahoma City, OK, United States

[3]**Department of Health Promotion and Behavioral Sciences, UT Health School of Public Health, Austin, TX, United States**

[4]Department of Family and Preventive Medicine, University of Oklahoma Health Sciences Center, Oklahoma City, OK, United States

[5]**Department of Biostatistics and Epidemiology, Hudson College of Public Health, The University of Oklahoma Health Sciences Center, Oklahoma City, OK, United States**

Background: Adults with greater motivation to avoid smoking tend to be at lower risk for smoking lapse during quit attempts. Identification of internal states that are associated with changes in motivation to avoid smoking may provide key contextual information that could be targeted in future smartphone-based just-in-time adaptive interventions. This study aims to examine the extent to which individual variations in negative affect and stress were associated with changes in motivation to avoid smoking during a planned smoking cessation attempt.

Methods: The present study made use of data collected from adults (N=72, 51% female, 67.5% White, M_{Age}=50 years, SD_{Age}=11.6) who participated in a pilot randomized controlled trial that compared three smoking cessation interventions. In particular, participants completed up to five ecological momentary assessments (EMAs) per day during the first four weeks of a quit attempt. On average, participants completed 124 EMAs (SD=37) and answered questions about their current motivation to avoid smoking, negative affect, and stress. Multilevel models were conducted to examine changes in cessation motivation after accounting for age, sex, education, race, intervention group, motivation in the previous prompt, and heaviness of smoking at baseline. Within- and between-person negative affect and stress were decomposed and included in the analyses.

Results: Results indicated that on occasions when individuals' negative affect and stress were higher than usual, their motivation to avoid smoking tended to decrease from the prior occasion (γ=-0.05, p<.01; γ=-0.10, p<.01, respectively). Additionally, those who tended to have higher negative affect and stress during the quit attempt on average also tended to show more of a decrease across consecutive occasions in their motivation to avoid smoking (γ=-0.04, p<.01; γ=-0.19, p<.01, respectively).

Conclusion: Higher momentary negative affect and stress are associated with momentary reductions in motivation to avoid smoking within a given day. Just-in-time adaptive interventions that include emotion regulation and distress tolerance skills when individual's

negative affect and/or stress are higher than usual may increase motivation to avoid smoking, and thus reduce the likelihood of smoking lapse during a quit attempt.

Funding: This study was supported by the Oklahoma Tobacco Settlement Endowment Trust (grant number R22-02) and used the mobile health shared resource of the Stephenson Cancer Center via an NCI Cancer Center Support Grant (grant number P30CA225520).

TSET Health Promotion Research Center

OU Health | Stephenson Cancer Center

Stress is Associated with Moment-to-Moment Change in Motivation during a Smoking Cessation Attempt

Jiwon Min, MS,[1,2] Lizbeth Benson, PhD,[2] Chaelin Karen Ra, PhD,[2]
Emily T. Hébert, PhD,[3] Darla E. Kendzor, PhD,[2,4] Summer Frank-Pearce, PhD,[2,5] & Michael S. Businelle, PhD[2,4]

[1]Department of Psychology, Oklahoma State University, [2]TSET Health Promotion Research Center, University of Oklahoma Health Sciences Center (OUHSC); [3]Department of Health Promotion and Behavioral Sciences, UT Health School of Public Health; [4]Department of Family and Preventive Medicine, OUHSC; [5]Department of Biostatistics and Epidemiology, OUHSC

Background

- Cigarette use = leading cause of preventable death worldwide
- Decreases in momentary motivation & self-efficacy are predictors of smoking lapse
- Stress is associated with lower motivation and self-efficacy for quitting smoking

Objective

- To use ecological momentary assessment (EMA) data collected during a scheduled quit attempt to determine if ***feelings of momentary stress predict subsequent changes in motivation and self-efficacy for quitting***

Study Design

Participants (N=71)
- 50.17 years old, 49% female.
- 64% White, 24% Black, 6% American Indian/Alaska Native, 3% Hispanic/Latino, 1% Native Hawaiian or other Pacific Islander, 5% Others

Procedures
- Randomized into 3 groups (Quitguide, TTRP, Smart-T2)
  - Quitguide: free NCI smoking cessation application
  - TTRP: standard in-person smoking cessation clinic care
  - Smart-T2: smartphone app that tailors intervention content in real-time
- Completed baseline assessment & 29 days of EMA post-quit 5x/day

Measures
- Baseline
  - Demographic information (i.e. sex, age, race, education)
  - Heaviness of Smoking Index (HSI)
- EMA (5-point Likert)
  - Stress ("I feel stressed")
  - Motivation ("I am motivated to AVOID smoking")
  - Self-Efficacy ("I am confident in my ability to AVOID smoking"

Analyses
- Bayesian multilevel models
  - DVs: Momentary motivation or self-efficacy
  - IVs: Previous stress & momentary motivation or self-efficacy
  - Covariates: Time (i.e., day of intervention), race, sex, intervention group, education, sample-mean-centered heaviness of smoking at baseline, whether they had smoked that day

Results

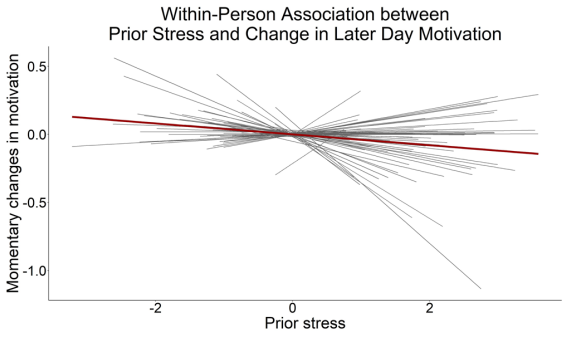

Figure 1. ***Higher momentary stress*** in the previous prompt is associated with a **decrease** in ***momentary motivation*** *from one moment to the next* (β_{2i} = -0.03, 95% CI = [-0.05, -0.01]. But not after controlling for all model covariates (β_{2i} = -0.02, 95% CI = [-0.05, -0.00])

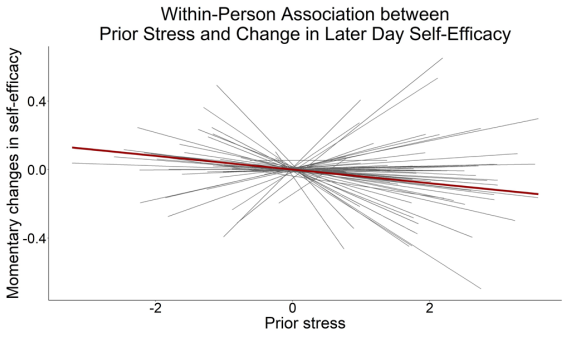

Figure 2. ***Higher momentary stress*** in the previous prompt is ***not*** associated with decrease in ***momentary self-efficacy*** from one moment to the next(β_{2i} = -0.03, 95% CI = [-0.05, -0.00]., even after controlling for all covariate variables (β_{2i} = -0.02, 95% CI = [-0.05, -0.00])

Discussion

- When a participant's feeling of stress was higher than their usual level of stress, their subsequent motivation decreased as measured during the next EMA (i.e, ~ 3.4 hours later, SD = 2.0 hours)
  - Effect not credible after controlling for all covariates
- Participant's feelings of stress were not associated with changes momentary self-efficacy
  - Even after controlling for all covariates

Limitations:

- ***Measurement:***
  - Motivation, self-efficacy, & stress were each assessed using a single EMA item.
- ***Generalizability:***
  - Small sample size
  - Sample was made up of smokers from one state (Oklahoma)

Future directions:
- ***Generalizability:***
  - Examine if findings are replicated with larger samples outside of Oklahoma
- ***Extension***
  - Examine if other internal states (e.g. negative affect) also predict changes in motivation and self-efficacy
  - Develop and test interventions that directly target stress management when one's stress is higher than usual & examine if intervention results in increase in subsequent motivation
    - Coping strategies
    - Distress tolerance
    - Emotion regulation

Acknowledgements

- Funding:
  - Oklahoma Tobacco Settlement Endowment Trust (grant number R22-02)
  - Mobile health shared resource of the Stephenson Cancer Center via an NCI Cancer Center Support Grant (grant number P30CA225520).

EPIDEMIOLOGY OF LUNG CANCER IN OKLAHOMA, 1999-2018

Shayla R. Morin, Ami E. Sedani MPH, Janis E. Campbell PhD
Department of Biostatistics and Epidemiology, Hudson College of Public Health, The University of Oklahoma Health Sciences Center

Introduction: Lung and bronchus cancer (e.g., lung cancer) is the leading cause of cancer death and the second most frequently diagnosed cancer in both men and women in the United States (U.S.). Although smoking rates in the U.S. have decreased over time, current and former smokers remain at high-risk for developing lung cancer. This project aimed to describe a summary for lung cancer incidence, mortality, and trends in Oklahoma from 1999 to 2018.

Methods: A surveillance study was used to assess lung cancer incidence and mortality rates among residents in Oklahoma. Data on incident cases of lung cancer were obtained from the Oklahoma Central Cancer Registry (OCCR), the CDC's National Program of Cancer Registries (NPCR), and the NCI's Surveillance, Epidemiology, and End Results (SEER) program. Mortality data were from Oklahoma Vital Statistic and the CDC's National Vital Statistics System (NVSS). We assessed incidence and mortality trends from 1999-2018 comparing Oklahoma and the U.S. Over the same period, we compared trends in rates by sex in Oklahoma. From 2014 to 2018, we further analyzed rates in Oklahoma by race/ethnicity and 10-year age groups. All rates used were age-adjusted to the 2000 US standard population and per 100,000 population. All data sources used in this project were publicly available and provided de-identified data.

Results: In Oklahoma, from 2014-2018, there were 15,609 lung cancer cases and 11,616 lung cancer deaths; correspondingly ranked as the 8th worst in incidence and 5th worst in mortality in the U.S. From 1999-2018, overall trends in rates for both the U.S. and Oklahoma decrease over time. However, Oklahoma decreases at a slower rate compared to the U.S. and maintains consistently higher rates compared to the national averages. From 1999-2018, men had higher lung cancer incidence and mortality rates compared to women. The age-adjusted incidence and mortality rates among the non-Hispanic, American Indian population have disproportionately higher rates than all other racial/ethnic groups within Oklahoma. Age-adjusted rates by 10-year age groups show that the highest rates are among those 75-84 years old.

Discussion: This project contains the most precise Oklahoma estimates currently available. Findings reveal that while progress has been made, continued evidence-based tobacco control and prevention efforts are needed to ensure further reductions in lung cancer rates in Oklahoma. Additionally, several opportunities exist to increase lung cancer screening participation among eligible individuals to reduce lung cancer mortality in the state.

Epidemiology of Lung Cancer in Oklahoma, 1999-2018

HUDSON COLLEGE OF PUBLIC HEALTH
The UNIVERSITY of OKLAHOMA HEALTH SCIENCES CENTER

Shayla R. Morin; Ami E. Sedani, MPH; Janis E. Campbell, PhD

Department of Biostatistics and Epidemiology, Hudson College of Public Heath,
The University of Oklahoma Health Sciences Center

Background

- Lung cancer is the leading cause of cancer death and second most frequently diagnosed cancer in the U.S.
- Tobacco smoking is the leading risk factor for lung[1] cancer and attributes to a majority of cases[2]
- Smoking rates have decreased over time, but current and former smokers remain at high-risk[2,3]

Aim

To summarize lung cancer incidence, mortality, and trends in Oklahoma from 1999-2018

Methods

- Surveillance study assessing incidence & mortality within Oklahoma
- Research involved the analysis of existing, publicly available de-identified data from 1999-2018
- Incidence data obtained from:
  - Oklahoma Central Cancer Registry (OCCR)
  - CDC's National Program of Cancer Registries (NPCR)
  - NCI's Surveillance, Epidemiology, and End Results (SEER) program
- Mortality data obtained from:
  - Oklahoma Vital Statistics
  - CDC's National Vital Statistics System (NVSS)
- Incidence and Mortality rates assessed by:
  - Comparison to national trends
  - Sex
  - Race/Ethnicity
  - 10-year age groups
- All rates were age-adjusted to the 2000 US standard population and per 100,000 population

Results

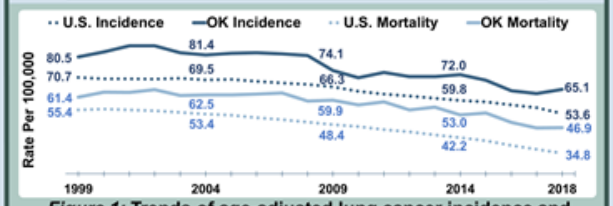

Figure 1: **Trends of age-adjusted lung cancer incidence and mortality rates in OK and the U.S., 1999-2018**

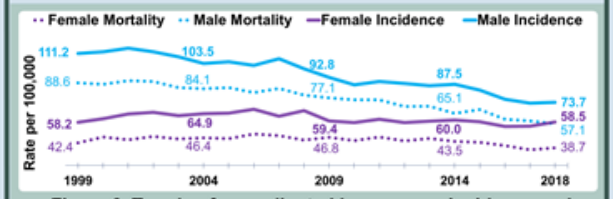

Figure 2: **Trends of age-adjusted lung cancer incidence and mortality rates by sex, Oklahoma, 1999-2018**

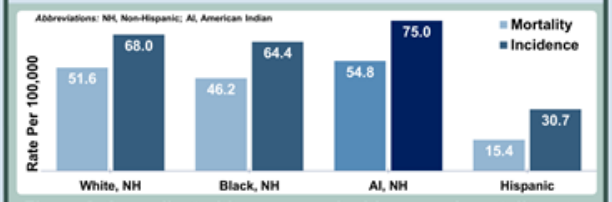

Figure 3: **Age-adjusted lung cancer incidence and mortality rates by race in Oklahoma, 2014-2018**

Figure 4: **Lung cancer incidence and mortality rates by 10-year age groups, Oklahoma, 2014-2018**

Results (cont.)

- Oklahoma declines at a slower rate and maintains higher incidence and mortality than the national averages
- Men have consistently higher rates compared to women
- Non-Hispanic, American Indian populations are disproportionally affected with the highest rates
- The highest incidence and mortality rates are seen for those 75-84 years old

Conclusion

- This report contains a complete summary of the most current estimates available for lung cancer in Oklahoma
- Findings reveal:
  - Continued efforts for tobacco control and prevention are needed to further reduce incidence rates in Oklahoma
  - A concerning uptick in incidence and mortality over the last 5 years that needs to be addressed with continued efforts towards encouraging screening for those who are eligible

References and Data Sources

- [1]US Cancer Statistics Working Group. U.S. Cancer Statistics Data Visualizations Tool, based on 2020 submission data (1999-2018): U.S. Department of Health and Human Services, Centers for Disease Control and Prevention and National Cancer Institute; www.cdc.gov/cancer/dataviz. Accessed Aug. 19, 2021.
- [2]Alberg AJ, Brock MV, Ford JG, et al. Epidemiology of lung cancer: diagnosis and management of lung cancer, 3rd ed: American College of Chest Physicians evidence-based clinical practice guidelines. Chest. 2013;143(5 suppl):e1S-e29S.
- [3]Samet, J. M. (1991). Health benefits of smoking cessation. Clinics in chest medicine, 12(4), 669-679.
- Oklahoma State Department of Health (OSDH), Center for Health Statistics, Health Care Information, Vital Statistics, on Oklahoma Statistics on Health Available for Everyone (OK2SHARE). https://www.health.state.ok.us/stats/Registries/cancer/FinalImortality.shtml
- Oklahoma State Department of Health (OSDH), Disease, Prevention, & Preparedness Service, Chronic Disease Service, Oklahoma Central Cancer Registry (OCCR), on Oklahoma Statistics on Health Available for Everyone (OK2SHARE). https://www.health.state.ok.us/stats/Registries/cancer/FinalStatistics.shtml
- Surveillance, Epidemiology, and End Results (SEER) Program (www.seer.cancer.gov) SEER*Stat Database: U.S. Population (1990-2018), National Cancer Institute, DCCPS, Surveillance Research Program, Surveillance Systems Branch, released April 2020.

Acknowledgement

- This poster reflects an Oklahoma lung cancer report that is a part of a series of cancer data briefs established by the Stephenson Cancer Center

THE RELATION BETWEEN INSOMNIA SEVERITY AND SMOKING CESSATION OUTCOMES AMONG ADULTS PARTICIPATING IN TREATMENT: A LONGITUDINAL STUDY

Chaelin K. Ra, Ph.D;[1] Summer Frank-Pearce, Ph.D, MPH;[1,3] Sarah J. Ehlke Ph.D;[1] Michael S. Businelle, Ph.D.[1,2] Darla E. Kendzor, Ph.D[1,2]

[1]TSET Health Promotion Research Center, Stephenson Cancer Center, University of Oklahoma Health Sciences Center, Oklahoma City, OK, United States

[2]Department of Family and Preventive Medicine, University of Oklahoma Health Sciences Center, Oklahoma City, OK, United States

[3]Department of Biostatistics and Epidemiology, Hudson College of Public Health, The University of Oklahoma Health Sciences Center, Oklahoma City, OK, United States

Significance: There is preliminary evidence that experiencing insomnia is associated with a lower likelihood of smoking cessation among those making a quit attempt. Yet, few studies have used longitudinal data to examine the association between insomnia and smoking cessation.

Methods: Data from a community-based tobacco cessation program for adults (N=649) were used to examine the association between insomnia and smoking cessation at follow-up. On the scheduled quit date, the Insomnia Severity Index was administered to assess insomnia severity during the previous two weeks. Biochemically-verified 7-day point prevalence abstinence was measured at four time points (i.e., quit date, 4-, 12-, and 26-weeks post-quit-date). Repeated measures logistic regression analyses were conducted to evaluate the odds of achieving abstinence at each follow-up given insomnia severity (i.e., none/subthreshold vs. moderate/severe), after adjustment for covariates. The potential interaction between insomnia severity and time was evaluated in the model.

Results: On average, participants were 51.9 (SD=12.1) years old with 12.5 (SD=2.2) years of education. Participants were predominantly female (58.1%), White (58.4%) or Black (27.3%), and most had a household income below $21,000 (61.6%). Participants reported smoking an average of 17.0 (SD=10.3) cigarettes per day for an average of 30.2 (SD=14.1) years at baseline. Analyses indicated that insomnia severity was not significantly associated with abstinence on the quit date (OR: 0.79, CI: 0.54-1.15) or at 4-weeks post-quit follow-up (OR: 0.73, CI: 0.53-1.01). However, those with moderate/severe insomnia had a significantly lower likelihood of achieving abstinence at 12- and 26-weeks post-quit follow-up (OR: 0.64, CI: 0.46-0.88 and OR: 0.50, CI: 0.28-0.88, respectively).

Conclusion: While insomnia severity was not related to abstinence early in treatment, it was associated with a lower likelihood of abstinence at later follow-ups. Future research should explore whether insomnia screening and treatment before and during a smoking cessation attempt might increase the likelihood of smoking cessation.

Acknowledgments: This research was supported by Oklahoma Tobacco Settlement Endowment Trust (TSET) grant R21-02, and NCI Cancer Center Support Grant P30CA225520 awarded to the Stephenson Cancer Center.

INTRA-SESSION RELIABILITY IN 1ST-RAY FORCE CONTRIBUTION TO PUSH-OFF DURING NEUROTOXIC CHEMOTHERAPY

Josiah Rippetoe[1,3], Chao Xu, PhD[4], Debra Richardson, MD[2], Kathleen Moore, MD, MS[2], Elizabeth Hile, PT, PhD[1,3]

[1]OU Health Stephenson Cancer Center, Cancer Rehabilitation, Oklahoma City, OK

[2]OU Health Stephenson Cancer Center, College of Medicine, Department of Obstetrics and Gynecology, Oklahoma City, OK

[3]The University of Oklahoma Health Science Center, College of Allied Health, Department of Rehabilitation Sciences, Oklahoma City

[4]The University of Oklahoma Health Sciences Center, College of Public Health, Department of Biostatistics and Epidemiology, Oklahoma City, OK

***Presenting speaker's email**: Josiah-Rippetoe@ouhsc.edu*

Introduction: Chemotherapy-induced peripheral neuropathy (CIPN) can cause activity restriction, mobility disability, and falls. The earliest CIPN gait changes are not well-characterized, and would inform clinical surveillance for dose reduction and rehabilitation. As a length-dependent polyneuropathy, CIPN sensory and strength changes begin at the toes, so we hypothesize that early CIPN changes will alter First Ray Force Contribution to Push-off (FRCP), making FRCP a valid biometric correlate of CIPN for use in clinical and research CIPN surveillance. Testing this hypothesis in future studies requires first establishing the intra-session reliability of FRCP values at baseline (pre-chemo) in women with cancer. FRCP is known to increase with gait speed in healthy adults, so we hypothesize that earliest CIPN-induced changes may be detected only at fast pace. For this reason, we will test intra-session reliability at both usual and fast pace.

Methods: This is a secondary analysis of baseline data from an ongoing prospective feasibility study to observe mobility and CIPN symptoms over 3-6 consecutive cycles of taxane chemo for breast & gynecologic cancers. We included data from the 14 (45% of 31) women who enrolled with no evidence of mobility-impacting neuromuscular conditions. Participants completed 20-ft walks at usual & fast pace, 4-8 passes each, on high-resolution Strideway™ (Tekscan®, Boston). For each step, FRCP (%) = (1^{st} ray force/total plantar force) X 100 at the timepoint of push-off (defined as 2^{nd} peak of stance phase pressure plot). We calculated intra-session reliability by side (R, L) and pace (usual, fast) as ICCs using 2-way mixed-effects & absolute agreement (SPSS 25) over 14 total steps per participant, and with/without normalization to gait speed.

Results: Women were 64.0 (12.8) years of age, 78% white, 0.98 (0.20) m/sec usual gait speed and 1.34 (0.32) m/sec fast gait speed. At usual pace, intra-session reliability by ICC was 0.587-0.588 without gait speed normalization, 0.449-0.502 when normalized. At fast pace, reliability was 0.610-0.618 without & 0.690-0.766 with normalization.

Conclusions: Intrasession reliability of FRCP is moderate in midlife and older women with breast and gynecologic cancers before 1st taxane dose. Reliability is highest when walking at fast pace, particularly when normalized to gait speed. Unexpectedly, normalizing to gait speed reduced between-step agreement at usual pace. Pressure-based gait parameters have low to moderate reliability even in healthy adults. Comparatively, the agreement of these FRCP ICC values obtained from steps taken by women with cancer in a single baseline session is acceptable to continue this line of questioning, toward the use of FRCP as an early indicator of CIPN gait changes during chemo. As technology becomes more accessible, monitoring gait parameters beyond speed could advance CIPN surveillance for earlier detection.

Funding: Presbyterian Health Foundation, Oklahoma Tobacco Settlement Endowment Trust, NCI Cancer Center Support Grant P30CA225520 to OU Stephenson Cancer Center.

Intra-Session Reliability in 1st-Ray Force Contribution to Push-off During Neurotoxic Chemotherapy

Josiah Rippetoe[1,3], Chao Xu, PhD[4], Debra Richardson, MD[2], Kathleen Moore, MD, MS[2], Elizabeth Hile, PT, PhD[1,3]
[1]OU Health Stephenson Cancer Center, Cancer Rehabilitation, Oklahoma City, OK
[2]OU Health Stephenson Cancer Center, College of Medicine, Department of Obstetrics and Gynecology, Oklahoma City, OK
[3]The University of Oklahoma Health Science Center, College of Allied Health, Department of Rehabilitation Sciences, Oklahoma City
[4]The University of Oklahoma Health Sciences Center, College of Public Health, Department of Biostatistics and Epidemiology, Oklahoma City, OK

INTRODUCTION

- Chemotherapy-induced peripheral neuropathy (CIPN) can cause activity restriction, mobility disability, and falls.[1]
- The earliest CIPN gait changes are not well-characterized, and could inform clinical surveillance for dose reduction & rehabilitation.
- As a length-dependent polyneuropathy, CIPN sensory & strength changes begin at the toes,[2] so we hypothesize that early CIPN changes will alter First Ray Force Contribution to Push-off (FRCP). If so, FRCP could be a valid biometric correlate of CIPN for use in clinical and research CIPN surveillance, but to test this hypothesis in future studies we must first establish the reliability of FRCP values from consecutive passes in a single session (intra-session).
- Force and pressure are known to increase with gait speed in healthy adults,[3] so we hypothesize that earliest CIPN-induced changes may be evident only at fast pace.

We aim to quantify the intra-session test-retest reliability of FRCP at usual and fast pace, in women with breast & gynecologic cancers who are scheduled to begin neurotoxic chemotherapy.

METHODS

- **Design**: Secondary analysis of baseline data from an ongoing feasibility study to observe mobility and CIPN symptoms over 3-6 consecutive taxane (± platinum) chemotherapy cycles for breast & gynecologic cancers.
- **Inclusion:** Of 31 women with baseline data, we included only the 13 (42%) with usual and fast pace passes and no evidence of mobility-impacting neuromuscular conditions.
- **Data**: 4-8 passes of 20-feet each across a high-resolution Strideway™ (Tekscan®, Boston) walking at usual pace, and then fast pace.

METHODS: ANALYSES

Analysis: FRCP was calculated at the time of push-off (*push-off =2nd peak of stance phase pressure plot*) as:

FRCP (%) = (1st ray force/total plantar force) X 100

- We calculated ICC by side (R,L) & pace (usual, fast) using 2-way mixed-effects & absolute agreement over 14 total steps per participant, and with/without normalization to gait speed.
- We performed sensitivity analyses for two sub-groups, with usual pace ≤0.8 m/s (n=4) & usual pace ≥ 1.0 m/s (n=4).

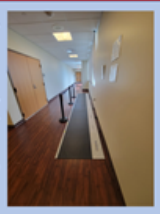

Figure 1: Tekscan™ Strideway® at the Cancer Rehab Research Laboratory (CRRL) at OUHSC/OU Health Stephenson Cancer Center. The walkway consists of 7 high-resolution pressure-sensing panels.

RESULTS

Table 1: Participant Demographics

Group	Mean Age (SD) years	Race/Ethnicity	Height Mean (SD) m	Weight Mean (SD) Kg	BMI Mean (SD) Kg/m^2	Usual Gait Speed Mean (SD) m/s	Fast Gait Speed Mean (SD) m/s
All n=13	64.4 (12.4)	92% White, 8% Black	1.60 (1.0)	79.0 (20.5)	30.8 (7.9)	0.90 (0.16)	1.32 (0.28)
Usual pace ≤0.8 n=4	71.4 (7.6)	100% White	1.66 (0.08)	86.4 (15.5)	43.5 (3.5)	0.71 (0.08)	1.09 (0.09)
Usual pace ≥1.0 n=4	63.2 (7.3)	100% White	1.56 (0.14)	67.5 (4.2)	28.6 (6.9)	1.09 (0.07)	1.46 (0.25)

Table 2: Intra-Session Test-Retest ICC Values by Group and Foot

Group	Foot	Mean FRCP (SD) %/m/s				ICC (p-value)			
		Usual Pace		Fast Pace		Usual Pace		Fast Pace	
			Normalized		Normalized		Normalized		Normalized
All n=13	Left	23.46 (13.83)	28.80 (19.66)	28.75 (12.22)	23.40 (12.02)	0.627 (<0.001)	0.755 (<0.001)	0.610 (<0.001)	0.690 (<0.001)
	Right	25.20 (12.20)	29.65 (17.0)	31.80 (11.05)	25.98 (11.83)	0.619 (<0.001)	0.744 (<0.001)	0.618 (<0.001)	0.766 (<0.001)
Usual pace ≤0.8 n=4	Left	28.19 (16.85)	41.71 (26.25)	36.67 (13.49)	33.82 (13.19)	0.758 (<0.001)	0.810 (<0.001)	0.588 (<0.001)	0.573 (<0.001)
	Right	27.51 (11.39)	41.14 (19.91)	33.19 (8.58)	30.29 (8.11)	0.558 (<0.001)	0.737 (<0.001)	0.351 (<0.001)	0.242 (0.002)
Usual pace ≥1.0 n=4	Left	24.75 (12.95)	23.22 (12.82)	29.91 (8.27)	21.37 (7.34)	0.583 (<0.001)	0.619 (<0.001)	0.160 (0.026)	0.461 (<0.001)
	Right	29.98 (9.02)	27.80 (8.83)	35.80 (8.55)	25.26 (7.29)	0.222 (0.004)	0.325 (<0.001)	0.148 (0.024)	0.360 (<0.001)

DISCUSSIONS AND CONCLUSIONS

- Overall, First Ray Contribution to Push-off (FRCP) is ***moderately reliable*** in this small sample of mid-life and older women with gynecologic cancers who are scheduled to begin neurotoxic chemotherapy. 70% of ICC values fall within values published for healthy younger adults (0.49 to 0.98).[4] It is important to consider that some variability is normal in gait.
  - Normalizing by gait speed appears to improve reliability.
  - Reliability may be lowest at fastest speeds, although group sizes were very small.
- When comparing data across women in this sample, FRCP during usual-paced gait differed up to 60%, and often differed between right & left feet of the same woman. ***Accurate interpretation of serial FRCP assessments over a course of neurotoxic chemotherapy will require a pre-chemo baseline value for each foot of each patient.***
- *Limitations*: Small n, especially for sub-analyses.
- We will confirm results in a larger, more diverse sample before testing FRCP as a biometric indicator of CIPN onset or progression in women with cancer.

ACKNOWLEDGEMENTS

- All participants for their time and effort
- Ashley Fox, Abby Cha, and Kayla Jencks for their help with data collection and cleaning.
- Funding: Presbyterian Health Foundation (PHF), Oklahoma Tobacco Settlement Endowment Trust (TSET), National Cancer Institute (NCI) Cancer Center Support Grant P30CA225520 awarded to the University of Oklahoma Stephenson Cancer Center. *The content is solely the responsibility of the authors and does not necessarily represent the official views of the PHF, NIH/NCI, or Oklahoma TSET.*

LITERATURE CITED

1. Battaglini E. JCO 2020;38(15_suppl.): E24080.
2. Kneis S, et al. Clin Neurophysiol. 2016;127(2):1481-1490.
3. Kirmizi M, et al. Acta Bioeng Biomech Orig Pap. 2020;22(3).
4. Zammit, GV, et al. J Foot Ankle Res 2010;3(11):1-9.

SECONDHAND SMOKE EXPOSURE ALTERS DRUG TRANSPORTERS AND INDUCES CISPLATIN-RESISTANT IN HEAD AND NECK CANCER CELLS

Balaji Sadhasivam[1*], Jimmy Manyanga[1,2*], Vengatesh Ganapathy[1], Célia Bouharati[1], Toral Mehta[1], Basil Mathews[1], Samuel Castles[1], David Rubenstein[4], Alayna P. Tackett[5,6], Pawan Acharya[3], Daniel Zhao[3], and Lurdes Queimado ✉[1,2,5]

Departments of [1]Otolaryngology Head and Neck Surgery, [2]Cell Biology, and *[3]Biostatistics, [5]TSET Health Promotion Research Center, Stephenson Cancer Center, The University of Oklahoma Health Sciences Center, Oklahoma City OK-73104, USA.*

[4]Department of Biomedical Engineering, Stony Brook University, New York, New York, United States of America.

[6]Department of Population and Public Health Sciences, Keck School of Medicine, University of Southern California Los Angeles CA-90032, USA.

* Equal contribution

Purpose: One in four Americans, are involuntarily exposed to secondhand smoke (SHS). Yet, the impact of SHS exposure on cancer treatment is unknown. A recent study has shown that exposure to SHS during head and neck squamous cell carcinoma (HNSCC) therapy is a significant independent predictor of HNSCC recurrence. Our study examines the effect of SHS smoke exposure on HNSCC cisplatin treatment and investigates the potential mechanisms leading to the observed effects.

Methods: Side-stream (SS) smoke, the main component of SHS, was extracted as previously described. Three different human HNSCC cell lines (UM-SCC1, WSU-HN6, and WSU-HN30) were exposed to SS smoke extract for 48 hours at doses mimicking the nicotine levels observed in the saliva of passive smokers. Then, cancer cells were treated
with cisplatin (0.1-100 µM) in the presence of SS smoke extract. Cancer cell death and indefinite survival capacity were assessed with trypan blue staining and clonogenic survival assay, respectively. The cisplatin half-maximal inhibitory concentration (IC50) was determined using GraphPad Prism software. qPCR and Western blot analysis were used to measure ABCG2 expression. Linear regression analysis was performed to evaluate the overall effect.

Results: Exposure to SS smoke extract significantly decreased cell death ($P<0.0001$) and increased clonogenic survival capacity ($P<0.017$) in the cancer cells treated with cisplatin in the presence of SS smoke extract, compared to cisplatin-treated but unexposed HNSCC cells. Cisplatin sigmoidal dose-response curves indicate that cancer

cells exposed to SS extract significantly increased their cisplatin resistance when compared to respective control cells: UM-SCC1 ($p<0.0001$), WSU-HN6 ($p<0.0035$), and WSU-HN30 ($p<0.0001$). These data indicate that in the presence of SS smoke extract, significantly higher concentrations of cisplatin need to be used to reach IC50 in all three HNSCC cells. Compared to control, cells treated with SS extract showed a significant increase in both mRNA and protein expression of ABCG2, a cisplatin drug efflux transporter, in all cell lines. The linear regression analysis strengthens the relevance of the observed overall increase in ABCG2 expression ($p<0.0001$). Our data suggest there is an active cisplatin efflux mechanism in the SS-treated cells.

Conclusions: Our study documents for the first time that even short-term exposure to SHS can lead to cisplatin resistance in head and neck cancer cells by altering the expression of multidrug resistance and the ability to evade cisplatin-induced cell death. Further studies in HNSCC patients-based observation are warranted. Our data stresses the urgent need for clinicians to consider the potential role of SHS exposure on treatment outcomes and to advise cancer patients or caregivers about the potential risks of SHS exposure during cancer treatment.

Funding: This work was partially supported by the National Cancer Institute of the National Institutes of Health (R33CA202898, R01CA242168, and P30CA225520), the Oklahoma Tobacco Settlement Endowment Trust, and the Oklahoma Center for Advancement of Science and Technology (HR16-007). Dr. Queimado holds a Presbyterian Health Foundation Endowed Chair in Otorhinolaryngology Position.

TSET Health Promotion Research Center

OU Health | Stephenson Cancer Center

SECONDHAND SMOKE EXPOSURE ALTERS DRUG TRANSPORTERS AND INDUCES CISPLATIN-RESISTANT IN HEAD AND NECK CANCER CELLS

Balaji Sadhasivam[1*], Jimmy Manyanga[1,2*], Vengatesh Ganapathy[1], Célia Bouharati[1], Toral Mehta[1], Basil Mathews[1], Samuel Castles[1], David Rubenstein[4], Alayna P. Tackett[5,6], Pawan Acharya[3], Daniel Zhao[3], and Lurdes Queimado[1,2,5]

Departments of 1Otolaryngology Head and Neck Surgery, 2Cell Biology, and 3Biostatistics, 5TSET Health Promotion Research Center, Stephenson Cancer Center, OUHSC, OK-73104, USA. 4Department of Biomedical Engineering, Stony Brook University, New York. 6Department of Population and Public Health Sciences, Keck School of Medicine, University of Southern California LA.

Background

- Active smoking during head and neck squamous cell carcinoma (HNSCC) treatment leads to poor chemo response, lower disease-free survival and five-year overall survival.
- In US, about 20% Americans are involuntarily exposed to secondhand smoke (SHS).
- Though mainstream (MS) and SHS smoke share similar chemicals, the impact of SHS exposure during HNSCC treatment outcome is understudied.
- A recent sole study showed that exposure to SHS during HNSCC therapy is a significant independent predictor of recurrence.
- How does the exposure to SHS affect cisplatin treatment outcome in head and neck cancers?

Objective

- To determine the effect of SS smoke exposure on HNSCC cells viability, cisplatin treatment efficacy and indefinite survival capacity during cisplatin therapy.
- To unearth the potential mechanisms responsible for the observed effects.

Study Design

- Three distinct human HNSCC cell lines (UM-SCC1, WSU-HN6, WSU-HN30) were used for this study.
- To mimic human exposure, cells were exposed to SS smoke (major component of SHS) extract for 48h at a dose delivering 48 ng/ml nicotine (observed in passive smokers' saliva).
- HNSCC cells exposed to SS smoke extract for 48h, followed by SS smoke extract and cisplatin for another 48h to assess cell death, IC50 and indefinite survival capacity.
- Cisplatin IC50 was determined using GraphPad Prism software.
- ABCG2 expression was measured by qPCR and Western blot analysis.
- Linear regression was analysis performed to evaluate the overall effect after adjusting cell lines.

Results

Figure 1. Exposure to SS Smoke Reduces Cell Death in HNSCC

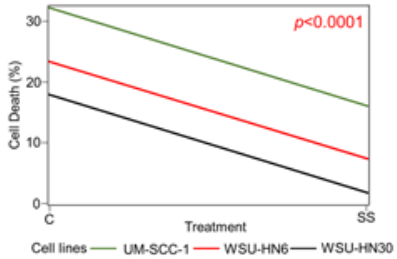

Figure 2. Exposure to SS Smoke Extract Increases Cisplatin Resistance in HNSCC

		Cisplatin IC50	
		IC50 [95% CI] µM	P-value
UM-SCC-1			
	Control	3.5 [2.9 to 4.3]	1
	SS	6.7 [5.6 to 7.8]	**<0.0001**
WSU-HN6			
	Control	7.9 [6.2 to 9.96]	1
	SS	12.2 [10.2 to 14.6]	**0.0035**
WSU-HN30			
	Control	3.0 [2.4 to 3.8]	1
	SS	6.1 [5.0 to 7.4]	**<0.0001**

Figure 3. Exposure to SS Smoke Increases HNSCC Clonogenic Survival

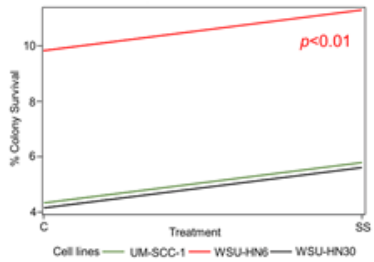

Results (cont.)

Figure 4. Exposure to SS Smoke Increases the Expression of Multidrug Resistance Protein ABCG2 in HNSCC

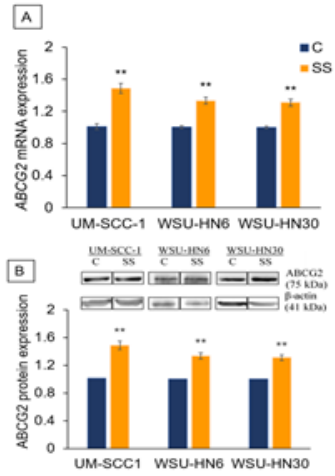

(A) Gene expression; (B) Western blot and protein quantification. Data represented as mean ± SEM. *p <0.05, **p <0.01. Overall effect assed by linear regression analysis for ABCG2 mRNA (p<0.0001) and protein (p<0.0001).

Conclusions

- Our study is the first to report, that even short-term exposure to SHS during cisplatin treatment can lead to cisplatin resistance in HNSCC.
- By altering the expression of multidrug resistance proteins, SHS can allow cancer cells to evade cisplatin-induced cell death.
- Our finding stress the urgent need for clinicians to consider the potential effect of SHS exposure on HNSCC treatment outcomes and to advise cancer patients and caregivers about the potential risks of SHS exposure during cancer treatment.
- Further studies on the effect of SHS in HNSCC patient outcomes are warranted.

Funding : NCI (NIH) R33CA202898, R01CA242168, and P30CA225520, TSET, OCAST (HR16-007). Dr. Queimado holds a PHF Endowed Chair in Otorhinolaryngology Position.

FACILITATORS AND BARRIERS TO LUNG CANCER SCREENING IMPLEMENTATION IN THE U.S: A SYSTEMATIC REVIEW

Authors: Ami E. Sedani[1], Olivia C. Davis[2], Shari C. Clifton[3], and Ann F. Chou[4]

[1]Department of Biostatistics and Epidemiology, Hudson College of Public Health, University of Oklahoma Health Sciences Center, Oklahoma City, OK

2College of Medicine, University of Oklahoma Health Sciences Center, Oklahoma City, OK

[3]Robert M. Bird Health Sciences Library, University of Oklahoma Health Sciences Center, Oklahoma City, OK.

[4]Department of Family and Preventive Medicine, College of Medicine, University of Oklahoma Health Sciences Center, Oklahoma City, OK

Introduction: The purpose of this study is to undertake a comprehensive systematic review to describe multi-level factors (barriers and facilitators) that may influence the implementation of low-dose computed tomography (LDCT) for lung cancer screening in the U.S.

Methods: Systematic literature searches were performed using six online databases and citation indexes for peer-reviewed studies, for articles published between January 1, 2013 to April 1, 2021. Covidence, a Cochrane technology web-based platform, was utilized for title and abstract screening, full text review, reference management, and data extraction. Studies were initially screened by title and abstract by two independent reviewers. Disagreements were resolved through discussion, or by a third reviewer when no decision was reached. The same screening process was repeated for full text screening, data extraction, and risk of bias. For thematic synthesis, the identified barriers and facilitators for each study included in our final review were then coded and categorized into domains that encompassed the Consolidate Framework for Implementation Research (CFIR). Risk of bias of individual studies was appraised using Mixed Methods Appraisal Tool (MMAT v. 2018). A protocol was registered with PROSPERO (CRD4202124767).

Results: Initial searched yielded 6,181 published studies. After automatic elimination of duplicates in Covidence, 2,473 were retained for title and abstract screens and 37 were included in this review. Five studies explored factors to implementation from the system level perspective, 16 at the provider level, 13 at the patient level, and 3 explored both patient and provider perspectives. Using the CFIR framework, a total of 21 constructs (out of 36) relating to 5 all domains were extracted for inclusion in this synthesis. The major emerging factors mentioned were those related to characteristics of the individual, intervention characteristics, and outer setting domains. These included: *knowledge & beliefs about the intervention* (n=37), *patients' needs and resources* (n=25), and *the evidence strength & quality* (n=24) constructs. The data were too heterogenous to perform a meta-analysis.

Discussion: Findings from this review summarizes the growing body of literature on the multi-level complexity of implementing high quality lung cancer screening program. Applying the CFIR domains and constructs to understand and specify factors facilitating uptake of lung cancer screening, as well as cataloguing the lessons learned from previous efforts, help to inform the development and implementation processes of lung cancer screening programs in the community setting.

Facilitators And Barriers To Lung Cancer Screening Implementation In The U.S: A Systematic Review

Ami E. Sedani[1], Olivia C. Davis[2], Shari C. Clifton[3], and Ann F. Chou[4]

[1]Department of Biostatistics and Epidemiology, Hudson College of Public Health, University of Oklahoma Health Sciences Center, Oklahoma City, OK
[2]College of Medicine, University of Oklahoma Health Sciences Center, Oklahoma City, OK
[3]Robert M. Bird Health Sciences Library, University of Oklahoma Health Sciences Center, Oklahoma City, OK.
[4]Department of Family and Preventive Medicine, College of Medicine, University of Oklahoma Health Sciences Center, Oklahoma City, OK

INTRODUCTION

- Despite guidelines issued by the US Preventive Services Task Force (USPSTF), health insurance coverage, and scientific evidence of screening, the implementation of lung cancer screening with Low-Dose CT (LDCT) has remained sub-optimal.

Purpose

- This **systematic review** uses the Consolidated Framework for Implementation Research (CFIR) to describe multi-level factors that may influence the implementation of LDCT for lung cancer screening.

Figure 1. Timeline of Lung Cancer Screening

METHODS

Protocol and Registration

- A protocol was registered with PROSPERO (CRD4202124767)

Search Strategy

- Key word searches in Ovid MEDLINE, Embase, PsycINFO, CINAHL, PubMed, and Web of Science databases
- Published: Jan. 2013 to Apr. 2021

Data Collection Process

- EndNote (v. X9) library
- Covidence, Cochrane technology web-based platform
- Mixed Methods Appraisal Tool (MMAT v. 2018)

Inclusion Criteria.

- Data collection completed after USPSTF recommendation (2013)
- Identified perceived barriers and/or facilitators to LDCT lung cancer screening
- Data from at least 1 perspective (e.g., system, provider, patient)
- Study conducted in the U.S
- Reported on original collection of data
- Full text article available

Synthesis Methods

- Findings were classified into 3 perspective levels: system, healthcare provider, and patient
- Then were subdivided into the 5 domains of the CFIR framework and further divided into 39 subcategories (constructs) (**Figure 2**)

Figure 2. Consolidated Framework for Implementation Research.*

Figure 3. Review Flow Diagram.

Figure 4. Comparison Of Overlap By Most Common Factors.

RESULTS

- A total of 37 studies were selected for inclusion (**Figure 3**)
  - 5 studies examined factors at the system level, 13 at the patient level, 16 at the provider level, and 3 at both patient and provider levels.
  - A total of 21 constructs (out of 36) relating to 5 all domains were extracted for inclusion in this synthesis.
  - The data were too heterogenous to perform a meta-analysis.

System Perspective (n= 5)

1. External policy and incentives
2. Executing implementation according to plan

Provider Perspective (n=19)

1. Knowledge and beliefs about the intervention
2. Evidence strength and quality
3. Implementation climate
4. Patients' needs and resources

Patient Perspective (n=16)

1. Knowledge and beliefs about the intervention
2. Engaging (e.g., education)
3. Patients' needs and resources

CONCLUSION

- Three key constructs areas emerged as key factors to implementation: knowledge and beliefs about the intervention, patient needs and resources, and evidence strength and quality.
- Findings can help to inform the development and implementation processes of lung cancer screening programs in the community setting.

For further information
Please contact Ami Sedani, Ami-Sedani@OUHSC.edu

*Reference: https://cfirguide.org; Kirk et al., 2016; A systematic review of the use of the Consolidated Framework for Implementation Research, Implement Sci., 11: 72-72.

GAIT ANALYSIS USING DATA-DRIVEN LEARNING METHODS ON SPATIOTEMPORAL PLANTAR FORCE DATASET BY TEKSCAN STRIDEWAY SYSTEM

Kangjun Seo (kangjun.seo@ou.edu), Hazem H. Refai, and Elizabeth S. Hile
Department of Electrical and Computer Engineering

The fundamental form of human gait is a well-learned, highly repeatable movement pattern. However, gait characteristics such as step length or stride duration naturally vary across multiple gait cycles to accommodate changing environmental conditions. The amount of gait variation depends on a performer's health and the environmental conditions, typically increasing with age and pathology. The study aims to find general features of gate events (initial and final foot contacts on the ground) that are stable and consistent even in the presence of the gait variations.

The plantar force dataset was collected with gait at self-selected usual pace over 20 feet TekScan Strideway floor sensory system at the Cancer Rehab Research laboratory (CRRL) at OUHSC/OU Health Stephenson Cancer Center (SCC). The Strideway system is a modular pressure measurement platform for human gait analysis, providing information on spatiotemporal plantar force across multiple gait cycles. We applied the data-driven dynamical analysis method, Dynamic Mode Decomposition (DMD), on normal adult's spatiotemporal plantar force at 12 different areas on both left and right feet during the 24 gait cycles, leading to 576 samples per person.

To capture the general features of a particular patient's gait cycle with varying gait characteristics (force duration and peak force) in the time domain, we performed the spectral analysis by decomposing the dataset into the dynamic modes or the eigenvectors of the Hankel matrix form of the dataset. For example, the temporal plantar force on the left metatarsal rises gradually upon the ground strike with multiple peaks (maximum peak at 131.63 ± 50.14 kPa) during the pressure-time (0.47 ± 0.06 seconds) across 24 multiple gait cycles, revealing the wide deviation of the highest force in each gait cycle. The dynamic modes for each gait cycle consist of a linear combination of the decaying harmonic functions of time, which form the orthonormal basis of the temporal plantar force in the spectral domain. Optimizing the number of the dynamic modes followed by the machine learning clustering produces 3 complex harmonics and their complex conjugates with the mean frequencies (FR) at 0.95Hz, 2.50Hz, and 4.45Hz and the decay rate (DR) at 0.14 ± 0.02s, 0.18 ± 0.06s, and 0.32 ± 0.21s, respectively.

In summary, the gait event at a particular plantar area for each gait cycle shares a feature quantified by a pair of values: FR and DR of the dynamic modes. The pair together is mapped to a point (a feature point) on a 2-dimensional feature space, made of the FR and DR. Then, the feature points generated across the multiple gait cycles form clusters at particular frequencies with a range of decay rate. We show the unsupervised machine learning algorithm captures the characteristic feature (FR and DR range) for the gait event at specific plantar areas. This preliminary result addresses the potential application of the data-driven learning system to quantify gait events under challenging conditions.

DATA-DRIVEN LEARNING METHODS TO FIND PLANTAR FORCE GAIT CONSISTENCIES IN WOMEN WITH CANCER

KANGJUN SEO, PhD[1], HAZEM H. REFAI, PhD[1], and ELIZABETH S. HILE, PT, PhD[2,3]

[1]OU Department of Electrical and Computer Engineering

[2]OUHSC College of Allied Health Department of Rehabilitation Sciences

[3]OU Health Stephenson Cancer Center Rehabilitation Research Laboratory

INTRODUCTION

- Uterine and other cancers may increase the risk for falls.[1] Mechanisms are not certain, but may include changes in postural control systems that impact safe walking (gait).
- In normal gait, foot (plantar) contact transitions from the heel to the toes with each step. This transition can be mapped using TekScan® Strideway™ (**Fig 1**). A single individual's progression of plantar pressures is generally repeatable across multiple gait cycles, and can even be used for identification.[2]
- While some gait variation is normal, excessive variation may signal pathology, especially of the nervous system.[3] We suspect that ***an early signal of imbalance with cancer may be a subtle drift from an individual's typical gait pattern, toward one of greater variability.*** Testing this theory will require dynamical modeling of complex datasets generated for plantar force distribution.
- Dynamic Mode Decomposition (DMD), a data-driven dynamical modeling algorithm, is suitable for the feature extraction in complex datasets,[4] such as plantar force progression during gait. Machine learning can then characterize unique features of a patient's identity through their temporal pattern of plantar force progression, with consideration of their own variability.
- We believe that, just as each person has unique dynamics for plantar force progression during gait,[2] they also have unique patterns of variation across multiple steps. ***Changes in these patterns could signal decline in balance, physical function, and possibly even health, during cancer treatment.*** This would inform dose adjustments and supportive care referrals.

OBJECTIVE

We seek a method to characterize "normal" variability in an individual's unique plantar force progression with gait, specifically in individuals with cancer who have baseline comorbidity affecting the nervous system. Such comorbidities may place the individual at higher risk for neurologic sequelae of cancer and cancer treatment. As first steps, in this developmental work, we will:

(1) Determine if DMD, a state-of-the-art computing technique, can be used to generate a dynamical model of walking-generated plantar force distribution using temporal datasets from a woman with uterine cancer and baseline neuropathic symptoms before exposure to neurotoxic chemotherapy.

(2) Extract the universal features of temporal development for unsupervised machine learning, to classify her unique patterns by extracted features.

METHODS

PARTICIPANT/DATA: Footfalls of a single participant (71 year old female with uterine cancer and diabetes, report of mild diabetic neuropathy) for multiple passes over a 20-foot high-resolution TekScan® Strideway™ (**Fig 1**) at self-selected pace; baseline data from an ongoing longitudinal feasibility study to observe symptoms and mobility with repeated exposure to neurotoxic chemotherapy.

TekScan® software divides the plantar force distribution into 12 spatial regions (**Fig2**), returns pressure in a region of interest (**Fig 1 - Red squares**) at recorded moments in the walk. **Fig 3** is a pressure-time plot for the combined pressure across segments Metatarsal (M1) + Big toe (T1) of the right foot. ***Purple-shading*** = Pressure X Time for one right step. Note the variability across 22 steps (3 passes).

Fig1. TekScan® Stride™ generates a spatiotemporal plantar force distribution.

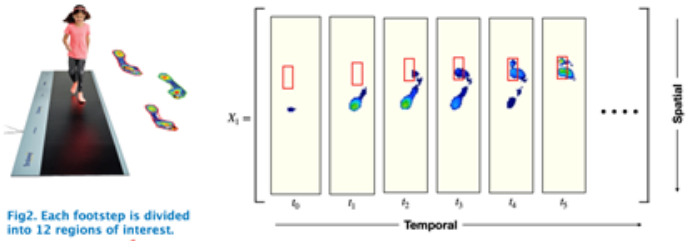

Fig2. Each footstep is divided into 12 regions of interest.

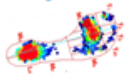

Fig3. Temporal plantar force on Metatarsal(M1)+ Big toe(T1) of Right Foot

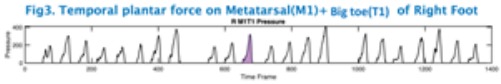

DYNAMIC MODE DECOMPOSITION (DMD) is a state-of-the-art computational method to generate a data-driven dynamic model using eigenvalues and the corresponding dynamic modes of the Koopman operator K that governs the nonlinear time evolution of the data signal: $X(t+1)=KX(t)$, where $X(t)$ is a data matrix of the signal as shown in **Fig1** as X_1 and $X(t+1)$ is a time-advanced data matrix of $X(t)$.

The DMD method employs a singular value decomposition (SVD) of K, optimizing its dimensionality and producing the eigenvalues and dynamic modes, which are characterized by **Frequency** and **Decay Rate** as shown in **Figure 4.**

Fig4. TekScan® Stride™ generated plantar forces and the corresponding Dynamic Modes.

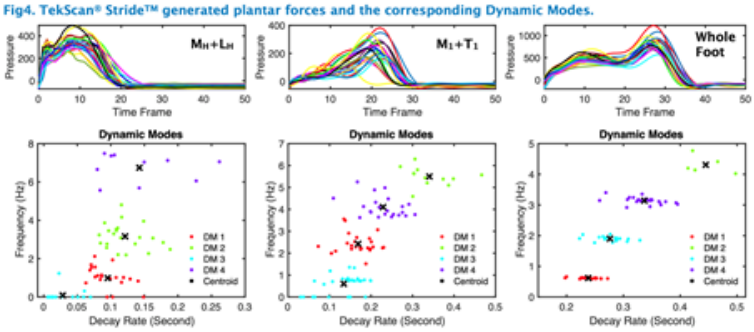

RESULTS

- For this woman with uterine cancer and mild diabetic neuropathy, the optimized dynamic modes are 9 complex numbers determined by the most dominant singular values, producing 198 points in the Frequency and Decay Rate space during 22 gait cycles (**Fig 4 – *Bottom set of plots***).
- The variability across gait cycles of this single participant generates variability in Frequencies and Decay Rates, yet they form **several well-defined clusters**, implying the characteristic Frequency and Decay Rate for each region of interest per patient.
- For 3 important plantar regions (M_H+L_H, M_1+T_1, Whole Foot) corresponding to key gait events (Heel-Strike, Toe-Off, Stance Phase), the unsupervised machine learning (K-mean with the optimized number of dynamic modes) algorithm produces the centroids of the clusters in the table below.

Table of Results: Centroids

		Heel	Meta+Big toe	Whole Foot
Frequency (Hz)	Left	{0.00, 0.77, 2.95, 5.39}	{0.00, 1.23, 3.26, 5.22}	{0.63, 1.93, 3.22, 3.37}
	Right	{0.09, 1.0, 3.16, 6.74}	{0.60, 2.43, 4.10, 5.50}	{0.62, 1.90, 3.14, 4.31}
Decay Rate (Second)	Left	{0.02, 0.09, 0.10, 0.13}	{0.06, 0.13, 0.15, 0.27}	{0.26, 0.30, 0.35, 0.43}
	Right	{0.03, 0.1, 0.12, 0.14}	{0.13, 0.17, 0.23, 0.34}	{0.24, 0.28, 0.34, 0.45}

CONCLUSIONS

We showed that the data-driven dynamic mode decomposition and an unsupervised machine learning algorithm together capture the characteristic feature (FR & DR range) for gait events associated with key plantar areas in this woman with uterine cancer who will receive neurotoxic chemotherapy. The resulting features are consistent, even in the presence of baseline gait variability.

We believe the capability of our data-driven learning systematic algorithm to identify baseline step consistencies will enable us to automate the identification of significant deviations from an individual's characteristic performance as they accumulate exposure to neurotoxic chemotherapy.

REFERENCES

1. Mohile SG, Fan L, Reeve E, Jean-Pierre P, Mustian K, Peppone L, Janelsins M, Morrow G, Hall W, Dale W. Association of cancer with geriatric syndromes in older Medicare beneficiaries. J Clin Oncol. 2011 Apr 10;29(11):1458-64. doi: 10.1200/JCO.2010.31.6695.
2. Pataky TC, Mu T, Bosch K, Rosenbaum D, Goulermas JY. Gait recognition: highly unique dynamic plantar pressure patterns among 104 individuals. J R Soc Interface. 2012 Apr 7;9(69):790-800. doi: 10.1098/rsif.2011.0430.
3. Moon Y, Sung J, An R, Hernandez ME, Sosnoff JJ. Gait variability in people with neurological disorders: A systematic review and meta-analysis. Hum Mov Sci. 2016 Jun;47:197-208. doi: 10.1016/j.humov.2016.03.010.
4. N. Parmar, et al., "A Survey on the Methods and Results of Data-Driven Koopman Analysis in the Visualization of Dynamical Systems," in IEEE Transactions on Big Data, doi: 10.1109/TBDATA.2020.2980849.

ACKNOWLEDGEMENT:

The project is supported by Presbyterian Health Foundation, Oklahoma Tobacco Settlement Endowment Trust, NCI Cancer Center Support Grant P30CA225520 to OU Stephenson Cancer Center.

Cancer Therapeutics

CANNABIS USE AMONG ADULTS UNDERGOING CANCER TREATMENT

Amy L. Barnett,[1,2] Amy M. Cohn,[2,3] Munjireen Sifat,[2] Laili Kharazi Boozary,[1,2] Sarah J. Ehlke,[2]
Susanna V. Ulahannan,[4] Christina Henson,[5] Adam C. Alexander,[2,6] Kathleen Moore,[7]
Laura L. Holman, [7] and Darla E. Kendzor[2,6]
[1] Department of Psychology, Cellular and Behavioral Neurobiology,
The University of Oklahoma, Norman, OK
[2] TSET Health Promotion Research Center
[3] Department of Pediatrics
[4] Department of Medical Oncology/Hematology
[5] Department of Radiation Oncology
[6] Department of Family and Preventive Medicine
[7] Department of Obstetrics and Gynecology
Stephenson Cancer Center, The University of Oklahoma Health Sciences Center,
Oklahoma City, OK

Little is known about cannabis use among individuals with cancer. Adults undergoing cancer treatment at the Stephenson Cancer Center completed an online survey that included questions about sociodemographic characteristics, history of COVID-19 infection, cannabis and other substance use, medical reasons for cannabis use, and perceptions of symptom relief following cannabis use (*N*=212). Past 30-day cannabis users and non-users were compared on their personal characteristics, and the prevalence of having a medical cannabis license and reasons for medical use were described. The most commonly reported cancers among participants were breast (18%, *n*=38), colorectal (10%, *n*=21), ovarian (9%, *n*=20), prostate (8%, *n*=16), and lung (7%, *n*=14). A total of 17% (*n*=35) of participants reported that they had a medical cannabis license and 24% (*n*=51) reported past 30-day cannabis use. Compared to non-users, past 30-day cannabis users were younger (*M*=55 vs. 60 years, *p*<0.05), more likely to be male (45% vs. 28%, *p*<0.05), and more likely to report an annual household income <$50,000 (32% vs. 23%, *p*<0.01). Cannabis users reported greater pain intensity over the past 7 days than non-users (*M*=4.5 vs. 3.3, *p*=0.05), and they were more likely to report past 30-day prescription pain medication use (41% vs. 24%, *p*<.05). Although rates of past 30-day smoking and alcohol use were higher among cannabis users, these differences did not reach significance. Non-users were more likely to have breast cancer (22% vs. 9%, *p*<.05) or colorectal cancer (12% vs. 2%, *p*<.05) than cannabis users, and users were more likely to report ever testing positive for COVID-19 than non-users (19% vs. 6%; *p*<0.01). Participants with a medical cannabis license most commonly sought their license for: physical pain (76.5%), cancer (73.5%), sleep problems/insomnia (70.6%), anxiety (52.9%), and nausea/vomiting (44.1%). Licensed participants perceived that cannabis delivered very much/extreme relief for nausea/vomiting (66.7%), sleep problems/insomnia (60%), physical pain (59.3%), and anxiety (47.4%), while fewer participants perceived very much/extreme relief from cancer (23.1%). Findings provide initial information about medical cannabis use among adults with cancer and the perceived medical benefits. Additional research will be needed to determine whether there is a causal association between cannabis use and physical/psychological symptom relief among individuals with cancer.

Funding: This research was supported by Oklahoma Tobacco Settlement Endowment Trust (TSET) Grant #R21-02 and National Cancer Institute (NCI) Cancer Center Support Grant P30CA225520 awarded to the Stephenson Cancer Center.

TSET Health Promotion Research Center

OU Health | Stephenson Cancer Center

Cannabis Use Among Adults Undergoing Cancer Treatment

Amy L. Barnett[1,2], Amy M. Cohn[2,3], Munjireen Sifat[2], Laili Kharazi Boozary[1,2], Susanna V. Ulahannan[4], Christina Henson[5], Adam C. Alexander[2,6], Kathleen Moore[7], Laura L. Holman[7], and Darla E. Kendzor[2,6]

[1]Departmentment of Psychology, Cellular and Behavioral Neurobiology, [2]TSET Health Promotion Research Center, [3]Department of Pediatrics, [4]Department of Medical Oncology/Hematology, [5]Department of Radiation Oncology, [6]Department of Family and Preventive Medicine, [7]Department of Obstetrics and Gynecology, Stephenson Cancer Center, The University of Oklahoma Health Sciences Center, Oklahoma City, OK

Background

- Medical marijuana was legalized in Oklahoma in June 2018, and the first medical marijuana licenses were issued in 2018.
- By January 2022, nearly 10% of the state population had been issued a medical marijuana license.
- Little is known about the prevalence, benefits, and consequences of cannabis use among patients with medical conditions, including cancer.
- Previous research has indicated that the national prevalence of past-month cannabis use is 8.4%, compared with rates of up to 30% within various samples of individuals with cancer.
- In general, cannabis has shown efficacy primarily for pain management, with limited evidence of benefit for other conditions.
- Little is known about the medical benefits of cannabis use specifically among patients with cancer.

Objectives

- To characterize the prevalence of licensed and unlicensed cannabis use among adults receiving cancer care.
- To compare the sociodemographic and personal characteristics of cannabis users and non-users.
- To compare the cannabis use characteristics of licensed and unlicensed past 30-day cannabis users.
- To characterize reasons for medical use and perceptions of medical benefit among licensed and unlicensed cannabis users.
- To describe and compare the cannabis use modalities of licensed and unlicensed cannabis users.

Study Design

- Individuals receiving cancer care at the Stephenson Cancer Center completed an online survey regarding sociodemographic characteristics, history of COVID-19 infection, cancer type, cannabis and other substance use, medical reasons for cannabis use, and perceptions of symptom relief following cannabis use.
- Participants were recruited by medical care providers when they were attending patient appointments, and also via Stephenson Cancer Center social media sites.
- Patient status was verified via the electronic medical record.

Acknowledgements: This research was primarily supported by Oklahoma Tobacco Settlement Endowment Trust (TSET) grant R21-02 and National Cancer Institute Cancer Center Support Grant P30CA225520 awarded to the Stephenson Cancer Center. Please direct correspondence to Darla-Kendzor@ouhsc.edu.

Results

- Participant characteristics (*N*=212) are presented in Table 1.
- Among participants, the most commonly reported cancers were breast (18%, *n*=38), colorectal (10%, *n*=21), ovarian (9%, *n*=20), prostate (8%, *n*=16), and lung (7%, *n*=14).
- Overall, 17% (*n*=35) of participants reported having a medical cannabis license and 24% (*n*=51) reported past 30-day cannabis use.
- Compared with non-users, cannabis users were significantly younger, less likely to be female, less likely to earn <$50,000 annual income, less likely to have breast cancer or colorectal cancer, more likely to have tested positive for COVID-19, and more likely to have a medical cannabis license and to have used prescription pain medications in the past 30 days. See Table 1.
- Participants with a medical cannabis license most commonly sought their license for: physical pain (76.5%), cancer (73.5%), sleep problems/insomnia (70.6%), anxiety (52.9%), and nausea/vomiting (44.1%).

Table 1. Participant characteristics (*N*=212)

	N	All Participants (*N*=212)	Cannabis Use, Past 30 days (*n*=51)	No Cannabis Use, Past 30 days (*n*=161)	*p*
SOCIODEMOGRAPHIC		Mean (SD) or % (n)			
Age, years, M (SD)	212	58.64 (13.3)	55.12 (13.8)	59.7 (13)	**0.032**
Sex, % female	212	67.9 (144)	54.9 (28)	72 (116)	**0.022**
Race/Ethnicity, % Hispanic or non-White	209	4.2 (9)	5.9 (3)	3.7 (6)	0.450
Education, % > high school	212	98.6 (209)	96.1 (49)	99.4 (160)	0.144
Annual Household Income, % <$50,000	205	75.12 (154)	68 (34)	77.4 (120)	**.005**
HEALTH					
Breast Cancer, %	212	17.92 (38)	7.84 (4)	21.12 (34)	**0.031**
Colon/Rectum Cancer, %	212	9.91 (21)	1.96 (1)	12.42 (20)	**0.029**
Ovarian Cancer, %	212	9.43 (20)	11.76 (6)	8.7 (14)	0.513
Prostate Cancer, %	212	7.55 (16)	9.8 (5)	6.83 (11)	0.484
Lung/Bronchial, %	212	6.6 (14)	5.88 (3)	6.83 (11)	0.812
Pain Rating, past 7 days, M (SD)	206	3.52 (2.73)	4.45 (2.9)	3.25 (2.6)	**0.053**
ATSQ (respiratory symptoms), M (SD)	207	15 (6.83)	17.17 (8)	14.31 (6.31)	0.065
COVID-19, ever tested positive, %	207	8.7 (18)	18.75 (9)	5.66 (9)	**0.005**
SUBSTANCE USE					
Medical Cannabis License, %	209	16.75 (35)	57.14 (28)	4.35 (7)	**<0.001**
Smoking, past 30 days, %	212	10.38 (22)	15.69 (8)	8.7 (14)	0.154
Alcohol Use, past 30 days, %	212	22.64 (48)	27.45 (14)	21.12 (34)	0.346
RX Pain Medication Use, Past 30 days, %	212	27.83 (59)	41.18 (21)	23.6 (38)	**0.015**
Non-Rx Pain Medication Use, Past 30 Days, %	212	58.02 (123)	52.94 (27)	59.63 (96)	0.399

Results (cont.)

- Licensed participants were most likely to perceive that cannabis delivered very much or extreme relief from nausea/vomiting, sleep problems/insomnia, and physical pain, while participants were less likely to perceive very much or extreme relief from arthritis, muscle spasms, and arthritis. See Figure 1.
- Overall, past 30-day cannabis users were most likely to consume cannabis via edibles and by smoking cannabis. Surprisingly, licensed participants were more likely to smoke cannabis than unlicensed participants. See Table 2.
- Licensed cannabis users had higher CUDIT-SF scores days than unlicensed cannabis users (p=0.045).

Figure 1. Cannabis Relief Among Licensed Users

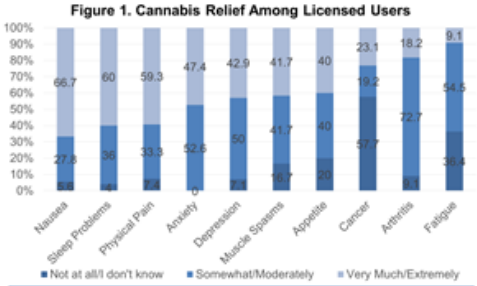

Table 2. Cannabis use modalities among past 30-day cannabis users.

	All Users (*N*=51)	Licensed Users (*n*=28)	Unlicensed Users (*n*=21)	*p*
	Mean (SD) or % (N)			
Ate, %	63.39% (34)	75% (21)	61.9% (13)	0.363
Smoked, %	53.06% (26)	67.86% (19)	33.33% (7)	**0.022**
Vaped, %	26.53% (13)	28.57% (8)	23.81% (5)	0.710
Applied to skin, %	18.37% (9)	17.86% (5)	19.05% (4)	0.600
Dabbed, %	14.29% (7)	14.29% (4)	14.29% (3)	0.654
Used some other way, %	14.29% (7)	14.29% (4)	14.29% (3)	0.654
Dissolved in mouth, %	10.2% (5)	7.14% (2)	14.29% (3)	0.362
Drank cannabis, %	6.12% (3)	3.57% (1)	4.76% (1)	0.679

Conclusions

- Findings provide initial information about medical cannabis use among adults with cancer and the perceived medical benefits.
- Additional research will be needed to determine whether there is a causal association between cannabis use and physical/psychological symptom relief among individuals with cancer.

MECHANISM OF MISMATCH REPAIR DEFICIENCY PREDICTS POOR OUTCOMES WITH PEMBROLIZUMAB IN RECURRENT ENDOMETRIAL CANCER

Lindsay E Borden, MD[1], Justin D Dvorak, PhD[2], Zachary CW Barrett[2], Kai Ding, PhD[2], Ana Valente, MD[1], Kathleen G Essel, MD[3], Kathleen N Moore, MD[1]

[1] Division of Gynecologic Oncology, Stephenson Cancer Center, University of Oklahoma
[2] Department of Biostatistics & Epidemiology, University of Oklahoma Health Sciences Center
[3] Tennessee Oncology

Objective: To determine response rate, recurrence-free survival, and overall survival to pembrolizumab in recurrent endometrial adenocarcinomas based upon mechanism of mismatch repair (MMR) deficiency.

Methods: A retrospective study was conducted among all women with recurrent endometrial adenocarcinomas treated with single-agent pembrolizumab at our institution from 2017 to 2021. Cases were included if complete mismatch repair data were available and were categorized based upon MMR status – germline Lynch Syndrome mutation (gLS), somatic Lynch Syndrome mutation (sLS) or MLH1 promoter hypermethylation (hMLH1). Clinical and pathologic data were abstracted by chart review and included patient demographics, tumor characteristics, recurrence date, and treatment. Continuous predictors were compared between groups using two-sample *t*-tests. Ordinal predictors such as stage and grade were compared using Wilcoxon rank-sum tests. Categorical predictors were compared using Fisher's exact tests, due to small counts. Unadjusted differences in survival were compared with log-rank tests and visualized with Kaplan-Meier curves. Cox proportional-hazards models were used to compare differences in survival between groups after adjusting for BMI. All statistical tests were conducted in R v3.5.1 with an alpha level of 0.05.

Results: Eighteen patients were categorized into two groups based upon results of tumor MMR testing and germline genetic testing: gLS/sLS (n = 6, 33.3%) or hMLH1 (n = 12, 66.7%). The hMLH1 patients had a higher mean BMI than gLS/sLS patients (40.9 vs. 28.5, $P = 0.003$). Demographic and tumor characteristics were otherwise well-matched between groups. Median follow-up was 9.45 months with a response rate of 44.4%. When stratified by MLH1 hypermethylation status, response rate was 83.3% in gLS/sLS patients and 25.0% in hMLH1 patients ($P = 0.043$). Recurrence-free survival (RFS) was significantly decreased among hMLH1 patients ($P = 0.031$). Median RFS was not reached (NR) in gLS/sLS vs. 4.0 mo in hMLH1 patients. Overall survival (OS) was similarly

significantly decreased for these patients (*P* = 0.037), shown in Figure 1. Median OS was NR in gLS/sLS vs. 8.5 mo in hMLH1 patients.

Conclusions: Recurrent dMMR endometrial cancers are currently treated as one entity. These data show women with MLH1 promoter hypermethylation may not respond comparably to pembrolizumab, as RFS and OS are decreased in these patients compared with germline and somatic Lynch Syndrome patients. While these data are exciting for Lynch Syndrome patients, it suggests an area of high unmet need for hMLH1 patients. The mechanism of dMMR should be considered as stratification schema in future trials.

Figure 1. Overall survival of hMLH1 patients vs. gLS/sLS patients.

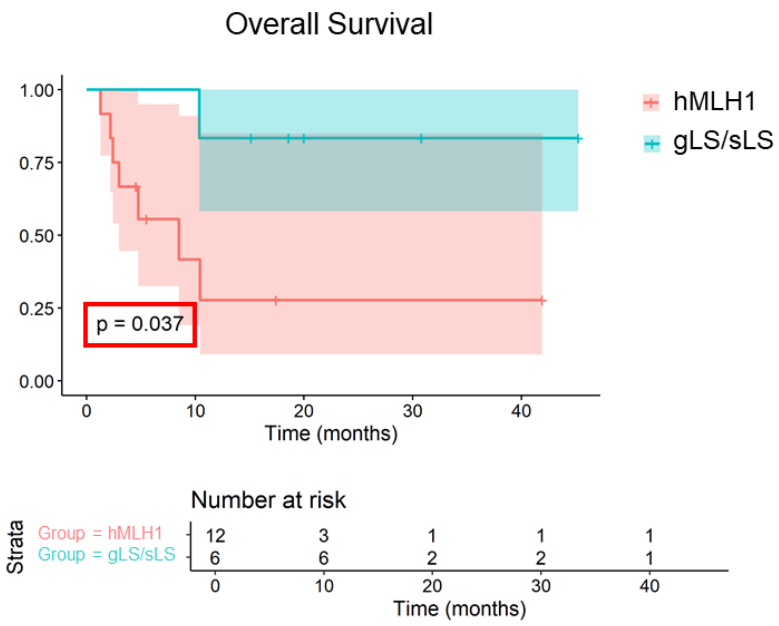

MLH1 hypermethylation predicts poor outcomes with pembrolizumab in recurrent endometrial cancer

Lindsay E Borden, MD[1], Justin D Dvorak, PhD[1], Zachary CW Barrett[1], Kai Ding, PhD[1], Ana Valente, MD[1], Kathleen G Essel, MD[2], Kathleen N Moore, MD[1]

[1] Division of Gynecologic Oncology, Stephenson Cancer Center, University of Oklahoma, [2] Tennessee Oncology

Background

Advanced or recurrent endometrial cancers have a poor prognosis, but the recent approval of immune checkpoint inhibitors (ICIs) in mismatch repair deficient (dMMR) and microsatellite instability-high (MSI-H) tumors has brought new optimism into treatment of this subgroup. Approximately 30-40% of endometrial cancers may be dMMR/MSI-H, either through germline mutations of the associated MMR genes, approximately 25% of dMMR tumors, or epigenetic changes of the MLH1 promoter, approximately 75%.[1,2] Two anti-programmed death 1 ICIs are approved in advanced or recurrent dMMR tumors: pembrolizumab and dostarlimab.[3] Little is known about outcomes with ICIs in MLH1 hypermethylation versus germline or somatic MMR mutation tumors.

Objectives

To determine response rate to pembrolizumab, recurrence-free survival, and overall survival in recurrent endometrial adenocarcinomas based upon mechanism of MMR deficiency.

Methods

- Retrospective, single-institution study 2017 – 2021
- Included all women with recurrent endometrial adenocarcinomas treated with pembrolizumab
- Stratify patients based upon MMR deficiency:
  - Germline Lynch Syndrome mutation (gLS)
  - Somatic Lynch Syndrome mutation (sLS)
  - MLH1 promoter hypermethylation (hMLH1)
- Statistical analyses completed by two-sample t-tests, Wilcoxon rank-sum tests, Fisher's exact tests, and survival differences by log-rank tests

Results

Total cohort n = 18

- Median follow-up: 9.5 mo
- Overall response rate: 44.4% (8/18)

Demographics

- No difference in age, race, stage at diagnosis, nor histologic grade between two groups
- BMI 28.5 in gLS/sLS vs. 40.9 in hMLH1 (P = 0.003)

Figure 1. Total cohort stratified by mechanism of MMR deficiency. Germline (g) and somatic (s) mutations pooled into gLS/sLS group.

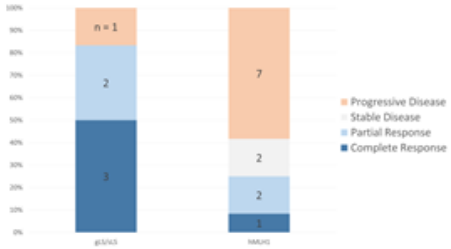

Figure 2. Best response to pembrolizumab by mechanism of MMR deficiency. Response rate for gLS/sLS 83.3% vs. hMLH1 25.0% (P = 0.043).

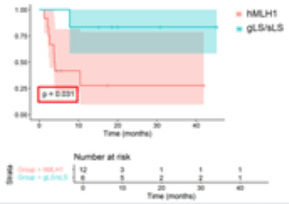

Figure 3. Recurrence-free survival (RFS) in gLS/sLS vs. hMLH1 patients (P = 0.031). Median RFS in gLS/sLS not reached vs. 4.0 months in hMLH1.

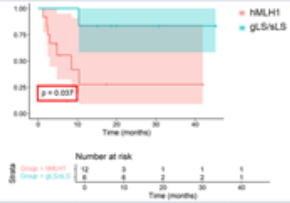

Figure 4. Overall survival (OS) in gLS/sLS vs. hMLH1 patients (P = 0.037). Median OS in gLS/sLS not reached vs. 8.5 months in hMLH1.

Conclusions

- Recurrent dMMR endometrial cancers are currently treated as one entity, regardless of epigenetic vs. somatic vs. germline mutations
- Consistent with Bellone et al, hMLH1 tumors may not respond as robustly to ICIs as gLS/sLS tumors[4]
- These data suggest an area of high unmet need for patients with hMLH1 tumors

Future Work

Ongoing collaboration with multisite Endometrial Cancer Molecularly Targeted Therapy Consortium at Duke University to validate findings.

[1] Oaknin A, et al. Clinical Activity and Safety of the Anti-Programmed Death 1 Monoclonal Antibody Dostarlimab for Patients With Recurrent or Advanced Mismatch-Repair Deficient Endometrial Cancer. JAMA Oncol. 2020;6(11):1766-1772.

[2] McMeekin DS, et al. Clinicopathologic Significance of Mismatch Repair Defects in Endometrial Cancer: An NRG Oncology/Gynecologic Oncology Group Study. J Clin Oncol. 2016;34(25):3062-3068.

[3] National Comprehensive Cancer Network. NCCN Guidelines Version 1.2022: Endometrial Carcinoma.

[4] A phase II evaluation of pembrolizumab in recurrent microsatellite instability-high (MSI-H) endometrial cancer patients with Lynch-like versus MLH-1 methylated characteristics (NCT02899793). Ann Oncol. 2021;32: 1045-1046.

IN VIVO RANGE VERIFICATION USING SINGLE PULSE PROTON INDUCED ACOUSTIC SIGNALS

J. Caron[1], G. Gonzalez[1], P. Pandey[2], S. Wang[2], K. Prather[1], L. Xiang[2], and Y. Chen[1]
1 University of Oklahoma Health Sciences Center, Department of Radiation Oncology, Oklahoma City, OK
2 University of California – Irvine, Department of Biomedical Engineering, Irvine, CA

Purpose: To investigate the feasibility of ionacoustic detection as an *in vivo* method for measuring proton dose depositions during patient treatments. Ionacoustic detection is seen as a cheap and efficient solution to reduce the current 1cm range uncertainty in patient plan delivery due to patient setup, patient motion, and machine deliverance. With pencil beam scanning being the most prevalent method of proton dose delivery, single pulse acquisitions are crucial in implementing this method of detection into the clinic.
Materials and Methods: Proton induced acoustic range measurements were performed with a proton synchrocyclotron (Mevion S250i Hyperscan) at energies ranging from 45.5MeV to 227.15MeV. The surface of a low-frequency 0.5MHz transducer (Olympus V389-SU) was placed in a water tank along the beam axis at approximately 33cm from the entrance window. The transducer was then connected to a two-stage amplification system placed in a borated-polyethylene shielding box, giving the signal a total 100dB amplification. The signal was then connected to a dispatch board and sent outside the treatment room to be viewed on a digital oscilloscope (Rigol DS1202). With the smallest single deposition of charge in patient treatments being 4pC, datasets were gathered with signal averaging ranging from 1024 to single pulse acquisitions and charges-per-pulse ranging from 3pC/pulse to 7pC/pulse. A post-processed Savitzky-Golay filter was applied to the signals. Five, five, and three signals were collected per depth for signals with 1024 averages, 4 averages, and single pulse acquisitions, respectively. Proton induced acoustic dosimetric measurements were performed in the same manner, with charge depositions ranging from 0.25pC to 7pC being delivered at an energy of 201.14MeV. The K-wave simulation toolbox was also used to provide insight on the signal propagation in the medium.
Results: With spots delivered with 3pC/pulse, variations in range for signals with 1024 averages were measured to be within 0.5mm of the mean for all energies, with a systematic shift of approximately 2mm. The largest standard error was calculated to be 0.2mm. With spots delivered with 4pC/pulse, variations in range for signals with 4 averages were measured to be within 1mm of the mean for all energies, with no systematic shift. The largest standard error was calculated to be 1.3mm. With spots delivered with 7pC/pulse, variations in range for single pulse signal acquisitions were measured to be within 1mm of the mean for all energies, with a systematic shift of approximately 2mm. The largest standard error was calculated to be 0.7mm.

Conclusion: With single pulse acquisitions having sub-millimeter range variations, ionacoustic detection is proven to be a viable *in vivo* method for measuring proton dose depositions with high precision during patient treatments.

Author Contact Information: joseph-caron@ouhsc.edu

Funding: This work was partially supported by the National Institute of Health (R37CA240806), American Cancer Society (133697-RSG-19-110-01-CCE), and The Oklahoma Center for Advancement of Science and Technology (OCAST HR19-131).

In Vivo Range Verification using Single Pulse Proton Induced Acoustic Signals

J. Caron[1], G. Gonzalez[1], P. Pandey[2], S. Wang[2], K. Prather[1], L. Xiang[2], and Y. Chen[1]
1 University of Oklahoma Health Sciences Center, Department of Radiation Oncology, Oklahoma City, OK
2 University of California – Irvine, Department of Biomedical Engineering, Irvine, CA

INTRODUCTION

- Ionacoustic detection proposes an efficient and low-cost solution to reduce the approximate 1cm range uncertainty in patient plan delivery due to patient setup, imaging, beam delivery, and dose calculations.
- With pencil beam scanning being the most prevalent method of proton dose delivery, single pulse acquisitions are crucial in implementing this method of detection into the clinic.

PURPOSE

- Reduce the approximate 1cm range uncertainty in clinical practice to have better utilization of the advantages of proton therapy.
- Investigate the feasibility of ionacoustic detection as an *in vivo* method for measuring proton dose depositions during patient treatments.

METHODS

- Proton induced acoustic range measurements were performed with a proton synchrocyclotron (Mevion S250i Hyperscan) at energies ranging from 45.5MeV to 227.15MeV.
- A low frequency 0.5MHz transducer was placed in a water tank along the beam axis for signal acquisitions and was connected to a two-stage amplification system. The signal was then connected to a digital oscilloscope and viewed outside of the treatment room.
- With the smallest single deposition of charge in patient treatments being 4pC, datasets were gathered with no signal averaging (single pulse acquisitions) and a charge-per-pulse of 7pC/pulse.
- Proton induced acoustic dosimetric measurements were performed in the same manner, with charge depositions ranging from 0.25pC to 7pC being delivered at an energy of 201.14MeV.

RESULTS

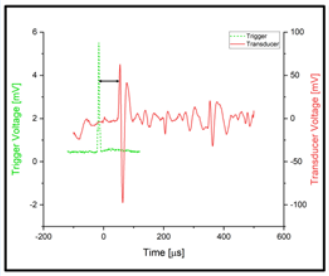

Figure 2: Typical Ionacoustic Signal.

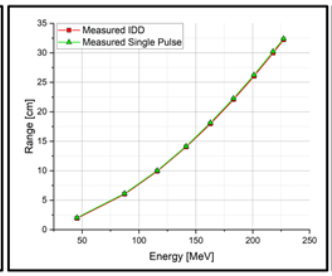

Figure 3: Energy-Range relationship of the proton system. Measured IDD obtained from an ion chamber.

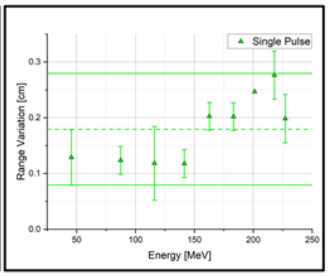

Figure 4: Range variation of the ionacoustic results from the measured IDD curve.

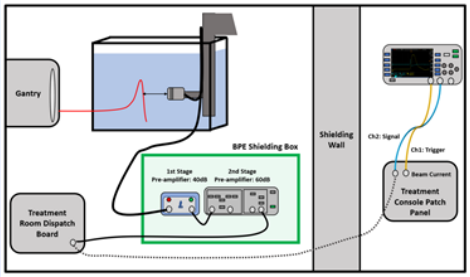

Figure 1: Setup.

- With spots delivered with 7pC/pulse, variations in range for single pulse signal acquisitions were measured to be within 1mm of the mean for all energies, with a systematic shift of approximately 2mm. The largest standard error was calculated to be 0.7mm.
- The linear trend shown in the dosimetric data means that there can be a relative means of assessment for relating the charge deposited in the medium to the deposited dose.

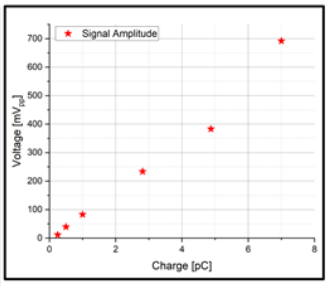

Figure 5: Dosimetric Data.

CONCLUSIONS & FUTURE APPLICATIONS

- With single pulse acquisitions having sub-millimeter range variations, ionacoustic detection is proven to be a viable *in vivo* method for measuring proton dose depositions with high precision during patient treatments.
- There are various ways this method could be implemented in the clinic.
  - It can be used to improve target position in patient setup by using transmit and receive modes on the transducer.
  - It can be used for *in vivo* range verification before and during patient treatments.
  - It can be used for a relative means of *in vivo* dosimetric verification during patient treatments.
  - It can be used with a log file comparison for adaptive post-treatment planning.

ACKNOWLEDGEMENTS

- This work was partially supported by the National Institute of Health (R37CA240806), American Cancer Society (133697-RSG-19-110-01-CCE), and The Oklahoma Center for Advancement of Science and Technology (OCAST HR19-131).

CONTACT INFORMATION

Email Joe Caron: joseph-caron@ouhsc.edu

OPTIMIZATION OF INJECTION MODE AND TEMPERATURE OF TARGETED PHOTOTHERMAL THERAPY OF BREAST CANCER

Authors: Gabriela N. F. Faria[1], Clement Karch[2], Alexis A. Woodward[2], Adam Aissanou[2], Roger Harrison[1].

[1]Chemical, Biological and Materials Engineering, University of Oklahoma; [2]Biomedical Engineering, University of Oklahoma. (faria.gabriela@ou.edu)

The lack of targeting treatments for triple negative breast cancer (TNBC) leads to poor prognosis, especially when metastasis has occurred, which spurs on the development of novel therapeutic strategies. We have developed a targeted photosensitizer for photothermal therapy (PTT) of solid tumors based on the functionalization of single-walled carbon nanotubes (SWCNT) to annexin A5 (ANXA5): SWCNT-ANXA5 conjugate. SWCNT efficiently convert near-infrared (NIR) light into thermal energy during PTT, aiming to ablate the primary tumor. ANXA5 is a protein that has specificity for cancer due to the strong binding to externalized phosphatidylserine (PS) on the surface of tumoral cells and tumor vasculature. PS is a biomarker of various types of cancers, including TNBC, but is absent on the surface of healthy cells.

ANXA5 was produced in *E. coli* and purified by affinity liquid chromatography in an immobilized-nickel column. The high purity protein (> 95%) is then linked to SWCNT with a linker (DSPE-PEG-MAL), which interacts hydrophobically with SWCNTs and bonds to ANXA5 through the cysteine reactive maleimide group. EMT6 cells, a TNBC tumor model, were orthotopically injected in BALB c/J female mice. When the tumors averaged 5 mm in diameter, the mice were treated with 980 nm NIR laser at 1 W/cm^2. For the first experiment, SWCNT-ANXA5 was injected either intravenously (IV) or intratumorally (IT), and the cytokine TNF-α in the serum 1 day after PTT was measured by ELISA. Secondly, using IT injection, the tumors were subjected to PTT, and treatment ceased when the tumor surface reached different peak temperatures (45, 50, 55 and 60˚C). Cytokine levels in serum were analyzed. Lastly, a long-term survival test was performed using IT injection and irradiation until the tumor surface temperature reached 45˚C in combination with checkpoint inhibition of anti-PD-1 (three intraperitonial injections of 200 μg/mouse, 1 and 4 days before irradiation, and 4 days after irradiation).

IT injection was the only method that induced a statistically significant increase in the level of TNF-α. When comparing the irradiation temperatures, 45˚C was the group that was more effective in increasing the level of cytokines TNF-α and IL-12. Furthermore, the optimized combination therapy resulted in complete tumor recession and survival at 100 days of 50% of mice in the anti-PD-1 + PTT group.

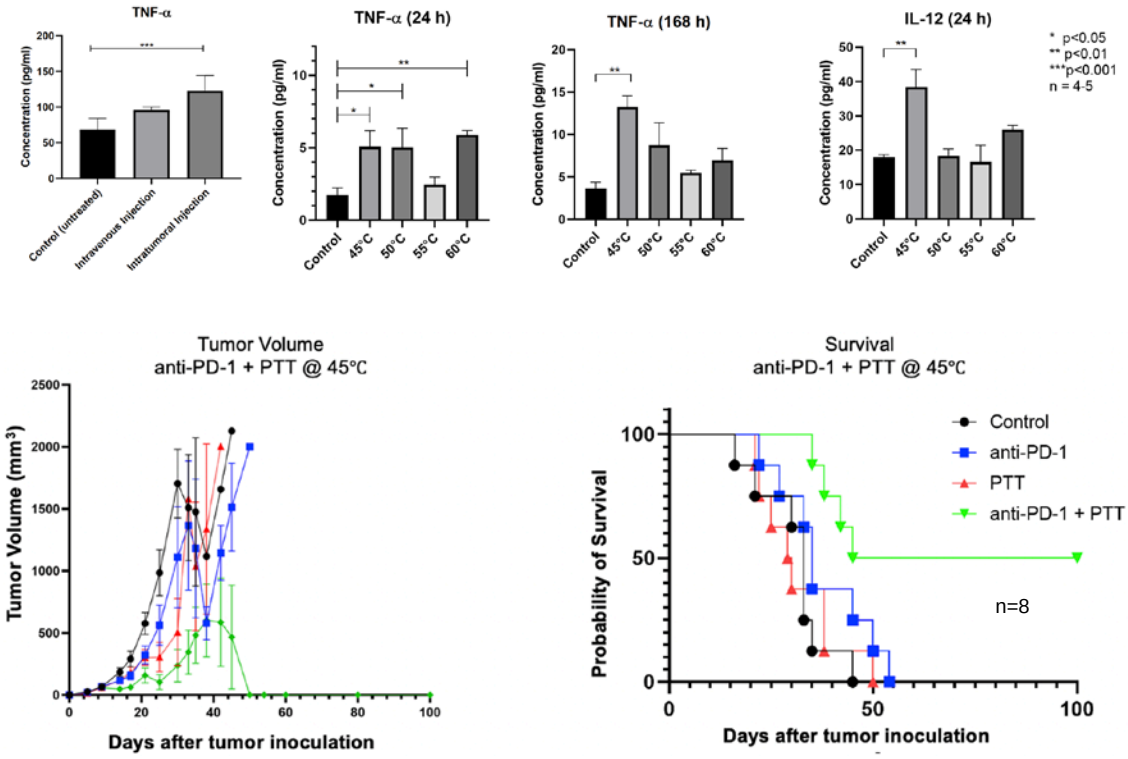

There is evidence that IT injection and PTT at 45˚C are more effective at generating immune responses. Because EMT6 tumor models are known to stablish metastatic tumors very early in the tumor development, the long-term survival is one evidence that the combination therapy of PTT and anti-PD-1 elicits a systemic antitumoral response that efficiently suppresses metastatic tumors.

Funding: IBEST-OUHSC Funding for Interdisciplinary Research; Jean Wheeler Sparks and Baxter Abbott Sparks Breast Cancer Research Fund; Universidad Nacional de San Agustin (Peru).

Optimization of the Activation of Immune Response in Targeted Photothermal Therapy of Breast Cancer

Gabriela N F Faria[1], Clemént Karch[2], Alexis Woodward[2] , Adam Aissanou[2], Roger Harrison[1]

University of Oklahoma – Chemical, Biological and Materials Engineering[1], Stephenson School of Biomedical Engineering[2]

School of Chemical, Biological and Materials Engineering

Abstract

Here we present the optimization of the combination therapy of targeted single walled carbon nanotube (SWCNT) – mediated photothermal therapy (PTT) and check point inhibition for the treatment of breast cancer. The protein annexin A5 (ANAX5) binds tightly to the anionic phospholipid phosphatidylserine (PS), which is overexpressed in breast cancer. Due to its high absorbance in the near infrared light range, SWCNT was conjugated to ANXA5, producing an efficient targeted photosensitizer that transforms light into heat. PTT, which is the irradiation of tumor by infrared light, eliminates the primary tumor and induces the release of tumor antigens that are internalized by antigen presenting cells. Checkpoint inhibition (anti-CTLA 4 or anti-PD-1) blocks the receptors in the regulatory T cells and preevents the downregulation of the immune response. The antigen presenting cells activate the cytotoxic and helper T cells, inducing a cell-mediated immune response against metastases.

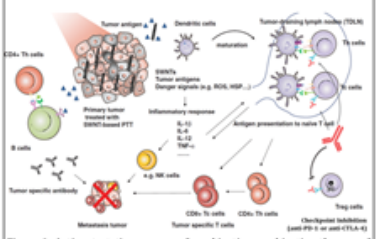

Figure 1: Anti-metastatic response of combination combination therapy of PTT and checkpoint inhibition. Image adapted from: Wang, C. et al. Adv. Mater. 26, 8154–8162 (2014)

There is a need to optimize the combination of photothermal therapy and checkpoint inhibition to maximize the possibility of translating this method to the treatment of human cancers.

Background

Breast Cancer:
- All subtypes express PS
- Triple-negative breast cancer has the lowest 5-year survival of all breast cancer subtypes because it cannot be targeted by current therapies in clinics.

Phosphatidylserine (PS) – Target:
- Exclusively found on inner leaflet of healthy cells
- Ubiquitously expressed on tumor vasculature and tumor cells

Annexin A5 (ANXA5) – Targeting agent:
- Binds to PS with high affinity in presence of calcium (K_D < 1 nM)

Anti-CTLA-4/anti-PD-1 – Check point inhibitor:
- Triggers anti-tumoral immune response
- Blocks action of regulatory T-cells

CoMoCat SWCNT – Photosensitizer:
- Produced at high quality and high purity using cobalt-molybdenum catalyst
- High absorbance in the near-infrared light range

SWCNT-ANXA5 Conjugation

Figure 2: Conjugation of ANXA5 to SWCNT. The DSPE-PEG-maleimide (1,2-distearoyl-sn-glycero-3-phosphoethanolamine-N-[maleimide(polyethylene glycol)]) is used as a linker between ANXA5 and SWCNT. The hydrophobic tail of the linker interacts hydrophobically with the SWCNT. Polyethylene glycol shields the nanoparticle from the immune system. The maleimide group has a specific chemistry that reacts with the cysteine residue in ANXA5.

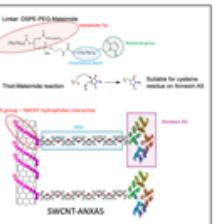

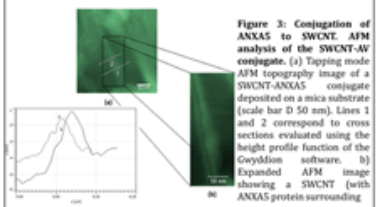

Figure 3: Conjugation of ANXA5 to SWCNT. AFM analysis of the SWCNT-AV conjugate. (a) Tapping mode AFM topography image of a SWCNT-ANXA5 conjugate deposited on a mica substrate (scale bar D 50 nm). Lines 1 and 2 correspond to cross sections evaluated using the height profile function of the Gwyddion software. b) Expanded AFM image showing a SWCNT (with ANXA5 protein surrounding its surface. The SWCNT is surrounded by the protein, which is represented with brighter pixels. (c) Cross section height profiles for two different regions of the SWNT. The profile plotted with a darker line corresponds to the cross section #1, while the lighter line represents the region defined by the cross section #2. From plots for several images, the height of the SWNT-protein conjugate was determined to be between 2.5 and 5.0 nm. Source: Neves, L. F. F. et al. Nanotechnology 24, (2013).

Previous Studies

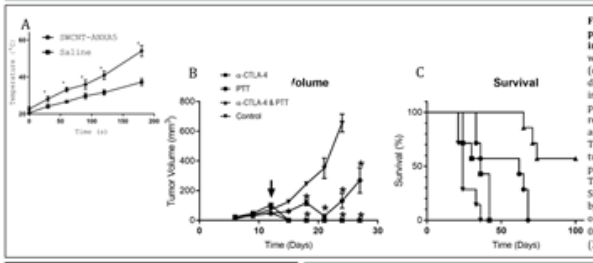

Figure 4: Results of combinatorial photothermal therapy (PTT) and checkpoint inhibition (anti-CTLA-4) in EMT6 tumors. Mice with well-developed orthotopic syngeneic tumors (d ≥ 5 mm) were administered an IV systemic dose of 1.2 mg/kg SWCNT-ANXA5. Tumors were irradiated with a NIR laser at an energy and power density of 175 J/cm2 and 1 W/cm2, respectively (t = 175 s). Select groups received anti-CTLA-4 (100 μg) on days 8, 11, and 16. A) Thermal kinetics resulting from radiation of tumors with NIR light at 980 nm. Data are presented as mean +/- SE (n = 3, *p < 0.05). B) Tumor volume shown as mean ± SE (n = 7). Significance compared to the control is indicated by *p < 0.05. C) Survival curve of the combination of PTT and anti-CTLA-4 (n = 7, *p < 0.05). McKernan *et al. Nanoscale Res Lett* **16,** 9 (2021).

Optimization of Injection Type

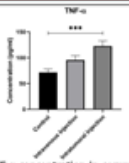

Figure 5: TNF-α concentration in serum 24 h after PTT in mice treated with IV or IT injection of the conjugate in EMT6 tumors. Level of TNF-α in the serum of treated mice or untreated mice as a control. Laser wavelength was 980 nm and power density 1.0 W/cm². (n = 4-5, ***p<0.001).

Optimization of Tumor Surface Temperature

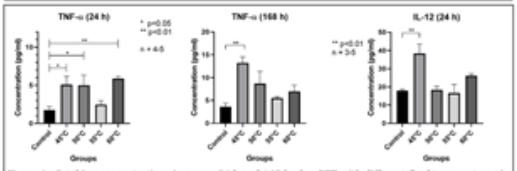

Figure 6: Cytokine concentrations in serum 24 h and 168 h after PTT with different final temperatures in EMT6 tumors. The diagram shows the level of TNFα and IL-12(p70) in the serum of mice treated with IT injections of conjugate, or untreated mice as a control. Photothermal therapy was performed until reaching a final temperature of 45, 50, 55, or 60°C. Laser wavelength was 980 nm and power density 1.0 W/cm².
(n = 4-5, *p<0.05, **p<0.01 and ***p<0.001)

Optimized Combination Therapy

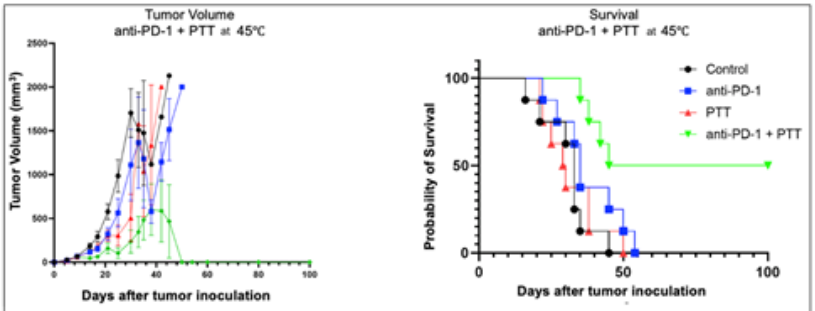

Figure 7: Results of optimized combinatorial photothermal therapy (PTT) and checkpoint inhibition (anti-PD-1) in EMT6 tumors. Mice with well-developed orthotopic syngeneic tumors (d ≥ 5 mm) were administered an IT dose of 1.2 mg/kg SWCNT-ANXA5. Tumors were irradiated with a NIR laser at a power density of 1 W/cm² until tumor surface temperature reached 45 C. Select groups received anti-PD-1 (200 μg) on days 8, 11, and 16. A) Tumor volume shown as mean ± SE (n = 7). Significance compared to the control is indicated by (* p < 0.05) . B) Survival curve of the combination of photothermal therapy and immune checkpoint inhibition (p < 0.05, n = 7).

Conclusions

- There is evidence that IT injection and PTT at 45 °C are more effective at generating immune responses.
- The optimized combination therapy induced complete tumor recession in half of the mice in the anti-PD-1 + PTT group and they survived for 100 days.

Future Work

- Determine how the immune therapy modulates the immune response to photothermal therapy.
- Irradiate tumors with cycles of on/off to maintain surface temperature at 45°C for longer times (1 min, 2 min, 5 min).
- Test the optimized combined therapy in a less immunogenic tumor model (4T1).
- Combine PTT with other checkpoint inhibitors (anti-PD-L1, anti-OX40, anti-B7-H3, anti-CD73)

Funding Acknowledgements

We thank Universidad Nacional de San Agustin (Peru) for funding, IBEST-OUHSC Funding for Interdisciplinary Research, Jean Wheeler Sparks and Baxter Abbott Sparks Breast Cancer Research Fund.

IMPLEMENTATION OF A STANDARD SAME DAY DISCHARGE PROTOCOL FOR MINIMALLY INVASIVE HYSTERECTOMIES IN THE DIVISION OF GYNECOLOGIC ONCOLOGY: A QUALITY IMPROVEMENT PROJECT

Authors: Mikaela S. Katz*¥, Anjalika R. Gandhi*, Ana L. Valente*, Debra L. Richardson*, Laura L. Holman*

*Department of Obstetrics and Gynecology, OU Health and Stephenson Cancer Center
¥ *Presenting author: mikaela-katz@ouhsc.edu*

Objectives: To determine the safety and feasibility of a same-day discharge (SDD) protocol for minimally invasive hysterectomies (MIH) within the oncologic patient population.

Study Design: This was a retrospective cohort study of all MIH between December 1, 2019-February 28, 2020 (pre-intervention cohort "PRE") and November 23, 2020-February 18, 2021
(post-intervention cohort "POST") at the University of Oklahoma. We educated staff on standard operating procedure (SOP) in November, 2020. Measures of patient safety included phone calls, emergency room (ER) visits, and 30 day re-admissions. Quality was measured by adherence rates to the SOP. The "POST" group ranked their satisfaction on a scale of 1-100 on several parameters using an electronic survey. Data was collected in REDCap. Descriptive statistics were used to summarize data, and t-tests were used to compare cohorts (α=0.05).

Results: 97 patients were eligible in PRE cohort and 59 in POST cohort. Zero patients in PRE cohort underwent SDD compared to 34 (59.7%) in POST cohort. By SOP-specified criteria, 54.6% of PRE cohort were eligible for SDD. Average stay in hospital midnights per patient was 1.09 and 0.51 in PRE and POST cohorts, respectively ($p<0.0001$).

SDD patients from POST cohort were observed for mean of 346 minutes in post-anesthesia care unit (PACU). Compliance rates with SOP were: observed >4 hours in PACU (91.2%), documented pre-op counseling (0.06%), narcotics prescribed prior to surgery (0.03%), receipt of enhanced recovery medications (79%), documented provider assessment prior to SDD (58.8%), and phone note on post-op day #1 (29.4%).

Mean number of patient-initiated calls and 30 day ER presentations for PRE and POST cohorts were 0.62 vs 0.52 ($p=0.783$) and 0.11 vs 0.049 ($p=0.40$). There were five and zero 30-day admissions in PRE and POST cohorts, respectively.

Patient survey response rate was 40.3% (17/42). Median satisfaction scores: 89% pre-operative counseling, 92% quality of care in PACU, 50% duration time in PACU, 80% pain control in PACU, and 90% overall satisfaction with SDD.

Conclusion: SDD for MIH resulted in significant reduction in hospital stays and was safe and feasible in an oncologic patient population. Additional provider education is required to improve adherence to SOP and improve patient satisfaction.

Implementation of a Standard Same Day Discharge Protocol for Minimally Invasive Hysterectomies in the Division of Gynecologic Oncology: A Quality Improvement Project

M. Katz[a], A. Gandhi[a], A. Valente[a], D. Richardson[a], L. Holman[a]

[a]*The University of Oklahoma Health Sciences Center, Stephenson Cancer Center, Oklahoma City, OK, USA*

Background

- Hysterectomy - most common gynecologic surgery in the US - 600,000 cases annually [1]
- Minimally invasive hysterectomy (MIH) compared to open with faster recovery, shorter hospital stay, decreased wound infection rates, decreased narcotic usage [2,3]
- Same day discharge (SDD) safe in benign gynecologic population [4,5]
- Gynecologic oncologic population high risk, but SDD deemed safe in some institutions [6-9]
- Gynecologic oncology division at OUMC implemented SDD protocol with aims to assess safety, quality, and patient satisfaction

Methods

- **Design:** Retrospective cohort study of all MIH in gynecologic oncology at OUMC between
  - December 1, 2019-February 28, 2020 (pre-intervention cohort "PRE") and
  - November 23, 2020-February 18, 2021 (post-intervention cohort "POST")
- **Outcomes**
  - **I. Protocol Performance**
  - **II. Adherence to SDD Protocol**
  - **III. Patient Satisfaction**
- **Statistical Analysis**
  - Descriptive statistics were used to summarize data, and t-tests were used to compare cohorts (α=0.05).

Results

I. Protocol Performance

	PRE (n=97)	POST (n=59)
Same day discharge	0%¶	57.6%
Average hospital stay (days)*	1.09	0.51
ER visits	0.11	0.049
Re-admissions	5	0
Patient-initiated Phone Calls	0.62	0.52

¶54.6% of the PRE cohort were eligible for SDD
*statistically significant p<0.0001

Reasons for no SDD

	n=25
Management of comorbidities	12 (48%)
Surgery completed after 5pm	5 (20%)
Anesthesia, analgesia, or operative concern	6 (24%)
Failed ABT, declined immediate home foley	4 (16%)
More than 1 reason charted	3 (12%)

II. Adherence to Protocol

- Documented pre-op counseling (0.06%)
- Narcotics prescription prior to surgery (0.03%)
- Receipt of enhanced recovery medications (79%)
- Observed >4 hours in PACU (91.2%)
- Documented provider assessment prior to SDD (58.8%)
- Phone note on post-op day #1 (29.4%)

III. Patient Satisfaction

- Patient survey response rate was 40.3% (17/42).
- Median satisfaction scores (0-100)
- Pre-operative counseling – 89
- Quality of care in PACU – 92
- Duration time in PACU – 50
- Pain control in PACU – 80
- Overall satisfaction with SDD - 90

Conclusion

Same day discharge for minimally invasive hysterectomy resulted in significant reduction in hospital stays and was safe and feasible in an oncologic patient population

Future Directions

- Provider education on performance related to quality metrics
- Repeat provider and nursing education on protocol with attention to documentation and communication
- Repeat data collection after the above with repeat focus on patient satisfaction and experience

References

1. Wu, J. M., Wechter, M. E., Geller, E. J., Nguyen, T. V. & Visco, A. G. Hysterectomy rates in the United States, 2003. *Obstet. Gynecol.* **110**, 1091–1095 (2007).
2. Choosing the Route of Hysterectomy for Benign Disease. https://www.acog.org/en/Clinical/Clinical Guidance/Committee Opinion/Articles/2017/06/Choosing the Route of Hysterectomy for Benign Disease.
3. Fleming, N. D. *et al.* Analgesic and antiemetic needs following minimally invasive vs open staging for endometrial cancer. *Am. J. Obstet. Gynecol.* **204**, 65.e1-65.e6 (2011).
4. Gan, T. J. M. *et al.* Consensus Guidelines for the Management of Postoperative Nausea and Vomiting. *Anesth. Analg.* **118**, 85–113 (2014).
5. Ramirez-Caban, L. *et al.* Factors that Lengthen Patient Hospitalizations Following Laparoscopic Hysterectomy. *JSLS J. Soc. Laparosc. Robot. Surg.* **24**, (2020).
6. Melamed, A. *et al.* Same-Day Discharge After Laparoscopic Hysterectomy for Endometrial Cancer. *Ann. Surg. Oncol.* **23**, 178–185 (2016).
7. Lee, S. J. *et al.* The feasibility and safety of same-day discharge after robotic-assisted hysterectomy alone or with other procedures for benign and malignant indications. *Gynecol. Oncol.* **133**, 552–555 (2014).
8. Lee, J. *et al.* The safety of same-day discharge after laparoscopic hysterectomy for endometrial cancer. *Gynecol. Oncol.* **142**, 508–513 (2016).
9. Gien, L. T., Kupets, R. & Covens, A. Feasibility of same-day discharge after laparoscopic surgery in gynecologic oncology. *Gynecol. Oncol.* **121**, 339–343 (2011).

INNATE IMMUNE RESPONSES ACTIVATED BY A COMBINATION OF LOCAL ABLATION AND IMMUNOSTIMULATION FOR CANCER TREATMENT

Kaili Liu, Ashley Hoover, and Wei R. Chen

Stephenson School of Biomedical Engineering, Gallogly College of Engineering, University of Oklahoma, Norman, Oklahoma 73019, USA

We have developed a novel localized ablative immunotherapy (LAIT), which combines photothermal therapy (PTT) with intratumor administration of an immunostimulant N-dihydrogalactochitosan (GC), for treatment of metastatic cancers. LAIT has been shown to be able to activate adaptive immune system, through B cells and T cells, to effectively control treated primary tumors and untreated distant metastases. However, the effect of LAIT on the host innate immune system has not been adequately studied. Natural killer (NK) cells are critical to the innate immune system and they provide responses to tumor formation. In this study, we used LAIT to treat mammary tumors in mouse mammary tumor virus-polyoma middle T (MMTV-PyMT) transgenic mice and used single-cell RNA sequencing (scRNAseq) to investigate the infiltration and activation of NK cells in the tumor microenvironment (TME). Our results showed that among the activated tumor-infiltrating NK cells, PTT significantly upregulated response of tumor necrosis factor, while GC and LAIT (PTT+GC) induced immune effector process as well as cytokine production pathways. We also found that LAIT specifically elicited the interferon response pathway. Furthermore, we observed that breast cancer patients had significantly extended survival time if they had elevated expression of genes in NK cells that were also induced by LAIT, but not by GC or PTT alone, suggesting that NK cells may be a potential cellular target to remodel the TME by LAIT for cancer treatment.

Keywords: Natural killer (NK) cells, mammary tumors, photothermal therapy (PTT), N-dihydrogalactochitosan (GC), localized ablative immunotherapy (LAIT)

Single-cell transcriptomic profiling reveals anti-tumor remodeling of tumor-infiltrating NK cells by localized ablative immunotherapy

Kaili Liu[1], Ashley R. Hoover[1,2], Jason R. Krawic[3], Christa I. DeVette[3], Xiao-Hong Sun[2], William H. Hildebrand[3], Mark L. Lang[3], Robert C. Axtell[2,3] and Wei, R. Chen[1]

[1] *Stephenson School of Biomedical Engineering, University of Oklahoma, Norman, OK, 73019*
[2] *Arthritis & Clinical Immunology Research Program, Oklahoma Medical Research Foundation, Oklahoma City, OK, 73104*
[3] *Department of Microbiology and Immunology, University of Oklahoma Health Sciences Center, Oklahoma City, OK, 73104*

Stephenson CANCER CENTER — the UNIVERSITY of OKLAHOMA

Introduction

As an important member of host innate immunity, natural killer (NK) cells play a crucial role in cancer immunology and immunotherapy. We previously reported the activation signaling pathways in tumor-infiltrating B cells responding to localized ablative immunotherapy (LAIT) in MMTV-PyMT breast tumor mice. However, whether LAIT affects NK cells are unknown. To address this, we performed single-cell RNA-seq (scRNAseq) analysis for the transcriptome of NK cells upon treatments of photothermal therapy (PTT), N-dihydrogalactochitosan (GC), and LAIT (PTT+GC) within the tumor microenvironment (TME). Our results showed that all the treatments activated tumor-infiltrating NK cells, among which PTT upregulated response of tumor necrosis factor, while GC and LAIT induced immune effector process as well as cytokine production pathways. By dissecting the relations of treatment-triggered differentially expressed genes (DEGs), we found LAIT specifically elicited the interferon response pathway, an important gene cassette playing the anti-tumor function. We also observed that breast cancer patient survival time was positively correlated with expression level of genes in NK cells that were also induced by LAIT, but not by GC or PTT alone, suggesting NK cell as a potential cellular target to remodel in TME for LAIT-based cancer therapy. In summary, our findings show that LAIT promote interferon signatures in NK cells and associate with positive clinical outcomes for breast cancer patients.

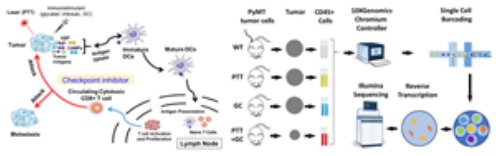

Figure 1. Schematic of LAIT mechanism

Figure 2. ScRNA-seq workflow

Results

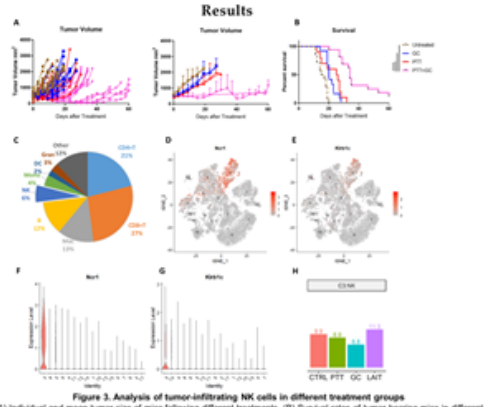

Figure 3. Analysis of tumor-infiltrating NK cells in different treatment groups

(A) Individual and mean tumor size of mice following different treatments. (B) Survival rates of tumor-bearing mice in different treatment groups. Log-rank (Mantel-Cox) test was used for statistical analysis. (C) Pie chart showing the proportions of different immune cell types in MMTV-PyMT tumors (combining all groups). NK cells, consisting of 6% of total immune cells, were analyzed in this study. Mac: macrophages; NK: natural killer cells; Mono: monocytes; DC: dendritic cells; Gran: granulocytes. (D, E) Feature plots (t-SNE) showing expressions of NK marker gene Ncr1 and Klrb1c that identify tumor-infiltrating NK cells. (F, G) Violin plots showing expressions of NK marker gene Ncr1 and Klrb1c that identify tumor-infiltrating NK cell clusters from other immune cell clusters. (H) Proportion of NK cells among all immune cells in each treatment group, in comparison with CTRL group. The ratio of NK cells in each treatment group was divided by the number of all tumor-infiltrating CD45+ immune cells in the same treatment group.

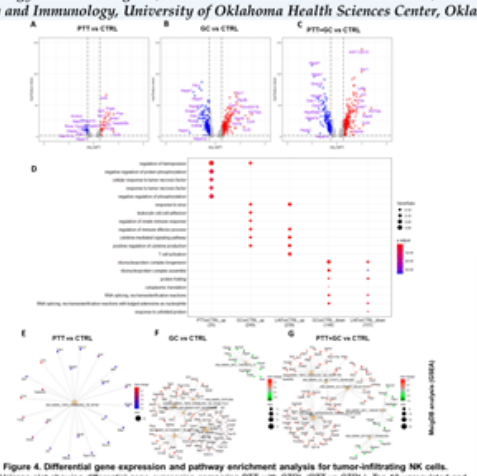

Figure 4. Differential gene expression and pathway enrichment analysis for tumor-infiltrating NK cells.

(A) Volcano plot showing differential gene expression comparing PTT with CTRL (PTT vs CTRL). Top 10 upregulated and downregulated genes are labeled. (B) Volcano plot showing differential gene expression comparing GC with CTRL. (C) Volcano plot showing differential gene expression comparing PTT+GC with CTRL. (D) Dot plot showing biological process (BP) of gene ontology (GO) analysis using over-representation analysis (ORA) method for both upregulated (up) and downregulated (down) genes for PTT vs CTRL, GC vs CTRL, and PTT+GC vs CTRL. (E) Network plot showing gene set enrichment analysis (GSEA) for DEGs from PTT vs CTRL using MsigDB hallmark gene sets. (F) Network plot showing the GSEA for DEGs from GC vs CTRL. (G) Network plot showing the GSEA for DEGs from PTT+GC vs CTRL.

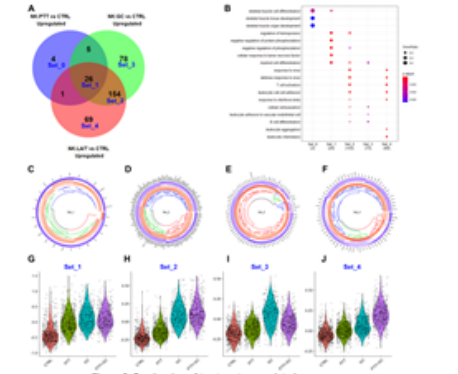

Figure 5. Overlapping of treatment-upregulated genes.

(A) Venn diagram showing upregulated genes from comparisons of PTT vs CTRL, GC vs CTRL, and PTT+GC vs CTRL. Five gene sets, from Set_0 to Set_4, are labeled. (B) Dot plot for BP of GO analysis of genes in Set_1 to Set_4. (C) Circular heatmap showing the expression of genes from upregulated set 1 (Set_1) in each treatment group. Heatmap columns for groups of CTRL, PTT, GC and PTT+GC were arranged from outside to inside. Higher expression was colored in red while lower in blue. (D) Circular heatmap showing the expression of genes from upregulated set 2 (Set_2) in each treatment group. (E) Circular heatmap showing the expression of genes from upregulated set 3 (Set_3) in each treatment group. (F) Circular heatmap showing the expression of genes from upregulated set 4 (Set_4) in each treatment group. (G) Violin plot showing relative gene signature scores from Set_1 in each treatment group. (H) Violin plot showing relative gene signature scores from Set_2 in each treatment group. (I) Violin plot showing relative gene signature scores from Set_3 in each treatment group. (J) Violin plot showing relative gene signature scores from Set_4 in each treatment group.

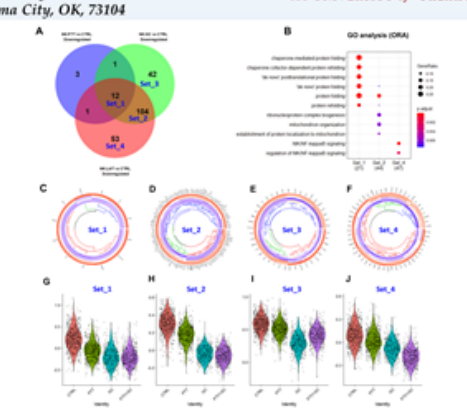

Figure 6. Overlapping of treatment-downregulated genes.

(A) Venn diagram showing downregulated genes from comparisons of PTT vs CTRL, GC vs CTRL, and PTT+GC vs CTRL. Five gene sets, from Set_0 to Set_4, are labeled. (B) Dot plot for BP of GO analysis of genes in Set_1 to Set_4. (C) Circular heatmap showing the expression of genes from downregulated set 1 (Set_1) in each treatment group. Heatmap columns for groups of CTRL, PTT, GC and PTT+GC were arranged from outside to inside. Higher expression was colored in red while lower in blue. (D) Circular heatmap showing the expression of genes from downregulated set 2 (Set_2) in each treatment group. (E) Circular heatmap showing the expression of genes from downregulated set 3 (Set_3) in each treatment group. (F) Circular heatmap showing the expression of genes from downregulated set 4 (Set_4) in each treatment group. (G) Violin plot showing relative gene signature scores from Set_1 in each treatment group. (H) Violin plot showing relative gene signature scores from Set_2 in each treatment group. (I) Violin plot showing relative gene signature scores from Set_3 in each treatment group. (J) Violin plot showing relative gene signature scores from Set_4 in each treatment group.

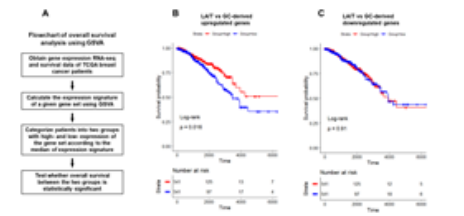

Figure 6. BC patients with a higher expression of the upregulated genes found in PTT+GC samples exhibited prolonged survival compared to the patients with lower expression

(A) Flowchart for analyzing overall survival of breast cancer patient using GSVA method. (B) Kaplan–Meier plots showing the significant difference in survival time (days) between breast cancer patients in groups with "high" and "low" expression of PTT+GC vs GC-derived upregulated genes. Patient groups were stratified by the median of enrichment score calculated by GSVA. Log-rank method was used for statistical analysis. (C) Kaplan–Meier plots showing the insignificant difference in survival time (days) between breast cancer patients in groups with "high" and "low" expression of PTT+GC vs GC-derived downregulated genes. Patient groups were stratified by the median of enrichment score calculated by GSVA. Log-rank method was used for statistical analysis.

References

1. Liu K, Hoover AR, Krawic JR, DeVette CI, Sun XH, Hildebrand WH, et al. Antigen presentation and interferon signatures in B cells driven by localized ablative cancer immunotherapy correlate with extended survival. Theranostics. 2022;12(2):639-56. Epub 2022/01/04. doi: 10.7150/thno.65773. PubMed PMID: 34976205; PubMed Central PMCID: PMCPMC8692917.

2. Hoover AR, Liu K, DeVette CI, Krawic JR, West CL, Medcalf D, et al. ScRNA-seq reveals tumor microenvironment remodeling induced by local intervention-based immunotherapy. bioRxiv. 2020:2020.10.02.323006. doi: 10.1101/2020.10.02.323006.

Acknowledgements

This research is supported in part by a grant from NIH/NCI (R01 CA205348) and by grants from the OCAST (HR16-085, HF20-019). The authors also acknowledge the support of Charles and Peggy Stephenson Chair endowment fund.

ARID3A IS EXPRESSED IN A SUBSET OF CHRONIC LYMPHOCYTIC LEUKEMIAS

Ankur Sharma [1], Murali K. Mamidi [4], Mariana T. Mendez[4], James Hocker[1], Mark L. Lang[2], Asish K. Ghosh[4,5] and Carol F. Webb[1-4]

[1]Department of Medicine, [2]Microbiology and Immunology, and [3]Cell Biology, University of Oklahoma Health Sciences Center, Oklahoma City, OK, 73104, USA

[4]Stephenson Cancer Center and [5]Department of Pathology, The University of Oklahoma Health Sciences Center, Oklahoma City, OK, USA.

Chronic lymphocytic leukemia (CLL) is an adult B-cell malignancy with a highly variable disease course. Despite morphological homogeneity as a cancer of B lymphocyte origin, more than twenty subtypes with overlapping characteristics have been identified. Subtypes have been based on immunoglobulin repertoires, transcriptomics and B cell differentiation states, and oncogenic drivers of carcinogenesis. The effectiveness of various therapeutics including tyrosine kinase inhibitors, BCL2 Inhibitors and monoclonal antibody therapies are varied and influences life expectancy. New sub-type specific treatments are needed to personalize and improve therapy options. The subtype of B lymphocyte from which CLLs are derived is controversial, as is the definition of a human B1 B lymphocyte, the supposed origin of many CLLs. In the mouse, fetal B1 lineage B cells require the DNA binding protein ARID3a for their development. However, ARID3a has not been examined as a marker for CLLs. We hypothesized ARID3a, in combination with other markers, will identify a unique subset of human B1-like CLLs. Further, we propose that inhibition of ARID3a in such cells may have therapeutic implications. We used flow cytometry to determine if we could detect ARID3a expression in 25 pre-therapy CLL samples, and examined those samples for other common B cell surface markers as well. Our data suggested those samples could be subdivided into 8 different groups, one of which exhibited high levels of ARID3a expression and made up 20% of the samples evaluated. This novel finding indicates that ARID3a expression may define a new subset of human CLLs. Experiments to determine if ARID3a inhibition of existing CLLs in this subset may affect their viability and growth in both human and mouse models are in progress. Preliminary data in the *Eμ-TCL1* transgenic CLL mouse model indicate that vivo-morpholinos against ARID3a reduce ARID3a expression and may limit tumor loads. These findings suggest that ARID3a inhibition has potential to be therapeutically useful.

Funding: This study was funded by Presbyterian Health Foundation (PHF), Team Science Grant to Webb, Ghosh, Lang.

ARID3a IS EXPRESSED IN A SUBSET OF CHRONIC LYMPHOCYTIC LEUKEMIAS

Ankur Sharma [1], Murali K. Mamidi [4], Mariana T. Mendez[4], James Hocker[1], Mark L. Lang[2], Asish K. Ghosh[4,5] and Carol F. Webb[1-4]

[1]Department of Medicine, [2]Microbiology and Immunology, and [3]Cell Biology, University of Oklahoma Health Sciences Center, Oklahoma City, OK, 73104, USA
[4]Stephenson Cancer Center and [5]Department of Pathology, The University of Oklahoma Health Sciences Center, Oklahoma City, OK, USA.

Abstract

Chronic lymphocytic leukemia (CLL) is an adult B-cell malignancy with a highly variable disease course. Despite morphological homogeneity as a cancer of B lymphocyte origin, more than twenty subtypes with overlapping characteristics have been identified. Subtypes have been based on immunoglobulin repertoires, transcriptomics and B cell differentiation states, and oncogenic drivers of carcinogenesis. The effectiveness of various therapeutics including tyrosine kinase inhibitors, BCL2 Inhibitors and monoclonal antibody therapies are varied and influences life expectancy. New sub-type specific treatments are needed to personalize and improve therapy options. The subtype of B lymphocyte from which CLLs are derived is controversial, as is the definition of a human B1 B lymphocyte, the supposed origin of many CLLs. In the mouse, fetal B1 lineage B cells require the DNA binding protein ARID3a for their development. However, ARID3a has not been examined as a marker for CLLs. We hypothesized ARID3a, in combination with other markers, will identify a unique subset of human B1-like CLLs. Further, we propose that inhibition of ARID3a in such cells may have therapeutic implications. We used flow cytometry to determine if we could detect ARID3a expression in 25 pre-therapy CLL samples, and examined those samples for other common B cell surface markers as well. Our data suggested those samples could be subdivided into 8 different groups, one of which exhibited high levels of ARID3a expression and made up 20% of the samples evaluated. This novel finding indicates that ARID3a expression may define a new subset of human CLLs. Experiments to determine if ARID3a inhibition of existing CLLs in this subset may affect their viability and growth in both human and mouse models are in progress. Preliminary data in the *Eμ-TCL1* transgenic CLL mouse model indicate that vivo-morpholinos against ARID3a reduce ARID3a expression and may limit tumor loads. These findings suggest that ARID3a inhibition has potential to be therapeutically useful.

Background

CLL is common and heterogeneous adult leukemia of B lymphocytes in the blood. Currently, multiple subsets of CLL have been identified that vary in surface marker expression, Ig repertoire characteristics, mutated drivers of carcinogenesis, and epigenetic subtypes associated with B cell differentiation stages that confer specific clinical outcomes. At least twenty subtypes have been identified with overlapping characteristics. Despite in the progress of treatments, such as Brutons's tyrosine kinase inhibitors, BCL2 Inhibitors, and monoclonal antibody therapy, patient with various subtypes differ in life expectancy and effectiveness of treatments.

Mouse CLL models are derived from fetal B1 lineage B cells characterized by surface expressions of CD5 and CD19 markers ARID3a is an AT rich interacting domain DNA binding protein required for mouse B1 B cell development. Human B1 B cell characterization remains controversial and the role of ARID3a in regulating human B1 cells is unclear.

Gating Scheme and Representative flow cytometric staining of CLL samples: B1 B cell panel; B cell panel; CLL panel

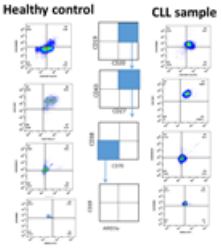

Figure 1: Represents flow cytometric staining of healthy control and CLL samples. B1 B cells are identified as ($CD19^+CD20^+CD43^+CD27^+CD38^-CD70^-$). The B1 B cells with ARID3a in healthy controls are shown at 2.81% and are generally less than 5%.

ARID3a expression in these cells from a CLL samples was observed at 72.9%.

Hypothesis

ARID3a, in combination with markers, identifies a unique subset of human B1-like CLL cells in mice. Treatment of mice with ARID3a inhibitors will reduce the expression of ARID3a and reduce or ameliorate disease processes and mouse CLL expansion.

Results

Gating Scheme and Representative flow cytometric staining of CLL sample with (A) B-cell panel and (B) CLL panel

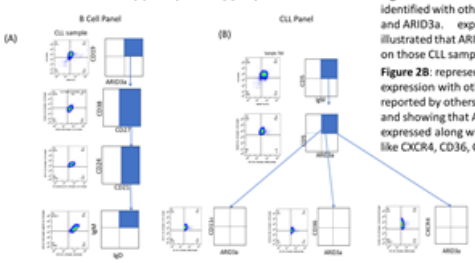

Figure 2A: shows a B cell panel identified with other B cells markers and ARID3a. expression and illustrated that ARID3a is expressed on those CLL samples.

Figure 2B: represent the ARId3a expression with other CLL markers reported by others in CLL samples and showing that ARID3a is expressed along with other makers like CXCR4, CD36, CD11c and CD5.

CLL Subsets with ARID3a

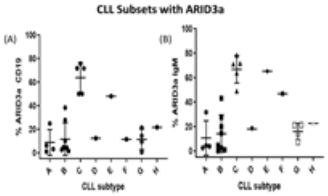

Fig.3. Expression of ARID3a (A) and (B) on subset of CLL
ARID3a appears consistently expressed on group C subset of the tested CLL samples.

Table 1: Identification of 8 Sub-groups observed in CLL patient samples.
Identification of patient sub-groups was done according to B1B cell$^+$ and ARID3a$^+$ expression in combination with CD19$^+$; ARID3a$^+$; IgM$^+$ and ARID3a$^+$ expression in each sample.

CLL Sub Type	sample (N)	Stain panel 1	Stain panel 2	
		B1 B cells+ ARID3a+	CD19+ ARID3a+ Mean (SD)	IgM+ ARID3a+ Mean (SD)
A	3	-/-	3.5 (2.5)	3.6 (5)
A1	1	-/-	24.9	31.7
B	3	+/-or +/+	4.1 (2.7)	7.8 (8.8)
B1	2	+/-or +/+	33.1 (7.4)	35.3 (11)
B2	1	+/+	4.05	0.87
C	5	+/+	63.9 (12.7)	66.8 (11.2)
D	1	-/+-	12.4	18
E	1	-/+ -	48.1	65.2
F	1	+ -/+	31.5	46.8
G	3	-/+	15.1 (6)	18.9 (1.9)
G1	1	-/-	0.49	7.2
H	1	+/+-	21.6	22.6

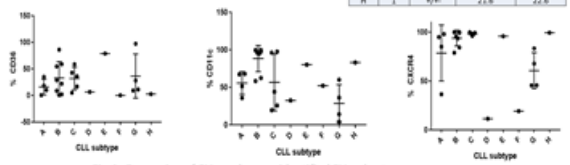

Fig.4. Expression of CLL markers on identified CLL subsets.
The markers identified by others do not appear to identify consistently the CLL phenotype.

Morpholino treatment of Mouse CLL Model

Table 2: Mouse model for ARID3a Vivo morpholinos

Experimental setup	Untreated Control	ARID3a Vivo morpholinos (Dose 1)	ARID3a Vivo morpholinos (Dose 2)
Mouse (N)	5	5	5
Treatment	Saline / vehicle	1mg / Kg	5mg / Kg
Mice were treated via tail vein injection once per week with either saline or ARID3a vivo morpholinos.			

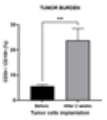

Figure 5: The tumor burden of the pre-treated mice was assessed in peripheral blood via flow cytometry. Mean tumor burden was estimated to be between 20-25% using the B1 surface markers CD5 and CD19 .

Flow Cytometry of peritoneal cells from mice with CLL: assessing treatment with Vivo Morpholinos.

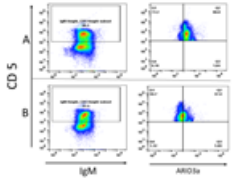

Figure 6: Representative flow cytometric staining of peritoneal cells from PBS treated control (A) and 5mg/kg ARID3a morpholino treated mice (B) shows ARID3a inhibition in CD5+ Cells.

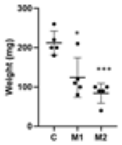

Figure 7: Spleen weights of control and morpholinos treated mice. (C) untreated; (M1) 1mg/kg and (M2) 5mg/kg treatments are shown with mean spleen mass and standard deviation. Significant differences, as compared to the untreated samples, are indicated by *p<0.0135 and *** p<0.001 .

Summary/key findings

- Our data suggest that a subset of human CLL samples express high levels of ARID3a expression. This subset was nearly 20% in our analyzed samples.
- This novel finding indicates that ARID3a expression may define a new subset of human CLLs.
- Preliminary data showed that vivo morpholinos may effectively reduce tumor loads mouse CLL models.
- These data suggest the exciting possibility that inhibition of ARID3a in human CLLs may be effective in a subset of patients.

Future directions

- *In vitro* inhibition study of vivo morpholinos on Human CLL
- To repeat and complete *in vivo* inhibition study.

ACKNOWLEDGEMENTS

This study was funded by Presbyterian Health Foundation (PHF), Team Science Grant to Webb, Ghosh, Lang.

EXPLORING ASSOCIATIONS BETWEEN TUMOR MUTATIONAL BURDEN AND CLINICAL BENEFIT OF IMMUNE CHECKPOINT INHIBITION IN ENDOMETRIAL CANCER

Ana Valente MD, Amy Gin MS4, Allison Wells, Kai Ding PhD, Kathleen Moore MD

Objective: Tumor mutations are key in the generation of anticancer immunity, and it is hypothesized that highly mutated tumors are more likely to harbor neoantigens that make them targets of activated immune cells. These highly mutated tumors may have superior or prolonged response to immuncheckpoint inhibitors (ICI). Recently published biomarker analysis of KEYNOTE-158 reported that tumors with high Mutational Burden (TMB-high) had a higher objective response to pembrolizumab monotherapy than non-TMB-high tumors leading to FDA approval of Pembrolizumab in TMB-high solid tumors. Reported objective response in endometrial cancer cohort was 46.6% in TMB-high (7/15) vs 4.9% (4/67) non-TMB high. In our study, we aimed to further investigate this identified association between TMB-high status and response as well as duration of response to ICI in endometrial cancers.

Methods: We conducted a retrospective review of patients with endometrial cancer at our academic institution who had received an ICI for management of recurrent or progressive endometrial cancer, as part of standard or care or clinical trial, who had TMB determined by next generation sequencing. TMB was reported as Very Low (<5), Low (5-10), Intermediate (10-15) or High (>15) mutations per megabase. We grouped patients together as TMB-int/high (>10) or TMB-very low/low for comparisons. Complete response (CR), partial response (PR), stable disease (SD) and progressive disease (PD) were assessed by RECIST criteria. Clinical Benefit was defined as SD+PR+CR. Durable clinical benefit was defined as no progressive disease for ≥ 6 months. Fisher's exact test was used to determine if associations existed with significance set at p<.05.

Results: We identified 21 patients who carried a diagnosis of endometrial cancer, had been treated with ICI as part of their therapy (on or off trial) and had TMB reported by next generation sequencing. All patients had advanced or recurrent disease. 9/21 (42.8%) were TMB-High/Intermediate (TMB >10) and 12/21 (57.1%) were TMB-Low/Very Low (TMB<10). Clinical benefit was seen in 7/9 (77.8%) TMB-high/intermediate vs 6/12 (50%) TMB-low/very low (*p=.36).*When further evaluating the population of patients who achieved clinical benefit, 7/7 (100%) of TMB-int/high while only 2/5 (40%) of TMB-very low/low achieved durable benefit. This finding was significant with *p=.0455*.

Conclusion: Our exploratory analysis suggests a correlation between TMB-int/high (TMB >10) status and duration of clinical benefit in patients with endometrial cancer treated with ICI. This finding may be clinically significant as recent literature suggests association between duration of response and overall survival and improved quality of life in patients treated with immunotherapy. Further evaluation is warranted to confirm our findings as we are limited by a small sample size. *All authors are associated with University of Oklahoma Health Science Center

Exploring Tumor Mutational Burden Status and Clinical Benefit of Immune Checkpoint Inhibitors in Endometrial Cancer

Introduction

- Marabelle et al 2020 biomarker analysis of KEYNOTE-158 found that patients with High Mutational Burden (TMB-high) tumors had a higher objective response to Pembrolizumab monotherapy than non-TMB-high tumors leading to 2020 FDA approval of Pembrolizumab in TMB-high solid tumors.
- McGrail et al. 2021 reported that TMB-high status did NOT predict immune checkpoint inhibitor response across solid tumors, but did predict response in tumor types where CD8 cells positively correlated with TMB high status.
- **We aimed to further investigate association between TMB-high status and the clinical benefit of immunecheckpoint inhibition in patients with endometrial cancer**

Methods

- Retrospective review of patients at our institution with a diagnosis of recurrent or progressive endometrial cancer and received immune checkpoint inhibitor therapy as part of standard or care or clinical trial and had TMB determined by next generation sequencing.
- We grouped patients together as TMB-intermediate/high (>10) or TMB-very low/low (<10) for comparisons and assessed response by RECIST Criteria
- **Clinical Benefit** was defined as SD+PR+CR.
- **Durable Clinical Benefit** was defined as no progressive disease for ≥ 6 months.
- Fisher's exact test was used to determine if associations existed with significance set at p<.05.

Conclusions

- **Our exploratory analysis suggests a positive correlation between TMB-int/high (TMB >10) status and duration of clinical benefit in patients with endometrial cancer treated with immune checkpoint inhibitors.**
- **Further evaluation is warranted to confirm our findings as we are limited by a small sample size**

Valente A, Gin A, Ding K, wells A, Moore K

[1] *The University of Oklahoma, Stephenson Cancer Center, Oklahoma City, OK*

Table 1: Patient Characteristics

Ethnicity	n(%)
Black	4(19.1%)
Caucasian	10 (47.6%)
Hispanic	2 (9.5%)
Native American	4 (19.1%)
Asian	1 (4/7%)
Histology	
Endometriod	10 (47.6%)
Serous	5 (23.8%)
Clear Cell	2 (9.5%)
Carcinosarcoma	2 (9.5%)
Dedifferentiated	1 (4.7%)
Unknown	1 (4.7%)
BMI	
<25	1 (4.7%)
25-30	6(28.6%)
>30	14 (66.6%)
Best Response to ICI	
CR	2 (9.5%)
PR	5 (23.8%)
SD	6 (28.6%)
PD	8 (38.1%)
TMB	
Int/High (>10)	9 (42.9%)
Low/Very Low (<10)	12 (57.1%)

Clinical benefit was seen in 7/9 (77.8%) TMB-high/intermediate vs 6/12 (50%) TMB-low/very low *[p=.36]*

7/7 (100%) of TMB-int/high vs 2/5 (40%) of TMB-very low/low achieved durable benefit. This finding was statistically significant *[p=.0455]*

HOLISTIC TREATMENT OF TRIPLE NEGATIVE BREAST CANCER USING A NOVEL ANXA5-DM1 CONJUGATE IN COMBINATION WITH RAPAMYCIN AND ANTI-PD-1

Alexis Woodward[1], Gabriela N F Faria[2], Benjamin Southard[1], Roger Harrison[2]

1. Stephenson School of Biomedical Engineering, University of Oklahoma
2. School of Chemical, Biological & Material Engineering, University of Oklahoma

The need to target both the primary triple-negative breast cancer tumors and metastatic lesions has never been greater. Here we report a novel protein drug conjugate, consisting of annexin A5 (ANXA5) and emtansine (DM1), that targets and exploits cancer's upregulation of phosphatidylserine (PS). ANXA5 (~36 kDa) is a naturally occurring mammalian protein that binds with high affinity (Kd ~ 1 nM) to PS in the presence of calcium. In healthy cells, PS is almost exclusively found on the inner cytosolic leaflet and regulates phagocytotic cell death when it is extracellularly expressed. The tumor, metastatic lesions, and tumor vasculature all have an upregulated external expression of PS, making it a useful biomarker for cancer therapy.

DM1 is a microtubule inhibitor that induces apoptosis. While DM1 was a promising anticancer drug because of its high cytotoxicity, it induced widespread systemic toxicity, limiting its therapeutic potential. By conjugating DM1 to ANXA5, we have harnessed DM1's therapeutic potential while decreasing systemic side effects. On top of DM1 being an attractive cytotoxic agent, it has shown to induce immunogenic cell death (ICD), which leads to the activation of professional antigen-presenting cells and T-cells causing antitumoral immunity. ANXA5-DM1 increases the therapeutic potential for checkpoint inhibitors such as anti-PD-1. Additionally, ANXA5-DM1 also targets the tumor vasculature cutting off the tumor's nutrient supply, inducing growth in the presence of hypoxia as a result of the activation of hypoxia-inducible factor-1 (HIF-1). Mammalian target of rapamycin (mTOR) inhibitors (I.e. rapamycin,) are thought to reduce angiogenesis by indirectly reducing the synthesis of HIF-1 subunits. By combining ANXA5-DM1, anti-PD-1 antibody, and rapamycin, a holistic treatment regime is established.

DM-1 was linked to ANXA5 using sulfosuccinimidyl 4-(N-maleimidomethyl) cyclohexane-1-carboxyalte (Sulfo-SMCC). Six DM1 molecules were successfully loaded per ANXA5 molecule. The conjugate has been tested both *in vitro* and *in vivo*. When compared to the free DM1, the ANXA5-DM1 conjugate was 130 to 370 times more effective, against two murine triple negative breast cancer cell lines, when comparing the IC50 values (concentration where the cell viability is reduced by 50%). For the *in vivo* studies, Balb/cJ female mice were inoculated orthotopically with 4T1 or EMT6 cancer cells. Once the tumor reached ~5 mm in diameter, treatment began. The optimization study found that

the dose of 0.025 mg/kg gave the lowest tumor volume of the doses. A holistic combination approach (ANXA5-DM1, rapamycin, and anti-PD-1) was also explored against 4T1 and EMT6 cancers. When compared to the PBS control, this combination resulted in tumor volume sizes being 2.2 times smaller for 4T1 tumors and 4.3 times smaller for EMT6 tumors. Further studies exploring ANXA5-DM1 intratumoral injections are ongoing.

Holistic Treatment of Triple Negative Breast Cancer using a Novel ANXA5-DM1 Conjugate in Combination with Rapamycin and anti-PD-1

Alexis Woodward*[1], Gabriela N F Faria[2], Benjamin Southard[1], Roger Harrison[2]

University of Oklahoma – [1] Stephenson School of Biomedical Engineering, [2] Chemical, Biological and Materials Engineering

Abstract

Here we present a novel protein drug conjugate consisting of annexin A5 and emtansine (ANAX5-DM1) for the targeted treatment of triple negative breast cancer. ANAX5 binds tightly to the anionic phospholipid phosphatidylserine (PS) which is overexpressed in triple negative breast cancer. We have successfully conjugated 6 +/- 2 molecules of DM1 to 1 ANAX5 protein. ANXA5-DM1 has proved to be superior in cytotoxicity against free DM1 drug in both 4T1 and EMT6 TNBC cells and selectively targets breast cancer cells over healthy cells. The therapeutic efficacy of ANXA5-DM1 was tested against 4T1 and EMT6 cells, orthotopically, in six-week year old BALB/cJ mice. ANAX5-DM1 was given once every 7 days for 21 days. When combined with rapamycin and anti-PD1 tumor volume is reduced by 2.2 time for 4T1 TNBC and 4.4 times for EMT6 TNBC.

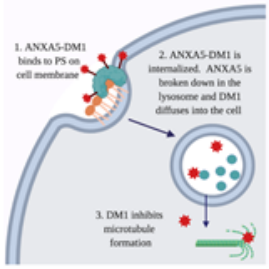

There is a need to develop novel targeted therapies for triple negative breast cancer to reduce systemic toxicity and increase cytotoxic payload to the tumor.

Background

Triple Negative Breast Cancer:
- Defined by the lack of estrogen, progesterone, and HER2 receptors
- Highly metastatic and aggressive
- Lowest 5-year survival of all breast cancer subtypes
- Untargeted systemic chemotherapy, surgery, and radiation remain the standard of care

Phosphatidylserine (PS):
- Exclusively found on inner leaflet of healthy cells
- Ubiquitously expressed on tumor vasculature and tumor cells

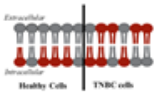

Annexin A5 (ANXA5)
- Binds to PS with high affinity in presence of calcium (K_D < 1 nM)
- Endocytosed via trimer network formation

Emtansine (DM1)
- Discovered by National Cancer Institute in the 1970s
- Toxic microtubule inhibitor

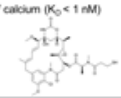

ANAX5-DM1 Conjugation and Quantification

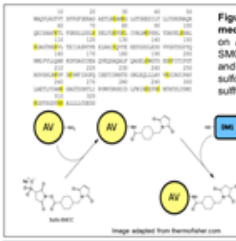

Figure 1: ANXA5-DM1 reaction mechanism. First the lysine resides on ANXA5 are activated with sulfo-SMCC. Second, DM1 is introduced and the maleimide on the ANXA5-sulfo-SMCC reacts with the lone sulfhydryl group on DM1 [1].

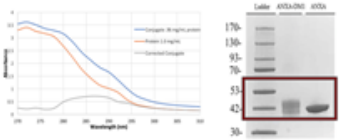

Figure 2: ANAX5-DM1 conjugation quantification. DM1 concentration was determined via spectroscopy. The conjugate absorbance was read at 288 nm. Blank ANXA5 was also read at 288 nm. The absorbance difference between the conjugate and blank protein is a result of DM1 addition and compared to a DM1 standard at 288 nm. An SDS-PAGE confirmed a protein shift consistent with 6 2+/- DM1 molecules to 1 ANAX5 protein. Mass Spec analysis confirmed drug loading.

ANAX5-DM1 *In Vitro* Cytotoxicity

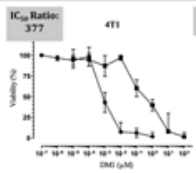

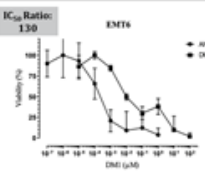

	IC50, uM
Cell line	ANXA5-DM1
4T1	0.85
EMT6	0.21
HUVEC	4.10
MCF10A	77.7

Figure 3: In vitro cytotoxicity of ANXA5-DM1 drug conjugate against TNBC and healthy cell lines. Cells were treated with ANXA5-DM1 or free drug for 72 hours. After treatment, viability was determined via an Alamar Blue assay. The inhibitory concentration at 50% (IC50) for healthy HUVEC and MCF10A cells is 5 to 370 times higher than the TNBC cells. Data depicted with mean +/-SD.

ANAX5-DM1 with a Holistic Dosing Regime

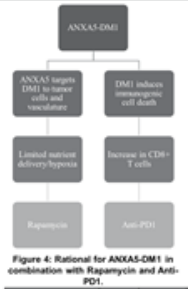

Figure 4: Rational for ANXA5-DM1 in combination with Rapamycin and Anti-PD1.

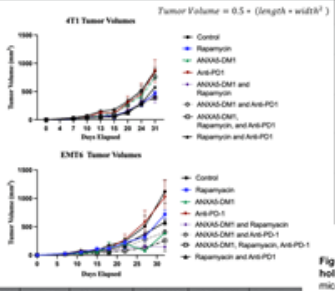

	Control	Rapamycin	ANXA5-DM1	Anti-PD1	ANXA5-DM1 and Rapamycin	ANXA5-DM1 and Anti-PD1	ANXA5-DM1, Anti-PD1, and Rapamycin	Anti-PD1 and Rapamycin
Median Survival (days)								
4T1	32	26	33.5	22	26	35 (*)	31	34
EMT6	34	34	21.5	32	25	33	32	30

Log-Rank (Mantel-Cox) curve comparison (*) p=0.0304

Group	4T1 Tumor Volume Day 21 mm³ (+/- SD)	4T1 Tumor Volume Day 21 Size ratio to control	EMT6 Tumor Volume Day 21 mm³ (+/- SD)	EMT6 Tumor Volume Day 21 Size ratio to control
Control	868 (+/-113) n=4		1119 (+/-412) n=4	
ANXA5-DM1	751 (+/-64) n=3	1.15	593 n=3	2
ANXA5-DM1 and PD1	758 (+/-106) n=5	1.145	403 (+/-307) n=3	2
ANXA5-DM1, PD1, and Rapamycin	389 (+/-64) n=6	2.23	255.51 (+/-187) n=3	4

Figure 5: 4T1 and EMT6 tumor volumes with holistic dosing regime. 6-week-old female Balb/cJ mice (n=6) were inoculated with an orthotopic injection of 10^5 cells in the 4th mammary fat pad. Mice were treated when tumors reached 5 mm in diameter with 0.025 mg/kg ANXA5-DM1 once every 7 days, 5 mg/kg rapamycin daily, and anti-PD1 on days 1, 5, and 9 of treatment. Mice treated with all three drugs had statistically significant tumor volumes on days 7, 10, 13, 15, 20, and 31 (p<0.05) for 4T1 tumors (one way ANOVA with post-hoc Tukey). Data depicted as mean +/- SEM.

ANXA5-DM1 Intratumoral Injections

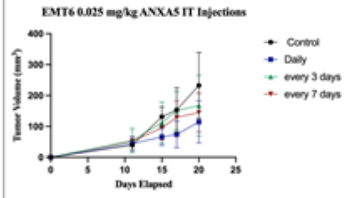

Figure 6: EMT6 tumor volume with intratumoral ANXA5-DM1 injections. 6-week-old female Balb/cJ mice (n=6) were inoculated with an orthotopic injection of 10^6 cells in the 4th mammary fat pad. Mice were treated when tumors reached 5 mm in diameter with 0.025 mg/kg ANXA5-DM1, daily, every 3 days, or every 7 days for 1 week. Daily ANXA5-DM1 injections decreased tumor volume by 1.6 times compared to PBS control. Data depicted as mean +/- SD.

Conclusions

- DM1 has been successfully conjugated to ANAX5
- Against 4T1 and EMT6 breast cancer cells, ANXA5-DM1 was 130 to 377 times more effective than the free drugs
- The IC50 for healthy vascular and breast cells were 5 to 370 times higher than TNBC cells when treated with ANXA5-DM1
- When combining ANXA5-DM1 with rapamycin and anti-PD1, tumor volumes were 2.2 to 4.3 times smaller than the control
- Daily intratumoral injections decreased tumor volumes by 1.6 times when compared to the control

Future Work

- Explore higher doses of ANXA5-DM1 for intratumoral injections
- Combine intratumoral ANXA5-DM1 with checkpoint inhibitor therapy
- Determine immune cell population changes in spleen and tumor

References

1. Thermo Fisher Scientific. Sulfo-SMCC. (2019)
Please Contact alexiswoodward@ou.edu for Questions

Funding Acknowledgements

We thank the Oklahoma Center of Advancement of Science and Technology and the Jean Wheeler Sparks and Baxter Abbott Sparks Breast Cancer Research Fund at 10
.The University of Oklahoma Foundation for funding.

Pre-symposium Poster Session

PATIENT DERIVED XENOGRAFTS (PDXs) OF HIGH GRADE SEROUSE OVARIAN CANCER AS A VALUABLE TOOL IN CANCER RESEARCH

Magdalena Cybula, Lin Wang, Summer Wang, Ana Luiza Drumond Bock, Maria Rostworowska, Magdalena Bieniasz

Oklahoma Medical Research Foundation, Aging and Metabolism Research Program

magdalena-cybula@omrf.org

A major obstacle in oncology is a scarcity of pre-clinical models that faithfully recapitulate the heterogeneity of human tumors and can be utilize in pre-clinical drug testing. Widely used tools for cancer research, including cancer cell lines and cell line-based mouse xenografts, do not preserve the complexity of tumors and have poor predictive power for clinical response. There is a need for development of more advanced tumor models that overcome these barriers. In recent years, PDXs emerged as a powerful tool in cancer research. These models are established by engrafting of patient tumor tissue directly into mice without prior in vitro manipulation, assuming that they preserve the diversity and complexity of human tumors and are more powerful tool in pre-clinical drug testing. Established PDX models can be propagated for multiple passages, however it raise the question whether PDXs change their characteristics over time. There is a need to assess the extent of genetic drift in these models. We developed a method to interrogate genetic drift in a panel of high grade serous ovarian cancer PDXs using SNP genotyping. We demonstrated that this method can be successfully utilized to assess genetic drift across PDX passages and detect PDX contamination with lymphoproliferative tissues. Our PDX model remain largely stable throughout propagation with marginal genetic drift. We performed a detailed histological characteristics and showed that PDXs retain the histological features of original patients' tumor even following multiple passages in mice. Moreover, our established PDX models faithfully recapitulate the therapeutic response of their corresponding patients. In conclusion, patient derived xenografts are a powerful tool in cancer research that can accelerate the process of translation of new therapies from pre-clinical studies to patients.

Funding: This research was funded in part by the McCasland Foundation, which supported the development of PDX models within the PDX-PCT Core Facility at OMRF in Oklahoma. Research reported in this publication was also supported in part by the National Cancer Institute Cancer Center, Support Grant P30CA225520, awarded to the University of Oklahoma Stephenson Cancer Center. The content is solely the responsibility of the authors and does not necessarily represent the official views of the National Institutes of Health

STRATEGIC TARGETING OF DNA DAMAGE REPAIR PATHWAYS TO IMPROVE THERAPEUTIC RESPONSE IN CERVICAL CANCER

Sugantha Priya Elayapillai[1], Bethany Hannafon[1], and Katherine Moxley[2]

[1]Department of Obstetrics and Gynecology, Peggy and Charles Stephenson Cancer Center, The University of Oklahoma Health Sciences Center, Oklahoma City, OK, [2]Department of Obstetrics and Gynecology, University of Michigan, Ann Arbor, MI
Email: suganthapriya-elayapillai@ouhsc.edu

Introduction: Cervical cancer (CC) is the fourth most common cancer among women worldwide. CC is most commonly induced by oncogenic strains of the human papillomavirus (HPV), which manipulates DNA damage repair (DDR) pathways, promoting viral replication and enhancing the survival of transformed cells. Moreover, due to the expression of HPV-viral oncoproteins activation of p53 is impaired, resulting in a deficient G1-S cell cycle checkpoint and ATM-mediated homologous recombination (HR) repair. CC cells become more reliant upon ATR-mediated HR and the Poly (ADP-ribose) Polymerase (PARP) non-homologous end joining (NHEJ) DNA repair pathway at the intact G2 checkpoint. We hypothesized that abrogating the G2 cell cycle checkpoint by ATR inhibition would sensitize cells to subsequent PARP inhibition resulting in synthetic lethality. The objective of this study was to investigate dual blockade of DDR proteins (ATR and PARP) alone and in combination as a novel therapeutic approach for the treatment of HPV-medicated CC.

Methods: The cytotoxicity of the ATR inhibitor AZD6738 (ATRi) and the PARP inhibitor Olaparib (PARPi) alone and in combination was determined by MTS assay *in vitro* using two HPV-positive CC cell lines (CaSki and SiHa). The combination index (CI) and dose reduction index (DRI) was determined by isobologram analysis based on the Chou-Talalay method. CC cells were either simultaneously or sequentially treated with ATRi and PARPi *in vitro*. The combinatorial effect of dual PARP and ATR inhibition was also evaluated *in vivo* in a mouse xenograft model. The effect of drug treatment on the expression of primary drug targets and downstream DNA damage repair pathway proteins (PARP, ATM, ATR, p-chk1 and pchk2) were evaluated by western blot.

Results: The CI of simultaneous ATRi/PARPi drug treatment indicated synergism in CaSki and moderate synergism in SiHa cells. PARPi pretreatment indicated strong synergism in CaSki and strong antagonism in SiHa cells. Whereas ATRi pretreatment indicated strong and very strong synergism in both CaSki and SiHa cell lines respectively. The DRI for ATRi pretreatment was higher than both PARPi pretreatment and simultaneous drug treatment. With an average DRI for ATRi pretreatment 13.4-fold less than the single-dose in CaSki cells and 176.7-fold less in SiHa cells. Treatment with ATRi and PARPi resulted in a significant reduction in tumor growth in vivo. Total PARP expression was increased following treatment with ATRi, and reduced significantly with PARPi in both CC cell lines. ATR inhibition decreased p-chk1 and p-chk2 protein levels indicating impaired ATR signaling. Increased PARP cleavage was observed in the combination drug-treatment groups resulting in increased cell death in the CC cell lines.

Conclusion: Our study showed a combination of ATR and PARP inhibition is a highly promising strategy to overcome HPV-positive cervical cancers in the pre-clinical setting.

Funding: Pilot grant from Memorial Sloan Kettering Cancer Center.

E-CIGARETTE AEROSOL ALTERS THE EXPRESSION OF ANTIOXIDANT AND DETOXIFICATION ENZYMES AND INFLAMMATORY MARKERS IN LUNG CELLS

Vengatesh Ganapathy[1], Daniel Brobst[1], Jimmy Manyanga[1,2], and Lurdes Queimado[1-3]

Departments of [1]Otorhinolaryngology and [2]Cell Biology; [3]TSET Health Promotion Research Center, [4]Stephenson Cancer Center, The University of Oklahoma Health Sciences Center, Oklahoma.

Background: Smoking is the leading cause of preventable disease and death. E-cigarettes (e-cigs) have emerged as a novel tobacco smoke harm reduction tool, but their health effects are unknown. Recent reports show that e-cig users increase their risk of respiratory disease. This is likely attributed to e-cig aerosols containing harmful and potentially harmful substances, e.g., nicotine, carbonyl compounds, heavy metals, carcinogens, and reactive oxygen species (ROS). When e-cig users vape, the above toxic substances accumulate in the lungs, causing lasting damage that can contribute to various types of toxicity, disease, and cancer. Our previous *in vitro* study showed that e-cig aerosols can suppress cellular antioxidant defenses and induce significant oxidative DNA damage. However, the molecular mechanisms contributing to the underlying e-cig induced oxidative stress are unknown.

Aims: To assess whether e-cig aerosol alters the expression of antioxidant and detoxification enzymes, and contributes to inflammatory signals in lung cells.

Methods: Human epithelial normal bronchial cells (Nuli1) cells were exposed every other day for 2 weeks, to e-cig extracts. E-cig aerosols extracts (18 mg/ml of nicotine; tobacco flavor) were prepared from two distinct e-cig brands. Standard tobacco extracts were used as positive control. The quantification of 37 key biomarkers of inflammation, including IL8, IL10, IL 22, TNF superfamily proteins, IFN family proteins, Treg cytokines, and MMPs, was performed on Nuli1 cell extracts and media with a BioRad multiplex kit. The expression of super oxide dismutase (SOD2), heme oxygenase 1 (HMOX1), and CYP1B1 proteins was quantified by western blotting. Data were analyzed by Student's t-test.

Results: Exposure to e-cig aerosol extracts for 2 weeks resulted in altered the expression of proteins involved in defense against oxidative stress. HMOX1, a protein with a role in cell protection, inflammation, and oxidative stress, was increased after exposure to specific e-cig extracts. A significant increase in the detoxification enzyme CYP1B1 was consistently observed after exposing to e-cig aerosols extracts. Significant alterations in cytokines that play major roles in inflammation and immune modulation were observed after exposure to e-cig aerosol extract, including significant decreases in the expression of IL8, IL10, and IL 22 proteins.

Conclusion: E-cig aerosol exposure significantly changed inflammatory markers and increased the expression of HMOX1 and CYP1B1 proteins. HMOX1 increase might modulate inflammation and immune response by altering cytokines levels. CYP1B1 is a protein with a key role in the bioactivation of tobacco pro-carcinogens and the regulation of redox homeostasis. The increase

in HMOX1 and CYP1B1 proteins might put the cell under additional oxidative stress which can have major biological implications.

Grant support: This work was supported by a seed grant from the Health Promotion Research Center (Ganapathy), the National Institutes of Health/National Cancer Institute (R01CA242168), and the Oklahoma Tobacco Settlement Endowment Trust.

NEW PORTABLE TECHNOLOGY TO QUANTIFY TOE STRENGTH IN CHEMOTHERAPY-INDUCED PERIPHERAL NEUROPATHY

Mustafa Ghazi[1,4,5], Hongwu Wang[1,5,2,6], Raghuveer Chandrashekhar[2,6], Josiah Rippetoe[1,4,5], Ashely Fox[4,5], and Abby Cha[4,5], and Elizabeth Hile, PT, PhD[1,3,4,5]

[1]Department of Rehabilitation Sciences, College of Allied Health, [2]Department of Occupational Therapy, College of Public Health and Health Professions, [3]OU Health, [4]Cancer Rehabilitation Research Lab, Stephenson Cancer Center, [5]University of Oklahoma Health Sciences Center, Oklahoma City, Oklahoma, [6]University of Florida, Gainesville, Florida

Introduction: Chemotherapy-induced peripheral neuropathy (CIPN) is a cancer sequela prioritized by NCI, as relevant to both quality of life and survival. Currently, there is no evidence-based cure or prevention, so oncologists use CIPN sensory symptoms of numbness and tingling to titrate chemo dose in hopes of preventing persistence. CIPN is also motor, but patients cannot perceive early weakness. As a result, motor decline is understudied, yet known to impact balance and gait in other populations, leading to falls and reduced physical activity. Like sensory symptoms, CIPN motor manifestations start at the toes. Unable to find a sufficiently reliable, accurate, and responsive clinical approach to quantify toe strength in patients at risk for CIPN, we aim to develop low-cost portable technology. Specifically, the device must quantify (1) the strength of great toe extension, for clearing the foot during gait, and (2) the pressure the great toe can exert downward, for pushing off to achieve a functional walking pace.

Methods: We developed a device informed by healthy young adults (ages 20-30), clinicians, and women with gyn & breast cancers. Core design features: (1) A “toe cap” mounted to 100 N load cell, (2) cap stability while toe pulls upward with foot securely attached to a rigid base plate, (3) onboard electronics to transmit the force data over USB to laptop where data are logged and analyzed. We used an aluminum base plate after preliminary testing determined aluminum is more rigid for its size, and yields more reliable readings. We developed multiple design iterations for the toe cap to allow for optimum load transfer, hygiene, and patient comfort. We also added a visual feedback display for more consistent peak performance.

Results: Our second-generation prototype is acceptable to clinicians and patients. We have early evidence of concurrent validity with Manual Muscle Testing, but also discriminant validity based on specific MMT value (Fig. 1). Our standardized test protocol is embedded in 2 ongoing studies: (1) CIPN onset during taxane chemo for women’s cancers, (2) focal vibration for management of persistent CIPN. Patent US20200408622A is under review at the US Patent Office.

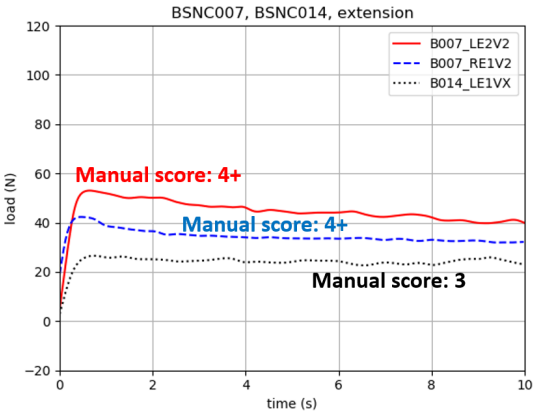

Figure 1. Device output compared to manual muscle testing.

Conclusion: Our 2nd generation prototype has proven acceptable to clinicians and women's cancers patients, and feasible for serial assessment in future trials of cancer therapeutics, and pharmacologic & behavioral preventions / interventions for CIPN. Future directions include continued device refinement, especially wireless data transfer, and production of copies as we seek SBIR opportunities and integrate the device into NIH funding applications to establish clinical phenotypes of sensorimotor CIPN.

Funding: NCI Cancer Center Support Grant P30CA225520 to OU Stephenson Cancer Center. Presbyterian Health Foundation, Oklahoma Tobacco Settlement Endowment Trust.

DRUG AND TARGET DISCOVERY AT THE OKLAHOMA CENTER FOR THERAPEUTIC SCIENCES

Matthew J. Hart

The Center for Therapeutic Sciences (CTS) at University of Oklahoma is a trans-institutional hub for drug discovery and development. The CTS comprises the Laboratory for Drug and Target Discovery (DTD), the Med Chem Laboratory (MCL) and the Pharmacology Laboratory (PHL), that coordinately support a multi-entry pipeline of both target and drug discovery and drug development. The DTD is a state-of-the-art technological hub that provides lab space, cell culture facilities and a full suite of integrated detection, robotic and imaging equipment designed to enable HTS in 96, 384-or 1536 well microplate formats. The goal of the DTD is to enable the translation of basic discoveries into therapeutics by working along with investigators during each stage of the drug discovery process, including screen design, high throughput screening, candidate identification and lead validation. DTD has also added structure-guided drug identification and development to its portfolio of services available to investigators. Drug candidates are then optimized through medicinal chemistry at the MCL and ADME and PD/PK among other parameters are defined at the PHL to generate intellectual property as novel therapeutics. Dr. Matthew Hart, Director of the CTS and the DTD has over 25 years of experience in drug and target discovery using high throughput screening technologies. Dr. Hart will discuss activities at the CTS and how CTS can add to the translational directions available to OUHSC investigators.

IMPACTS OF EXPOSURE TO CORRECTIVE STATEMENTS AND FEDERAL COURT FINDINGS ON SMOKING CESSATION

James D. Matheny, M.P.H.[1]; Sixia Chen, Ph.D.[2]; Joseph J. C. Waring[3]; Summer G. Frank-Pearce, Ph.D.[1,2]; Darla E. Kendzor, Ph.D.[1,4]

[1] TSET Health Promotion Research Center, Stephenson Cancer Center, OUHSC; [2] Department of Biostatistics and Epidemiology, Hudson College of Public Health, OUHSC; [3] Johns Hopkins Bloomberg School of Public Health, Baltimore, Maryland; [4] Department of Family and Preventive Medicine, OUHSC

Presenting Author's Email Address: james-matheny@ouhsc.edu

Funding: This work was supported by the Oklahoma Tobacco Settlement Endowment Trust (TSET) grant 092-016-0002 and the NCI Support Grant P30CA225520 awarded to the Stephenson Cancer Center.

Introduction: A federal court found tobacco companies in violation of civil racketeering laws and ordered them to disseminate corrective statements. Prior research suggests that the corrective statements alone may provide little benefit to public health. This study examined potential impacts of the corrective statements and the corresponding federal court findings among adults trying to quit smoking.

Methods: Participants (n=582) were adults enrolled in tobacco cessation treatment. Data were collected from October 2018 through September 2021. Participants were asked to read the 18 corrective statements and 10 court findings, and to report their prior awareness of each. Using a 9-point scale (1 = "not at all" to 9 = "extremely"), they rated the extent to which the information evoked emotions and then reported their likelihood of quitting smoking. Reported smoking status was verified via a carbon monoxide breath sample at 4, 12, and 26 weeks after the quit day. All regression analyses were adjusted for age, sex, race/ethnicity, education, and pre-quit cigarettes smoked per day.

Results: Participants were mostly female (56.4%), White (63.4%) or Black (25.4%), with a mean age of 52.5 (SD = 12.3) years. Nearly half reported they had ≤ a high school education (43.3%, n = 252). Participants had smoked an average of 16.6 (SD = 10.4) cigarettes per day (pre-quit) for 31.1 (SD = 14.7) years. Cessation rates were 25.3%, 19.3%, and 12.5% at 4, 12, and 26 weeks after the scheduled quit date, respectively. On average, participants reported awareness of 13.3 (SD = 4.6) of the 18 corrective statements, and 4.1 (SD = 3.8) of the 10 court findings. Substantial proportions of participants reported the statements/findings made them feel extremely (rating=9) afraid (28.4%), angry toward tobacco companies (43.8%), worried about the health risks of smoking (45.9%) and worried about the health risks of secondhand smoke (47.8%). Many reported that after reading this information they were more likely to quit smoking for good (80.4%) and to support a law banning smoking in all workplaces (71.0%). Of those who had not already adopted personal smoking bans, many reported that they were more likely to ban smoking in their home (68.4%) or in their vehicles (72.8%). Greater

awareness of the 10 court findings was associated with smoking abstinence at 4 weeks ($p = 0.023$) and 12 weeks ($p = 0.001$) post-quit, but not at 26 weeks post-quit ($p = 0.124$). Awareness of the corrective statements was not associated with abstinence at any follow-up. Females ($p = 0.003$) were less likely to be aware of the court findings.

Discussion: Smokers' awareness of court findings from the ongoing federal racketeering case against tobacco companies may evoke strong emotions while aiding smoking cessation. This finding may warrant substantial and sustained public education efforts to highlight the tobacco companies' egregious behaviors that led to the court-ordered corrective statements.

SMARTPHONE OWNERSHIP AND MEDIA USE BY ADULTS EXPERIENCING HOMELESSNESS: AVENUES FOR FUTURE INTERVENTIONS

Audrey Montgomery[1], Jordan M. Neil [1,2], Michael B. Cannell,[3] Jennifer Gonzalez[4], Ashley Cole[5], Chaelin Ra[1], Jillian Robison[1], Krista Kezbers[1], Darla E. Kendzor[1,2], & Michael S. Businelle[1,2]

[1]TSET Health Promotion Research Center, Stephenson Cancer Center, University of Oklahoma Health Sciences Center, Oklahoma City, OK, United States; [2]Department of Family and Preventive Medicine, University of Oklahoma Health Sciences Center, Oklahoma City, OK, United States; [3]School of Public Health, University of Texas Health Sciences Center, Dallas, TX, United States; [4]The Meadows Mental Health Policy Institute, Dallas, TX; [5]Department of Psychology, Oklahoma State University, Stillwater, OK, United States; The Meadows Mental Health Policy Institute, Dallas, TX

Background: Homelessness is associated with negative physical and mental health comorbidities, including substance use, chronic stress and health conditions, and early mortality. Technology-based interventions may reduce access barriers to empirically validated interventions in this underserved population. The current descriptive study examines the prevalence of technology and social media use, and the perceived utility of health-related mobile health applications (apps) among homeless adults recently released from incarceration.

Methods: Baseline data from a large NIH funded randomized controlled trial conducted in Dallas, Texas were analyzed for this study. Participants self-reported demographic information, duration of homelessness, and answered questions about smartphone ownership, social media/internet use, and frequency of technology engagement. Participants were also asked if they had previously used smartphone apps to manage health behaviors, and if they believed apps could help them improve their health behaviors. Descriptive analyses were conducted in R.

Results: Participants (n=244) were predominantly male (86.5%), African American (60.7%), 40.6 years old on average (SD=11.0) and had been homeless for 30 months (median). Nearly one-fourth (22.1%) of participants reported that they currently owned a smartphone (98.1% Android), and nearly all (94.6%) had an active data plan. Most participants (89.7%) reported that they used the internet at least weekly. Most reported that they used email (79.5%) and Facebook (70.1%; 89.8% accessed Facebook at least weekly), but fewer reported that they used Instagram (25.8%), Snapchat (14.3%), Twitter (9.4%) or LinkedIn (8.2%). Few participants (8.2%) reported that they do not use social media at all. Most participants (86.4%) believed that a smartphone app could help them improve their health, but only 26.2% had ever used a smartphone app for this purpose.

Conclusion: Findings indicated that most adults experiencing homelessness regularly access and use social media and the internet. Further, most participants believed that smartphone apps could help them to manage health behaviors, but few had used apps for this purpose. Future research should examine if standalone, and/or adjunctive internet-, social media-, and/or smartphone app-based health behavior change interventions are effective for adults experiencing homelessness.

Funding: This research was supported by the National Institute of Minority Health and Health Disparities (R01MD01073301; PIs: MSB, JRG). This work was also supported by the Oklahoma Tobacco Settlement Endowment Trust -(TSET) grant 092-016-0002, and the Mobile Health Technology Shared Resource which is a component of the NCI Support Grant P30CA225520 awarded to the Stephenson Cancer Center.

DELAY OF NEOADJUVANT CHEMOTHERAPY REDUCES PATHOLOGIC COMPLETE RESPONSE RATE IN TRIPLE NEGATIVE BREAST CANCERS

Shreya Nuguri[1], Macall Leslie[2], Rashmi Pathak[2], William Dooley[3], Inna Chervoneva[4], Takemi Tanaka[2, 5]

1)University of Oklahoma Health Sciences Center, College of Medicine, 975 NE, 10th, Oklahoma City, OK 73104; 2)University of Oklahoma Health Sciences Center, Stephenson Cancer Center, 975 NE, 10th, Oklahoma City, OK 73104; 3)University of Oklahoma Health Sciences Center, School of Medicine, Dept. of Surgery, 800 Stanton L. Young Blvd., Oklahoma City, OK 73104; 4)Thomas Jefferson University, Division of Biostatistics, Department of Pharmacology and Experimental Therapeutics, 1015 Chestnut St., Suite 520, Philadelphia, PA 19107; 5)University of Oklahoma Health Sciences Center, School of Medicine, Dept. of Pathology, 800 Stanton L. Young Blvd., Oklahoma City, OK 73104

Breast cancer is the second leading cause of cancer-related deaths among women in the US. Although it makes up only about 14% of cases, Triple Negative (i.e.- hormone receptor and HER2-negative) breast cancer is more aggressive and has poorer prognosis than other subtypes. Triple Negative breast cancer is typically treated with neoadjuvant chemotherapy followed by surgery. Pathologic complete response (pCR), the absence of residual invasive disease, at the time of surgery is a predictor of survival. Currently, there is a lack of information on how time to initiation of neoadjuvant therapy (TTN) may impact disease outcomes, including pCR. Thus, the purpose of this study is to investigate the impact of the time interval between diagnosis to initiation of neoadjuvant chemotherapy on pCR. Using the National Cancer Database, a retrospective cohort analysis was conducted to assess the relationship between TTN and pCR in Stage I-III Triple Negative breast cancer treated with neoadjuvant chemotherapy between 2010-2017. After exclusions, the cohort included 8,071 Triple Negative cases, 35.5% of whom achieved pCR. The proportion of patients who achieved pCR decreased with increasing TTN. Multivariable logistic regression models showed that TTN $\geq$45 days is associated with 23.7% (OR 0.76, 95% CI 0.66-0.88) lower likelihood of achieving pCR. Therefore, delay of neoadjuvant therapy over 45 days after diagnosis negatively impacts pCR in Triple Negative breast cancer patients.

Funding: NA
Email Address: snuguri@ouhsc.edu

INFLUENCE OF OBESITY ON TUMOR SIGNALING PATHWAYS IN BREAST CANCER PROGRESSION

Queen Pierre[1], Ty Milligan[1], Alexander Filatenkov[2], William Dooley[3,7], Chao Xu[5], Elizabeth Wellberg[2,6, & 7] and Bethany Hannafon[4,7]

[1] College of Medicine, [2]Department of Pathology, [3]Department of Surgery, [4]Department of Obstetrics and Gynecology, [5]Department of Biostatistics and Epidemiology, College of Public Health, [6]Harold Hamm Diabetes Center,[7]Stephenson Cancer Center, University of Oklahoma Health Sciences Center, Oklahoma City, OK

Email Address: Queen-Pierre@ouhsc.edu

Ductal carcinoma in situ (DCIS) is a benign breast condition with the potential to progress to invasive ductal carcinoma (IDC). While research indicates that obesity affects breast cancer incidence and risk of IDC after DCIS diagnosis, it is not well understood how obesity influences pro-tumorigenic programs in DCIS and IDC relative to patients without obesity. We hypothesize that gene expression differences are present between patients with and without obesity diagnosed with DCIS or IDC that may contribute to cancer progression.

Archived FFPE blocks were obtained from patients diagnosed with DCIS or IDC. These patients were divided into categories based on diagnosis (DCIS or IDC) and body mass index (BMI; normal BMI <30 kg/m^2, high BMI 30> kg/m^2). RNA was extracted from sections cut from FFPE blocks and analyzed using the Nanostring Tumor Signaling 360 Panel. Initial data was composed of 23 post-menopausal subjects: high BMI DCIS (n=6); normal BMI DCIS (n=6); high BMI IDC (n=6); and normal BMI IDC (n=5). Raw expression counts were normalized, and fold-change (FC) was calculated. Significant differences were determined by t-test and immune cell types were profiled using nSolver Software (4.0).

The largest differences in gene expression were found between DCIS to IDC, and high BMI DCIS vs IDC relative to normal BMI DCIS vs IDC. Among the DCIS and IDC comparison CXCL9 (FC=9.57), CXCL10 (FC=10.9), ASXL2 (FC=1.3), STAT3 (FC=1.43), and IDO1 (FC=10.6) showed higher levels of gene expression in the IDC group compared to the DCIS group. In the high BMI DCIS vs high BMI IDC comparison, gene expression differences were observed between IDO1 (FC=48.1), PMAIP1 (FC=4.62), CXCL9 (FC=26.4), CXCL10 (FC=35.1), and EZH2 (FC=4.1). These genes are involved in chemokine signaling, myeloid immune evasion, apoptosis, adipocyte differentiation, immortality, and epigenetic and transcriptional regulation. Alterations to the populations of immune cell types were observed in high BMI DCIS vs. IDC relative to normal BMI DCIS vs. IDC.

The major pathways dysregulated by the differentially expressed genes observed among the high BMI DCIS vs IDC relative to normal BMI DCIS vs IDC involved inflammatory and immune response pathways. These gene expression changes corresponded to changes in immune cell type populations present in high BMI groups relative to normal BMI. While gene expression differences were observed, the major limitation to this initial data set is the lack of statistical significance after multiple hypothesis testing, likely due to the heterogeneity of human tumors and the small sample size. Currently, only 23 patient samples have been analyzed thus far. However, preliminary data indicate that obesity may alter the expression of genes involved in

immune response and alter populations of immune cell types. Inclusion of more samples per group, and further analysis of the identified genes involved in immune signaling, chemokine signaling, epigenetic regulation and adipocyte differentiation may be worth further investigation.

Funding: Nanostring Technologies Institutional Grant Program and Harold Hamm Diabetes Center-Stephenson Cancer Center Pre-Team Science Grant

RELATIONS BETWEEN DISTRESS TOLERANCE AND PSYCHOSOCIAL VARIABLES IN ADULTS EXPERIENCING HOMELESSNESS

Jillian Robison (jillian-robison@ouhsc.edu),[1] Jordan Neil,[1] Michael Brad Cannell,[2]Jennifer Reingle Gonzalez,[3] Michael Zvolensky,[4] Chaelin Karen Ra,[1] Lorra Garey,[4] Darla Kendzor,[1, 5] Ashley Cole,[6] Krista Kezbers,[1] Audrey Montgomery,[1] & Michael S. Businelle[1, 5]

[1]TSET Health Promotion Research Center, Stephenson Cancer Center, University of Oklahoma Health Sciences Center, 655 Research Parkway, Oklahoma City, OK, 73104; [2]School of Public Health University of Texas Health Sciences Center, Dallas, TX; [3]Meadows Mental Health Policy Institute, Dallas, Texas; [4]Department of Psychology, University of Houston; [5]Department of Family and Preventive Medicine, the University of Oklahoma Health Sciences Center; [6]Department of Psychology, Oklahoma State University, 116 Psychology Building, Stillwater, OK 74078, USA

Funding: This research was supported by the National Institute of Minority Health and Health Disparities (R01MD01073301; PIs: MSB, JRG). This research was supported by the Oklahoma Tobacco Settlement Endowment Trust (TSET) grant R21-02 and used the mHealth Shared Resource which is partially funded by the NCI Cancer Center Support Grant P30CA225520 awarded to the Stephenson Cancer Center.

Background: Recent research suggests that a small set of transdiagnostic vulnerability factors may underly causes of many psychological symptoms and disorders, as well as comorbid behavioral health problems. Compared with domiciled adults, adults experiencing homelessness are more likely to suffer from anxiety, depression, chronic stress, and drug use. Distress Tolerance (DT) is a transdiagnostic factor that may be particularly relevant to mental and physical health problems among individuals experiencing homelessness.

Methods: This study used baseline data from a randomized controlled trial that tested a novel smartphone-based intervention for recently incarcerated adults experiencing homelessness. A series of linear regressions were conducted to examine relationships between DT subscales (i.e., tolerance, appraisal, regulation, and absorption) and psychosocial variables (e.g., depression, aggression, hostility, anxiety, and urban life stress). The subscales measured the participant's ability to tolerate negative emotional states (tolerance), the participant's own assessment of distress (appraisal), mechanisms used to cope with distress (regulation) and the estimated level of attention consumed by distress (absorption). All models were adjusted for age, sex, race/ethnicity, education, and duration of homelessness.

Results: Participants (*n*=244) were predominantly Black/African American (60.7%) and male (86.5%) with a mean age of 40.6 years (*SD*= 11.0). Lower DT Appraisal was significantly associated with higher depression symptoms, anxiety, hostility, and stress. Lower DT Absorption was significantly associated with higher aggression, anxiety, and stress. Similarly, lower DT Tolerance was significantly associated with greater levels of hostility. All but one of the results were consistent with hypotheses (all $p<.05$).

Conclusion: This research extends previous work and indicates that lower DT, particularly the Appraisal and Absorption subscales, was associated with more depression symptoms, anxiety,

hostility, and stress among adults experiencing homelessness. Future research should assess the feasibility of interventions with individuals experiencing homelessness that enhance DT Appraisal and Absorption coping.

POLYAMINE METABOLISM IS IMPORTANT FOR IL-22 EXPRESSION IN GROUP 3 INNATE LYMPHOCYTES (ILC3S)

Prakash Sah* and Lauren Zenewicz

Department of Microbiology and Immunology, College of Medicine, The University of Oklahoma Health Sciences Center, Oklahoma City, OK, 73104, USA
prakash-sah@ouhsc.edu

Abstract

Group 3 innate lymphocytes (ILC3s) are rare, tissue resident immune cells and are a major source of the cytokine interleukin-22 (IL-22). IL-22 is a critical regulator of tissue repair and inflammation. However, IL-22 can also promote cancer in the gastrointestinal tract and other tissues. IL-22 is a potential therapeutic target for many inflammatory conditions and a better understanding of its regulation is critical for development of effective therapeutics. While the functions of IL-22 have been studied very well, much less is known about regulation of IL-22 production. Polyamines are low molecular weight, polycationic alkylamines that regulate many fundamental cellular processes. Polyamines are also known to be regulators of immune cell functions, including Th17 cells, the adaptive immune cell counterparts of ILC3s. Ornithine decarboxylase (ODC), encoded by *Odc1*, is the rate-limiting enzyme in polyamine synthesis pathway. In this study, we investigated the role of ODC in activation of ILC3s. NanoString analysis of metabolic gene expression of MNK3 cells, a mouse ILC3-like cell, revealed *Odc1* as a significantly upregulated metabolism gene during immune cell activation. Inhibition of ODC resulted in decreased IL-22 production, which was rescued by addition of the polyamine, putrescine. Our results implicate a role for polyamine metabolism in regulation of IL-22 production in ILC3s.

Funding: This work is supported by P20 GM134973. Research reported in this abstract was supported in part by the National Cancer Institute Cancer Center Support Grant P30CA225520 awarded to the University of Oklahoma Stephenson Cancer Center and used the Molecular Biology Shared Resource.

TRANSCRIPTION AND REPLICATION DIFFERENCES DRIVING MYC-INDUCED B AND T CELL LEUKEMIAS

Arpan A. Sinha, MD[1]; Clay Foster, PhD,[1]; Courtney Sansam, PhD[2]; Pilar I. Andrade, MS[1]; Katie Foster, PhD[1]; Megan Malone-Perez, BS[1]; Hayley Harris, BS[1]; Christopher Sansam, PhD[2]; J. Kimble Frazer, MD, PhD[1,3,4]

[1]Jimmy Everest Section of Pediatric Hematology/Oncology, Department of Pediatrics, OUHSC, Oklahoma City, OK; [2]Cell Cycle & Cancer Biology Research Program, OMRF, Oklahoma City, OK
[3]Department of Cell Biology, OUHSC, Oklahoma City, OK; [4]Department of Microbiology & Immunology, OUHSC, Oklahoma City, OK
E-mail: Arpan-Sinha@ouhsc.edu

Acknowledgement of funding: This project is supported by the Presbyterian Health Foundation of Oklahoma City - Team Science Award.

MYC is central to acute lymphoblastic leukemia (ALL) – the most common and second most lethal malignancy in children. ALL afflicts even higher numbers of adults. Much of MYC's oncogenic function is as a transcription factor, but MYC has also been shown to deregulate DNA replication independent of transcription. *We hypothesize that MYC alters both RNA expression and DNA replication (the spatio-temporal process where genomic domains replicate in either early or late S-phase) in B- and T-ALL, and that these perturbations—some shared, others unique to one ALL type—drive leukemogenesis.*

We utilize a novel transgenic *rag2:hMYC* zebrafish ALL model that we established, which is the only animal model to develop both highly penetrant B- and T-ALL. In this model, B- and T-ALL are each induced by human MYC *(hMYC)* regulated by a zebrafish (*Danio rerio*) *rag2* promoter. We use several transgenic markers (*lck*:*GFP*, *lck*:*mCherry*, *cd79a*:*GFP*, *cd79b*:*GFP*) to identify T- and B-ALL in these animals and to FACS-purify cells for study. To date, we have collected 30 ALL samples (18 T, 12 B) and completed two types of analyses on 15 of these. We established gene expression profiles (GEP) for both ALL types by RNA-seq; multiple analyses demonstrate B- and T-ALL are distinct. To assess DNA replication, we generated Replication Timing (RT) profiles by FAC-sorting cells based on cell cycle phase (G1 vs. S; defined by DNA content) and then performing whole-genome sequencing to derive RT profiles from the same ALL analyzed by RNA-seq. We identified differentially-replicating regions by comparing RT of B-vs. T-ALL, revealing loci where replication consistently shifts either early → late or late → early based on ALL type.

Despite their shared MYC genetic driver, we found RT differences distinguishing B- vs. T-ALL across ~30% of the genome. Most differences affect large genomic domains, suggesting abnormal chromatin structure in ALL. An additional unexpected result was that many ALL samples showed read count differences across large chromosomal regions, demonstrating highly-recurrent and lineage-specific aneuploidies/copy number aberrations.

Together, our data reveal differences in RNA transcription, DNA replication, and hotspots of genomic instability that are lineage-specific, despite a shared oncogenic driver. Future studies

will examine which of these deranged loci are also perturbed in human ALL, with an overarching goal of finding prognostic biomarkers and therapeutic targets. MYC hyperactivity is not unique to ALL, present in ~70% of human malignancies, potentially making our findings informative not only to ALL, but also many other cancer types where MYC acts as an oncogenic driver.

RELATIONSHIP BETWEEN SLEEP QUALITY AND READINESS TO CHANGE WEIGHT RELATED HEALTH BEHAVIORS IN SMOKERS UNMOTIVATED TO QUIT

Clayton Ulm,[1] Krista M. Kezbers,[1] Lizbeth Benson,[1] Darla E. Kendzor,[1,2] Summer Frank-Pearce,[1,3] Jordan Neil[1,2], Irene De La Torre,[1] & Michael S. Businelle[1,2]

[1]TSET Health Promotion Research Center, Stephenson Cancer Center, University of Oklahoma Health Sciences Center, Oklahoma City, OK, United States; [2]Department of Family and Preventive Medicine, University of Oklahoma Health Sciences Center, Oklahoma City, OK, United States; [3]Department of Biostatistics and Epidemiology, Hudson College of Public Health, The University of Oklahoma Health Sciences Center, Oklahoma City, OK, United States

Background: Prior research has demonstrated that smoking cessation can lead to weight gain, which may demotivate smokers from quitting. Improved sleep can mitigate weight gain and ameliorate withdrawal symptoms, improving the likelihood of cessation. This study explored associations between sleep quality and readiness to change health behaviors related to weight.

Methods: The current study used baseline data collected during a randomized controlled trial of a novel smartphone application designed to increase motivation for smoking cessation. Participants reported self-rated health (*Would you say your health, in general, is…* from *Excellent* = 1 to *Poor* = 5) and sleep quality and duration. Readiness to lose weight, exercise more, and eat more fruit and vegetables were rated by participants (e.g., *I have decided not to try to lose weight for my lifetime* indicated "1" as the lowest level of readiness to change). Pearson correlations were run between self-rated health, sleep measures, and readiness to change.

Results: Participants (N=152) were primarily female (68%) and White (74%) and reported an average of 11.9 days (SD = 10.9) of inadequate sleep in the past 30 days. A majority of participants (61%) reported snoring and a minority of participants (5.3%) reported falling asleep while driving in the past 30 days. Average duration of sleep was relatively low (*M* = 6.7 hours, SD = 1.5). Most participants reported they did not get enough exercise (61%), did not eat enough fruit and vegetables (53%), and 56% were unhappy with their weight. Overall, 31% of participants reported plans to initiate weight loss in the next 30 days, 14% reported plans to eat more fruit and vegetables in the next 30 days, and 11% reported plans to start exercising more in the next 30 days. Correlation analyses indicated that duration of sleep was associated with self-rated health (r = .36, $p < .001$). Further, number of days of inadequate sleep was related to dissatisfaction with weight (r = .16, $p = .048$), but not motivation to lose weight (r = -.18, $p = .058$).

Conclusion: Although many participants had plans or were actively trying to lose weight, few had plans to exercise more or eat more fruit and vegetables, which could hinder their weight loss goals. Inadequate sleep was associated with greater weight dissatisfaction and marginally related to motivation to lose weight. The baseline component of this present study exhibited between-person differences in the associations between sleep and health behaviors related to

weight; further analysis of the longitudinal component of this study is needed to verify the same with-person associations over time.

Funding or acknowledgments: This work was supported by the Oklahoma Tobacco Settlement Endowment Trust (TSET) grant 092-016-0002, and the Mobile Health Technology Shared Resource which is a component of the NCI Support Grant P30CA225520 awarded to the Stephenson Cancer Center.